
PPAR α in peroxisome proliferation:
molecular characterisation and species differences

by

Munim A I Choudhury; B.Sc., M.Sc.

Being a thesis presented in accordance with the regulations
governing the award of the degree of Doctor of Philosophy at
the University of Nottingham

May 2000

Abstract

Peroxisome proliferators (PPs) cause proliferation of peroxisomes and hepatocarcinogenesis in rodent liver, mediated by Peroxisome Proliferator-Activated Receptor-alpha (PPAR α). There are marked species differences in peroxisome proliferator-induced responses, and the functionality of PPAR α may be an important determinant factor in species sensitivity to PPs. Primary hepatocytes were investigated for a highly responsive marker induced by PPs to study the effects of transfected PPAR α . CYP4A1 was highly induced in rat hepatocytes that require hydrocortisone for maximal induction. Hepatocytes were cultured in hydrocortisone-deficient media to determine if reduced endogenous PPAR α was associated with lowered induction of CYP4A1. However, there was residual induction of CYP4A1 by peroxisome proliferators. Primary hepatocytes from PPAR α knock-out (-/-) mice were investigated as they lack endogenous PPAR α . *In vitro* and *in vivo* studies demonstrated that *Cyp4a10* and *14* were highly inducible by PPs in the hepatocytes of wild-type but not in -/- mice. However, addition of either mouse or guinea pig PPAR α in -/- hepatocytes did not induce the expression of these marker genes, although both receptors showed trans-activation ability in a reporter assay. The failure of added PPAR α to activate endogenous genes responsive to PPs, whilst at the same time activating episomal DNA containing response elements of PP-inducible gene, suggests that the endogenous genes require PPAR α to remain in an accessible conformation.

Although hamster is considered to be a partially-responsive species to PPs, their response to PPs is poorly characterized. Three CYP4A genes (CYP4A17, 18 and 19) were cloned from hamster liver cDNA, and hepatic CYP4A17 was found to be highly inducible by PPs. In addition, PPAR α was cloned from hamster liver and shows higher identity to rat and mouse PPAR α than to human and guinea pig. Hepatic expression of PPAR α mRNA was compared between mouse, hamster and guinea pig. The level of PPAR α transcript was found to correlate well with species response to PPs, i.e. mouse (highly responsive species) has the highest level and guinea pig

(non-responsive) the lowest, while hamster (partially-responsive) has an intermediate level. This is consistent with a model where the level of expression of hepatic PPAR α determines species response to PPs.

Expression of PPAR α and transcriptional coactivators, such as PBP, SRC-1 and CBP/p300, were confined to mouse liver at the RNA level, but in each case expression showed homogenous distribution within the liver acinus and was non-inducible by PPs. Mouse PPAR α ligand binding domain (LBD) was bacterially expressed as a histidine-tagged protein and soluble proteins were purified using affinity and column chromatography. Functional LBD may serve as a useful bait in protein-protein interaction studies for the identification of any novel PPAR α interacting coactivator protein.

TABLE OF CONTENTS

1 INTRODUCTION	19
1.1 Peroxisome Proliferation: an overview	19
1.1.1 Peroxisomes and their function	19
1.1.2 β-oxidation of fatty acids in peroxisomes	20
1.1.3 Peroxisome Proliferators	23
1.1.4 Acute effects of peroxisome proliferators	25
1.1.5 Biochemical changes associated with peroxisome proliferation	26
1.1.6 Hyperplastic response to peroxisome Proliferators	27
1.1.7 Chronic exposure to peroxisome proliferators	28
1.1.8 Peroxisome proliferators are non-genotoxic carcinogens	28
1.1.9 The oxidative stress model	28
1.1.10 Peroxisome proliferators as tumour promoting agents	30
1.2 Cytochrome P450 mono-oxygenase system	32
1.2.1 Cytochrome P450 4A subfamily	35
1.2.2 Expression of CYP4A genes	37
1.2.3 Role of CYP4A in fatty acid metabolism and renal function	38
1.2.4 Role of CYP4A in peroxisome proliferation	39
1.3 Cloning of a steroid receptor activated by PPs	40
1.3.1 The steroid hormone receptor superfamily	41
1.3.2 The PPAR family and tissue-specific expression	43
1.3.3 Regulation of PPARα gene expression	45
1.3.4 PPARα activators and ligands	47
1.3.5 Peroxisome proliferator response elements (PPREs)	48
1.3.6 PPARα-RXRα heterodimer binds to PPRE	50
1.3.7 Regulation of PPARα-induced transactivation by receptor cross-talk	51
1.3.8 Coactivator proteins in steroid hormone receptor function	55
1.3.9 Functional loss of PPARα and its implications	56
1.4 Species differences in peroxisome proliferation	57
1.4.1 Peroxisome proliferation in responsive species	58
1.4.2 Peroxisome proliferation in non-responsive species	59
1.4.3 Peroxisome proliferation in primates	59
1.5 Aims of the thesis	61

2 MATERIALS & METHODS	63
2.1 Animal Studies	63
2.1.1 Guinea pigs	63
2.1.2 Mice	63
2.1.3 Hamster	64
2.1.4 Rats	64
2.2 Primary Hepatocytes: Isolation & Culture	64
2.2.1 Primary Hepatocyte Isolation	64
2.2.2 Viability count and quantification of hepatocytes	66
2.2.3 Hepatocyte Culture	67
2.2.4 Dosing of primary hepatocytes	67
2.2.5 Measurement of DNA Synthesis	67
2.2.6 Histochemical staining of peroxisomes	69
2.2.7 Detection of apoptosis in hepatocyte culture	69
2.3 Transient Transfection Studies	70
2.3.1 Preparation of lipofectin reagent	70
2.3.2 Transfection of primary hepatocytes	71
2.3.3 β-Galactosidase histochemistry	71
2.3.4 Dual luciferase assay	72
2.4 General Molecular Biology Techniques	73
2.4.1 E. Coli growth media	73
2.4.2 Preparation of calcium competent E. Coli	74
2.4.3 Preparation of electro-competent E. Coli	74
2.4.4 Plasmid transformation into CaCl_2 competent E.coli	75
2.4.5 Plasmid transformation into electro-competent E.coli	75
2.4.6 Phenol:Chloroform extraction of nucleic acids	76
2.4.7 Ethanol precipitation of nucleic acids	76
2.4.8 Restriction digestion of plasmid DNA	77
2.4.9 Agarose gel electrophoresis (non-denaturing)	77
2.4.10 Agarose gel electrophoresis (denaturing)	78
2.4.11 Denaturing polyacrylamide gel electrophoresis	78
2.4.12 DNA gel purification by geneclean	79
2.4.13 Alkaline Phosphatase treatment of DNA	80

2.4.14	DE81 test for nucleotide incorporation	80
2.4.15	Labelling of DNA ladder	81
2.4.16	Extraction and Purification of Nucleic Acids	82
2.4.16.1	Purification of plasmid DNA by alkaline lysis method	82
2.4.16.2	Purification of plasmid DNA on Qiagen Mini- and Maxi-prep columns	83
2.4.16.3	Mini-prep method	83
2.4.16.4	Maxi-prep method	84
2.4.17	Extraction and Purification of RNA	85
2.4.17.1	Preparation of equilibrated Phenol	85
2.4.17.2	RNA extraction from liver	85
2.4.17.3	Lithium chloride/ urea method	86
2.4.17.4	Guanidinium thiocyanate method	87
2.4.17.5	From primary hepatocytes	88
2.4.17.6	Isolation of total RNA for cDNA cloning	89
2.4.18	Purification of polyA+ RNA	90
2.5	Gene Cloning: PCR Cloning of cDNA	90
2.5.1	PCR Amplification of cDNA	91
2.5.2	Purification of PCR products	93
2.5.3	Ligation of amplified DNA fragment	93
2.5.4	Selection of recombinant plasmids	94
2.5.5	Amplification of 5'-cDNA ends	94
2.5.6	Purification of First strand product	95
2.5.7	Homopolymeric tailing of cDNA	96
2.5.8	PCR of dC-tailed cDNA	96
2.5.9	Cloning of putative 5'-cDNA RACE products	97
2.6	DNA Sequencing and analysis	97
2.7	Gene Expression Studies	100
2.7.1	RNase Protection Assay	100
2.7.1.1	Template Generation	100
2.7.1.2	RNA transcription in vitro	101
2.7.1.3	Probe Hybridisation	101
2.8	In situ Hybridization	103
2.8.1	Tissue preparation and sectioning	103

2.8.2 Probe Labelling and Hybridisation	103
2.8.2.1 Purification of the probe	105
2.8.2.2 Hybridisation	105
2.8.2.3 Stringency Washes	106
2.8.2.4 Emulsion Autoradiography	107
2.9 Protein Methodologies	107
2.9.1 Bradford Assay	107
2.9.2 SDS-Polyacrylamide gelelectrophoresis (SDS-PAGE)	108
2.9.3 Coomassie staining	109
2.9.4 Immunoblotting	110
2.9.5 Electrophoretic transfer of proteins	110
2.9.6 Probing of transferred protein with antibody	111
2.9.7 Expression of bacterially expressed recombinant protein	111
2.9.8 Induction of His-tagged Protein	111
2.9.9 Affinity Chromatography	112
2.9.10 FPLC Chromatography	114
2.10 Data Presentation and Analysis	114
2.10.1 Illustration	114
2.10.2 Statistical Analysis	114
3 RESULTS	116
3.1 In vitro study of peroxisomal events	116
3.2 Primary rat hepatocyte culture system	116
3.2.1 DNA synthesis in primary hepatocyte culture	116
3.2.1.1 Mitogenic stimulation by epidermal growth factor	117
3.2.1.2 PP-induced DNA synthesis in primary rat hepatocyte culture	118
3.2.2 Effect of peroxisome proliferators on apoptosis	121
3.2.3 Induction of CYP4A1 in primary rat hepatocyte culture	122
3.2.3.1 Extraction of in vitro and in vivo RNA	122
3.2.3.2 Expression and induction of rat CYP4A1 in liver and kidney	123
3.2.3.3 Effects of hydrocortisone on the induction of CYP4A1 in hepatocytes	125
3.2.3.4 Effects of culture conditions on the induction of CYP4A1	128
3.3 Expression of Cyp4a genes in PPAR α wild-type and -/- mice	132
3.3.1 Induction of murine Cyp4a gene family	133

3.3.1.1 Effects of PPs on Cyp4a10 expression.	133
3.3.1.2 Effects of PPs on Cyp4a14 expression.	134
3.3.1.3 Effects of PPs on Cyp4a12 expression.	136
3.3.2 Primary mouse hepatocyte culture system	138
3.3.2.1 Induction of Cyp4a genes in primary mouse hepatocytes	138
3.3.2.2 Transient transfection of mouse hepatocytes.	140
3.3.2.3 Transfection of PPAR α in primary mouse hepatocytes.	142
3.3.2.4 Expression of transfected PPAR α in mouse hepatocytes	144
3.4 Peroxisome proliferation in primary rat hepatocytes	147
3.5 PCR cloning of hamster CYP4A genes	148
3.6 Identification of multiple hamster CYP4A genes	152
3.6.1 Restriction analysis of putative CYP4A clones	152
3.6.2 Sequence analysis of hamster CYP4A genes	156
3.6.3 Presence of mispliced CYP4A mRNA species in hamster.	158
3.6.4 Peroxisome proliferator-induced CYP4A induction in hamster liver.	160
3.7 Cloning of hamster PPAR α cDNA	161
3.7.1 Cloning of 5' end of hamster PPAR α	164
3.7.2 Hamster PPAR α cDNA and deduced amino acid sequence.	167
3.7.3 Sequence analysis of the PPAR α amino acid sequence	169
3.7.4 Phylogenetic analysis of PPAR α genes	172
3.7.5 Expression of PPAR α in mouse, hamster and guinea pig Liver.	173
3.8 The mPPAR α ligand binding domain (mPPAR α -LBD).	176
3.8.1 Induction of mPPAR α -LBD protein.	176
3.8.1.1 Effect of temperature on protein solubility	177
3.8.1.2 Effect of IPTG concentration on protein solubility	178
3.8.2 Affinity purification of mPPAR α -LBD protein	179
3.8.3 FPLC purification of mPPAR α -LBD protein.	181
3.9 Localisation of RNA in mouse liver	182
3.9.1 Region-specific distribution of mPPAR α mRNA	183
3.9.2 Expression of co-activator proteins in the liver	185
4 DISCUSSION	187
4.1 The role of PPAR α in peroxisome proliferation	187
4.1.1 Peroxisome proliferation in rat primary hepatocytes	187

4.1.2	Induction of DNA synthesis in rat primary hepatocytes	188
4.1.3	Peroxisome proliferator-induced DNA synthesis	189
4.1.4	Influence of culture components on DNA synthesis	189
4.1.5	Suppression of apoptosis by MCP	191
4.1.6	Induction of CYP4A1 mRNA as marker of peroxisome proliferation	192
4.1.7	CYP4A1 induction in primary hepatocytes	193
4.1.8	Modulation of CYP4A1 expression	194
4.1.9	Endogenous versus reporter gene activation to study of PPARα function	196
4.2	Characterization of the induction of murine Cyp4a genes	198
4.2.1	Induction of murine Cyp4a family	199
4.2.2	Effects of transfected PPARα in the hepatocytes knock-out mice	202
4.3	Hamster response to peroxisome Proliferators	206
4.3.1	Cloning of hamster CYP4A cDNA	207
4.3.2	Cloning of three CYP4A cDNAs in hamster	208
4.3.3	Sequence analysis of hamster CYP4A genes	208
4.3.4	Functions of putative hamster P4504A proteins	210
4.3.5	Evidence of mis-spliced CYP4A mRNA in MCP-treated hamster liver	211
4.3.6	Induction of hamster CYP4A by peroxisome proliferators	213
4.4	Cloning of hamster PPARα	215
4.4.1	Sequence analysis of hamster PPARα	216
4.4.2	Hamster PPARα function	219
4.4.3	Molecular phylogeny of PPARα genes	219
4.4.4	Hepatic expression of PPARα in species with differing responses to PPs	221
4.5	Distribution of PPARα and interacting coactivator proteins	225
4.6	Heterologous expression and purification of mPPARα-LBD	227
4.7	Conclusions	229
5	REFERENCES	233

Figure 1.1 Peroxisomal β -oxidation of a long chain fatty acid.	22
Figure 1.2 Chemical structure of some peroxisome proliferators	24
Figure 1.3 The catalytic cycle of cytochrome P450 mono-oxygenase.	35
Figure 1.4 Functional domains of nuclear hormone receptors.	43
Figure 1.5 Cartoon of PPAR α and its heterodimerization partner, RXR α , on a PPRE.	52
Figure 2.1 Sequencing strategy for hamster PPAR α	98
Figure 3.1 Immunochemical detection of BrdUrd labelled cells.	117
Figure 3.2 Peroxisome proliferator-induced DNA synthesis in rat hepatocytes.	118
Figure 3.3 Induction of DNA synthesis in primary rat hepatocyte cultures.	119
Figure 3.4 Effect of medium components and culture conditions on DNA synthesis.	120
Figure 3.5 Suppression of apoptosis by peroxisome proliferators.	121
Figure 3.6 Agarose gel electrophoresis of total liver RNA.	123
Figure 3.7 Diagrammatic representation of CYP4A1 template.	124
Figure 3.8 Expression of and induction of CYP4A1 gene in rat tissue.	125
Figure 3.9 Effects of hydrocortisone on induction of CYP4A1.	127
Figure 3.10 Induction of rat CYP4A1.	128
Figure 3.11 Effects of dosing period in the induction of CYP4A1.	129
Figure 3.12 Induction of CYP4A1 after different dosing periods.	130
Figure 3.13 Cartoon of <i>Cyp4a10</i> , <i>12</i> (A) and <i>14</i> (B) templates.	133
Figure 3.14 <i>Cyp4a10</i> expression in PPAR α wild-type and knock-out mice.	134
Figure 3.15 <i>Cyp4a14</i> expression in PPAR α wild-type and knock-out mice.	135
Figure 3.16 <i>Cyp4a-12</i> expression in PPAR α $+/+$ and $-/-$ mice.	136
Figure 3.17 Induction of <i>Cyp4a10</i> and <i>14</i> in $+/+$ mice.	137
Figure 3.18 Expression of <i>Cyp4a14</i> in hepatocytes of PPAR α $+/+$ and $-/-$ mice.	138
Figure 3.19 Induction of <i>Cyp4a14</i> in primary mouse hepatocytes.	139
Figure 3.20 Transfection of pRSV- β -GAL in (A) rat and (B) mouse hepatocytes.	140
Figure 3.21 Optimisation of transfection efficiency (A) DNA and (B) lipofectin reagent.	141
Figure 3.22 Effect of transfected PPAR α on expression of <i>Cyp4a14</i> in hepatocytes.	143
Figure 3.23 Guinea pig PPAR α mRNA after transfection into hepatocytes of $-/-$ mice.	144
Figure 3.24 Effect of PPAR α on reporter gene in hepatocytes of $-/-$ mice.	146
Figure 3.25 Peroxisome proliferation in rat primary hepatocytes.	148
Figure 3.26 Design of PCR primers from alignment of CYP4A proteins.	149

Figure 3.27 cDNA (A) and amino acid (B) sequence of hamster CYP4A17.	150
Figure 3.28 PCR of CYP4 genes from hamster liver.	151
Figure 3.29 Restriction analysis of hamster CYP4A clones.	153
Figure 3.30 cDNA (A) and amino acid (B) sequence of hamster CYP4A18.	154
Figure 3.31 cDNA (A) and amino acid (B) sequence of hamster CYP4A19.	155
Figure 3.32 Alignment of three CYP4A proteins from hamster	156
Figure 3.33 Mis-spliced CYP4A mRNA species in MCP-treated hamster liver.	159
Figure 3.34 Cartoon of hamster CYP4A17 template.	160
Figure 3.35 CYP4A induction in hamster liver by MCP and Wy-14,643.	161
Figure 3.36 Induction of hamster CYP4A by MCP and Wy-14,643	162
Figure 3.37 Design of PCR primers from alignment of PPAR α proteins.	163
Figure 3.38 PPAR α amplified from hamster liver cDNA.	164
Figure 3.39 5'RACE products from hamster PPAR α cDNA.	165
Figure 3.40 Restriction analysis of 5'-clones of hamster PPAR α	167
Figure 3.41 cDNA sequence of hamster PPAR α	168
Figure 3.42 Deduced amino acid sequence of hamster PPAR α	169
Figure 3.43 Alignment of hamster PPAR α with known PPAR α proteins.	171
Figure 3.44 Phylogenetic relationship of PPAR α proteins.	172
Figure 3.45 Cartoon of hamster (A), mouse (B) and guinea-pig (C) PPAR α templates . .	173
Figure 3.46 PPAR α mRNA in hamster (A), guinea pig (B) and mouse (C) liver.	174
Figure 3.47 Comparative hepatic expression of PPAR α	175
Figure 3.48 Induction of mPPAR α -LBD in <i>E. coli</i>	177
Figure 3.49 Solubility of mPPAR α -LBD; effect of temperature.	178
Figure 3.50 Effect of IPTG on induction and solubility of mPPAR α -LBD.	179
Figure 3.51 Affinity purification of mPPAR α -LBD.	180
Figure 3.52 Detection of mPPAR α -LBD by Western blotting.	181
Figure 3.53 FPLC of PPAR α -LBDwt.	182
Figure 3.54 Distribution of glutamine synthase mRNA in mouse liver.	184
Figure 3.55 <i>In situ</i> hybridisation with anti-sense (A) and sense (B) PPAR α	185
Figure 3.56 Localisation of coactivator mRNA expression in mouse liver.	186

LIST OF TABLES

Table 1.1 Enzymes induced by peroxisome proliferators	26
Table 1.2 Members of the CYP4A subfamily identified in different species.	36
Table 1.3 Members of PPAR family identified from different species	43
Table 1.4 PPRE sequences in peroxisome proliferator responsive genes.	49
Table 2.1 Sequence primers used for hamster PPAR α	99
Table 2.2 Sequence of primers for hamster CYP4A cDNA.	99
Table 2.3 List of oligo primers used for in situ hybridisation	104
Table 3.1 Grouping of hamster CYP4A clones by restriction digestion.	153
Table 3.2 Identity of hamster CYP4A proteins.	157
Table 3.3 Comparison of hamster and rat CYP4A genes.	157
Table 3.4 Comparison of hamster CYP4A proteins with other species.	158
Table 3.5 Similarity between hamster PPAR α and other PPARs.	170
Table 4.1 Induction of reporter genes	197

Abbreviations

A	Adenine
ACO	Acyl-CoA oxidase
AF-1	TransActivating Function-1
Amp	Ampicillin
APS	Ammonium Persulphate
Chl	Chloramphenicol
CoA	Coenzyme
BSA	Bovine Serum Albumin
bp	Base Pair
BrdU	BromodeoxyUridine
C	Cytosine
CBP	CREB binding protein
CTP	Cytosine triphosphate
CYP4A	Cytochrome P450 4A subfamily
COUP-TF	Chicken ovalbumin upstream promoter-transcription factor
DBD	DNA Binding Domain
DNA	Deoxyribonucleic acid
cDNA	Complementary DNA
DEN	Diethylnitrosoamine
DEPC	Diethyl Pyrocarbonate
DEHA	Di(2-ethylhexyl)adipate
DEHP	Di(2-ethylhexyl)phthalate
DMSO	Dimethyl Sulphoxide

DOPE	L-a-phosphatidylethanolamine, dioleoyl(C18:1,[cis]-9)
DOTMA	(N-[I-(2,3-dioleoyloxy)propyl]-N,N,N-triethylammonium
DR1	Direct Repeat element with a single nucleotide spacer
DTT	Dithiothreitol
EDTA	Ethylenediaminetetraacetic acid (disodium salt)
EET	Epoxyeicosatetraenoic acid
EGF	Epidermal Growth Factor
ER	Estrogen Receptor
ERE	Estrogen Receptor Response Elements
FPLC	Fast Protein Liquid Chromatography
G	Guanine
GR	Glucocorticoid Receptor
GSP	Gene Specific Primer
H ₂ O ₂	Hydrogen Peroxide
HETE	Hydroxyeicosatetraenoic acid
HNF-4	Hepatic Nuclear Factor-4
IAA	Isoamyl alcohol
IPTG	Isopropyl-β-D-thiogalactopyranoside
JAK-STAT	Janus Kinase-Signal Transducer and Activator of Transcription
kb	Kilobase
kDa	Kilodalton
KRHB	Krebs Ringer Hydrocarbonate Buffer
KRPB	Krebs ringer Phosphate Buffer
L15	Leibovitz medium

LB	Luria-Bertani Broth
LBD	Ligand Binding Domain
LCR	Locus Control Region
MCP	Methylclofenapate
MgCl ₂	Magnesium Chloride
NH ₄ Ac	Ammonium Acetate
PAGE	Polyacrylamide Gel Electrophoresis
PBS	Phosphate Buffered Saline
PBP	PPAR-gamma Binding Protein
PCR	Polymerase Chain Reaction
PFDA	Perfluorodecanoic Acid
PGC-1	PPAR-gamma Coactivator-1
PPs	Peroxisome Proliferators
PPAR	Peroxisome Proliferator-Activated Receptor
PPRE	Peroxisome Proliferator Response Element
4A6z	Cytochrome P450 4A6 gene PPRE with consensus 5'flanking sequence
PVDF	Polyvinylidene Difluoride
RAR	Retinoic Acid Receptor
RIP-140	Receptor Interacting Protein-140
RNA	Ribonucleic Acid
mRNA	Messenger RNA
RXR	Retinoid X Receptor
RZR α	Retinoid Z Receptor alpha
SDS	Sodium Dodecyl Sulphate

SRC-1	Steroid Receptor Coactivator-1
SRS	Substrate Recognition Site
T	Thymine
TAE	Tris/EDTA/Glacial acetic acid Buffer
TBE	Tris-borate-EDTA Buffer
TBS	Tris-buffered Saline
TTBS	Tween-TBS
TEMED	N, N, N', N',-tetramethylethylenediamine
Tet	Tetracyclin
TR	Thyroid Hormone Receptor
TZD	Thiazolidinedione
UHP	Ultra High Purity
VDR	Vitamin D Receptor
VLCFA	Very Long Chain Fatty Acid Coenzyme A
Wy-14,643	[4-chloro-6(2,3-xylidino)-2-pyrimidinylthio] acetic acid
X-Gal	5-bromo-4-chloro-3-indolyl- β -D-galactopyranoside

Acknowledgements

I wish to acknowledge the support and scientific guidance of my project supervisor, Dr David Bell, whose enthusiasm and scientific endeavour has been a constant source of encouragement throughout my PhD. My sincere thanks to him for the critical discussion and the successful completion of this project. Also, I would like to thank my industrial supervisor Dr Ruth Roberts for her role and helpful comments on the preparation of this thesis. I wish to acknowledge MRC and Zeneca CTL for their funding of this project.

A very special thanks to Neill Horley for teaching me how to isolate “good” hepatocytes and for his advice and encouragements to see the project through on occasions when things were difficult (respect due!). I would like to thank “computer Guru” Simon Tomlinson for his help on GCG sequence analysis and of course for keeping all our computers networked! I would like to thank Dave Fox, Neill, Declan, Sunny and Brett for their assistance in animal dosing.

Thanks to all past and present members of the “Bell Lab” for maintaining the working spirit of the lab, for their good humour and stimulating scientific discussions in the coffee bar! They are Neill Horley (would you give?), Yee Heng (surf dude!), Alex Gage, Sunny Chahal (Mum-rrraaahhhh!), Brett Jeffery (Net-Boy), Chris Mee (the player). Thanks to Declan Brady (“perfectly proportional”), Gareth Murtagh, Alex Bell, Paul Clark, Fan Ming Qi, Sharon Kuo and members of Zeneca cancer biology group for their positive contributions during my PhD. Many thanks to Yee and Sunny for their hospitality when I visited Nottingham from time to time during my writing-up.

Lastly, but not least, I would like to thank my family for their encouragements and moral support.

For Mum & Dad

Chapter 1 Introduction

Section 1.1 Peroxisome Proliferation: an overview

Section 1.1.1 Peroxisomes and their function

The discovery of peroxisomes as distinct biochemical entities by Christian De Duve and their subsequent study by other workers has paved the way for better understanding of the metabolism of fatty acids and cholesterol (Baudhuin *et al.*, 1965; De Duve and Baudhuin, 1966). Peroxisomes are so called because they contain one or more enzymes that use molecular oxygen to remove hydrogen atoms from specific organic substrates in an oxidative reaction that produces hydrogen peroxide. Peroxisomes are single-membrane bound organelles, generally spherical in shape with a finely granular matrix. They are found in all eukaryotic cells, particularly abundant in hepatocytes with a diameter of up to 0.5 μ m (Wilcke *et al.*, 1995). They contain oxidative enzymes, such as catalase and urate oxidase, at such high concentrations that in the cells of some species, rat liver for example, the peroxisomes stand out in electron micrographs because of the presence of a crystalloid core, largely composed of urate oxidase (Baudhuin *et al.*, 1965). However, crystalloid cores are absent in human peroxisomes (Usada *et al.*, 1988). Peroxisomes are detected histochemically by utilizing the peroxidase activity of catalase that converts 3, 3'-diaminobenzidine into a brown precipitate at alkaline pH. Peroxisomes are most abundant in liver and kidney where there can be as many as 600 individual peroxisomes in a single cell, occupying up to 2% of cell volume (Masters and Crane, 1995).

Peroxisomes fulfill a crucial role in cellular metabolism, and as many as 50 enzymatic activities have been identified in mammalian peroxisomes (Mannerts and van Veldhoven, 1993), some of which are restricted to peroxisomes whereas others have their counterparts in other organelles. Peroxisomal enzymes are involved in a number of catabolic and anabolic processes, including fatty acid oxidation, alcohol oxidation, synthesis of cholesterol, bile acids and ether lipids, and

metabolism of purines, polyamines and amino acids (Van den Bosch *et al.*, 1992; Masters and Crane, 1992; Masters, 1996).

The importance of peroxisomal functions in maintaining normal tissue homeostasis has been exemplified by the recognition of a number of fatal inherited diseases involving either a defect in the biogenesis of peroxisomes or a deficiency of one or more peroxisomal enzymes. Patients with Zellweger syndrome lack functional peroxisomes and are characterized by a number of biochemical abnormalities. For example, impairment of the β -oxidation of fatty acids results from the deficiency of all peroxisomal β -oxidation enzymes, which results in the accumulation of very long chain fatty acids in tissues and blood (Schutgens *et al.*, 1986; Moser, 1987; Lazarow and Moser, 1989). Accumulation of very long chain fatty acids also occurs in X-linked adrenoleukodystrophy, a single gene disorder associated with a defect in the peroxisomal enzyme VLCFA-CoA synthase (Wanders *et al.*, 1988; Lazo *et al.*, 1988). Other peroxisomal disorders of generalized impairment include adrenoleukodystrophy and the infantile type of Refsum disease (Moser, 1993). In conditions such as the rhizomelic type of Chondrodysplasia Punctata and Zellweger-like syndrome a limited number of peroxisomal functions are impaired (Van den Bosch *et al.*, 1992).

Section 1.1.2 β -oxidation of fatty acids in peroxisomes

A major function of the oxidative reactions carried out in mammalian peroxisomes is the breakdown of fatty acid molecules, particularly very long chain fatty acids which are exclusively metabolized by peroxisomal β -oxidation system. During β -oxidation the alkyl chains of fatty acids are shortened sequentially by blocks of two carbon atoms at a time that are converted to acetyl-CoA and exported from the peroxisomes to the cytosol for reuse in biosynthetic reactions. Free fatty acids must be activated to a CoA derivative before being degraded by β -oxidation. This esterification reaction is carried out in the cytoplasm by a variety of acyl-CoA synthetases. Fol-

Following activation, the acyl-CoA derivatives of fatty acids are carried to the peroxisomes where they are subjected to oxidation by acyl-CoA oxidases. Acyl-CoA oxidases are multi-subunit flavoproteins containing FAD as a prosthetic group that require molecular O₂ for the oxidation of fatty acids, yielding hydrogen peroxide in the process (Van den Bosch *et al.*, 1992; Schultz, 1991). The next two steps of β -oxidation pathway are hydration, followed by dehydrogenation. A single bifunctional enzyme has been found to carry out these two reactions. Bifunctional enzyme of the rat liver peroxisomes has been shown to possess an extra enzymic activity of 3,2-enoyl-CoA isomerase in addition to 2-enoyl-CoA hydratase and 3-hydroxyacyl-CoA dehydrogenase activities (Palosaari and Hiltunen, 1990). The final step of β -oxidation in peroxisomes is the thiolytic cleavage of oxo-acyl-CoA (3-ketoacyl-CoA) by CoA-SH catalysed by 3-keoacyl-CoA thiolase. (Figure 1.1 shows an example of peroxisomal β -oxidation of a fatty acids)

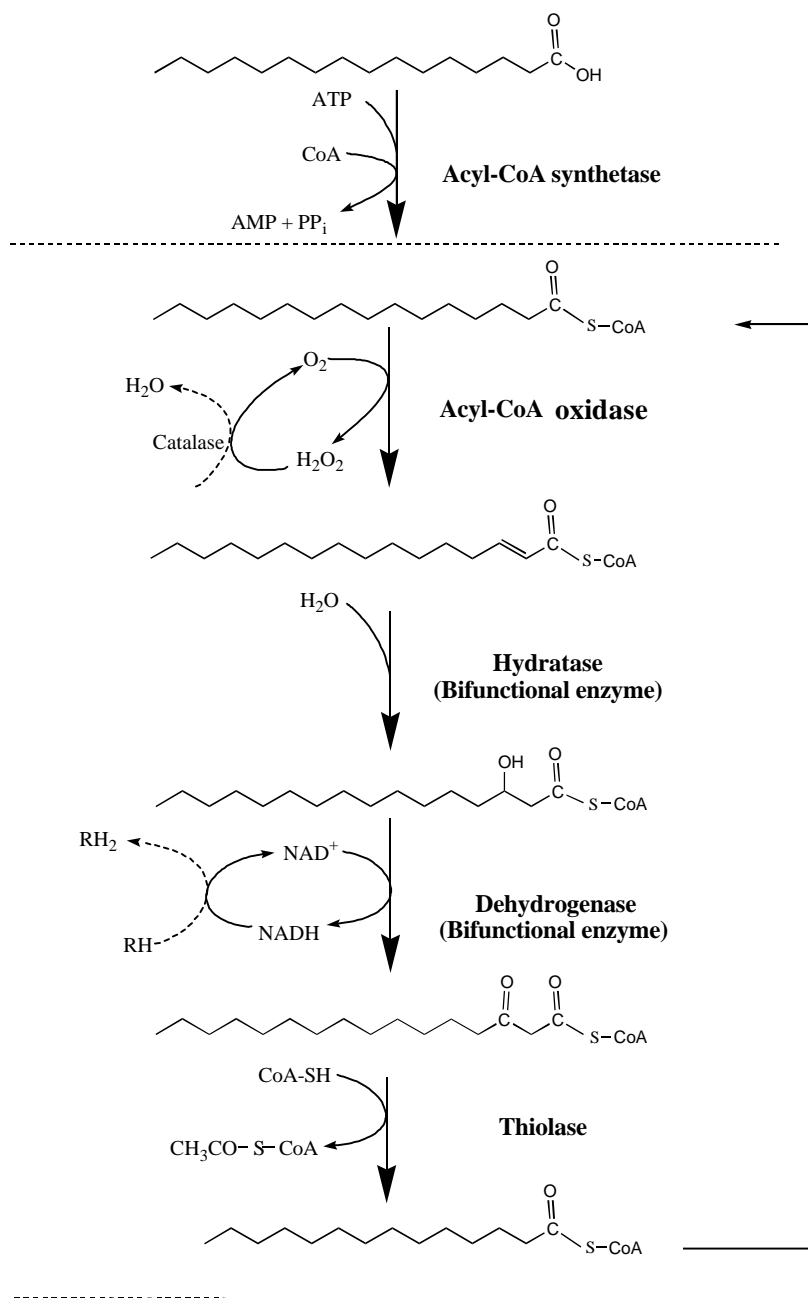


Figure 1.1 Peroxisomal β -oxidation of a long chain fatty acid. (modified from Osmunden *et al.* 1991). Essential metabolic features of peroxisomal β -oxidation of a saturated fatty acid (C_{16}) are presented. The enzymes of the β -oxidation are contained within the peroxisomal membrane (dashed line) and the reaction pathway are shown by solid arrows. For completeness, reaction of catalase are shown in the left-hand side of the reaction pathway.

The products of peroxisomal β -oxidation are chain shortened acyl-CoAs, acetyl-CoA, NADH and hydrogen peroxide (H_2O_2). Acyl-CoA is able to undergo further cycles of β -oxidation or they may be utilized for the synthesis of more complex lipids. However, medium chain fatty acyl-CoAs can be utilized by carnitine acetyl transferases present in the peroxisomes to generate

carnitine derivatives. The carnitine derivative can be further oxidized by mitochondria to generate ATP in the process. Hydrogen peroxide is rapidly degraded by catalase present in the peroxisome producing O₂ and H₂O in the process. Catalase utilizes H₂O₂ to oxidize a variety of other substrates, including phenol, formic acid, formaldehyde and alcohol (Van den Bosch *et al.*, 1992; Schultz, 1991; Gibson and Lake, 1993). This type of oxidative reaction is particularly important in the liver and kidney cells whose peroxisomes detoxify various toxic molecules that may enter the blood stream.

Section 1.1.3 Peroxisome Proliferators

Peroxisome proliferators (PPs) are a class of non-genotoxic carcinogens which upon administration to some rodents results in profound biochemical and morphological changes of the liver known as peroxisome proliferation (Reddy *et al.*, 1980; Lock *et al.*, 1982). Peroxisome proliferators are structurally diverse with no easily identifiable common molecular structure or physical property (see Figure 1.2 for some examples). However, a large number of PPs contain

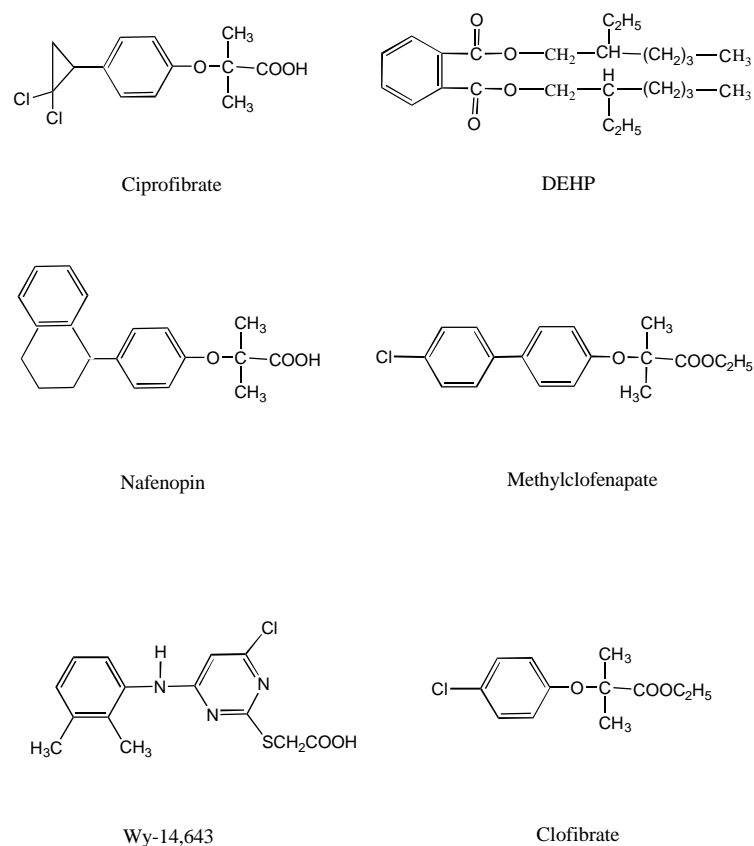


Figure 1.2 Chemical structure of some peroxisome proliferators.

a carboxylic acid moiety or a group that can be converted into one (McGuire *et al.*, 1992) or an acidic group. The requirement for an acidic group to elicit peroxisome proliferation has been shown in the case of hypolipidaemic drug LY-171883, where substitution of the tetrazole group into an analog that can not form an acidic group abolishes its ability to cause peroxisome proliferation (Sakuma *et al.*, 1992). Peroxisome proliferating chemicals constitute a group that has widespread clinical and industrial use including hypolipidaemic drugs, plasticizers and herbicides (Moody *et al.* 1991; Bently *et al.*, 1993).

Certain pathophysiological conditions such as high-fat diets, cold temperature, starvation and conditions such as diabetes mellitus also cause peroxisome proliferation in the liver (Reddy and Lalwani, 1983). When administered to rodents, PPs cause a pleiotropic cellular response, in-

volving an increase in the number and size of peroxisomes that appears to be most pronounced in the liver, kidney and heart (Reddy and Chu, 1996; Lock *et al.*, 1989; Reddy and Lalwani, 1983).

Section 1.1.4 Acute effects of peroxisome proliferators

Despite the lack of structural homology between PPs, acute exposure to these xenobiotics results in a series of biochemical and morphological changes in the liver, leading to liver enlargement, hepatomegaly (Styles *et al.*, 1988; Barrass *et al.*, 1993). There is a rapid initial increase in liver size following administration of a potent PP, with up to 3-fold increase in liver mass by day three and reaching a maximum size by day fourteen (Marsman *et al.*, 1988; Reddy and Lalwani, 1991; Eacho *et al.*, 1991). This augmentative liver growth is sustained for the duration of the exposure and upon cessation of exposure, the liver regresses to its original size and mass (Cohen and Crasso, 1981).

Peroxisome proliferator-induced hepatomegaly is a consequence of hypertrophic and hyperplastic response. Hypertrophy results from an increase in the size of individual hepatocytes due to an increase in subcellular organelles such as smooth endoplasmic reticulum, Golgi bodies, mitochondria and peroxisomes (Reddy *et al.*, 1980; Lock *et al.*, 1989). The major organelle affected by PPs, however, is the peroxisome which undergoes significant increase in both size and number (Moody and Reddy 1978; Reddy *et al.*, 1980; Samboda and Azarnoff, 1966). Treatment with PPs has been shown to increase the number of peroxisomes to up to 25% of the cytoplasmic volume of the hepatocyte, compared to untreated cell where less than 2% of cytoplasmic volume is occupied by peroxisomes (Moody and Reddy, 1976; Nemali *et al.*, 1989). The collective volume and surface area of the smooth endoplasmic reticulum is increased up to 3-fold by PPs (Moody and Reddy, 1976).

Section 1.1.5 Biochemical changes associated with peroxisome proliferation

Concurrent with the increase in size and numbers of peroxisomes, specific peroxisomal enzymes are induced (Hawkins *et al.*, 1987; Auwerex *et al.*, 1996; Lazarow and De Duve, 1976; Lazarow, 1977; Norseth and Thomassen, 1983; Veerkamp and Van Moerker, 1986), including enzymes of the β -oxidation pathway. However this selective induction of peroxisomal enzymes is differentially regulated. For example, a marked induction of acyl-CoA oxidase activity (30-fold) was observed with PPs compared to a modest increase in catalase activity (3-fold) (Reddy and Lalwani, 1983; Lock *et al.*, 1989). The proliferation of smooth endoplasmic reticulum is associated with a high level of microsomal lauric acid ω -hydroxylase activity resulting from high level of induction of cytochrome P-4504A family (Kimura *et al.*, 1989, Bell and Elcombe, 1991a). Induction of CYP4A1 precedes the induction of peroxisomal acyl-CoA oxidase after administration of the peroxisome proliferator MCP (Bell *et al.*, 1991), suggesting that the induction of peroxisomal and microsomal genes are regulated in a coordinate manner. Due to their early and high level of induction during peroxisome proliferation, induction of CYP4A1 and acyl-CoA oxidase by PPs are routinely used as markers of peroxisome proliferation. Table 1.2 shows a list of some of the enzymes induced by PPs.

Enzyme	Cellular Localization	Reference
Cytochrome P450 4A1	Smooth ER	Gibson <i>et al.</i> , 1982
Acyl-CoA oxidase	Peroxisome	Osumi <i>et al.</i> , 1984
Bifunctional enzyme	Peroxisome	Reddy <i>et al.</i> , 1986
Thiolase	Peroxisome	Baumgart <i>et al.</i> , 1990
Catalase	Peroxisome	Pacot <i>et al.</i> , 1993
Malic enzyme	Cytosolic	Sakuma <i>et al.</i> , 1992
HMG-CoA Synthase	Mitochondrial	Rodriguez <i>et al.</i> , 1994
Carnitine Palmitoyl-CoA transferase	Total cellular	Sakuma <i>et al.</i> , 1992
Fatty acid binding protein	Cytosolic	Kaikaus <i>et al.</i> , 1993
Urate oxidase	Peroxisome	Reddy <i>et al.</i> , 1988

Table 1.1 Enzymes induced by peroxisome proliferators.

Enzyme	Cellular Localization	Reference
Epoxide hydrolase	Cytosolic	Schladt <i>et al.</i> , 1987

Table 1.1 Enzymes induced by peroxisome proliferators.

Section 1.1.6 Hyperplastic response to peroxisome Proliferators

Peroxisome proliferator-induced hepatomegaly is a consequence of both hypertrophic and hyperplastic response of the hepatocytes. Hypertrophy results from increase in cell size while hyperplastic response is due to an increase in the number of parenchymal cells. The mitogenic effect of PPs has been shown by the induction of DNA synthesis (Styles *et al.*, 1988; Roberts *et al.*, 1995; Marsman *et al.*, 1988). Measurement of DNA synthesis by bromodeoxyuridine incorporation shows that at high doses of MCP (25mg/kg) replicative DNA synthesis is induced to maximal between 20-30 hours after dosing (Styles *et al.*, 1988). Induction of DNA synthesis has been shown predominantly to be localized in the periportal region of the liver acini (Roberts *et al.*, 1995; Barrass *et al.*, 1993). Further, work by Styles and coworkers (1988) demonstrated that this induction in DNA synthesis is mainly confined to binucleated hepatocyte population. Their work also suggest that those responding binucleated hepatocytes undergo amitotic cytokinesis to form 4N cells following their stimulation to S-phase, since the proportion of 2x2N cells was reduced while the fraction of 4N cells was increased by MCP treatment.

The molecular nature of PP-induced liver growth is not well understood. Expression of a number of immediate early genes, such as the proto oncogenes *c-fos*, *c-myc* and *c-jun*, has been investigated during PP-induced augmentative liver growth. Work by Coni and coworkers (1993) and Hasmall and coworkers (1997) demonstrate that expression of proto-oncogenes *c-fos* and *c-myc* is not increased during PP treatment and therefore suggest that the molecular mechanism of PP-induced direct hyperplasia is different from compensatory hyperplasia induced by partial hepatectomy or CCl₄ (Goldsworthy *et al.*, 94; Coni *et al.*, 1993; Hasmall *et al.*, 1997).

Section 1.1.7 Chronic exposure to peroxisome proliferators

Sustained increase in peroxisome proliferation due to long-term administration of PPs results in the formation of hepatocellular carcinoma in rodents (Lake, 1995; Reedy and Lalwani, 1983). Many PPs have been found to be carcinogenic in rats and mice but their carcinogenic potential varies considerably between compounds. For example, potent PPs MCP and Wy-14,643 give 100% incidence of tumours in rat liver after 12 months of exposure whereas the weaker agent DEHP causes a lower incidence of tumour formation that requires high doses and even longer exposure periods (over 2 years) (Reedy *et al.*, 1982; Rao *et al.*, 1984; Cattley *et al.*, 1987; Kluwe *et al.*, 1982).

Section 1.1.8 Peroxisome proliferators are non-genotoxic carcinogens

Classical carcinogens such as aflatoxin are genotoxic mutagens, that is, their direct interaction with DNA results in DNA lesions (mutation), leading ultimately to tumour formation. Despite their carcinogenic effect in rodent bioassays, PPs have been shown to be non-mutagenic in the *Ames Salmonella* mutagenesis assay (Warren *et al.*, 1980; Reedy and Lalwani *et al.*, 1983; Bentley *et al.*, 1987). The genotoxic potential of PPs has been studied extensively using tests such as ³²P-post labelling assay for DNA adduct formation (Gupta *et al.*, 1985), unscheduled DNA synthesis (Cattley *et al.*, 1986), chromosomal aberrations (Nilsson *et al.*, 1991) and DNA repair assay (Butterworth *et al.*, 1989). Taken together, all of these of *in vitro* and *in vivo* genotoxic studies failed to identify PPs as direct mutagens, and PPs are therefore termed non-genotoxic carcinogens, PPs cause hepatocellular carcinoma without directly damaging the DNA (Ashby *et al.*, 1994). However, the mechanism by which PPs cause liver cancer is not well understood and multiple hypotheses have been put forward to explain PP-induced hepatocarcinogenesis. Each model is based upon a different aspect of the observed effects following dosing with PPs.

Section 1.1.9 The oxidative stress model

In the oxidative stress hypothesis, the indirect effects of PPs cause DNA damage and subsequent

carcinogenesis (Reddy and Lalwani, 1983). This hypothesis postulates that chronic administration of PPs produces sustained oxidative stress in rodent hepatocytes due to an imbalance in the production and degradation of H_2O_2 (Rao and Reddy, 1987 and 1991; Reedy and Rao, 1989). The differential induction of peroxisomal enzymes by PPs results in a marked increase in the β -oxidation enzymes, especially acyl-CoA oxidase. This increase in β -oxidation activity can potentially generate a large increase in the cellular level of hydrogen peroxide since the cyclic oxidation of a long chain fatty acid molecules results in the production of several molecules of H_2O_2 (Lazarow and De Duve, 1976; Lake, 1993; Reddy and Rao, 1989). This hypothesis further postulates that cellular defence mechanisms that normally detoxify H_2O_2 are perturbed in such a way as to allow a rise in cellular H_2O_2 levels. The excess H_2O_2 can diffuse out of the peroxisome and may react either directly or indirectly, via reactive oxygen species, to form DNA adducts. Catalase, a peroxidase, that normally neutralizes H_2O_2 produced during β -oxidation is only marginally induced by PPs, approximately two to three fold above control values (Nemali *et al.*, 1988). Rao and Reddy postulated that this induction would not be sufficient to rapidly metabolize additional hydrogen peroxide produced by the increased level of peroxisomal β -oxidation, and this would result in elevated intra-peroxisomal H_2O_2 levels over a sustained period. Thus the proposed increase in cellular H_2O_2 levels and the concurrent rise in reactive oxygen species like superoxide anion would lead to an increased incidence of DNA adduct formation and therefore an increased mutation rate. Further, PPs have been shown to reduce the expression of other enzymes involved in the removal of H_2O_2 , such as superoxide dismutase (Ciriolo *et al.*, 1982; Elliott and Elcombe, 1987), glutathione-S-transferase (Foliot *et al.*, 1986; Lake *et al.*, 1989; Furukawa *et al.*, 1985; Tamura *et al.*, 1990b) and glutathione peroxidase (Tamura *et al.*, 1990a and 1990b; Furukawa *et al.*, 1985).

To accept the oxidative stress hypothesis, evidence is required to demonstrate the transient increase in H_2O_2 level and its reactivity to DNA by PPs as they are central to the proposed hy-

pothesis. To substantiate/validate such a hypothesis, a number of experimental investigations had focused on the effect of PPs on the levels of β -oxidation, production of H_2O_2 and DNA adduct formation. PPs, in the presence of saturating substrate concentration, have been shown to cause a small increase in intracellular H_2O_2 (Lake, 1993) despite the high level of induction of acyl-CoA oxidase (Foerster *et al.*, 1981; Handler *et al.*, 1988).

One of the major adducts formed through oxidative damage is 8-hydro-2-deoxyguanosine (8-OHdG) (Clayson *et al.*, 1994). Treatment with a number of PPs has been reported to increase levels of 8-OHdG in rat hepatic DNA. However such increases are very small, between 0.5-2.5-fold (Kasai *et al.*, 1989; Takagi *et al.*, 1990 and 1991; Huang *et al.*, 1994; Catley and Glover, 1993). Most studies of 8-OHdG have utilized whole liver homogenates that contain both nuclear and mitochondrial DNA, thus making the interpretation of the result more difficult since mitochondrial DNA is 16-fold more susceptible to oxidative damage than nuclear DNA (Richter *et al.*, 1988). Sausen *et al.* (1995) found that 8-OHdG adducts in DNA isolated from whole liver homogenate increased up to 2-fold following treatment with Wy-14,643 and clofibric acid, but the increase was found to be due to an increase in background levels arising from a 3-fold increase in mitochondrial DNA levels. Cattley and Glover (1993) found that when isolated hepatic nuclei were examined, no increase in 8-OHdG levels was found for some PPs tested. Also, a few studies have examined the effects of PPs on other modified DNA bases and DNA strand breaks, and concluded that PPs have no significant effect on these parameters (Elliott and Elcombe, 1987; Tamara *et al.*, 1991). In summary, there is little evidence to support the idea that oxidative damage to nuclear DNA might be solely responsible for PP-induced hepatocarcinogenesis.

Section 1.1.10 Peroxisome proliferators as tumour promoting agents

Non-genotoxic carcinogens such as phenobarbitone, phorbol esters and dioxin are considered

to be tumour “promoters” rather than initiators. Since PPs do not produce positive results in initiation studies it is likely that they could also act as tumour promoters. Keeping in mind the multi-step nature of carcinogenesis, it is possible that promotion and progression of spontaneously initiated cells could be influenced by the action of PPs. To support this, PPs have been shown to induce hepatocyte cell replication which is clearly important in the promotion and progression of initiated cells into tumours (i.e. clonal expansion). Non-parenchymal liver cells do not undergo cell proliferation in response to PPs, and hepatocytes that are stimulated to DNA synthesis are mainly restricted to the periportal hepatocytes (James and Roberts, 1996, Prince *et al.*, 1992; Melchiorri *et al.*, 1993; Ohmura *et al.*, 1996; Styles *et al.*, 1988; Lake *et al.*, 1993; Lalwani *et al.*, 1997). In a number of cases, PPs have been shown to produce a burst of cell replication in rodent hepatocytes during the initial 2-7 day period of dosing, (Eldridge *et al.*, 1990; Styles *et al.*, 1988). In some, but not in all, studies PPs have caused a sustained stimulation of DNA synthesis (Marsman *et al.*, 1988; Eacho *et al.*, 1991; Chem *et al.*, 1994; Price *et al.*, 1992). The majority of these studies have employed the more sensitive continuous infusion (osmotic pump), rather than pulse-labelling techniques, to administer DNA precursor to measure DNA synthesis. Apart from intrinsic compound potency, dose is an important factor in determining whether a particular PP can produce either a transient or sustained stimulation of cell replication in rodent hepatocytes. Thus low doses of Wy-14,643, MCP and nafenopin do not produce a sustained stimulation of replicative DNA synthesis whereas higher doses do produce this effect (Price *et al.*, 1992; Lake *et al.*, 1993).

The ability of PPs to act as tumour promoters have been studied in chemically-initiated liver, and it was found that PPs are efficient promoters of certain genotoxic carcinogen-induced lesions (Cattley and Popp, 1989; Ward *et al.*, 1983, 84 and 86; Glauent and Clarke, 1989; Garney *et al.*, 1987). For example, DEHP has been reported to promote N-nitrosodiethylamine (DEN)

initiated focal hepatocellular proliferative lesions in mouse (Ward *et al.*, 1986), and co-administration of DEN and clofibrate in rats resulted in a significant increase in the number of hepatic tumours formed over rats given DEN alone (Mochizuki *et al.*, 1983). Further evidence to support the hypothesis that PPs act as tumour promoters of spontaneously initiated cells comes from age-related susceptibility to increased tumour incidence in rats and mice. There is a high incidence of pre-neoplastic lesion in the livers of untreated old rats and mice, and are thought to result from spontaneously initiated cells that accumulate during the life span of the animal. This suggests that PPs should be a better promoter of hepatocarcinogenesis in older animals. Indeed, nafenopin and Wy-14,643 produced more liver adenomas and carcinomas in older rats than younger rats (Cattley *et al.*, 1991; Kraupp-Grasl *et al.*, 1991).

In addition to cell replication and promotion of initiated cells, PPs have been shown to affect the apoptotic process of the liver that may play an important role in the promotion of PP-induced liver carcinogenesis. PPs were found to suppress both spontaneous and TGF β induced apoptosis in rat hepatocytes (Bayly *et al.*, 1993; Roberts *et al.*, 1995; James and Roberts, 1996) and in the FAO hepatoma cell line (Bayly *et al.*, 1993). It is thought that PPs induce liver cancer by inducing cell proliferation and at the same time suppressing apoptosis. Thus, DNA damaged cells that are normally removed by apoptosis are allowed to survive, and upon PP-induced mitogenic stimulation they may proliferate (clonal expansion) and accumulate further genetic changes that may ultimately lead to liver cancer.

Section 1.2 Cytochrome P450 mono-oxygenase system

The cytochrome P450 mixed function mono-oxygenase system is a collection of isoenzymes that act as terminal electron donors in many mono-oxygenation reactions. All proteins of this P450 superfamily are haemoproteins that possess an iron protoporphyrin IX as the prosthetic group and the monomer of the enzyme has a molecular weight of 52-60 kDa. A characteristic

of all cytochrome P450 proteins is that in the reduced state they bind carbon monoxide giving an absorption maximum at 450nm. To date over 500 cytochrome P450 genes have been sequenced from species as divergent as mammals and bacteria (Unger, 1986). Mammalian P450 enzymes are membrane-bound within the endoplasmic reticulum and are closely associated with NADPH cytochrome P450 reductase, another component of mixed function oxidase system.

A nomenclature system for naming the growing number of newly identified members of the P450 gene superfamily has been devised which is based on their protein sequence homology with other P450 enzymes (Nelson *et al.*, 1996). Cytochrome P450 genes are named with the italicized root symbol 'CYP' ('Cyp' for mouse and *Drosophila*). Gene families are designated by numbers and subfamilies are represented by letters followed by a number for the individual gene. For example, the rat CYP4A1 is the first member of the A subfamily which belongs to the fourth family of the cytochrome P450 super family. Generally, cytochrome P450 molecules are defined as being within the same family if there is a minimum of 40% amino acid identity between the two proteins. Proteins belonging to the same subfamily have >70% amino acid identity.

Biotransformation of a wide range of xenobiotics as well as many endogenous compounds are carried out by the P450 enzyme family. They are capable of carrying out diverse monooxygenase activities, the common aspect of all the oxidative reactions being the insertion of one atom of molecular oxygen into the substrate. Since most xenobiotics are highly lipophilic in nature the purpose of this phase I reaction is to introduce a functional group into the substrate, rendering it more water soluble. Thus, phase I biotransformation plays a crucial role in the disposal of toxic compounds (both endogenous and foreign) in the body. As well as playing an important role in the detoxification of many xenobiotics, P450 enzymes can activate a chemical to more

toxic metabolite as in the case of procarcinogen benzo[a]pyrene which is activated to a carcinogenic epoxide derivative. Normally phase II biotransformation convert reactive epoxides into more soluble derivatives such as diols (by hydration). However, the metabolic activation of procarcinogens to carcinogenic epoxides can arise when this second stage (phase II) is prevented by steric hindrance.

The catalytic cycle of the P450 enzyme is summarised in Figure 1.3. Substrate binding occurs in the vicinity of the haem region of the enzyme and takes place when the iron is in the oxidised, ferric state (Fe^{3+}). Substrate binds close to the haem region of the enzyme (step 1). By channeling an electron from NADPH via the NADPH-reductase, the iron atom is reduced from ferric to ferrous state (step 2). The reduced cytochrome P450-substrate complex then binds molecular O_2 and undergoes a rearrangement (step 3), after which a second electron is transferred from NADPH via P450-reductase to the complex (step 4). Finally the complex rearranges with insertion of one atom of oxygen into the substrate to yield the product (step 5 and 6) while the other

oxygen atom is reduced to water.

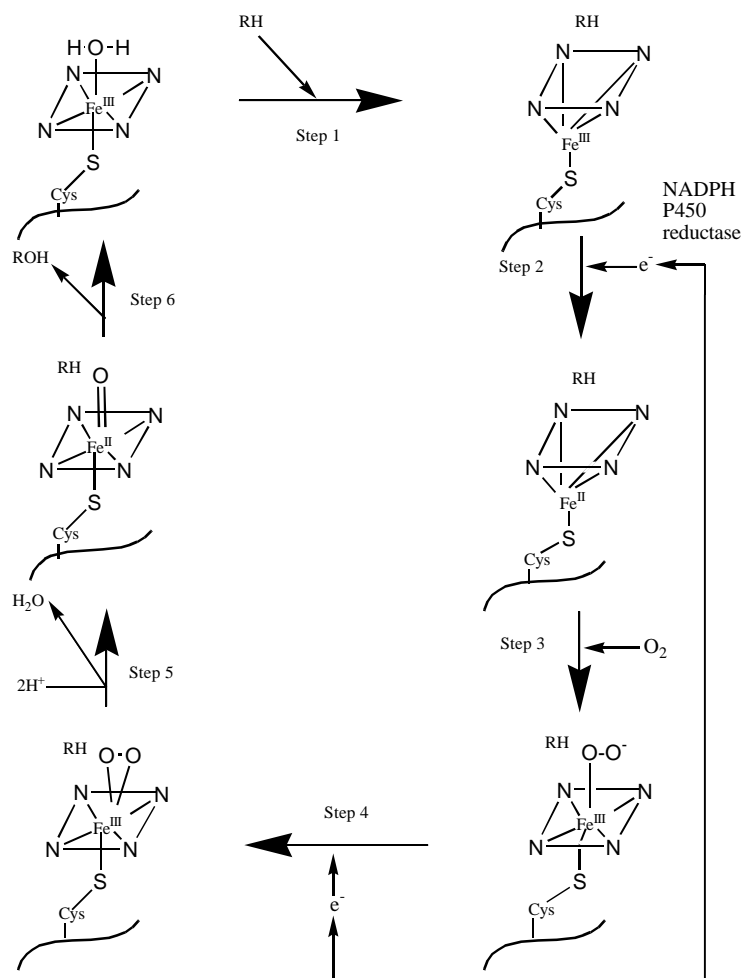


Figure 1.3 The catalytic cycle of cytochrome P450 mono-oxygenase. (modified from JA Timbrell, introduction to toxicology, second edition). The sequence of metabolic reactions during mono oxygenation of substrate (RH) is shown with particular emphasis on oxidation state of iron of the haem prosthetic group.

Section 1.2.1 Cytochrome P450 4A subfamily

Induction of P450 activities is a characteristic feature of a number of xenobiotics and has an important bearing on the elimination of toxic compounds from the circulation. Orton and Parker first demonstrated the induction of lauric acid ω -hydroxylase activity in the rat liver following the administration of clofibrate (Orton and Parker, 1982). Subsequent studies have purified a microsomal P450 with ω -hydroxylase activity from a number of different species, including rat liver (Tauburini *et al.*, 1984; Gibson *et al.*, 1982), rabbit intestine (Kaku *et al.*, 1984), rabbit lung (Willams *et al.*, 1984), human and rat kidney (Kawashima *et al.*, 1992). The CYP4 gene family

was first identified when rat CYP4A1 was cloned and sequenced, and as the predicted amino acid sequence was less than 36% identical to other P450 known at the time it was designated as the first member of the new 4A subfamily (Nebert *et al.*, 1987). Now it is generally accepted that CYP4A subfamily encodes several cytochrome P450 enzymes that are capable of hydroxylating the terminal ω -carbon and, to a lesser extent, the $\omega-1$ position of saturated and unsaturated fatty acids (Sharman *et al.*, 1989). The enzymes are also active in the ω -hydroxylation of various prostaglandins (Matsubara *et al.*, 1987; Yamamoto *et al.*, 1984). So far 15 isoenzymes have been identified as members of this subfamily from a number of species such as rat, mouse, human, guinea pig and rabbit (see table 1.2.). The genomic sizes of CYP4A subfamily genes are between 10 to 15kb long and produce mRNAs of around 1.5kb encoding 509 amino acids. Tissue distributions of P4504A vary and many of these genes are expressed at high levels in the liver and kidney while others are expressed in sex and tissue specific patterns.

P450 4A Gene	Species	cDNA/Genomic	Reference
CYP4A1	Rat	cDNA Genomic	Hardwick <i>et al.</i> , 1987 Kimura <i>et al.</i> , 1989
CYP4A2	Rat	Genomic	Kimura <i>et al.</i> , 1989
CYP4A3	Rat	cDNA	Kimura <i>et al.</i> , 1989
CYP4A4	Rabbit	cDNA Genomic	Matsubara <i>et al.</i> , 1987 Palmer <i>et al.</i> , 1993
CYP4A5	Rabbit	cDNA	Johnson <i>et al.</i> , 1990
CYP4A6	Rabbit	cDNA Genomic	Yokotani <i>et al.</i> , 1989 Muerhoff <i>et al.</i> , 1992
CYP4A7	Rabbit	cDNA	Yokotani <i>et al.</i> , 1989
CYP4A8	Rat	cDNA	Stromstedt <i>et al.</i> , 1990
CYP4A9	Human	cDNA	Kawashima <i>et al.</i> , 1994
<i>Cyp4a10</i>	Mouse	cDNA	Henderson <i>et al.</i> , 1990
CYP4A11	Human	cDNA	Palmer <i>et al.</i> , 1993
<i>Cyp4a12</i>	Mouse	cDNA	Bell <i>et al.</i> , 1993
CYP4A13	Guinea Pig	cDNA	Bell <i>et al.</i> , 1993
<i>Cyp4a14</i>	Mouse	Genomic	Heng <i>et al.</i> , 1997

Table 1.2 Members of the CYP4A subfamily identified in different species.

Section 1.2.2 Expression of CYP4A genes

Four members of the CYP4A family have been identified in rat, two of which are genomic clones (CYP4A1 and CYP4A2) while the other two are cDNA clones (CYP4A3 and CYP4A8). The CYP4A1 gene, the most extensively studied member of CYP4 family, is constitutively expressed in the rat liver and kidney. Exposure to PPs such as clofibrate results in a large induction of this gene, especially in the liver (Kimura *et al.*, 1989). Expression of CYP4A1 in the kidney was found to be in proximal convoluted tubule while in the liver constitutive and induced expression was localized mainly in the centrilobular region (Bell *et al.*, 1991). Expression of CYP4A2 was found to be regulated in a sex specific manner (Waxman *et al.*, 1991). In the male rat liver, constitutive expression of CYP4A2 occurs at a low level which is highly induced by clofibrate. In male kidney the gene is expressed constitutively at high levels which are slightly induced by treatment with PPs (Kimura *et al.*, 1989). CYP4A2 was also detected in male seminal vesicle, prostate, brain cortex, cerebellum and brainstem (Stromstedt *et al.*, 1994). Expression of CYP4A2, however, was not detectable in female liver and kidney (Sundseth and Waxman, 1992). This apparent sex specific expression is regulated by the different growth hormone profiles between the sexes (Waxman *et al.*, 1991). CYP4A3 was found to be expressed in liver and kidney, and is highly inducible by PPs (Kimura *et al.*, 1989). CYP4A3 was also detected in other extrahepatic tissues, very much similar to CYP4A2 expression. But unlike CYP4A2, it is not expressed in the seminal vesicle (Stromstedt *et al.*, 1994). CYP4A8 is expressed mainly in the prostate and kidney but also weak expression was detected in the retina (Stromstedt *et al.*, 1994 and 1990).

Mouse liver microsomes from both control and MCP treated animals exhibited ω -hydroxylase activity (Henderson *et al.*, 1990), and immunoblotting detected an immunoreactive band using an antibody generated against rat CYP4A1. Using a PCR cloning strategy, Bell *et al.* (1993) identified *Cyp4a* cDNAs (*Cyp4a10*-a homologue of rat CYP4A1) in the mouse liver. Full length

cDNA was later cloned by screening a mouse liver cDNA library using a full-length rat CYP4A1 cDNA probe (Henderson *et al.*, 1994). *Cyp4a10* was found to be highly induced by PPs at the transcriptional level in mouse liver and in kidney to a lesser extent (Bell *et al.*, 1993). Two other murine *Cyp4a* genes have also been identified that are expressed in the liver. These are *Cyp4a12* and *14* which are homologues of rat CYP4A8 and 2, respectively. *Cyp4a14* is highly inducible by PPs in both male and female mouse liver (Heng *et al.*, 1997). The *Cyp4a12* gene is expressed at high levels in the male liver and kidney and was not induced by treatment with MCP. However, there was a low level of expression of *Cyp4a12* mRNA in the female liver and kidney, which was greatly induced by treatment with MCP (Bell *et al.*, 1993).

Four CYP4A genes (CYP4A4, CYP4A5, CYP4A6 and CYP4A7) have been identified in rabbit and the genomic sequences of CYP4A4 and CYP4A6 are known. CYP4A6 is expressed at very low level in the liver and kidney, and was highly induced by clofibrate treatment (Yokotani *et al.*, 1989; Roman *et al.*, 1993). In contrast, CYP4A7 was expressed at high constitutive levels in the liver, kidney and small intestine, but its expression was enhanced only in the liver by clofibrate treatment (Yokotani *et al.*, 1989; Roman *et al.*, 1993). CYP4A5 was found to be expressed in liver and kidney and was slightly induced in the liver by clofibrate treatment (Roman *et al.*, 1993). CYP4A13 was isolated as a partial cDNA clone from guinea pig liver and was found to be non-inducible by PPs (Bell *et al.*, 1993). CYP4A11 was cloned from human (Palmer *et al.*, 1993b; Imaoka *et al.*, 1993). Expression of CYP4A11 was detected in a number of tissues including liver, kidney and lung among others (Palmer *et al.*, 1993).

Section 1.2.3 Role of CYP4A in fatty acid metabolism and renal function

Metabolism of arachidonic acid, a fatty acid derivative, results in a number of important biological mediators that are involved in the control of inflammation (inflammatory response). Leukotriene B₄ is one such mediator produced by lipooxygenase-dependent arachidonic acid

metabolism (Samuelsson, 1983). Since leukotriene B₄ is a potent chemotactic and chemoketic agent, biological inactivation of leukotriene B₄ is very important in the control of inflammation. CYP4A has been shown to play an important role in the metabolism of leukotriene B₄. Catabolism of leukotriene B₄ was found to be induced in primary hepatocytes from clofibrate treated rats, and studies on animal models shows that the duration of inflammatory response is prolonged in mice resistant to Cyp4a induction by PPs (Devchand *et al.*, 1996)

Arachidonic acid can also be metabolized by members of the CYP4A protein family to hydroxyicosatetraenoic acids (HETEs), epoxyicosatetraenoic acids (EETs) and dihydroxyicosatetraenoic acids (DHTs), all of which play important biological roles including platelet aggregation and renal functions (Fitzpatrick and Murphy, 1988). Inhibition of CYP4A activity by 17-octadecynoic acid, a suicide substrate of CYP4A enzymes, inhibited the formation of 20-HETE (a hydroxylated product of HETE) as well as EET and DHT (Zouel *et al.*, 1994 and 93). Microsomes from dog renal arteries were found to produce 20-HETE in response to infusion with arachidonic acid (Ma *et al.*, 1993). 20-HETE is shown to be a potent vasoconstrictor of renal arteries and the inhibition of its formation results in an increase in urine flow and sodium excretion, whereas renal blood flow and glomerular filtration rate were not significantly altered (Zou *et al.*, 1994).

Section 1.2.4 Role of CYP4A in peroxisome proliferation

Pathophysiological stimuli or drug-induced peroxisome proliferation are associated with high levels of induction of a number of enzymes, including CYP4A1 (Sharma *et al.*, 1988; Bell and Elcombe, 1991). Perturbation of hepatic lipid metabolism by PPs is thought to result in peroxisome proliferation and, although the mechanism of peroxisome proliferation is not clear, it is thought that the induction of CYP4A protein plays an important and mechanistic role in peroxisome proliferation (Lock *et al.*, 1989; Sharma *et al.*, 1988). Following the induction of

CYP4A1, other genes are induced, particularly those of the β -oxidation pathway (Bell and Elcombe, 1991). Production of long chain dicarboxylic acids by CYP4A1 (formed through ω -hydroxylation) has been implicated in peroxisome proliferation. Long chain dicarboxylic acids have been detected in hepatocyte culture due to the activity of high levels of CYP4A1 (Lock *et al.*, 1989; Sharma *et al.*, 1988; Aoyama *et al.*, 1990), and long chain dicarboxylic acids has been shown to induce peroxisomal β -oxidation enzymes (Kaikaus *et al.*, 1993). The coordinate induction of CYP4A1 and peroxisomal acyl-CoA oxidase was studied by Bell and co workers, which demonstrate that the induction of CYP4A1 mRNA precedes the induction of acyl-CoA oxidase gene (Bell *et al.*, 1991; Bell and Elcombe, 1991).

Use of primary hepatocyte culture also demonstrated that MCP mediated induction of CYP4A1 mRNA was unaffected by the presence of the protein synthesis inhibitor cyclohexamide, while the induction of acyl-CoA oxidase was ablated. This suggests that induction of acyl-CoA oxidase required the production of a protein, possibly CYP4A1 (Milton *et al.*, 1991). Further evidence was provided by work which found that the specific inactivator of CYP4A1, 10-undecynoic acid, inhibited clofibrate-mediated induction of acyl-CoA oxidase mRNA but not the induction of CYP4A1 mRNA in hepatocytes (Kaikaus *et al.*, 1993). Taken together, these studies indicate that the CYP4A1 ω -oxidation pathway, or even the CYP4A1 protein itself, plays an important part in the induction of β -oxidation by PPs. Generation of CYP4A knock-out mice will provide further insight into the role of CYP4A family members in peroxisome proliferation and most importantly their physiological role in maintaining tissue homeostasis.

Section 1.3 Cloning of a steroid receptor activated by PPs

The rapid and co-ordinate transcriptional induction of microsomal and peroxisomal genes by PPs has long suggested that PPs could act by a mechanism similar to that of steroid hormones. Initially, a rat liver protein termed peroxisome proliferator binding protein (PPBP), was identi-

fied in affinity studies using labelled nafenopin (Lalwani *et al.*, 1983 and 1987). Further work has characterized this PPBP as a member of heat shock protein family HSP70 and the possibility that this protein could act as receptor in mediating the effects of PPs was unlikely. A more refined search specifically aimed at identification of steroid receptors that could be activated by PPs has led to the discovery of a steroid receptor termed PPAR α (peroxisome proliferator activated receptor alpha) (Isseman and Green, 1990). PPAR α was isolated by screening a mouse liver cDNA library using a probe based on the consensus sequence of the DNA binding domain of several nuclear receptors. Full-length PPAR α cDNA was found to encode a 468 amino acid protein with predicted molecular weight of 52 kDa. Analysis of the amino acid sequence demonstrated that PPAR α belonged to the steroid hormone receptor superfamily since it had all the typical characteristics of steroid receptor (Evans *et al.*, 1988). The PPAR α amino acid sequence displayed high homology to the DNA binding region of nuclear steroid hormone receptors such as the glucocorticoid receptor, estrogen receptor, retinoid X receptor, vitamin D receptor, thyroid receptor and retinoic acid receptor. The ability of PPs to activate PPAR α was determined by using a chimeric receptor construct containing regions encoding the putative ligand binding domain of the identified PPAR α and the N-terminal sequence and DNA binding domain of human estrogen receptor (hER-PPAR α) (Isseman and Green, 1990). In the presence of PP, hER-PPAR α was able to transcriptionally activate the expression of a reporter gene under the transcriptional control of estrogen receptor. In this transient transactivation assay a number of structurally dissimilar PPs, such as nafenopin, MCP, clofibrate, Wy-14,643, MEHP and trichloroacetic acid, were shown to be activators of PPAR α .

Section 1.3.1 The steroid hormone receptor superfamily

The actions of many lipophilic hormones are mediated by a group of structurally similar intracellular receptors called steroid hormone receptors (SHRs). SHRs are defined as ligand dependent transcription factors that exert their regulatory function at the gene level. Their immense

importance as a regulators of vital processes such as development, cell differentiation and organ physiology has been indicated by the early death of mice mutant for some of these receptors as in the case of the glucocorticoid hormone receptor (Cole *et al.*, 1995). This group of nuclear receptors represents the largest known family of transcription factors in eukaryotes, and includes the estrogen receptor, glucocorticoid receptor, mineralocorticoid receptor, progesterone receptor, retinoid receptor, vitamin D receptor, thyroid receptor and peroxisome proliferator activated receptor (Mangelsdorf *et al.*, 1983; Evans *et al.*, 1988). Most of the orphan receptors with no apparent ligand also belong to this group. Sequence comparison and subsequent experimental analysis has identified a number of modular domains that are characteristic of the steroid receptor superfamily as shown in Figure 1.4.(Evans *et al.*, 1988).

The N-terminal A/B domain contains a constitutive ligand-independent transactivation function (AF-1). The DNA binding domain (DBD) or C domain is the most conserved region, which targets the receptor to specific DNA sequences known as response elements. The DBD also has a role in receptor-receptor heterodimerisation. Domain D (hinge domain) is concerned with conformational alteration of the protein and is believed to be involved in receptor interaction with coactivators and repressors (i.e. protein-protein interactions). Domain E is the ligand binding domain (LBD) which may also have transactivating functions (AF-2). This domain functions as a modular unit whose transcriptional activities are switched on by ligand binding and receptor dimerisation. No specific functions have yet been attributed to the small variable C-terminal F domain but it may have a role in protein-protein interactions.

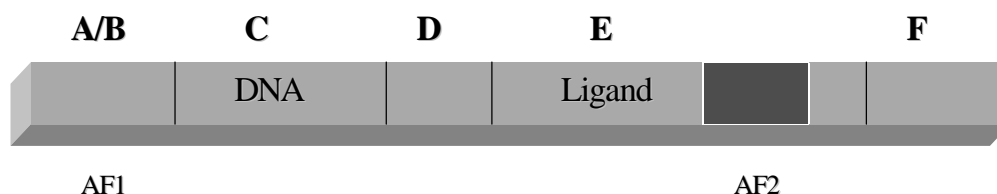


Figure 1.4 Functional domains of nuclear hormone receptors. DNA binding domain is shown by C (DNA) and ligand binding domain is shown by E (Ligand). AF1 and AF2 represents transactivation function 1 and 2 respectively.

Section 1.3.2 The PPAR family and tissue-specific expression

Soon after the initial description of mouse PPAR (later termed PPAR α), other groups demonstrated the existence of several types of PPAR in different species. So far, three different subtypes of PPAR have been identified termed α , β (also known as δ and FAAR) and γ from *Xenopus* (Krey *et al.*, 1993), mouse (Isseman and Green, 1990; Chen *et al.*, 1993; Kilewer *et al.*, 1994; Amni *et al.*, 1995), rat (Bocosc *et al.*, 1995; Xing *et al.*, 1995; Guardiola-Diaz *et al.*, 1999), human (Jow and Mukhergy, 1994; Green, 1995; Lamb and Tugwood, 1996; Elbrecht *et al.*, 1996), hamster (Aperlo *et al.*, 1995) and guinea pig (Bell *et al.*, 1998; Tugwood *et al.*, 1998) (see table 1.3). Two distinct isoforms of PPAR γ (PPAR γ 1 and PPAR γ 2) have been identified in mouse, rat and human. Both human and rat PPAR γ 1 and PPAR γ 2 are homologues of mouse PPAR γ 1 and PPAR γ 2, respectively, and have been shown to be the products of alternative promoter usage and differential splicing. Differential splicing is also observed for retinoid and thyroid hormone receptors and the relative expression of isoforms is important in the regulation of gene transcription.

PPAR isoform	Cloned from	Reference
mouse PPAR α	liver cDNA	Isseman & Green, 1990
<i>Xenopus</i> PPAR α	ovary cDNA	Dreyer <i>et al.</i> , 1992
rat PPAR α	liver cDNA	Gottlicher <i>et al.</i> , 1992

Table 1.3 Members of PPAR family identified from different species.

PPAR isoform	Cloned from	Reference
human PPAR α	liver cDNA	Dreyer <i>et al.</i> , 1993
guinea pig PPAR α	liver cDNA	Tugwood <i>et al.</i> , 1998
<i>Xenopus</i> PPAR β	ovary cDNA	Dreyer <i>et al.</i> , 1992
mouse PPAR β	brain cDNA	Chen <i>et al.</i> , 1993
human PPAR β	osteosarcoma	Schmidt <i>et al.</i> , 1992
<i>Xenopus</i> PPAR γ	liver cDNA	Dreyer <i>et al.</i> , 1992
mouse PPAR γ 1	liver cDNA	Zhu <i>et al.</i> , 1993
mouse PPAR γ 2	adipocyte cDNA	Kliwer <i>et al.</i> , 1994

Table 1.3 Members of PPAR family identified from different species.

Expression of the three PPAR subtypes was characterized in several tissues of rat and mouse (Braisant *et al.*, 1996; Jones *et al.*, 1995). Using specific probes for PPAR α , β and γ , Braisant *et al.* (1996) have localized the expression pattern of different PPARs in a number of rat tissues using *in situ* hybridisation. The highest level of expression of PPAR α was found in the liver, and a moderate to low level in kidney, stomach, brown adipose tissue, heart, small intestine and retina. PPAR β was expressed at a moderate level in a number of tissues including liver, kidney, heart, intestine and retina, except in the genital system where high level were observed. Compared to α and β subtypes, PPAR γ was expressed at very low levels in most tissues examined except in the white adipose tissue and the immune system where it was expressed at high levels. Jones *et al.* (1995) used a highly specific RNase protection assay to determine the expression pattern of three PPARs in mouse tissue. Their data demonstrate that PPAR α RNA is expressed at highest levels in the liver, with 20-fold lower levels of PPAR β and virtually negligible levels of PPAR γ . A moderate level of PPAR α expression was seen in kidney and brown adipose tissue and low levels elsewhere. PPAR β was expressed at moderate levels in liver, and low levels in other tissues. The highest level of expression of PPAR γ was found in adipose tissue and very low levels in other tissues. PPAR γ expression has also been examined by other groups in rat, mouse, hamster and human, and these studies found that PPAR γ mRNA expression was highest

in adipose tissue (Kliwer *et al.*, 1994; Tontonoz *et al.*, 1994a and 1994b, Aperlo *et al.*, 1995; Elbrecht *et al.*, 1996; Mukherjee *et al.*, 1997). Tissue-specific expression of PPARs, especially of PPAR α and γ , suggests that they have different physiological roles. The high level of expression of PPAR γ in adipose tissue suggests that this receptor plays an important role in lipid metabolism in this tissue, and recently PPAR γ has been linked with adipogenesis as over expression of PPAR γ converts pre-adipocytes into adipocytes. The high expression of PPAR α in the liver correlates well with the fact that PPs have their greatest effect in the liver; its expression in other tissues indicates that it may have important physiological functions, possibly in lipid homeostasis.

Section 1.3.3 Regulation of PPAR α gene expression

It was originally thought that as well as activating PPAR α itself, PPs could also induce the expression of their receptor PPAR α . A number of studies were carried out in rat to characterize the regulation of the PPAR α gene by PPs in cultured hepatocytes and cell lines as well as *in vivo* tumour and non-tumour liver tissues. Miller *et al.* (1996) found that long-term administration of Wy-14,643 resulted in significant induction of PPAR α mRNA in both tumour and non-tumour lesions of the rat liver, and the induction of PPAR α mRNA was slightly increased in tumour lesions as compared to the surrounding non-lesion liver tissue. However they used a mouse PPAR α probe to determine the expression of rat PPAR α in Northern blot analysis. Also in their study, the expression of albumin mRNA as an internal control was reduced in Wy-14,643 treated samples. McNae *et al.* (1994) found that clofibrate and perfluorodecanoic acid (PFDA) induced PPAR α mRNA expression, but other PPs examined in these study had no effect on PPAR α expression. Using an antibody raised against mouse PPAR α , Gebel *et al.* (1992) detected an immunoreactive protein of 52 kDa in the nuclear extracts of rats treated with fenofibrate but not in control animals. They also reported the induction of a 6kb mRNA species in fenofibrate-treated rat liver in Northern analysis using a probe derived from mPPAR α . Other

studies have found a small induction in primary hepatocytes and cell lines (Yamada *et al.*, 1995; Sterchele *et al.*, 1996). Although these studies shows that rat PPAR α is inducible by PPs, other studies conclude that PPs have no effect on the expression of PPAR α mRNA (Sterchele *et al.* 1995; Schoonjan *et al.*, 1996; Jones *et al.*, 1995). For example, Sterchele *et al.* (1995) found that in rat liver, PPAR α mRNA accumulated after treatment with PFDA. However, this accumulation in PFDA-treated rats appeared to be due primarily to hypophagia as pair-feeding control and complete caloric restriction result in a large increase in the concentration of this PPAR α mRNA in the absence of PP treatment. *In vivo* studies where the induction of PPAR α mRNA was reported did not include a pair-fed control group, and therefore the induction observed by these groups is likely to be due to a stress based induction mechanism, possibly arising from the dose of the PP used. Using the highly sensitive and specific RNase protection assay Jones *et al.* (1995) demonstrated that PPAR α mRNA expression was unaffected in the mouse liver treated with the potent peroxisome proliferator MCP. Recently it has been reported that rat PPAR α mRNA levels are modulated in brown adipose tissue during peroxisome proliferation induced by cold acclimatization. Here, PPAR α mRNA was found to decrease markedly after 5-hour of cold exposure and was almost undetectable after one day in the cold (Guardiola-Diaz *et al.*, 1999). However, the PPAR α mRNA level increased gradually to normal by four weeks of cold exposure of the rat.

The involvement of glucocorticoid hormones in lipid metabolism and in energy mobilization in stress has been recognized. Since PPAR α is involved in the direct regulation of genes involved in fatty acid oxidation, a number of studies have examined the regulation of PPAR α genes by glucocorticoid hormones. Dexamethasone, a synthetic glucocorticoid hormone, was found to stimulate the expression of PPAR α mRNA up to 15 times over control in primary rat hepatocytes and to a lesser degree in a hepatoma cell line (6-fold) (Steineger *et al.*, 1994). In the same

study insulin was found to inhibit the induction of PPAR α mRNA. Lamberger *et al.* (1994) also found that synthetic glucocorticoid analogue (dexamethasone and hydrocortisone) could induce the rat PPAR α gene in primary hepatocyte cultures, and hydrocortisone was also shown to induce the expression of PPAR α at the protein level in rat hepatocytes (Plant *et al.*, 1998). Glucocorticoids induced PPAR α mRNA in a dose dependent manner and this was inhibited by glucocorticoid antagonists. PPAR α is also stimulated by stress and follows a diurnal rhythm, but the pattern is somewhat different from glucocorticoid and its receptor (Lamberger *et al.*, 1996). The peak release of glucocorticoid hormone occurs at the light/dark switch and the peak expression of glucocorticoid receptor occurs around midnight (between 11 pm to 2 am). The peak expression of glucocorticoid receptor is out of synchronization with the circadian rhythm of PPAR α which has been found to peak in the late afternoon (between 5 to 6 pm) (Lamberger *et al.*, 1996). If glucocorticoid receptors regulate PPAR α gene expression then one would expect synchrony between the expression of glucocorticoid receptor and the expression of PPAR α . The expression of PPAR α gene in mice was unaffected by testosterone treatment (Jones *et al.*, 1995).

Section 1.3.4 PPAR α activators and ligands

Originally PPAR α , and indeed other subtypes, were isolated as orphan receptors with no known natural or synthetic ligands (Isseman and Green, 1990). Peroxisome proliferators (synthetic and endogenous fatty acids) were shown to be PPAR α activators, that is the ability of these chemicals to convert PPAR α into a transcriptionally active complex could be demonstrated in reporter gene assays, and therefore in that sense PPs are not true ligands. Although PPs were thought to be PPAR α ligands, evidence for direct interaction was lacking. Recently, using a high affinity radiolabelled ligand, thiazolidinedione (a synthetic anti-diabetic drug), a natural ligand for PPAR γ was identified, called prostaglandin J₂ (Kliwer *et al.*, 1997). In the past, using this classical ligand-binding approach, the identification of *bona fide* PPAR α ligands has been hindered

by the unavailability of a comparable, high-affinity PPAR α radioligand which does not produce unacceptable levels of non-specific binding. Recently a high affinity fibrate ligands GW2331 ($K_d = 140$ nM) for PPAR α has been identified. Using GW2331 radioligand in a competition binding assay Kliewer *et al.* (1997) has demonstrated that certain mono and polyunsaturated fatty acids (palmitic acid, oleic acid, petroselenic acid, linolenic acid, linoleic acid, arachidonic acid and hydroxy eicosatetraenoic acid) are ligands for PPAR α . Forman *et al* 1997 used a ligand-induced conformational change to identify PPAR α ligands indirectly. They have utilized the electrophoretic mobility shift assay to determine the enhanced binding of PPAR α -RXR α heterodimers (present at low levels) to a PPRE (peroxisome proliferator response element) induced by various PPs. This and number of other studies have demonstrated that certain fatty acids and their derivatives, hypolipidaemic drugs and leukotriene B₄ are ligands for PPAR α (Krey *et al.*, 1997; Dowell *et al.*, 1997; Devchand *et al.*, 1996). The most potent PPAR α ligands identified so far are 8-HETE ($IC_{50} = 500$ nM) and leukotriene B₄ ($K_d = 90$ nM) that bind to PPAR α in the nanomolar range.

Section 1.3.5 Peroxisome proliferator response elements (PPREs)

Steroid receptors are transcription factors and therefore modulate transcription of responsive genes by directly interacting with DNA sequences in the regulatory region found upstream of the gene promoter. This protein-DNA interaction, occurs through the DNA-binding domain (DBD) of the receptor, and is important in the differential regulation of genes whose promoter regions contain sequence specific motifs for receptor binding in addition to a TATA-box for the binding of basal transcription machinery. PPAR α , being a transcription factor, is thought to regulate transcription of a number of genes involved in both peroxisome proliferation and the β -oxidation of fatty acids by binding to specific DNA regulatory elements located in the upstream promoter region of these genes (Figure 1.5). Investigation of transcriptional regulation at the upstream promoter region of a rat acyl-CoA oxidase gene identified the first response element for

PPAR α , termed peroxisome proliferator response element (PPRE) (Osumi *et al.*, 1991; Tugwood, 1992; Green, 1992). The Upstream promoter region of a rat acyl-CoA oxidase gene was cloned in front of a β -globin promoter and linked to a CAT reporter gene. The putative response element-reporter gene construct was co-transfected in a mouse hepatoma cell line with an expression plasmid for mouse PPAR α . Expression of the reporter gene was higher in the presence of PPs while the stimulation of the reporter gene was comparatively low in the absence of PPAR α or PP. Through sequential deletion analysis, a small region of the response element was localized as the minimal PPRE. PPREs have also been identified in a number of other PP-responsive gene such as rabbit CYP4A6 (Muerhoff *et al.*, 1992), rat CYP4A1 (Aldridge *et al.*, 1995), rat HMG-CoA synthase (Rodriguez *et al.*, 1994), human fatty acyl-CoA oxidase (see table 1.4). PPREs consists of a tandem direct repeat of two hexameric nucleotide motifs (half-sites) spaced by a single nucleotide, termed direct repeat1 (DR1) (Tugwood *et al.*, 1992). Examination of rat bifunctional enzyme, human apolipoprotein A-I and rat acyl-CoA synthetase PPREs revealed a third half-site either two nucleotides 5' or three nucleotides 3' to the PPRE. However, the influence of these half sites on the functioning of the PPRE remains to be elucidated.

Gene	Minimal PPRE sequence	Reference
Rat CYP4A1	TCCCCT C TGACCT	Aldridge <i>et al.</i> , 1995
Rabbit CYP4A6 (z-element)	TCAACT T TGCCCT	Muerhoff <i>et al.</i> , 1992
Rabbit CYP4A6	TGACCC T TGCCCA	Palmer <i>et al.</i> , 1994
Rat acyl-CoA oxidase	TGACCT T TGTCCT	Tugwood <i>et al.</i> , 1992
Human fatty acyl-CoA	AGGTCA G CTGTCA	Varanasi <i>et al.</i> , 1996
Rat bifunctional enzyme	TGAACT A TTACCT	Zang <i>et al.</i> , 1992
Rat acyl-CoA synthase	TGACTG A TGCCCT	Schoonjans <i>et al.</i> , 1995
Rat malic enzyme	GGACCT G TGCCCT	Castelein <i>et al.</i> , 1994
Rat fatty acid binding protein	TGACCT A TGGCCT	Issemann <i>et al.</i> , 1992

Table 1.4 PPRE sequences in peroxisome proliferator responsive genes. Sequences of functional PPRE identified in the promoter region of peroxisome proliferator responsive genes. Minimal PPRE sequence are shown that are determined to be functional in reporter assay.

Gene	Minimal PPRE sequence	Reference
Rat acyl CoA binding protein	TCACCT T TGCACT	Elholm <i>et al.</i> , 1996
HMG-CoA synthase	AGACCT T TGGCCC	Rodriguez <i>et al.</i> , 1994
Human apolipoprotein A-I	TGACCC C TGCCCT	Vu-Dac <i>et al.</i> , 1994
Human apolipoprotein C-III	TGACCT T TGCCCA	Hertz <i>et al.</i> , 1995
Rat apolipoprotein C-III	TGACCT T TGACCA	Hertz <i>et al.</i> , 1995
Human lipoprotein lipase	TGCCCT T TCCCCC	Schoonjans <i>et al.</i> , 1996

Table 1.4 PPRE sequences in peroxisome proliferator responsive genes. Sequences of functional PPRE identified in the promoter region of peroxisome proliferator responsive genes. Minimal PPRE sequence are shown that are determined to be functional in reporter assay.

This DR-1 element was found to be optimal for PPAR binding and transactivation (Isseman *et al.*, 1993), since separation of half-sites by 0 or 2 nucleotides produce a weak response and no response at all when the spacing is greater than or equal to 3 nucleotides. Table 1.4 lists some of the genes regulated by identified PPREs and their sequences. As can be seen from table 1.4, the sequence specificity of each PPRE is not strict and the sequence of the PPRE can deviate from the consensus sequence by as many as 5 nucleotides but mutations of one or two nucleotide within a particular PPRE can diminish or completely abolish its PP responsiveness (Isseman *et al.*, 1993; Du-Dac *et al.*, 1994; Palmer *et al.*, 1994; Chen *et al.*, 1995).

Section 1.3.6 PPAR α -RXR α heterodimer binds to PPRE

Retinoid X receptor α (RXR α), a promiscuous binding partner for many steroid hormone receptors, has been shown to be the preferential binding partner for PPAR α receptor (Isseman *et al.*, 1993; Baudet *et al.*, 1993; Greig *et al.*, 1993; Keller *et al.*, 1992 and 1993). In electromobility shift assays, binding of PPAR α to its cognate PPRE has been found to occur only in the presence of its heterodimeric partner RXR α . A detailed study of the binding of PPAR α -RXR α heterodimer to rabbit CYP4A6 PPRE has been carried out. Two distinct elements, termed Z and X, have been identified as functional elements in the promoter region of the gene (Muerhoff *et al.*, 1992). The Z element was found to mediate the major portion of the response to PPs by CYP4A6 reporter construct in reporter assay, binding PPAR α -RXR α much more efficiently

than the other CYP4A6 PPRE. However, further work demonstrated that the typical PPRE motifs may not be sufficient to ensure a peroxisome proliferative response (Palmer *et al.*, 1994). Deletions within 6 nucleotides 5' of the DR-1 dramatically diminished PPAR α -RXR α binding but not the RXR α -RXR α homodimer binding. This and a number of other study clearly demonstrate the importance of 5' flanking sequence of the DR-1 in influencing the binding of PPAR α -RXR α heterodimers in preference to competitors like RXR α homodimers (Colling *et al.*, 1995; Osada *et al.*, 1997; Ijpenberg *et al.*, 1997).

Section 1.3.7 Regulation of PPAR α -induced transactivation by receptor cross-talk

Transcriptional modulation of PP-responsive genes occurs through the heterodimerisation of the PPAR α with the 9-cis retinoic acid receptor, RXR α , and subsequent binding to the DNA response element PPRE (Figure 1.5). Recently a number of proteins/receptors have been identified that are shown to influence this signalling pathway in a reconstituted system (*in vitro* studies). This “cross-talk” between PPAR and other cellular proteins (mainly steroid receptors) may occur by competition for binding to the PPRE or for the heterodimeric partner RXR α or even PPAR α itself. In the case of receptors competing for binding to either PPAR α or RXR α , the concentration of the competing receptor will be crucial in deciding how the signalling pathway is influenced. An excess of a low competing receptor may titrate out available PPAR α or RXR α , thus preventing the PPAR α -RXR α heterodimer from forming. In an artificial system excess hPPAR β has been shown to repress PP signalling by competing with hPPAR α for RXR α , thus forming hPPAR β -RXR α on a PPRE by displacing PPAR α (Jow and Mukherjee, 1995).

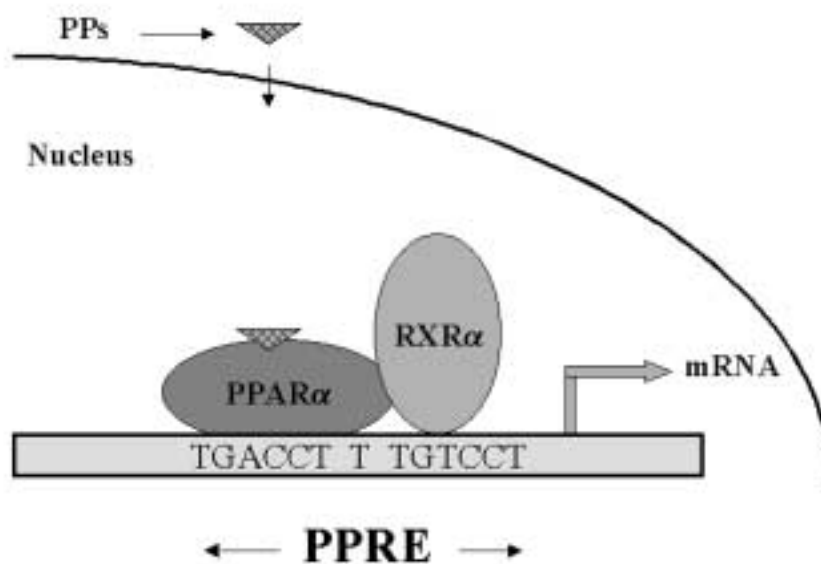


Figure 1.5 Cartoon of PPAR α and its heterodimerization partner, RXR α , on a PPRE.

Cross-talk between the orphan receptor RZR α (retinoid Z receptor) and PPAR α in the regulation of the peroxisomal hydratase-dehydrogenase (HD) gene has been reported by Winrow *et al.* (1998). RZR α has been shown to modulate PPAR α -RXR α dependent transactivation in a response-element dependent manner. Electrophoretic mobility shift analysis showed that RZR α bound specifically as a monomer to the HD-PPRE and did not form complexes with PPAR α or RXR α on the HD-PPRE. Further, RZR α stimulated ligand-mediated transactivation by PPAR α from an HD-PPRE luciferase reporter gene. RZR α , however, did not bind to the PPRE from an acyl-CoA oxidase (ACO) gene and had no effect on the PPAR α dependent transactivation of an ACO-PPRE reporter gene. This cooperation between RZR α and PPAR α in the regulation of the expression of the HD-gene, the second enzyme in the peroxisomal β -oxidation pathway, suggests that there are additional factors which may govern the peroxisomal β -oxidation.

Another nuclear orphan receptor TAK1/TR4 has been found to repress the PPAR α signalling pathway. TAK1 was able to bind rat HD-PPRE and ACO-PPRE (Yan *et al.*, 1998). Therefore

TAK1 represses PPAR α mediated transactivation by directly competing for binding to the PPRE. Two-hybrid analysis showed that TAK1 does not form heterodimers with either PPAR α or RXR α , indicating that this repression does not involve a mechanism by which TAK1 titrates out PPAR α or RXR α from PPAR α -RXR α complexes. Further, TAK1 has been shown to compete with PPAR α for RIP140 (a coactivator protein, see later) binding. These observations indicate that the antagonistic effects of TAK1 on PPAR α -RXR α transactivation can take place at least at two levels in the PPAR α signalling pathway by competing with PPAR α -RXR α for binding to PPRE as well as to common coactivators such as RIP140.

A significant level of cross-talk exists between the PP and thyroid hormone signalling pathways. In rodents PPs and thyroid hormones often regulate the same target genes, and some of these genes have been shown to carry both thyroid response elements and PPREs (Hertz *et al.*, 1996; Castelein *et al.*, 1994). Cross-talk between PPAR and thyroid receptor (TR) may occur by competition for binding to DNA (Miyamoto *et al.*, 1997; Hunter *et al.*, 1996) or for the common heterodimeric partner RXR α (Juge-Aubry *et al.*, 1995; Chu *et al.*, 1995; Ren *et al.*, 1996; Hunter *et al.*, 1996) or by formation of PPAR-TR heterodimers (Bogazzi *et al.*, 1994). TR and TR-RXR α binding to a PPRE has been observed, and high levels of TR could repress PPAR α -RXR α mediated signalling (Miyamoto *et al.*, 1997). This inhibitory action of TR was due to competition for DNA binding since a mutation in the DNA binding domain of TR abolishes its ability to repress PPAR α -RXR α signalling. Thus binding of the RXR α -TR heterodimer to a PPRE results in repression of PPAR α -RXR α mediated signalling. By binding to TR α or β isoform, PPAR α can also cross-talk with thyroid hormone signalling in either a positive or negative manner depending on the nature of response element (DR-2/4) (Bogazzi *et al.*, 1994).

Potential cross-talk between JAK-STAT (Janus Kinase-Signal Transducer and Activator of Transcription) and PPAR α has been described by Zhou and Waxman (1999). Inhibition of clof-

ibrate-induced peroxisomal β -oxidation by growth hormone (GH) has been described in rats (Yamada *et al.*, 1994; Sato *et al.*, 1995). This inhibition is thought to occur following binding of the GH to its membrane-bound receptor, leading to receptor dimerisation. This activity eventually leads to the activation of a cytoplasmic transcription factor STAT through JAK2 kinase mediated phosphorylation. GH inhibition of PPAR α activity was dependent upon the presence of active STAT5b and GH receptor. Since STAT5b was unable to bind HD-PPRE, the inhibitory effect of GH may be due to competition for an essential PPAR α coactivator or synthesis of a more proximal PPAR α inhibitor.

HNF4 and COUP-TF can also bind PPRES (Winrow *et al.*, 1994) and thus are likely to repress PPAR action by competing for PPRE. Fatty acyl thioester receptor HNF4 are involved in the transcriptional regulation of hepatic genes (Hertz *et al.*, 1998), and since fatty acids can activate PPAR α to regulate the expression of a number of liver genes, it is likely that cross-talk between HNF4 and PPAR α may occur. COUP-TF II is another steroid hormone receptor shown to repress PP-induced gene expression by competing with PPAR α -RXR α for PPRE binding (Miyata *et al.*, 199; Baes *et al.*, 1995; Marcus *et al.*, 1996). PPAR α -RXR α heterodimers have been shown to bind estrogen receptor response elements (ERE) and upregulate gene expression of a reporter gene under the control of the vitellogenin-A-ERE (Nunez *et al.*, 1997). The orphan nuclear receptor LXR α can cross-talk with PPAR α signalling as it binds either PPAR α or RXR α in solution but not as a heterodimer bound to a PPRE. The expression of LXR α in mammalian cells blocked PP signalling mediated by PPAR α -RXR α heterodimers (Miyata *et al.*, 1996).

Insulin and the PPAR γ ligand, TZD, act synergistically to increase the expression of an adipose-specific gene aP-2 (Zang *et al.*, 1996) in transfection study. Transfection with a dominant negative MAP-kinase kinase mutation resulted in a decrease in the effects of both insulin and TZD on PPAR γ activity, indicating that mitogen activated protein kinase is involved in the cross-talk

between PPAR and insulin. Mutational studies on potential MAP-kinase phosphorylation sites in PPAR γ resulted in the repression of EGF stimulated MAP-kinase dependent transcription (Camp and Tautri, 1997). Immunoprecipitation of endogenous PPAR α from rat adipocytes pre-labelled with [32 P]-orthophosphate and treated with phosphatase inhibitors (vanadate and okadaic acid) demonstrated that PPAR α is a phosphoprotein. Insulin, in the presence of phosphatase inhibitor, resulted in an increased level of PPAR α phosphorylation (Shalev *et al.*, 1996), suggesting that the insulin dependent MAP-kinase pathway may be in operation. However, the involvement of MAP-kinase dependent phosphorylation has not been established yet. These *in vitro* studies indicate the potential for cross-talk between steroid hormone receptors and the PPAR α signalling pathway but the significance of which, if any, of these pathways are important in the modulation of PPAR α functioning *in vivo* remains to be elucidated.

Section 1.3.8 Coactivator proteins in steroid hormone receptor function

Ligand-dependent transcription requires a highly conserved motif termed activating function-2 (AF-2), located at the C-terminus of the ligand binding domain (LBD) (Evans *et al.*, 1988). The crystal structure of the LBD of a number of steroid receptors, including PPAR γ , has been solved (Bourguet *et al.*, 1995; Brzozowski *et al.*, 1997; Renaud *et al.*, 1995; Wagner *et al.*, 1995; Nolte *et al.*, 1998). There is evidence that nuclear receptors require the ligand dependent recruitment of coactivator proteins to effectively stimulate gene transcription which is dependent on allosteric alterations in the AF-2 helical domain (Horwitz *et al.*, 1996), and this AF-2 domain is required for effective interactions with coactivators (Baretino *et al.*, 1994; Danielian *et al.*, 1992). Transcriptional regulation of nuclear hormone receptors involves the participation of basal transcription factors, including TATA-binding protein and TF-IIB. Other cofactors known as nuclear transcription coactivators and corepressors are also required that bridge the association between nuclear receptors and the basal transcription machinery (Janknecht and Hunter, 1996; Kamei *et al.*, 1996). The coactivators identified in recent years include CBP/p300 (Arany *et al.*,

1994; Chrivia *et al.*, 1993), SRC-1 (Onate *et al.*, 1995; Cavilles *et al.*, 1994), PBP (Zhu *et al.*, 1997) and RIP140 (Cavilles *et al.*, 1995) among others. Sequence and functional analysis of a number of coactivators has identified a signature motif LXXLL (where L is leucine and X is any amino acid) which is necessary and sufficient for the binding of coactivators to nuclear receptors (Heery *et al.*, 1997). Ternary complex containing the PPAR γ LBD, rosiglitazone (a PPAR γ ligand) and part of SRC-1 containing LXXLL reveal that glutamate and lysine residues that are highly conserved in the LBD of nuclear receptors form a charge clamp that contacts backbone atoms of the LXXLL helices of SRC-1. Screening a mouse liver cDNA library using PPAR γ LBD as bait in a yeast two-hybrid system, PBP and SRC-1 were identified as interacting proteins (Zhu *et al.*, 1996 and 97). SRC-1 and PBP have been shown to bind PPAR γ in a ligand dependent manner, and increased ligand-induced reporter activity of PPAR γ (Direzo *et al.*, 1997; Krey *et al.*, 1997). As well as interacting with PPAR γ , both SRC-1 and PBP also interact with PPAR α and increase PPAR α dependent transcriptional activity *in vitro*. Recently a cold-inducible coactivator protein PGC-1 has been identified from a brown fat cDNA library which interacts specifically with PPAR γ and a number of other nuclear receptors (Puigserver *et al.*, 1998). Interaction of PGC-1 greatly increases the transcriptional activity of PPAR γ but its influence on PPAR α transcriptional activity has not been established. A number of other coactivators such as CBP/p300 and RIP140 have been shown to interact with PPAR α . However, so far no specific coactivator for PPAR α or indeed for other steroid receptors has been assigned, and many of these coactivators interact with a number of steroid receptors. Although SRC-1 was identified as a PPAR interacting protein, its true physiological role still remains to be determined since knock-out studies demonstrated that mouse SRC-1 is not essential for PPAR α regulated gene expression and peroxisome proliferation (Qui *et al.*, 1999).

Section 1.3.9 Functional loss of PPAR α and its implications

The observations that PPAR α is activated by PPs and that PPAR α causes transcriptional induc-

tion of PPRE-containing reporter genes suggest that the pleiotropic effects of PPs are mediated by PPAR α . Direct evidence for the role of PPAR α in peroxisome proliferation is provided by the generation of PPAR α null mice by targeted disruption of the LBD of mPPAR α (Lee *et al.*, 1995). Mutant mice lacking functional PPAR α protein are viable and fertile, suggesting that it is not important for development, but are resistant to peroxisome proliferation and hepatocarcinogenesis induced by PPs. In knock-out mice, treatment with Wy-14,643 or clofibrate failed to cause induction of PP responsive genes such as acyl-CoA oxidase, bifunctional enzyme, cytochrome P4504A family and fatty acid binding protein. Studies using PPAR α knock-out mice showed alterations in fatty acid and lipoprotein metabolism, and accumulation of lipid droplets in the liver treated with PPs. This perturbation of lipid metabolism suggest that PPAR α is essential in maintaining the homeostasis of hepatic lipid metabolism (Aoyama *et al.*, 1998; Peters *et al.*, 1997; Leone *et al.*, 1999). Regulation of genes (e.g. CYP4A) by PPAR α involved in the metabolism of arachidonic acid and other inflammatory mediators has long suggested that PPAR α may be involved in the control of inflammation. This evidence is further supported by studies using PPAR α null mice which demonstrate that PPAR α is required for endotoxin-induced renal expression of the *Cyp4a* gene, and endotoxin-induced inflammation is prolonged in knock-out mice (Devchand *et al.*, 1996; Barclay *et al.*, 1999). Further studies using PPAR α knock-out mice will improve our understanding of the molecular mechanism of peroxisome proliferation and hepatocellular carcinogenesis induced by PPs.

Section 1.4 Species differences in peroxisome proliferation

Widespread use of PPs in the form of hypolipidaemic drugs and industrial and agrochemical agents means that humans are constantly exposed to the peroxisome proliferating chemicals. From a toxicological point of view, this human exposure and the fact that PPs are hepatocarcinogens in rodents has prompted much research in an effort to understand the underlying molecular mechanism of species differences in peroxisome proliferation. Since human

experimentation is not possible, a greater understanding of these species differences and similarities in peroxisome proliferation is required so that animal data could be extrapolated to humans for risk assessment.

Section 1.4.1 Peroxisome proliferation in responsive species

It is now well established that marked differences exist in species responses to PPs. All *in vitro* and *in vivo* studies have found that rats and mice are highly responsive to PPs. In the liver of these animals, PPs have been shown to cause high levels of induction of specific microsomal and peroxisomal enzyme activities, peroxisome proliferation, induction of DNA synthesis and a high incidence of hepatocellular carcinoma. These effects have been reproduced in primary hepatocytes of rats and mice. Treatment of hamster with MCP and Wy-14,643 caused hypolipidaemia as well as hepatomegaly (Choudhury *et al.*, 2000). Increases in liver weight have also been observed after dosing with other PPs such as DEHP, clofibrate and nafenopin (Lake *et al.*, 1986; 1989a and 1993). This increase in liver weight was associated with proliferation of peroxisomes but a concomitant reduction in their size (Gray *et al.*, 1984). There was a small but significant increase in peroxisomal β -oxidation, lauric acid ω -hydroxylation and a number of other enzymic activities that are typically induced in rats and mice by PPs (Lake *et al.*, 1986 and 1989a; Lhughermot *et al.*, 1988; Sakuma *et al.*, 1992). However, these observed effects are much smaller compared to those observed in rats. Nafenopin has been shown to suppress both spontaneous and TGF β induced apoptosis in primary hepatocytes isolated from hamster (James and Roberts *et al.*, 1996). There is conflicting evidence as to whether PPs can induce replicative DNA synthesis in hamster, since some studies have observed no increase in DNA synthesis (Price *et al.*, 1992; Lake *et al.*, 1993; James and Roberts, 1996) while others found a small induction using high doses of PPs (Styles *et al.*, 1988). Although this limited response to PPs has been observed, long-term administration of PPs did not result in liver cancer in hamsters (Tucker and Ortan, 1995; Schmezer *et al.*, 1988; Lake *et al.*, 1993 and 1995). Thus, from comparative

studies hamster is regarded as partially-responsive to peroxisome proliferation and “non-responsive” to PP-induced hepatocarcinogenesis.

Section 1.4.2 Peroxisome proliferation in non-responsive species

PPs DEHP, clofibrate, nafenopin and fenofibrate do not induce liver peroxisomal β -oxidation, do not cause peroxisome proliferation or increase in liver weight in guinea pig (Corma *et al.*, 1992; Corm-Chu *et al.*, 1995; Rao *et al.*, 1984; Sakuma *et al.*, 1992). However, hypolipidaemic effects of MCP and Wy-14,643 have been observed in guinea pig (Bell *et al.*, 1998). Some reports indicate a small increase in microsomal P-450 content associated with a small increase in ω -hydroxylase activity (Lake *et al.*, 1989a; Pacot *et al.*, 1996) while others have found no such inducibility or increase in P-450 content in guinea pig liver microsomes (Dirven *et al.*, 1993; Latruffe *et al.*, 1995). CYP4A13, the only identified member of CYP4A subfamily in guinea pig, has been shown to be non-inducible by MCP at the RNA level (Bell *et al.*, 1993). Consistent with these *in vivo* observations, guinea pig primary hepatocyte cultures show little or no evidence of peroxisome proliferation after incubation with PPs (Blauauboer *et al.*, 1990; Dirvan *et al.*, 1993). However, whereas guinea pig primary hepatocytes showed no evidence of increased replicative DNA synthesis following PP treatment, these cultures showed evidence of PP-induced suppression of apoptosis (James and Roberts, 1996). Therefore guinea pig is generally considered as non-responsive to PPs as opposed to rats and mice which are highly responsive. This difference in responsiveness to PPs between rats and guinea pig is not attributable to differences in pharmacokinetics or metabolism since when guinea pigs and rats were dosed with ciprofibrate, to give equivalent plasma levels, the rats showed peroxisome proliferation but the guinea pigs did not (Pacot *et al.*, 1996).

Section 1.4.3 Peroxisome proliferation in primates

Effects of PPs on three species of monkeys (rhesus, cynomolgous and marmoset) have been investigated, and although some studies report small increases in peroxisome number, liver

weight and β -oxidation, the majority of studies, however, indicate no increase in these parameters (Lake *et al.*, 1989a; Blaaubour *et al.*, 1990; Foxworthy *et al.*, 1990 and 1994; Cornu *et al.*, 1992; Elcombe and Mitchell, 1986; Reddy *et al.*, 1984; Gray *et al.*, 1984). Long-term exposure to PPs (up to 6 years) has been shown to have no effect on primates and therefore primates are considered to be non-responsive species.

A limited amount of information regarding the effects of PPs on human has been obtained through the use of primary hepatocyte cultures obtained from biopsies and through the use of transformed liver cell lines. Human primary hepatocytes dosed with most potent PPs showed no effects on the induction of peroxisomal β -oxidation or fatty acid metabolizing enzymes (Ducles *et al.*, 1997; Blaabour *et al.*, 1990; Butterworth *et al.*, 1989; Elcombe, 1985; Elcombe and Mitchell, 1986). However, studies using human hepatoma cell line Hep G2 demonstrated a small induction in palmitoyl-CoA and acyl-CoA oxidase activity and catalase activity (Duclos *et al.*, 1997; Latruffe *et al.*, 1995; Chance *et al.*, 1995; Scotto *et al.*, 1995). These small inductions observed in Hep G2 cells are probably biologically insignificant since no such induction was observed in primary hepatocytes, and the metabolism/biochemistry of primary hepatocytes mimics more closely to *in vivo* situation than the Hep G2 transformed cell line. A limited amount of information regarding the effects of PPs on human has been gained from volunteers exposed to hypolipidaemic fibrate drugs. Although these drugs are effective hypolipidaemic agents, morphological examination of liver biopsies from patient treated with gemfibrozil exhibited no changes in peroxisome number or size (De la Inglesia *et al.*, 1982; Blumcke *et al.*, 1983; Gariot *et al.*, 1987). Bently *et al.* (1993) found a 30% increase in peroxisomal volume in the liver of ciprofibrate-treated patients, and Hanefeld *et al.* (1983) found a 50% increase in peroxisome number in the liver of clofibrate-treated patients. Interpretation of these findings is limited by the fact that examination of all liver lobes could not be performed to exclude any

possibility of intra-regional variation. Also, a large number of data points is required to account for any inter-individual variation in human population (polymorphism). Epidemiological studies on patients treated with clofibrate or gemfibrozil for up to 5 years showed no significant rise in tumour incidence of the liver (Oliver *et al.*, 1978; Frick *et al.*, 1987). It is now generally accepted that humans are non-responsive to the adverse effects of PPs.

Section 1.5 Aims of the thesis

The pleiotropic effects of PPs, including peroxisome proliferation, are mediated by PPAR α (Lee *et al.*, 1995). However, marked variations in species response to PPs exist, where rats and mice are highly responsive, human and guinea pig are non-responsive and hamster is partially-responsive species (Lake *et al.*, 1995). These species differences are not due to the lack of functional PPAR α since transcriptionally active PPAR α has been cloned from both responsive and non-responsive species (Issemann and Green 1990; Tugwood *et al.*, 1998). Further, fibrate-induced hypolipidaemia has been observed in both human and guinea pig (De la Inglesia *et al.*, 1982; Bell *et al.*, 1998), an action that requires functional PPAR α (Peters *et al.*, 1998).

Qualitative differences of PPAR α between species may be an important determining factor in species response to PPs. Differences in the intrinsic activity of PPAR α , arising from differences in key amino acids for example, may affect their transcriptional activity. Therefore addition of PPAR α to a responsive system with low or zero level of endogenous PPAR α will enable a comparison of PPAR α activities from different species. Thus primary hepatocyte culture systems from rats and mice will be investigated as a useful model to study the functionality of PPAR α in the context of peroxisome proliferation.

Differences in PPAR α level (quantitative differences) between species may also be a contributing factor in differing species response to PPs as there are reports of lower levels of PPAR α transcripts in human and guinea pig liver than in mouse (Palmer *et al.*, 1998; Bell *et al.*, 1998;

Tugwood *et al.*, 1998). It may be that a different threshold level of PPAR α exists for PP-induced hypolipidaemia and for peroxisome proliferation, where hypolipidaemic responses require lower PPAR α levels, whereas higher levels are required for peroxisome proliferation. If such is the case then one would expect reduced or zero peroxisome proliferation in non-responsive species due to their lower level of PPAR α . To determine how PPAR α level varies between species, hepatic concentrations of PPAR α mRNA will be determined on a comparative basis in species showing different responsiveness to PPs.

Recently a number of transcriptional coactivators have been identified; as well as interacting with other steroid receptors, some of these coactivators have been found to enhance the transcriptional activity of PPAR (Zhu *et al.*, 1996; Puigserver *et al.*, 1998, for example). It is not known which, if any, coactivators are important in peroxisome proliferation. If the expression of PPAR α and any such coactivators are co-localized within the liver lobule of responsive species then this may indicate whether such coactivators are likely to be associated with peroxisome proliferation. Therefore, transcript localization of the PPAR α and a number of its interacting coactivators will be studied in the mouse liver. There may be specific, as yet unidentified, PPAR α coactivators present in responsive species that may play a significant role in peroxisome proliferation. Since steroid receptors interact with coactivators through their LBD, PPAR α -LBD could serve as a useful bait in a nuclear-pull down assay to identify any novel interacting proteins that may function as specific PPAR α coactivators. This project also aims to purify functional PPAR α -LBD to be utilized in protein-protein interaction studies.

Chapter 2 Materials & Methods

Section 2.1 Animal Studies

Section 2.1.1 Guinea pigs

Male Dunkin-Hartley Guinea Pigs (400g) were obtained from Harlan-Olac and were kept in a standard 12 hours dark/light cycle and had access to standard laboratory chow and water *ad lib*. For RNA extraction, animals were killed by cervical dislocation between 9-10am in the morning and the livers were removed, weighed and flash frozen in liquid nitrogen.

Section 2.1.2 Mice

S129 PPAR α wild type and knock-out mice were obtained from Dr. Frank Gonzalez (USA). A colony was established and experiments were conducted using these in-house bred animals. Adult males (25-30g) were kept in a standard 12 hours dark/light cycle and had access to standard laboratory chow and water *ad lib*. Mice were dosed daily by intra-peritoneal injection with 25mg/kg body weight of either methylclofenapate or Wy-14,643 in corn oil or vehicle control (in total volume of 100 μ l) for 3 consecutive days. At the end of the dosing period animals were sacrificed by cervical dislocation. Livers were removed, weighed and immediately flash frozen in liquid nitrogen, and stored at -80 $^{\circ}$ C until use.

C57B1/6 mice were obtained from Harlan, UK and were dosed with methylclofenapate for the study of the expression of coactivator proteins in liver using *in situ* hybridisation. Animals were kept under the same conditions as above. Adult males (25-30g) were dosed daily by intra-peritoneal injection with methylclofenapate (20mg/kg body weight) in a total volume of 100 μ l of corn oil or vehicle control for 7 consecutive days. At the end of the dosing period animals were sacrificed by cervical dislocation. Livers were removed, weighed and immediately flash frozen in liquid nitrogen, and stored at -80 $^{\circ}$ C until use.

Section 2.1.3 Hamster

Golden Syrian hamsters were from a colony maintained at Nottingham, and the animals were individually caged and kept in a standard 12 hours dark/light cycle and had access to RM3 pelleted diet and water *ad lib*. Adult males (150-180g) were dosed daily by intra-peritoneal injection with methyclofenapate or Wy-14,643 dissolved in sunflower oil (25mg/kg body weight) or vehicle control (in a total volume of 200 μ l for 3 consecutive days. At the end of the dosing period animals were sacrificed by cervical dislocation. Livers were removed, weighed and flash frozen in liquid nitrogen, and stored at -80°C until use.

Section 2.1.4 Rats

Adult male Wistar Rats (200-250g) were obtained from Harlan UK and were kept in a standard 12 hours dark/light cycle and had access to standard laboratory chow and water *ad lib*. These naïve animals were used for the preparation of primary hepatocyte cultures following liver perfusion.

Section 2.2 Primary Hepatocytes: Isolation & Culture

Section 2.2.1 Primary Hepatocyte Isolation

Composition of Reagents:

Collagenase H: [150 units/mg]

CL-15 Medium (Sigma, UK)

CaCl₂: [1M, filtered]

Krebs Ringer Phosphate Buffer (KRPB) and

Krebs Ringer Hydrogen Carbonate Buffer (KRHB):

Component	KRPB (mM)	KRHB (mM)
NaCl	150	142
KCl	4.97	4.37
KH ₂ PO ₄	1.24	1.24
MgSO ₄	0.62	0.62
MgCl ₂	0.62	0.62
NaHCO ₃	3.73	24.0
Na ₂ HPO ₄	4.84	-----

Male Wistar rats of 200-250g body weight were used for hepatocyte preparation. Hepatocytes isolation was performed essentially as described by Mitchell *et al.* (1984), based on the method of Rao *et al.* (1976). All solutions used for liver perfusion were sterile. Ca²⁺ free Krebs Ringer Phosphate Buffer (KRPB), pH 7.4 and Krebs Ringer Hydrogen Carbonate Buffer (KRHB), pH 7.4 were freshly made, and during perfusion, the buffers were maintained at 37 °C and gassed continuously with 95% O₂ : 5% CO₂.

The animal was terminally anaesthetized with diethyl ether. While the heart was beating, the exposed liver was cannulated through the hepatic portal vein at one end while another catheter was inserted through the right atrium to cannulate the superior vena cava. This creates a circulating system so that the liver can be perfused *in situ*. First, the liver was perfused with KRPB for 10 minutes, and then with KRHB for 5 minutes, at a flow rate of 40 ml/min. The liver was then perfused for a further 10-15 minutes with KRHB to which collagenase (14 units/200ml) and CaCl₂ (5mM final) were added. Collagenase digests the connective tissue meshwork that maintains the liver cells and its architecture, and therefore allows easy isolation of cells which are dissociated from their neighbours. The digested liver is easily recognised due to the drop in liver pressure. Liver lobes were removed and placed in a sterile beaker containing KRHB. The

tissue was gently minced and passed through a sterilized 120 μ m gauze using a total volume of 100ml of KRHB. Cells were washed three times with KRHB by centrifuging at 50g for 3 minutes in each wash. Finally, cells were resuspended in CL-15 medium and cell viability determined by trypan blue exclusion method. Viability of >85% was required to carry out subsequent experiments.

Hepatocytes from mouse liver were isolated using essentially the same perfusion procedure as for rat liver, but with slight modifications. Unlike rats, mice have a gall-bladder, and this must be removed to prevent contamination of the liver. The gall bladder was ligatured at the start of the isolation procedure, and removed by cutting below the ligature while pulling away from the liver. Here only the hepatic portal vein was cannulated, and through which perfusion was carried out and drained through the punctured heart. Perfusion was carried out at a flow rate of 20ml/min, and collagenase treated for 5-10 minutes.

Section 2.2.2 Viability count and quantification of hepatocytes

The Trypan blue exclusion method was used to determine the viability of the isolated hepatocytes. Dead or dying cells with damaged plasma membranes take up the dye and appear blue under the light microscope. These non-viable cells are easily distinguished from viable cells which are transparent white in their appearance. The viable fraction and cell concentration of a hepatocyte isolation can be determined using a haemocytometer. This was done by mixing 100 μ l of cell suspension with 100 μ l of Trypan blue, and the total number of blue and white cells were counted in five squares of a twenty-five square grid slide (improved Neubauer haemocytometer). Using this information, cell viability and concentration was calculated using the following equations:

Viable fraction = $[1 - \text{Total number of blue cells} / \text{Total number of cells}]$

Viability (%) = Viable fraction X 100

Viable cells (cell/ml) = $[\text{Total number of cell} \times 2 \times 5 \times 1 \times 10^4] \times \text{Viable fraction}$

Section 2.2.3 Hepatocyte Culture

25cm² Falcon tissue culture flasks were seeded with either 2x10⁶ or 1x10⁶ viable hepatocytes isolated from rat and mouse liver, respectively, in 4ml of CL-15 medium i.e. Liebowitz L15 media containing fetal bovine serum (8.3%), tryptose phosphate broth (8.3%), penicillin G (41.3U/ml), streptomycin sulphate (8.2mg/ml), glutamine (241mg/ml), insulin (10⁻⁶M), and hydrocortisone-21-hemisuccinate (10⁻⁵M). The flasks were then incubated at 37⁰C in a humidified non-CO₂ incubator. The medium was changed four hours later to remove unattached cells and replaced with 4ml of fresh medium. Cells were left overnight to form monolayer by completing attachment. Further changes (4ml of CL-15 medium) were made every 24 hours in following seeding.

Section 2.2.4 Dosing of primary hepatocytes

Test compounds were added at 24 hours after seeding and included in all subsequent changes. Chemical stocks were kept at -20⁰C for up to one week while diluted chemicals were prepared prior to dosing of the cells. The vehicles used for dissolving test chemicals were of tissue culture grade. The volume of test chemicals and their vehicle control never exceeded more than 1/400th of the total volume of the media.

Section 2.2.5 Measurement of DNA Synthesis

Composition of reagents:

Test Chemicals: [EGF (10mg/ml) in L-15 medium, MCP (12.2mg/ml) and Wy-14,643 (12.94mg/ml) in DMSO]

Bromodeoxyuridine (BrdUrd): [3mg/ml in PB buffer]

Phosphate Buffered Saline (PBS): [150mM NaCl, 15mM Na₂H₂PO₄]

Phosphate Buffer: [5.76g Na₂HPO₄, NaH₂PO₄·2H₂O in 1 litre water]

Fixing Solution: [70% Ethanol, 50mM Glycine, pH 2.0]

Denaturing Solution: [0.5M NaOH, 1.5M NaCl]

Neutralising Solution: [0.5M Tris-HCl (pH7.4), 1.5M NaCl]

Antibody: [Primary: mouse monoclonal anti-BrdUrd; Secondary: rabbit anti-mouse (binding site, UK)]

3,3'-Diaminobenzidine Tetrahydrochloride (DAB): [0.5mg/ml in PB]

A known hepatic mitogen, EGF (10ng/ml), was used to demonstrate that the primary culture was responsive to mitogenic stimulation. To show that PPs act as liver mitogens, Wy-14,643 and MCP were used to stimulate DNA synthesis. Both test chemicals were dissolved in DMSO and a concentration of up to 100µM was used to study DNA synthesis. Hepatocytes were exposed to BrdUrd (6µg/ml) between 6 and 30 hours after the start of the exposure to PPs (24-48 hours in the case of EGF). Cells that underwent replicative DNA synthesis incorporate the base analog BrdUrd which can be detected by immunocytochemistry.

At the end of the exposure period cells were fixed and prepared for immunocytochemical detection of BrdUrd. The cell monolayer of each flask was rinsed briefly in PBS and then fixed in 3ml of fixing solution for 20 minutes at -20 °C. Cells were washed three times in 3ml of UHP water and left to air dry. A mouse anti-BrdUrd monoclonal antibody was used which detects incorporated BrdUrd bases in DNA. Briefly, cells were rehydrated by washing in 3ml of PBST (PBS with 0.5% Tween-20) for 3 minutes. Cells were then incubated in 3ml denaturing solution for 30 minutes. Following denaturation, cells were returned to neutral pH by treatment with neutralising solution for 30 minutes, followed by three washes (5 minutes each) with PBST. Cells were then incubated with primary antibody (1:1600 diluted in PBST) for 2 hours at room temperature followed by three washes of PBST. The cells were then incubated for 1 hour with a secondary antibody: rabbit anti-mouse conjugated to horseradish peroxidase (1:100 diluted in PBST) and washed with PBST as before. At the end of incubation period, secondary antibody

was localised histochemically by incubating with developing solution containing 3,3'-Diaminobenzidine Tetrahydrochloride (DAB; 10µg/ml) for 10 minutes. Peroxidase converts DAB into a brown precipitate that can be visualised as light-brown colour under conventional light microscopy. Cells that incorporate BrdUrd have brown-stained nuclei. The total number of cells was counted at X160 magnification (three fields per flask and three flasks per data point) and also the total number of positive cells in each field. This was expressed as labelling index (LI%):

$$\text{LI (\%)} = \frac{\text{Number of positive cells}}{\text{Total number of cells}} \times 100$$

Section 2.2.6 Histochemical staining of peroxisomes

Peroxisomes in the cultured rat hepatocytes could be demonstrated by histochemical staining (modified from Foxworthy *et al.*, 1990). Catalase within the peroxisomes converts DAB into a dark-brown precipitate that can be visualised by light microscopy. To show peroxisome proliferation as well as DNA synthesis occurring in the cultured hepatocytes, cells were dosed with MCP for 48 hours. At the end of the dosing period monolayers were washed twice with 0.1M sodium cacodylate buffer containing 10% sucrose (4ml per flask). Cells were then fixed for 1 hour with 2.5% glutaraldehyde in 0.1M cacodylate buffer at 4 °C. The fixed cells were washed twice with 0.1M cacodylate buffer, and then incubated at 37 °C for 2 hours in staining solution under alkaline conditions (0.2% DAB, 0.05% H₂O₂, 5mM KCN and 50mM 2-amino-2-methyl 1,3 propandiol, pH 9.7). Cells were washed thoroughly with UHP water and air-dried.

Section 2.2.7 Detection of apoptosis in hepatocyte culture

Cell undergoing apoptosis display a number of characteristics, and one such feature is the condensation of the chromatin structure. This can be detected as increased intensity of nuclear staining when the cells are treated with Hoechst 33258 chromatin stain. Cells were dosed appropriately with MCP or Wy-14,643 and cultured for 48 hours. At the end of the dosing pe-

riod monolayers were washed briefly in PBS to remove residual medium. Cells were then fixed in 3ml of fixation solution (75% ethanol, 25% acetic acid) for 60 minutes at -20°C . Cells were washed thoroughly with UHP water and air-dried. Prior to staining, cells were rehydrated by washing three times in 3ml PBS for 3 minutes. Cells were then stained with Hoechst 33258 (8 mg/ml in UHP water) and incubated at room temperature for 10 minutes on a rocking platform. Flasks were washed thoroughly in UHP water and mountant (20mM citric acid, 50mM Na_2HPO_4 , 50% glycerol) was added. Cells were viewed under a fluorescence microscope (350nm-460nm range).

Section 2.3 Transient Transfection Studies

Section 2.3.1 Preparation of lipofectin reagent

Composition of reagents:

DOPE: L- α -phosphatidylethanolamine, dioleoyl (C18:1, [cis]-9) (Sigma), (10 mg / ml in chloroform)

DOTMA: (N-[1-(2,3-dioleoyloxy)propyl]-N,N,N-trimethylammonium)

(kindly provided by Dr Cliff Elcombe, Zeneca CTL)

Nitrogen Gas

Transfection reagent “lipofectin” is a liposome formulation of the synthetic cationic lipid N-[1-(2,3-dioleoyloxy)propyl]-N,N,N-trimethylammonium chloride (DOTMA), and L-dioleoyl phosphatidylethanolamine (DOPE). This liposome formulation was prepared in the laboratory but is also available commercially. The lipofectin was prepared as described by several workers (e.g. Felgner *et al.*, 1987). Briefly, 10mg of DOTMA was mixed and dissolved in 1ml of DOPE (10mg/ml in chloroform). The solvent was then evaporated to dryness under a constant stream of nitrogen. This step was carried out in a dark room to prevent direct exposure to light. The dried solid of DOTMA/DOPE mix was dissolved in 2ml of sterile UHP water and then sonicated in a 50-60Hz, 80watt Polaron Sonibath until the solution is homogeneous (usually for 5 minutes). The resulting opaque solution was stored in a light-tight vial at 4°C . Final concentration

of the DOTMA/DOPE mix was 5mg/ml.

Section 2.3.2 Transfection of primary hepatocytes

Composition of reagents:

Lipofectin reagent (DOTMA/DOPE)

Transfection vector (Quiagen purified plasmid DNA)

CL-15* medium (without insulin and serum)

CL-15 medium (normal)

Primary hepatocytes (24hr old culture)

A previously optimised transfection protocol was followed for the determination of transfection efficiency (pRSV- β -galactosidase) and transient transfection of PPAR α vector constructs (pSG5-mPAR α , pBK-CMV-gpPPAR α and cotransfected vector [ACO-PPRE]2.pGL3-LUC). Primary hepatocytes were isolated 24 hours before the transfection experiment and incubated overnight at 37 °C. Lipofectin reagent (5 μ l + 300 μ l CL-15*/flask) and plasmid DNA (5 μ g + 300 μ l CL-15*/flask) were prepared separately by mixing with CL-15* media and incubated at room temperature for 30 minutes in a class II cabinet. Lipid-DNA complexes were prepared by gently mixing the above solutions together and incubated at room temperature for a further 15-20 minutes. Whilst the lipid-DNA complexes were being incubated together, serum-containing medium in the flasks was removed and cells were incubated with CL-15* medium for 15-20 minutes. At the end of lipid-DNA complex formation, the CL-15* medium of the flask was removed and replaced with lipid-DNA complex solution diluted with 2.4ml of CL-15* medium. Flasks were incubated at 37 °C in a humidified non-CO₂ incubator for 4 hours. At the end of the incubation period transfection medium was removed and replaced with 4ml of normal CL-15 medium and cultured for a further 48 hours.

Section 2.3.3 β -Galactosidase histochemistry

Composition of reagents:

PBS: [150mM NaCl, 15mM Na₂H₂PO₄]

X-Gal: [40 mg/ml in DMSO]

Fixing Solution: [2% Formaldehyde (v/v), 0.2% Glutaraldehyde(v/v) in PBS]

Developing Reagent: [5mM K₃Fe(CN)₆, 5mM K₄Fe(CN)₆, 2mM MgCl₂ in PBS]

Histochemical analysis of β -Galactosidase activity was carried out as described by Sanes *et al.* (1986) for the determination of transfection efficiency. Culture medium was removed from the transfected cells and these were washed twice for 2 minutes with phosphate buffered saline (PBS). Cells were fixed for 5 minutes with 3ml fixing solution at 4 °C and washed with PBS as before. The monolayer was then overlaid with 3ml of developing reagent containing X-Gal (75 μ l/flask) and incubated at 37 °C for 24 hours. Due to their β -Galactosidase activity the transformed cells develop blue cytoplasm and can be easily distinguished from non-transformed cells. Transfection efficiency was expressed as the percentage of blue transfected cells.

Section 2.3.4 Dual luciferase assay

Composition of reagents:

PBS: [150mM NaCl, 15mM Na₂H₂PO₄]

Passive Lysis Buffer [5X] (Promega)

Luciferase Assay Reagent II (Promega)

Stop and Glow Reagent (Promega)

Mouse primary hepatocytes were transfected with appropriate expression vector (pSG5-mPPAR α , pBK-CMV-gppPAR α) along with their reporter vector (ACO-PPRE)₂.pGL3-LUC. At the end of the transfection period, medium from transfected flasks was removed and the monolayer was washed briefly with 4ml of PBS. To prepare cell extracts for the dual luciferase assay, PBS was removed and 900 μ l of passive lysis buffer (1x) was added to each flask. Flasks were incubated for 5 minutes at room temperature with gentle agitation on a four-way rocker. Lysed cells were removed from the flask by scraping with a sterile rubber policeman and then transferred

into a microfuge tube and kept on ice for luciferase assay.

Cell extracts prepared above using passive lysis buffer were used for dual luciferase assays. Twenty μl of cell extract was added to 100 μl luciferase assay reagent II. Immediately, the luminescence generated by the firefly luciferase reaction was measured over four 10 second intervals. The firefly luciferase activity was stopped by adding 100 μl of Stop & Glo reagent and the luminescence generated by the *Renilla* luciferase reaction was measured again over four 10 second intervals in a Packard (PICO-LITE) luminometer. The average luminescence for each luciferase assay was used as the final measurement.

Section 2.4 General Molecular Biology Techniques

Section 2.4.1 *E. Coli* growth media

Composition of Reagents:

Luria-Bertani (LB) Broth: [the following chemicals were dissolved in and made up to one litre with Ultra High Pure (UHP) water and autoclaved: 10g Bacto-tryptone, 5g Bacto-yeast extract, 10g NaCl]

LB-Agar was made by dissolving 5g of Bacto-agar in 1 litre of LB-broth and then autoclaved. To make LB-plates, autoclaved LB-agar medium was cooled to 55⁰C, then appropriate antibiotic(s) added and poured into 9cm Petri dishes. The following concentrations were used for antibiotics:

antibiotics	stock solution	concentration used
Tetracycline	5 mg/ml in ethanol	20-50 $\mu\text{g/ml}$
Ampicillin	100 mg/ml in water	50-100 $\mu\text{g/ml}$
Chloramphenicol	34 mg/ml in ethanol	25-50 $\mu\text{g/ml}$
Kanamycin	50 mg/ml in water	10-100 $\mu\text{g/ml}$

Section 2.4.2 Preparation of calcium competent *E. Coli*

Composition of Reagents:

LB broth + Tetracycline (for XL-1 & XL-2)

LB Broth + Chloramphenicol (for BL21 [DE3] pLysS)

CaCl₂: [0.1M, 0.22mM filtered]

CaCl₂/Glycerol: [0.1M CaCl₂, 10% Glycerol, 0.22mM filtered]

E. coli strains were stored at -80 °C as 10% glycerol stock and were used to streak fresh LB-agar plates containing appropriate selection antibiotics and incubated overnight at 37 °C. A single colony from an overnight streaked agar plate of either XL-1, XL-2 or BL21(DE3)pLysS *E. coli* strains was picked and inoculated in 10ml LB-Broth medium containing appropriate antibiotics. Cultures were grown in an orbital shaking incubator (200 rpm/min) overnight at 37 °C. Five millilitres of the overnight cultures were used to seed 500ml of LB-Broth medium and grown at 37 °C in an orbital shaker as before until an optical density of between 0.5-0.6 (OD_{600nm}) was reached. The cultures were chilled on ice for 10 minutes, then centrifuged in a JA21 rotor at 4000g for 15 min at 4 °C. Pelleted cells were resuspended in 50ml ice-cold sterile 0.1M CaCl₂ (10ml per 100ml original culture). This process of cell resuspension and pelleting was repeated again. Finally cells were resuspended in 20ml of ice-cold 0.1M CaCl₂ containing 10% glycerol (2ml per 50ml original culture). Cells were stored at -80 °C as 200µl aliquots.

Section 2.4.3 Preparation of electro-competent *E. Coli*

Composition of Reagents:

LB broth + Tetracycline (for XL-1 & XL-2)

LB Broth + Chloramphenicol (for BL21 [DE3] pLysS)

Sterile Ultra High Pure (UHP) Water

A single colony from an agar plate (streaked and grown at 37 °C overnight) of either XL-1, XL-2 or BL21(DE3)pLysS *E. coli* strains was picked and inoculated in 10ml LB-Broth medium con-

taining appropriate antibiotics. Cultures were grown in an orbital shaking incubator (200 rpm/min) overnight at 37 °C. Five millilitres of the overnight cultures were used to seed 500ml of LB-Broth medium and grown at 37 °C in an orbital shaker as before until an optical density of between 0.5-0.6 (OD_{600nm}) was reached. The cultures were chilled on ice for 10 minutes, then centrifuged in a JA21 rotor at 4 000g for 15 min at 4 °C. Pelleted cells were resuspended in 50ml ice-cold sterile UHP water (10ml per 100ml original culture). This process of cell resuspension and pelleting was repeated between four and five times with sterile UHP water. Finally cells were resuspended in 20ml of ice-cold sterile UHP water containing 10% glycerol (2ml per 50ml original culture). Cells were stored at -80 °C as 200µl aliquots.

Section 2.4.4 Plasmid transformation into CaCl₂ competent *E.coli*

Frozen cell aliquots were thawed on ice and mixed gently by flicking the tube. Cells were aliquoted into 100µl volumes (pre-chilled tubes and pipette tips were used) and kept on ice. Plasmid DNA <50ng in a total volume of 5µl or 10µl of a ligation reaction mixture was added to the cells and incubated on ice for 10 minutes. The cells were then heat-shocked at 42 °C for 60-90 seconds and then immediately placed on ice for 2 minutes. Following the addition of 900µl of LB-medium cells were cultured at 37 °C for 60 minutes. Cells were plated on LB-agar plates containing appropriate antibiotics for the selection of strains and plasmids. Different volumes of cells were spread (typically 10, 50 and 200µl) in order to obtain single colonies on the plate. Plates were incubated overnight at 37 °C.

Section 2.4.5 Plasmid transformation into electro-competent *E.coli*

Electroporation cuvettes and the cuvette holder were chilled on ice prior to use. Frozen aliquots of cells were thawed quickly using hand warmth and then immediately placed on ice. 50µl of cells were added to 10-25ng of plasmid DNA. For the transformation of ligation product, 1-5µl of ligation reaction mixture was added to 50µl of cells and put on ice. Cells were then electroporated at 1.8kV using a bio-rad electroporator. One millilitre of LB-broth was immediately added

and incubated at 37 °C for 1 hour. Either 50 or 100µl of transformed cells were spread on agar plates containing appropriate antibiotics and incubated overnight at 37 °C.

Section 2.4.6 Phenol:Chloroform extraction of nucleic acids.

Protein contaminants in DNA and RNA solutions can be effectively removed by phenol:chloroform extraction. One volume of phenol:chloroform (1:1) was added to the sample of nucleic acid, and then vortexed thoroughly. The samples were centrifuged at 15000 rpm for 5 minutes in a benchtop mini-centrifuge. This allows separation of nucleic acids into the upper aqueous phase while protein contaminants remain in the interface and organic phase. The aqueous phase is carefully removed and retained, which is ethanol precipitated as described below.

Section 2.4.7 Ethanol precipitation of nucleic acids

Composition of Reagents:

Absolute Ethanol

Ethanol: [70 %]

Sodium Acetate: [3 M, pH 5.2, 0.22µM filtered]

Ammonium Acetate: [7 M, 0.22µM filtered]

Autoclaved and DEPC-treated UHP water

The aqueous phase from phenol/chloroform treatments, or diluted nucleic acids needing to be concentrated, are ethanol precipitated. For the precipitation of DNA 0.1 volume of sodium acetate was added to the aqueous phase while for RNA 0.25 volume of ammonium acetate was used. Two volumes of absolute ethanol are added to the solution, mixed and placed on ice or at -20 °C for 20-30 minutes to precipitate the nucleic acid. Precipitated nucleic acids were pelleted by centrifugation at 15000 rpm for 20 minutes. Pellets were washed with 200-500µl of 70% ethanol by centrifuging as before. Any residual ethanol traces were removed and the pellets were air-dried. DNA pellets were resolubilised in UHP water and RNA pellets were resolubilised in DEPC treated water.

Section 2.4.8 Restriction digestion of plasmid DNA

Restriction digestion of plasmid DNA was performed using the optimal buffer supplied by the manufacturer for the particular enzyme. When double digests were carried out using non-compatible buffers, the buffer with the lowest salt concentration was used to perform a single digest first and then second digest was carried out. Alternatively salts were removed after the first digest by ethanol precipitation before the second digest could be carried out. Typically 2-10 μ g DNA was digested using 1X buffer and 5 units of enzyme in a 50 μ l volume, and incubated at 37 $^{\circ}$ C for 2 hours. The reaction mixtures were assembled in an Eppendorf tube in the order shown below for a single digest:

component	volume (μ l)
10X restriction buffer	5.0
DNA (1mg/ml)	10.0
UHP H ₂ O to make final volume of 50 μ l	33.0
Restriction enzyme (2 units/ μ l)	2.0

At the end of incubation period, reaction was terminated by the addition of either sodium acetate and ethanol for DNA precipitation or by DNA loading buffer. Restriction digest was analysed by agarose gel electrophoresis.

Section 2.4.9 Agarose gel electrophoresis (non-denaturing)

Composition of Reagents:

TBE [10X]: [107.8g Tris Base, 55g Boric Acid, 20ml EDTA (0.5M, pH 8.0) in 1 litre UHP H₂O]

TAE [50X]: [242g Tris base, 57.1ml Glacial Acetic Acid, 100ml EDTA (0.5M, pH 8.0) in 1 litre UHP H₂O]

DNA Loading Buffer [10X]: [0.25% Bromophenol Blue (v/v), 0.25% Xylene Cyanol FF (w/v),

30% Glycerol (v/v), 1X TBE]

Ethidium Bromide: [10mg/ml]

1 kb⁺ marker DNA ladder (0.1mg/ml): 75bp-12kbp

TBE was used for normal electrophoresis of DNA while TAE was used for gel purification purposes where DNA bands were excised and purified for subcloning. Agarose was dissolved to an appropriate concentration (0.7-1.5% w/v) by boiling in 1X TBE, and allowed to cool to approximately 55 °C. Ethidium bromide (10µg/50ml gel volume) was added and the gel mixture poured into a casting mould, containing an appropriate sized gel comb, on a flat surface. The gel was allowed to set at room temperature for thirty minutes. Samples were prepared using 1X DNA loading buffer as a final concentration. After loading of samples and DNA marker the gel was run in 1X TBE buffer at a constant voltage of 6V/cm until desired resolution was achieved. DNA bands were visualised by illumination with UV light and photographed.

Section 2.4.10 Agarose gel electrophoresis (denaturing)

For the separation and visualisation of total and polyA⁺ RNA denaturing agarose gel electrophoresis was used. RNA tends to form secondary structures and therefore requires denaturing condition so that it is separated on the basis of size. Preparation and running of denaturing gels is the same as non-denaturing gels except that 0.1% (v/v) SDS was included in the gel mixture before it was poured into the gel cast.

Section 2.4.11 Denaturing polyacrylamide gel electrophoresis

The following formulae were used to calculate the volume of 10X TBE, sequagel diluent and concentrate required to make a certain percentage of gel.

$$[1/10 * (\text{total gel volume})] = \text{volume of 10X TBE}$$

$$[(\% \text{ acrylamide gel need}) * (\text{volume of gel})] / 25 = \text{volume of sequa gel concentrate}$$

$$[\text{volume of gel} - (1/10\text{th volume of gel} + \text{volume of concentrate})] = \text{volume of diluent}$$

For example, to make a 6% gel of 10ml total volume 2.4ml of concentrate and 6.6ml of diluent and 1ml of 10X TBE was mixed. To start the polymerisation, 6 μ l of TEMED and 100 μ l of 10% APS were added and mixed. Immediately the gel solution was pipetted in the gel cast without introducing air bubbles. The comb was inserted into the gel and the gel was allowed to set for 30 minutes. The gel was then placed in the gel tank and 1X TBE was used to fill the anode and cathode compartments, and pre-run at 50 volts for 30 minutes. Prior to loading, unpolymerised acrylamide and crystalline urea were thoroughly washed out of each well with running buffer. The samples were loaded into the wells and separation was carried out at 120 volts until the Xylene cyanol FF dye front had travelled at least 75% through the gel (usually 90 minutes was sufficient for most probes used). The gel was fixed (in 10% methanol and 10% acetic acid) and dried under vacuum. Dried gel can then be used to obtain autoradiographs or quantified in the phosphor imager.

Section 2.4.12 DNA gel purification by geneclean

Composition of Reagents:

Agarose gel: [made with 1X TAE]

GeneClean II kit:

NaI solution: [6M]

Glassmilk Silica Matrix in UHP water

New Wash Buffer: [NaCl, ethanol, water]

UHP water, autoclaved and filtered

The GeneClean II kit contains “glassmilk” which is a silica matrix that binds single and double stranded DNA. DNA fragments to be purified from other contaminating fragments were first separated and resolved on a 1X TAE agarose gel. To minimise UV damage to the DNA, the gel is kept in its perspex casting tray and is visualised on a UV transilluminator. The band of interest was excised and weighed in a 1.5ml eppendorf tube. Three volumes (of gel slice) of NaI solution

were then added to the tube. The gel slice was dissolved by heating the tube to 55 °C for 15 minutes. 5µl of glassmilk (1µl per µg DNA) was added to the DNA solution and vortexed thoroughly. Ten minutes of incubation at room temperature was sufficient to allow binding of the DNA to the glassmilk. The glassmilk-DNA complex was then pelleted by centrifugation at 14000 rpm for 10 seconds and the supernatant was removed. The pellet was washed three times with 500µl of ice cold New Wash Buffer. After the final wash the glassmilk pellet was resuspended in 10µl of UHP water and incubated at 55 °C for 3 minutes to elute the bound DNA. DNA in solution was separated from the glassmilk by brief centrifugation (30 seconds at top speed). The supernatant was carefully removed and stored at -20 °C until required.

Section 2.4.13 Alkaline Phosphatase treatment of DNA

Composition of Reagents:

Shrimp Alkaline Phosphatase (SAP) Buffer [10X]: [200mM Tris-HCl (pH 8.0), 100mM MgCl₂]

Shrimp Alkaline Phosphatase Enzyme (SAP), (United States Biochemical-USB)

UHP water, 0.22µm filtered

Alkaline phosphatase treatment of linearised plasmid cloning vector was carried out to prevent it from re-circularising. Restriction digested DNA was first gel-purified by the GeneClean method and then alkaline phosphatase treated. Ten µl of GeneClean product was added to 5µl of 10X SAP buffer and the reaction volume was made up to 49µl with UHP water and the reaction was initiated by the addition of 1µl SAP enzyme. The reaction was incubated at 37 °C for 30 minutes and then heat inactivated for 15 minutes at 65 °C. The reaction mixture containing DNA was phenol:chloroform treated and ethanol precipitated and the DNA pellet was resuspended in 10µl of UHP water.

Section 2.4.14 DE81 test for nucleotide incorporation

Compositions of Reagents:

Na₂HPO₄ : [0.5M]

DE 81 Filters (Whatman)

Ethanol: [100 %]

Sterilized UHP water

Hi-Safe Liquid Scintillant

To determine the efficiency of transcription, an incorporation test was carried out using DE81 ion-exchange filters. One μl of DNase treated transcription mix (or reaction mix in the case of DNA ladder) was first diluted 10 fold using DEPC treated water, and then $1\mu\text{l}$ was spotted onto each half of a filter, and allowed to air-dry. One half of the filter was washed five times in 0.5M Na_2HPO_4 , twice in DEPC treated H_2O , and twice in absolute ethanol, one minute for each wash. The half filters were air-dried and counts per minute compared between washed and unwashed filter halves. To do this, half filters were placed in separate scintillation vials containing 3ml of scintillation cocktail and counted on a [$\alpha^{32}\text{P}$] program for 1 minute in a Packard 1900 TR liquid scintillation analyser. Transcription efficiency was expressed as % incorporation (washed/unwashedX100).

Section 2.4.15 Labelling of DNA ladder

Composition of reagents:

Labelling Buffer [5X]: [50mM Tris-HCl (pH 7.5), 250mM NaCl, 50mM MgCl_2]

dNTP Mix: [10mM of each nucleotide dATP, dTTP, dGTP (Pharmacia)]

100bp or 1kb DNA ladder: [1mg/ml, (Gibco BRL)]

[$\alpha^{32}\text{P}$] dCTP: [3.3 mM, (Dupont ICN)]

Klenow DNA polymerase: [5U/ μl] (Nbl)]

UHP water

The DNA ladder was radiolabelled so that it could be used for sizing double stranded RNA fragments in the RNase protection assay. The klenow fragment of E.coli DNA polymerase was used to label $5\mu\text{g}$ of DNA by filling in the 3' ends. The reaction was set up using the following com-

ponents:

component	volume (μl)
Labelling Buffer	3.0
dNTP Mix.	3.0
DNA Ladder	5.0
[α ³² P] dCTP	5.0
DNA Polymerase	1.0
UHP H ₂ O	13.0

The reaction was then incubated at room temperature for 3 hours, and the incorporation was determined using the DE81 test.

Section 2.4.16 Extraction and Purification of Nucleic Acids

Section 2.4.16.1 Purification of plasmid DNA by alkaline lysis method

Composition of Reagents:

Solution 1: [25mM Tris-HCl (pH 8.0), 10mM EDTA, 10mg/ml RNase A]

Solution 2: [0.2M NaOH, 1% SDS (v/v)]

Solution 3: [3M Potassium Acetate, 11.5% Glacial Acetic Acid (v/v)]

Phenol : chloroform [1:1 (v/v)]

Sodium Acetate: [3 M, pH 5.2]

Absolute Ethanol

Ethanol: [70%]

UHP water (0.22μm filtered)

For this crude miniprep, 2ml of overnight bacterial culture was pelleted by centrifugation at 15000 rpm for 2 minutes, and the supernatant discarded. The pellet was resuspended in 100μl of solution 1. Immediately 200μl of solution 2 (freshly prepared) was added and mixed by gently inverting the tube several times. The tube was then incubated at room temperature for 5 min-

utes. At the end of incubation period 150µl of ice cold solution 3 was added and mixed by inverting the tube several times. Proteins were precipitated by incubating the tube on ice for 10 minutes, and pelleted by centrifugation at 15000 rpm for 10 minutes. The supernatant was transferred to a fresh tube, phenol:chloroform treated and ethanol precipitated (section 2.4.6). The DNA pellet was washed in 70% ethanol and air-dried to remove any residual ethanol. Finally the DNA pellet was resuspended in 20µl of UHP water. Purified plasmid DNA was stored at -20 °C until required.

Section 2.4.16.2 Purification of plasmid DNA on Qiagen Mini- and Maxi-prep columns

Composition of Reagents:

Buffer P1: [50mM Tris-HCl (pH 8.0), 10mM EDTA, 10mg/ml RNase A]

Buffer P2: [200mM NaOH, 1% SDS (v/v)]

Buffer P3: [3M Potassium acetate (pH 5.5)]

Buffer QBT: [750mM NaCl, 50mM MOPS (pH 7.0), 15% Isopropanol (v/v), 0.15% Triton X-100 (v/v)]

Buffer QC: [1M NaCl, 50mM MOPS (pH 7.0), 15% Isopropanol (v/v)]

Buffer QF: [1.25M NaCl, 50mM Tris-HCl (pH 8.5), 15% Isopropanol (v/v), 70% Ethanol]

Autoclaved and 0.22µm filtered UHP water

Qiagen tip columns contain diethylaminoethanol (DEAE) anion exchange resin. The negative charge on the phosphate backbone of DNA causes the DNA to bind to this resin, and is only eluted from the column resin at high salt concentrations. Impurities such as RNA, protein, carbohydrates and small metabolites are washed from the resin in medium salt buffers.

Section 2.4.16.3 Mini-prep method

For sequencing purposes the Qiagen mini-prep method was used. Four millilitres of a 10ml overnight culture were pelleted by centrifugation at 15000 rpm for 2 minutes. The bacterial pellet was resuspended in 0.3ml of buffer P1. Immediately 0.3ml of buffer P2 was added and mixed thoroughly by inverting the tube several times, and incubated at room temperature for 5 min-

utes. At the end of incubation period 0.3ml of chilled buffer P3 was added and mixed by inversion as before. The sample was incubated on ice for 10 minutes. The sample was centrifuged at 15000 rpm for 15 minutes, then the supernatant was promptly removed and kept on ice. Meanwhile a Qiagen-tip 20 was equilibrated with 1ml of buffer QBT. The supernatant was applied to the column and allowed to drain through, using gravity to pull the solution through. The column was washed four times with 1ml of buffer QC. DNA was eluted with 0.8ml of buffer QF, and precipitated by the addition of 0.56ml of isopropanol. The solution was centrifuged at 15000 rpm for 30 minutes. The DNA pellet was washed with 1 ml of 70 % ethanol. 20 μ l of autoclaved UHP water was used to resolubilise the DNA. The concentration of DNA was determined by measuring the $A_{260\text{nm}}$ of a diluted sample. DNA samples were stored at -20 $^{\circ}$ C.

Section 2.4.16.4 Maxi-prep method

The Quiagen maxi-prep method was used for the large scale purification of plasmid DNA. This high quality DNA was used for either sequencing, synthesis of riboprobe or transfection of primary hepatocytes. An overnight culture of 200ml was pelleted by centrifugation at 7000 rpm in a JA-10 rotor for 15 minutes. The bacterial pellet was resuspended in 10ml of buffer P1. Immediately 10ml of buffer P2 was added and mixed thoroughly but gently by inverting the tube several times, and incubated at room temperature for 5 minutes. Ten millilitres of chilled buffer P3 was added and mixed as before. The sample was incubated on ice for 20 minutes and then centrifuged at 12000 rpm in a JA-20 rotor for 15 minutes, then the supernatant was promptly removed and stored on ice. A Qiagen-tip 500 was equilibrated with 10ml of buffer QBT, and the supernatant was applied to the column and allowed to drain through under gravity. The column was washed twice with 30ml buffer QC. DNA was eluted with 15ml of buffer QF, and precipitated by the addition of 10.5ml (0.7 volume of the eluant) of isopropanol. The solution was centrifuged at 12000 rpm for 30 minutes in a JA-20 rotor. The DNA pellet was washed with 5 ml of 70% ethanol. Finally the dried pellet, free of residual ethanol, was resuspended in 500 μ l

of filtered UHP water. The concentration of DNA was determined by measuring the $A_{260\text{nm}}$ of a diluted sample. DNA samples were stored at -20°C .

Section 2.4.17 Extraction and Purification of RNA

Section 2.4.17.1 Preparation of equilibrated Phenol

Phenol solutions were prepared from the crystalline solid and during the process any contaminants were removed and equilibrated to correct the pH for nucleic acid isolation. Five hundred grams of crystalline solid was melted at 68°C and then 0.1% (w/v) hydroxyquinoline was added. An equal volume of 0.5M Tris-HCl (pH 8.0) was added and stirred continuously for 20 minutes at room temperature. The mixture was then allowed to separate and the aqueous phase was discarded. The organic phenolic phase was then equilibrated with an equal volume of 0.1M Tris-HCl (pH 8.0) and again stirred for 20 minutes. The mixture was then allowed to separate into two phases and the aqueous phase removed. The phenol solution was equilibrated several times with 0.1M Tris-HCl until the desired pH (8.0) was achieved. The equilibrated phenol solution with a top layer of 0.1M Tris-HCl (pH 8.0) was stored in the dark at 4°C .

Section 2.4.17.2 RNA extraction from liver

Composition of Reagents:

Lysis Buffer: [5M Guanidinium Thiocyanate, 10mM EDTA, 50mM Tris-HCl, 8% 2-Mercaptoethanol (v/v)]

Precipitation Buffer: [4M Urea, 3M LiCl]

SDS-TE Buffer: [0.1% SDS (w/v), 1mM EDTA, 10mM Tris-HCl]

Phenol : Chloroform [1:1 (v/v)]

Ethanol: [90%, made with DEPC-treated water]

DEPC-treated water, autoclaved and filtered

To be utilised in RNase protection experiment, RNA was extracted from hamster liver using the method of Cathala *et al.* (1983). Frozen liver tissue (1-1.5g) was placed in RNase free polypropylene tube containing 5ml ice-cold lysis buffer and homogenised for 20-30 seconds using a Sil-

verstron homogeniser. To the homogenised samples 35ml of ice-cold precipitation buffer was added and mixed by gentle inversion for several times. The samples were left to precipitate at 4 °C overnight. Precipitated samples were centrifuged at 12 000g for 90 minutes at 4 °C in a JA20 rotor. The supernatant was removed and the pellet was resuspended in 5ml of ice-cold LiCl (3M). This was then centrifuged as before for 60 minutes and the supernatant was removed. The resulting pellet was resolubilised in 5ml of SDS-TE buffer and then mixed with an equal volume of phenol:chloroform. The sample was placed on ice for 20 minutes, vortexing for 30 seconds every 5 minutes. The sample was then frozen at -80 °C for 30 minutes and then thawed on ice. The sample was centrifuged at 10 000g for 15 minutes at 4 °C in a JA20 rotor. The aqueous phase was carefully extracted and phenol:chloroform treated as before. The resulting aqueous phase was ethanol precipitated at -20 °C overnight. Precipitated RNA was centrifuged at 10,000g for 15 minutes at 4 °C in a JA20 rotor. The pellet was washed twice in 5ml of 90% ethanol, and finally resuspended in 500µl DEPC treated water.

Section 2.4.17.3 Lithium chloride/ urea method

Composition of Reagents:

Lysis Buffer: [3M LiCl, 6M Urea, 10mM Sodium Acetate (pH 5.2)]

SDS: [10% (w/v)]

Aqueous Buffer: [18.8ml DEPC-treated Water, 200ml 1M Tris-HCl (pH 7.4), 1ml 10% SDS (w/v)]

Tris-Buffered Phenol (pH 8.0)

Chloroform : Isoamyl alcohol [24:1]

Absolute Ethanol

Ethanol: [70%, made with DEPC-treated water]

DEPC-treated Water, filtered and autoclaved

Frozen liver tissue (1-1.5g) was placed in an RNase free polypropylene tube containing 15ml of ice-cold lysis buffer and homogenised for 15 seconds, with a cooling period of 15 seconds, for

60 seconds using a Silverstron Homogeniser. To the homogenate 150 μ l of 10% SDS was added and the tube contents were mixed four times by gentle inversion, and left to precipitate at 4 $^{\circ}$ C overnight. The precipitated sample was centrifuged at 10 000g for 20 minutes at 4 $^{\circ}$ C in a JA20 rotor. The supernatant was discarded and the pellet was resuspended in 5ml of aqueous buffer. The solution was then transferred to a fresh clean tube containing 2.5ml of Tris buffered phenol and 2.5ml of chloroform:isoamyl alcohol. The solution was mixed by shaking vigorously on a rotary shaker for 15 minutes, and then centrifuged for 20 minutes as before. The aqueous phase was carefully transferred to a clean tube containing 2.5ml of phenol and 2.5ml of chloroform:isoamyl alcohol mix. This was mixed and centrifuged as before. The supernatant from this step was mixed with 5ml of chloroform:isoamyl alcohol, mixed by shaking and centrifuged for 10 minutes as before. The aqueous phase was then removed and ethanol precipitated at -20 $^{\circ}$ C overnight. Precipitated RNA was pelleted at 4 $^{\circ}$ C by centrifugation at 11 000g for 30 minutes in a JA-20 rotor. The pellet was washed in 70% ethanol, air-dried and resuspended in 250 μ l DEPC treated water. Resuspension was aided by incubating the tube at 65 $^{\circ}$ C for 10 minutes. RNA to be used immediately was stored at -20 $^{\circ}$ C, but for long term storage samples were kept at -80 $^{\circ}$ C.

Section 2.4.17.4 Guanidinium thiocyanate method

Composition of Reagents:

Denaturing Solution: [4M guanidinium thiocyanate, 25mM sodium citrate (pH 7.0),

0.5% sarcosyl (w/v), 0.1M 2-mercaptaethanol]

Sodium Acetate: [2M]

Phenol (water saturated)

Chloroform : isoamyl alcohol [49:1]

Liver tissue (0.1-0.2g) was homogenised in 10ml ice-cold denaturing solution for 30 seconds using a Silverstron Homogeniser. To the lysate, 0.1 volumes of sodium acetate, 1 volume of

phenol and 0.2 volumes of chloroform:isoamyl alcohol mixture were added sequentially. The homogenate was mixed thoroughly by inversion after the addition of each reagent. The final mixture was vortexed for 30 seconds and incubated on ice for 15 minutes. The aqueous and organic phases were separated by centrifugation at 10 000g for 20 minutes at 4 °C. The aqueous phase was carefully transferred to a clean tube and precipitated with 1 volume of isopropanol at -20 °C for 1 hour. Precipitated RNA was pelleted by centrifugation as before. The resulting pellet was washed with 70% ethanol and air-dried. The pellet was then dissolved in 200µl of DEPC water.

Section 2.4.17.5 From primary hepatocytes

Composition of Reagents:

Solution B: [4M Guanidinium Thiocyanate, 25mM Sodium Citrate (pH 7.0)]

Solution A: [Solution A was prepared by mixing Tris saturated Phenol, Solution B and 2M Sodium Acetate (pH 4.0)

in a ratio of 1:1:0.1. Prior to use, 720µl of β-mercaptoethanol was added to 100ml of solution A].

RNA was extracted from small amounts of tissue or from primary hepatocytes using the above method of Chomczynski and Sacchi (1987), as modified by Xie and Rothblum (1991). This method achieves greater yield on small amounts of tissue, and was therefore used to extract RNA from primary hepatocytes. At the end of culturing period, the monolayer was washed twice with cold PBS. The cells were lysed by directly pipetting 900µl of solution A (for 25cm² flask growth area) on to the cell monolayer, and the monolayer was harvested using a sterile RNase free cell scraper. The lysed cells were collected in a microfuge tube and placed on ice. To the lysate 100µl of chloroform:isoamyl alcohol was added and the phases mixed by vortexing for 10 seconds and then incubated on ice for 30 minutes. The aqueous and organic phases were separated by centrifugation at 14 000g for 20 minutes at 4 °C on a benchtop centrifuge. The aqueous phase was carefully transferred to a fresh Eppendorf tube and precipitated overnight

with 800 μ l (2 volumes) of ethanol at -20⁰C. The RNA was pelleted by centrifugation at 14 000g for 20 minutes at 4⁰C. The resulting pellet was washed with 70% ethanol and air-dried. The pellet was then resuspended in 20 μ l of DEPC water and stored at -20⁰C until required.

Section 2.4.17.6 Isolation of total RNA for cDNA cloning

Composition of Reagents:

RNA Isolation Reagent (Advanced Biotechnologies)

Chloroform

Isopropanol

Ethanol: [75%]

DEPC-treated water, 0.22 μ m filtered

Molecular cloning methodologies such as preparation of polyA⁺mRNA, PCR and 5' RACE require high quality RNA which is undegraded and free of protein and DNA contamination. For this reason Advanced Biotechnologies total RNA isolation kit was used for the extraction of hamster liver RNA which was subsequently used for the cloning experiment. RNA isolated using this kit is reported to produce very high quality RNA and is suitable for cloning purposes.

The protocol was followed according to the manufacturer instructions. Briefly, 0.5g of tissue was homogenized in 6ml of RNA reagent using a Polytron homogenizer. Following homogenization, the homogenate was stored at 4⁰C for 5 minutes to allow complete dissociation of nucleoprotein complexes. Five volumes of chloroform was added and shaken vigorously for 15 seconds and then placed on ice for 5 minutes. The homogenate was centrifuged at 14 000g for 15 minutes at 4⁰C. This allows the separation of RNA into the aqueous phase. The aqueous phase was transferred to a fresh tube containing equal volume of isopropanol and stored at 4⁰C for 10 minutes. Precipitated RNA was pelleted by centrifugation at 14 000g for 10 minutes at 4⁰C. The resulting pellet was washed with 70% ethanol and air-dried. The pellet was dissolved

in 500 μ l DEPC treated water by brief vortexing and incubation at 60 $^{\circ}$ C for 10 minutes.

Section 2.4.18 Purification of polyA+ RNA

Composition of Reagents:

Bind Buffer [5X]: [2.5M NaCl, 50mM Tris-HCl (pH 7.5), 0.5% Sarkosyl (v/v), 5mM EDTA (pH 8.0)]

DEPC-treated water, 0.22 μ m filtered

NaOH: [0.1M]

Oligo-dT resin (0.08g) was preswollen in 5ml of DEPC treated water at 4 $^{\circ}$ C for 1 hour. The swollen resin was then poured into a 2.5ml syringe barrel stuffed with siliconised and autoclaved glasswool at the base, and allowed to settle. The settled bed volume was approximately 0.5ml. The column resin was then washed with 20 volumes of 0.1M NaOH, followed by 30 volumes of DEPC treated water and then washed with 10 volumes of 1X Bind buffer. Total RNA, 1.25mg, was ethanol precipitated and resuspended in 1X bind buffer to give a final concentration of 0.5mg/ml. Prior to loading, the RNA sample was heated to 65 $^{\circ}$ C and loaded onto the centre of the resin-bed. The elute was collected and heated to 65 $^{\circ}$ C before being loaded onto the column resin again. This step was repeated once more. To remove unbound RNA, the column was washed with 5ml of 1X Bind buffer. Finally, bound RNA was eluted from the column by DEPC treated water. Ten 0.5ml aliquots of water, preheated to 65 $^{\circ}$ C, were loaded individually and their respective eluant fractions were collected separately in microfuge tubes. RNA in each eluant fraction was ethanol precipitated and then resolubilised in 10 μ l of DEPC treated water. Each RNA fraction was analysed on a 0.8% agarose gel (denaturing). The fractions containing polyA+ RNA were pooled and quantitated.

Section 2.5 Gene Cloning: PCR Cloning of cDNA

Synthesis of first strand cDNA

Composition of Reagents:

First Strand Buffer [5x]: [250 mM Tris-HCl (pH 8.3), 375mM KCl, 15mM MgCl₂, 100mM Dithiothreitol]

Superscript II Rnase H-Reverse Transcriptase: [(200U/ml) (Gibco BRL)]

Oligo-dT Primer: [12-18 Nucleotides Long (40µg/ml)]

DTT: [100mM]

dNTP Mix: [contain 10mM of the each nucleotide dATP, dGTP, dTTP and dCTP]

Total RNA of high quality was used for the synthesis of cDNA. Three separate reactions were carried out using three different amounts of total RNA (1, 2.5 and 5 µg). Appropriate amounts of RNA were added to tubes containing 500ng of oligo-dT primer and the total volume was adjusted to 12µl with DEPC treated water. This was heated to 70 °C for 10 minutes and then chilled on ice immediately. The tube contents were collected at the bottom by pulse-spin, and then 4µl of 5X first strand buffer, 2µl of DTT, 1µl of dNTP mix were added. Tubes were heated to 42 °C for 2 minutes, and the reaction was allowed to proceed by the addition of 1µl of superscript II enzyme and incubated at 42 °C for 45 minutes. The reaction was stopped by heat inactivating the enzyme at 70 °C for 15 minutes. The tubes were cooled on ice and 2µl of RNase H was added, and then incubated at 37 °C for 20 minutes. A DE81 incorporation test was carried out using 2µg RNA to show that cDNA synthesis has occurred. For this, a separate reaction was carried out using the same reagents and conditions as above but 1µl of [³H] dCTP was added to the reaction for the incorporation test.

Section 2.5.1 PCR Amplification of cDNA

cDNA synthesised from reverse transcribed hamster total RNA was used for the PCR amplification of putative hamster CYP4A and PPARα gene fragments. To generate CYP4A fragment, PCR primers were designed from regions of DNA sequence identity by sequence alignment of known CYP4A subfamilies of different species. For PPARα, primers were designed from regions of DNA sequence identity after alignment of PPARα genes from known species.

Primers used for CYP4A cloning:

HMcyp-P1: 5'-AAGCTTGAATTCTTGTCTGACAAGGACCTACGTGCTGAGGTGGACAC-3'

HMcyp-P2: 5'-AAGCTTGGATCCCATCTCACTCATAGCAAATTGTTTCCCAAT-3'

Primers used for PPAR α cloning:

HMppar-P1: 5'-CTCAGTACATGTCCCTGTAGAT-3'

HMppar-P2: 5'-TACGGAGTTCACGCATGTGAAGGCTGCAAGGGCTTCTT-3'

Composition of Reagents:

KlenTaq PCR Buffer: [400mM Tricine-KOH (pH 9.2 at 25 °C), 150mM KOAc, 35mM Mg(OAc)₂, BSA (750mg/ml)]

KlenTaq Polymerase Mix: [Taq start antibody:Antibody dilution buffer:DNA polymerase (1:4:1,v/v/v)]

dNTP mix: [10mM of each nucleotide: dATP, dGTP, dCTP, dTTP (Pharmacia)]

Autoclaved UHP water

The “good start” procedure was employed for the PCR reaction. Components were added to a 0.5ml PCR tube sitting on ice in the order shown: 16 μ l water, 2.5 μ l KlenTaq PCR buffer, 1.5 μ l 5'-primer (40 pmol), 1.5 μ l 3'-primer (40 pmol), 1 μ l dNTP mix, 2 μ l cDNA (in the case of positive controls <50ng of plasmid DNA was used while water was used for negative control), 0.5 μ l of KlenTaq polymerase mix. The tube contents were gently mixed by tapping and pulse-centrifuged to collect to the bottom. The reaction mix was then overlaid with 2 drops (~30 μ l) of mineral oil to prevent evaporation, and the tubes were transferred directly from ice to the thermal cycler block pre-equilibrated to 94 °C. PCR reaction was performed in a Perkin Elmer DNA thermal cycler using a three step cycle for a total of 25 cycles:

Step 1- denaturation: 94 °C for 1 minute

Step 2- primer annealing: 50 °C for 1 minute

Step 3- primer extension: 72 °C for 1 minute

The following formula was used to calculate annealing temperature of the primers.

$$81.5 + 16.6(-\log [\text{salt} +]) + 0.41 (\% \text{ GC}) - (675 / \text{number of nucleotides in primer})$$

5µl of each PCR reaction mixture was analysed on a 1% agarose gel, made with 1XTBE, prestained with syber green and run at 90 volts for 1 hour.

Section 2.5.2 Purification of PCR products

Composition of Reagents:

Quiaquick PCR Purification Kit:

PB Buffer

PE wash Buffer

Qiaquick Columns

Autoclaved UHP water

Each PCR reaction was diluted with 250µl of PB buffer. The sample was placed in a Qiaquick spin column and centrifuged for 30 seconds in a bench-top microcentrifuge (13,000 rpm), and the flow through was discarded. The column was washed with 0.7ml of PE buffer, and then centrifuged at 13,000 rpm for 30 seconds. The flow through was discarded and the column was centrifuged again at 12,000 rpm for a further 30 seconds to remove traces of residual PE wash buffer. DNA bound to the column was eluted with 40µl of water by centrifugation at 13,000 rpm for 60 seconds.

Section 2.5.3 Ligation of amplified DNA fragment

Components used:

Ligation kit, supplied by Promega

Cloning Plamid: [pGEM-T and pGEM-T easy vector (50ng/µl): pGEM-5Zf(+)

digested with EcoRV and 3' terminal thymidines added]

T4 DNA Ligase Buffer (10X): [300mM Tris-HCl (pH 7.8), 100mM MgCl₂, 100mM DTT, 5mM ATP]

T4 DNA Ligase: [10 units/μl in 10mM Tris-HCl (pH 7.4), 50mM KCl, 1mM DTT, 0.1mM EDTA, 50% Glycerol]

Purified PCR products were ligated into either pGEM-T or pGEM-T easy vector. Ligation reactions were assembled at room temperature using 1μl of 10X T4 DNA ligase buffer, 1μl pGEM-T/easy vector, 4μl PCR product, 3μl water and 1μl T4 DNA ligase. The tube contents were mixed and pulse-spun, and incubated at 4 °C overnight.

Section 2.5.4 Selection of recombinant plasmids

Ligated PCR products were transformed into electrocompetent *E.coli* XL-1 blue strain. One μl of ligation reaction product was used to transform 60μl of XL-1 blue cells. Blue/white selection was used for the screening of plasmid containing the insert. To do this, 100μl of transformed cells were plated on a Tet/Amp LB-agar plate containing 0.5mM IPTG and 80μg/ml X-gal. Cells carrying recombinant plasmid (containing an insert) appear as white colonies whereas those with non-recombinant plasmid appear as blue colonies on the selection plate. Individual colonies of 25 white and 2 blue colonies were picked and inoculated in 5ml of Tet/Amp LB-broth. Plasmid minipreps were carried out using the alkaline lysis method, and the DNA was analysed on a 1% agarose gel. Three independent colonies containing plasmids positive for the insert were Quiagen miniprepmed and the inserted fragment was sequenced from both directions.

Section 2.5.5 Amplification of 5'-cDNA ends

Gene Specific Primers (GSP):

RACE 1: 5'-GGCATTGTGGAAGCGGCAGTATTGGC-3'

RACE 2: 5'-CAGCTTCGATCACATTTGTCATACGCCAGC-3'

RACE 3: 5'-GAAGCCCTTGCAGCCTTCACATGCGTG-3'

Rapid Amplification of 5'-cDNA Ends (RACE) is a procedure for amplification of nucleic acid sequences from an mRNA template between a defined internal site and unknown sequences at the 5'-end of the mRNA. Gibco BRL 5' RACE kit was used for cloning the remainder of the 5'-end of the putative hamster PPAR α gene. Two parallel reactions were carried out using either 1 μ g of total RNA or polyA⁺ RNA. One μ l of GSP (RACE 1) was added to each tube and the final volume was adjusted to 15.5 μ l with DEPC treated water. The tubes were heated at 70 °C for 10 minutes to denature secondary RNA structures. The tubes were chilled on ice and then centrifuged briefly. The following components were added to the tubes and then incubated at 48 °C for 1 minute: 2.5 μ l of 10X PCR buffer, 2.5 μ l of MgCl₂, 1 μ l of dNTP mix and 2.5 μ l of DTT. The reactions was initiated by the addition of 1 μ l of Superscript II reverse transcriptase and incubated for a further 50 minutes at 42 °C. The reaction was terminated by heat denaturing the enzyme at 70 °C for 15 minutes. The tubes were briefly centrifuged and then 1 μ l of RNase mix was added to each tube. RNase treatment was carried out for 30 minutes at 37 °C.

Section 2.5.6 Purification of First strand product

Excess nucleotides and RACE1 primers were removed from the first strand cDNA product which otherwise will interfere in subsequent reactions, such as the homopolymeric tailing reaction. First strand cDNA product was purified using a Gibco BRL glassmax DNA isolation spin cartridge. After equilibrating the binding solution (6M NaI) to room temperature, 120 μ l of this solution was added to the first strand reaction, and the mixture was transferred to a spin cartridge. This was then centrifuged for 20 seconds at 13 000g. DNA bound to the column was washed four times with 0.4ml of cold wash buffer followed by two washes of 70% ethanol by brief centrifugation (20 seconds in each step). Finally, bound DNA was eluted with 40 μ l of sterilized water (preheated to 65 °C) by centrifugation at 13 000g for 25 seconds.

Section 2.5.7 Homopolymeric tailing of cDNA

Terminal deoxynucleotidyl transferase (TdT) was used to add a homopolymeric tail of dCTP's on the 3'-end of the purified cDNA. TdT-tailing was carried out on cDNA made from both total and polyA⁺ RNA. The following reaction components were added to each tube: 6.5µl of DEPC-treated water, 5µl of 5X tailing buffer, 2.5µl of 2mM dCTP was and 10µl of glassmax purified cDNA. To evaluate the specificity of the subsequent amplification reaction from the oligo-dC tail, a negative control was included that omits TdT in the reaction. The tubes were incubated at 94 °C for 3 minutes, and then chilled on ice for 1 minute. The contents of the tube were collected by brief centrifugation and then 1µl of TdT enzyme was added to each tube and the reactions were incubated at 37 °C for 10 minutes. The reaction was stopped by heat inactivating TdT at 65 °C for 10 mins.

Section 2.5.8 PCR of dC-tailed cDNA

PCR amplification of dC-tailed cDNA was carried out by employing the "hot start" procedure to improve the specificity of the reaction. All the reaction components were from RACE kit except the custom made internal genespecific primer and Taq polymerase (red hot polymerase mix, Advanced Biotechnologies). Components were added to 0.5ml PCR tubes sitting on ice in the order shown: 33.5µl water, 5µl PCR buffer, 3µl MgCl₂, 1µl 10mM dNTP mix, 1µl nested GSP2 (RACE1), 2µl anchor primer, 5µl dC-tailed cDNA. The contents of the tubes were mixed by gentle tapping and pulse-centrifuged to collect to the bottom. The tubes were then transferred to a thermal cycler block preequilibrated at 94 °C. Taq polymerase mix (0.5µl) was added directly to the tube sitting on the heat block and the reaction was overlaid with 2 drops (~30µl) of mineral oil to prevent evaporation. Two negative controls were included where one contained cDNA that underwent a dC-tailing reaction with TdT omitted while the other contained no cDNA. PCR reactions were performed in a Perkin Elmer DNA thermal cycler using a three step cycle for a total of 20 cycles:

Step 1- denaturation: 94 °C for 1 minute

Step 2- primer annealing: 65 °C for 1 minute

Step 3- primer extension: 72 °C for 1 minute

5µl of each PCR reaction was analysed on a 1% agarose gel, made with 1XTBE. PCR products from this first round were diluted 50-fold, and then 5µl of this was reamplified using GSP (RACE 2) and anchor primer for 25 cycles using the same reaction condition as above. PCR reaction products were analysed on a 1% agarose gel, made with 1XTBE. PCR products were purified using Qiagen Qiaquick PCR purification spin columns. A third round of PCR was performed using GSP (RACE 3) and the amplified products were purified as above.

Section 2.5.9 Cloning of putative 5'-cDNA RACE products

Purified RACE products were ligated into pGEM-T easy vector. The ligated products were transformed into electrocompetent *E.coli* XL2/blue cells. Blue/white selection was used to select for plasmids containing an insert. Individual colonies (25 white and 2 blue) were picked and inoculated in 5ml Tet/Amp LB-broth. Plasmid minipreps were carried out using the alkaline lysis method. Restriction digests were performed on all the plasmids DNA using EcoRI enzyme to determine the size of the cloned insert. Restriction digests were analysed on a 1% agarose gel. A diagrammatic representation of the PPAR α cDNA cloned into the cloning vector and the primers used for sequencing is outlined in Figure 2.1.

Section 2.6 DNA Sequencing and analysis

Quiagen purified DNA was sent to the Biomedical Synthesis and Analysis unit (Queens Medical Centre, Nottingham) for sequencing. An ABI prism dye terminator cycle sequencing kit (Perkin Elmer) was used for the PCR stage of the sequencing protocol, and the sequencing reactions were analysed on a 373A DNA sequencer (Perkin Elmer). Initially, T7 and SP6 primers

were used to obtain the first part of the sequence of the cloned DNA from both directions. Primers (“custom-made”) were then designed from this and used for subsequent sequencing to obtain the full sequence of the cloned fragment. A list of primers used for this oligonucleotide-directed sequencing of hamster PPAR α and CYP4A cDNA are shown in Table 2.1 and Table 2.2.

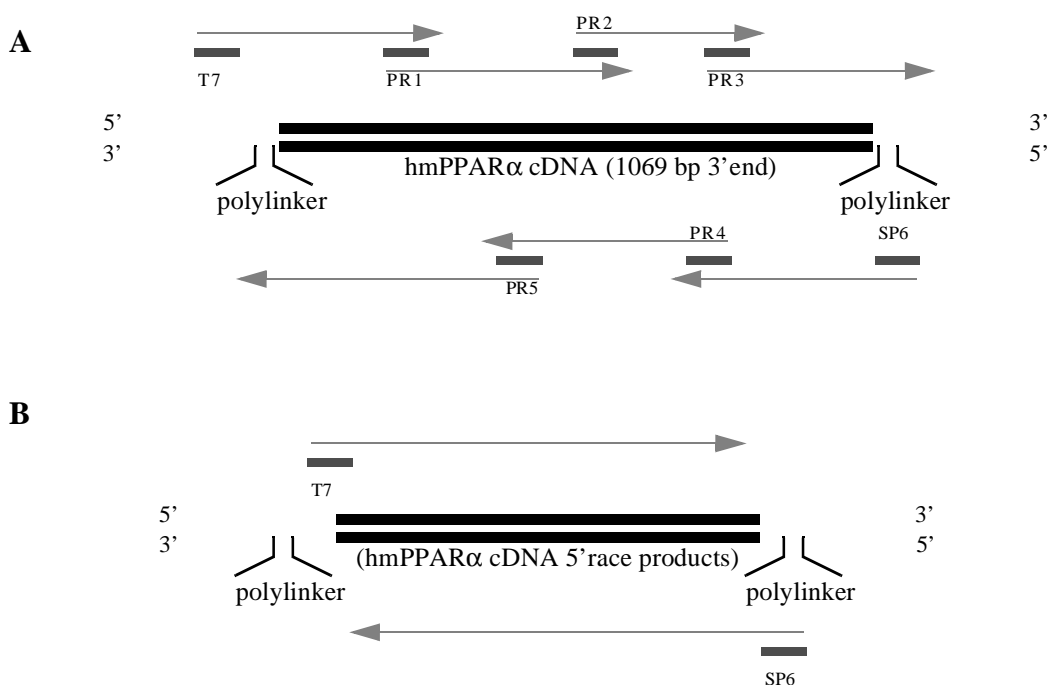


Figure 2.1 Sequencing strategy for hamster PPAR α . 1069 bp sequence from the 3' end of hamster PPAR α cDNA was cloned into pGEMT vector by PCR (A) and was sequenced with designed sequencing primers as indicated. The remaining 5' end of the PPAR α cDNA (B) was cloned using 5'RACE strategy. For 5'RACE gene specific primers were designed from the 1069 bp cloned fragment and the amplified fragment was cloned in pGEMT-Easy vector for sequencing. Primers used for sequencing are shown by arrows in the diagram and individual primer sequences are shown in Table 2.1 below. Cloned fragments are shown by solid lines.

primer name	primer sequence (5' to 3')
T7	TAATACGACTCACTATAGGGCGA
PR1	TCAACATGAATAAGGTCAAGGCC
PR2	ACATGGAGACCTTGTGTATGGCTGAG
PR3	CATAGGATACATTGAGAAGATGC
SP6	GTATTCTATAGTGTACCTAAAT
PR4	GTGCACGATACCCTCCTGCATCT
PR5	TTGCGAAGCCTGGGATGGCCTTG

Table 2.1 Sequence primers used for hamster PPAR α . The sequence of the primers used for sequencing cloned hamster PPAR α cDNA are shown on the right, and their name on the left.

primer used	primer sequence (5' to 3')	clone number
T7	TAATACGACTCACTATAGGGCGA	all clones
PR6	AAATGGAGAGTACAACCTGTGGCA	3, 4, 5, 8, 9
SP6	GTATTCTATAGTGTACCTAAAT	all clones
PR7	GATCCTCCATTACCTGGAATCAC	3, 4, 5, 8, 9
PR8	CATCAGGGAAGGTGACAGGTGTG	1, 6, 12-14, 15-18
PR9	ACCTGGGATCACCTGGACCAGAT	1, 6, 12-14, 15-18

Table 2.2 Sequence of primers for hamster CYP4A cDNA. The sequence of the primers used for sequencing cloned hamster CYP4A cDNA are shown on the right, and their name and clone number on the left.

Sequence chromatograms were viewed using CHROMAS software, and the raw DNA sequences were edited using GCG sequence analysis software (Winconsin Package, version 9.0). Within the GCG programme TED and SEQED were used for sequence editing; PILEUP, GAP and BESTFIT were used for sequence alignment and comparison; GELSTART, GELENTER, GELMERGE and GELASSEMBLE were used for the generation of consensus sequence; and MAP and TRANSLATE were used for obtaining protein sequences from consensus DNA se-

quences. Protein sequence alignments and phylogenetic analysis was done using GCG, CLUSTALW 1.6 (Thompson *et al.*, 1994), SAGA for optimised alignments (Notredame and Higgins 1996), Puzzle 4 for maximum likelihood analysis (Strimmer and von Haeseler, 1996), Genedoc (Nicholas and Nicholas 1997), and Treeview computer programs. Raw DNA sequences were inspected and edited using GCG sequence analysis software. The software programs used were, TED, SEQED, BESTFIT, GENASSEMBLE and MAP (Wisconsin Package Version 9.0).

Section 2.7 Gene Expression Studies

Section 2.7.1 RNase Protection Assay

Section 2.7.1.1 Template Generation

Composition of Reagents:

Ammonium Acetate: [7M]

Phenol:Chloroform [1:1 (v/v)]

Template DNA: [1mg/ml]

Proteinase K: [100mg/ml]

Ethanol: [70%]

Plasmid (pGEM7) containing rat or mouse CYP4A cDNA was used to generate the template for protection assay. Plasmid was linearised with NcoI which has a unique restriction site within the CYP4A1 sequence. When this linearised template is transcribed from a T7 promoter, a 200bp antisense probe is generated. To generate the template, 10µg of DNA was digested to completion (as determined by agarose gel) using NcoI. This was first proteinase K (10 µg/µl) treated for 1 hour at 37 °C in the presence of 0.1% SDS then phenol:chloroform treated, vortexed and centrifuged. DNA in the top aqueous layer was precipitated with two volumes of absolute ethanol and 0.25 volumes of 7M ammonium acetate. This was left on ice for 20 minutes and then centrifuged. The resulting pellet was washed with 70% ethanol and resuspended in

10 μ l of DEPC-treated H₂O.

Section 2.7.1.2 RNA transcription *in vitro*

RNA probes were prepared by incorporating radiolabelled [α^{32} P] CTP as the base analogue in the transcription reaction. The following reaction components were mixed at room temperature for transcription:

component	volume (μ l)
[5X] Transcription Buffer	4.0
100 mM DTT	1.0
RNA Guard	1.0
5 mM A, G & UTP mix	4.0
DEPC-treated H ₂ O	13.0
[α^{32} P] CTP	5.0
100 mM Cold CTP	1.0
DNA (1 μ g/ μ l)	1.0

To begin the reaction 1 μ l of T7 RNA polymerase was added and incubated at 37⁰C for 1 hour. At the end of incubation period the DNA template was removed by the addition of 1 μ l (10 Units/ μ l) DNaseI and incubated for further 15 minutes. Incorporation of radioactivity was determined by the DE-81 test. After DNase treatment, labelled probe was phenol:chloroform treated, ethanol precipitated, and centrifuged (as for template). The resulting pellet was resuspended in 15 μ l deionised formamide.

Section 2.7.1.3 Probe Hybridisation

Composition of reagents:

Total RNA: [10 μ g/ μ l]

Yeast tRNA: [10 μ g/ μ l in DEPC-treated water]

RNA probe, [α^{32} P] CTP labelled

Hybridisation Buffer: [80% Formamide, 40mM PIPES (pH 6.7), 5M NaCl, 0.4M EDTA]

RNase Buffer: [0.35 NaCl, 10mM Tris-HCl (pH 7.5), 5mM EDTA (pH 7.5)]

RNase A: [10 mg/ml]

Proteinase K: [100mg/ml]

SDS: [10% w/v]

Phenol:chloroform: [1:1 (v/v)]

Sodium acetate: [7M, pH5.2]

Protection Gel Load Buffer: [90% Formamide (v/v), 1X TBE,

0.25% Xylene Cyanol (w/v)], 0.2% Bromophenol Blue (w/v)]

Gel Running Buffer: [10X TBE]

Denaturing Urea-Acrylamide Gel: [6%]

Fixing Solution: [10% Methanol, 10% Glacial Acetic Acid]

Samples were prepared by precipitating 30µg total RNA by the ethanol/ammonium acetate precipitation method. To show the specificity of the hybridised probe, two lots of 30 mg of yeast tRNA were also precipitated and incubated in the presence or absence of RNase A following hybridisation reaction with the probe. These are termed tRNA^{+ve} (yeast tRNA treated with RNase A) and tRNA^{-ve} (yeast tRNA treated without RNase A). RNA pellets were stored at -20 °C until use. For hybridisation reactions, probe was diluted in the range of 1:100 to 1:500, depending on the percentage incorporation, in hybridisation buffer. Thirty µl of this buffer was used to hybridize 30µg of RNA sample. RNA pellets were resuspended by brief vortexing and then heated to 85 °C for 3 minutes to denature RNA secondary structure. Hybridisation was carried out overnight at 45 °C. After overnight incubation, samples were treated for 1 hour at 37 °C with 300µl RNase buffer containing 10mg/ml RNase A. RNase A was omitted from the tRNA^{-ve} sample. The samples were then incubated at 37 °C for one hour. Following RNase treatment, samples were treated with Proteinase K (10mg/ml) in the presence of 0.1% SDS for 45 minutes at 50 °C. Samples were then phenol:chloroform treated, and the aqueous phase was

ethanol precipitated with 7M ammonium acetate. The resulting pellet was resuspended in 10ml of protection load buffer by vigorous vortexing. Prior to loading on the gel, samples were heated at 85 °C for 3 minutes, cooled on ice and then briefly centrifuged to collect the tube contents. Samples were run on a 6% denaturing polyacrylamide gel, using 1X TBE buffer, at 120 volts for 90 minutes, after which the gel was placed in fixing solution for 30 minutes and dried on a vacuum gel dryer. For visualisation of signal, Kodak X-ray Hyper film was exposed to the gel at -80 °C and developed. The same gel was also used to quantify protected bands using a Bio-Rad molecular imager. To develop the exposed film the following steps were performed: soaked in 1X developer for 2 minutes, washed in water for 2 minutes, fixed in 1X fixing solution for 1 minute, and then allowed to air dry.

Section 2.8 *In situ* Hybridization

Section 2.8.1 Tissue preparation and sectioning

Localisation of PPAR α and steroid receptor-coactivator proteins mRNA in the liver mouse liver was carried out using *in situ* hybridisation as described by Srinathsinghji *et al.* (1990). Control and MCP (20mg/kg) treated liver were obtained as described in section 2.4.17. Liver sections were taken from lobes and frozen in Tissue-Tec and isopropanol on ice (by dropping in small volume of Tissue-Tec then placed on weighting boat on isopropanol on ice). Tissue-Tec containing liver lobes was frozen at -70 °C for cryo-sectioning. Slides were prepared 24 hours before sectioning by coating with Poly-L-Lysine (5mg/ml) and baked for 2 to 3 hours, and the slides were stored in a metal rack covered in aluminium foil until use. Cryo-sections of 1 μ m thickness were cut with a cryotome, placed on poly-L-lysine coated slides and stored in 95% ethanol at 4 °C. Sections were usually prepared 24 hours prior to the hybridisation experiment.

Section 2.8.2 Probe Labelling and Hybridisation

Sense and anti-sense oligo-probes of 45 nucleotides in length were designed from 5'-end of respective mouse gene concerned and synthesized by John Kyte (Biomedical Synthesis and Anal-

ysis unit, QMC, Nottingham). Sense and antisense oligo-probes used are listed in Table 2.3.

Primer	Sequence (5' to 3')
PBP sense	CCATACACTGATCCAGCTGACCTTATTGCAGATGCTGCTGGAAGC
PBP antisense	GCTTCCAGCAGCATCTGCAATAAGGTCAGCTGGATCAGTGTATGG
SRC-1 sense	AGCTCACAGCTGGATGAGCTCCTCTGTCCACCAACAACAGTAGAA
SRC-1 antisense	TTCTACTGTTGTTGGTGGACAGAGGAGCTCATCCAGCTGTGAGTC
CBP/p300 sense	GCAGGAGAGCAAGTACATAGAGGAGCTGGCAGAGCTCATCTCTGC
CBP/p300 antisense	GCAGAGATGGACTCTGCCAGCTCCTCTATGTACTTGCTCTCCTGC
GS sense	CAGTCTGAAGGCTCCAACAGCGACATGTACCTCCATCCTGTTGCC
GS antisense	GGCAACAGGATGGAGGTACATGTGCTGTTGGAGCCTTCAGACTG
RIP-140 antisense	GAGGAAGGACTGGCCTCGTTGTCAGTGGTCACGGCTCCATCTGTC
PGC-1 antisense	CTAGAGCTGAATGACTGAAGCAAAGAGGCCAGCAATGTGCTATCC

Table 2.3 List of oligo primers used for *in situ* hybridisation.

A Boehringer Mannheim TdT (terminal deoxynucleotidyl transferase) labelling kit was used to label both sense and anti-sense probes. Terminal transferase from calf thymus was used to label the 3' ends of single stranded oligo probes with radioactively labelled [$\alpha^{35}\text{S}$] dATP. The following components were mixed in a 0.5ml microfuge tube and incubated at 37 °C for 1 hour:

component	volume (μl)
[5X] TdT buffer	2.0
CoCl_2	1.0
TdT enzyme (25 units/ μl)	1.0
dATP [$\alpha^{35}\text{S}$] (12.5 mCi/ml)	1.0
Oligo-probe (4 ng/ μl)	2.5
DEPC-treated H_2O	2.5

The reaction was terminated by the addition of 40 μl H_2O

Section 2.8.2.1 Purification of the probe

Non-incorporated dATP was removed from the reaction mix using a Sephadex G-50 column. The matrix was prepared by suspending 5g of Sephadex G-50 in 100ml of TENS solution (5.84g NaCl, 1.58g Tris, 0.37g EDTA dissolved in 1 litre H₂O and adjusted to pH 8.0), stood overnight, DEPC treated and autoclaved. The Sephadex column was made by plugging the bottom of a 2ml syringe barrel with autoclaved siliconised glasswool and Sephadex suspension was poured and allowed to set. The tube was spun briefly at 2000g to drain residual liquid. Before the addition of the diluted reaction mix to the column 1µl was removed for scintillation counting (representing total radioactivity in the reaction). The probe preparation was added to the top of the column and spun at 2500 rpm at 4 °C for 10 minutes. Incorporation of radioactivity in the probe was measured by scintillation counting of 1µl of this spun sample and comparing this to the total radioactivity of the reaction. Two µl of 1M DTT was added to the purified probe and kept on ice until required.

Section 2.8.2.2 Hybridisation**composition of reagents**

Hybridisation Buffer:

To make 10ml of hybridisation buffer following components were added and warmed to 50 °C and then 1 gram of dextran sulphate gradually added and mixed to homogeneity.

component	volume (ml)
100% Deionised Formamide	5.0
20x SSC	2.0
0.5M Sodium Phosphate	0.5
0.1M Sodium Pyrophosphate	0.1
[10x] Denharts	0.5
Salmon sperm (10mg/ml)	0.2
Polyadenylic Acid (5mg/ml)	0.2
Sodium Heparin (120mg/ml)	0.01
1M DTT	0.2
DEPC-treated H ₂ O	~1.29

Slides containing tissue sections were removed from ethanol and air-dried in a fume hood. Probes were diluted in hybridisation buffer to a final radioactivity of 150,000 cpm/50 μ l. Fifty μ l of diluted probe was applied to the tissue section of each slide and then overlaid with the underside of NESCO film to prevent evaporation of the hybridisation solution. The slides were placed inside a sterile humidified (with DEPC-treated H₂O) bioassay dish and incubated overnight at 42 °C in sterile oven free from RNase contamination.

Section 2.8.2.3 Stringency Washes

Following hybridisation a series of washes with decreasing salt concentrations were performed with gentle agitation on four-way rocker to remove any non-hybridised probe. Slides were first washed for 20 minutes at room temperature in 1x SSC/0.5% β -mercaptoethanol [SSC = 1.75.3g NaCl, 88.2g Sodium Citrate per litre DEPC-treated H₂O, adjusted to pH 7.0]. Two 35 minutes washes were then carried out at 55 °C in 1x SSC, and then one wash with 0.1x SSC at room temperature. Slides were dehydrated by dipping first in 70% ethanol and then in 95% ethanol for 10 seconds and then air-dried.

Section 2.8.2.4 Emulsion Autoradiography

In order to detect radioactive signal on the tissue section, dried slides were coated with silver grain emulsion (Kodak liquid autoradiography emulsion) by dipping in the emulsion briefly in the dark and then air-dried. Coated slides were placed in a light-proof box and exposed at 4 °C until optimal signal could be detected. After an appropriate length of exposure, slides were developed as for normal autoradiography by placing in developer for 5 minutes, 2 minutes in water, 5 minutes in fixer and 20 minutes in water. Soon after fixation, tissue sections were stained with haematoxylin for 10 minutes, washed in running water for 10 minutes and then dehydrated in a series of alcohols: 70%, 90% and 100% ethanol for 1 minute each. Slides were dried at room temperature and coverslip was placed in between tissue sections and oil-based mountant. Slides were viewed under light-field microscopy for the detection of signal that appears as black silver grains over the cell nuclei.

Section 2.9 Protein Methodologies

Section 2.9.1 Bradford Assay

Composition of Reagents:

Bradford reagent:

the following chemicals were dissolved in and made up to 1 litre with UHP water and filtered through Whatman paper.

Serva blue G	100 mg
85% Phosphoric acid	100 ml
95% ethanol	50 ml

1M NaOH

Bovine Serum Albumin (2mg/ml)

Protein standards were prepared using Bovine Serum Albumin (BSA) to cover a protein concentration range of 0-40µg/ml. For assay purposes, 30µl of protein sample was mixed with 50µl

of 1M NaOH and then 950 μ l of Bradford reagent was added. The solution was vortexed thoroughly and incubated at room temperature for 5 minutes. Their absorbance was measured immediately at 590nm using a plastic cuvette. Each sample and protein standard were assayed in triplicate and the mean values were used. A linear plot ($r^2 > 0.95$) of BSA standard was used to determine the concentration of protein samples.

Section 2.9.2 SDS-Polyacrylamide gelelectrophoresis (SDS-PAGE)

Composition of Reagents:

SDS-PAGE Loading Buffer[5X]: [250mM Tris-HCl (pH 6.8), 0.5M DTT, 10% SDS (w/v),

0.5% Bromophenol Blue (w/v), 50% glycerol (v/v)]

Electrophoresis Buffer: [25mM Tris-HCl (pH 8.3), 250mM Glycine, 0.1% SDS (w/v)]

Coomassie Blue: [0.25g Coomassie Brilliant Blue R250 in 90ml Methanol:Water (1:1), 10ml Glacial acetic acid]

Destaining Solution: [30% methanol, 10% glacial acetic acid]

SDS-PAGE, first described by Laemmli 1970, separate proteins by molecular weight under denaturing conditions. Interaction of SDS with the amino acid chain of the protein results in a net negative charge, and therefore proteins are separated according to the length of the protein i.e. molecular weight. A 12% gel (resolution range 12-75 kDa) was used to separate the protein of interest which has a molecular weight of 33.3 kDa. Protein gels were prepared and run using a Bio-Rad Mini-PROTEAIN II electrophoresis kit as instructed by the manufacturer. Resolving and stacking gel mixes were premade separately by adding the following components and stored at 4 $^{\circ}$ C until required, with the exception of 10% APS, which was added to the required gel volume on the day of use prior to pouring into the gel plate:

Composition of a 12% Resolving & 5% Stacking Gel mix (100ml):

component	resolving gel (ml)	stacking gel (ml)
30% acrylamide/0.8% bisacrylamide (37.5:1)	40	17
1.5M Tris-HCl (pH 8.8)	25	---
1.0M Tris-HCl (pH 6.8)	---	13
Autoclaved UHP H ₂ O	33	68
10% SDS	1.0	1.0
TEMED	0.04	0.04
10% APS	1.0	1.0

Polymerisation of resolving gel was initiated by the addition of 10% APS, and the solution was immediately poured into the assembled gel plates. Soon after the pouring of the gel solution, it was overlaid with 300µl of 0.1% SDS and left to polymerise at room temperature for 30 minutes. SDS was decanted off the surface and cleaned with water. Stacking gel mix (containing SDS) was applied to the top of the resolving gel and a comb was inserted at the top of the gel plate. The gel was left to polymerize for 30 minutes.

Protein samples were prepared by mixing with 1x loading buffer and denatured by boiling in water for five minutes and then placed on ice. Appropriate amounts of protein samples were loaded into the gel and electrophoresis was carried out using electrophoresis buffer for 60 minutes. Initially a voltage of 20mA/gel was applied until the sample had fully entered the stacking gel, after which the current was increased to 75mA/gel.

Section 2.9.3 Coomassie staining

For visualisation of the resolved protein bands Coomassie blue staining was employed. Immediately after electrophoresis, the gel was immersed in Coomassie staining solution and stained for 2-3 hours with gentle agitation. The gel was then destained with several changes of destain-

ing solution until the protein bands were clearly visible. Gels were placed onto Whatman 3MM chromatography paper and dried under a vacuum at 80 °C for 60 minutes using Bio-Rad 583 gel dryer.

Section 2.9.4 Immunoblotting

Composition of reagents:

Methanol

Blocking Solution: [10% Marvel dried milk powder made with 1X TTBS]

1X TBS: [20mM Tris-HCl (pH 7.6), 500 mM NaCl]

1X TTBS: [1X TBS containing 0.1% Tween-20 (v/v)]

Transfer Buffer: [25 mM Tris-HCl, 192 mM glycine, 20% methanol (v/v), 0.1% SDS (w/v)]

Primary Antibody: [Rabbit Anti-mouse PPAR α polyclonal antibody]

Secondary Antibody: [Goat Anti-rabbit IgG (H+L) conjugated to horseradish peroxidase]

ECL Western Blotting detection kit (Amersham Life Science)

1X Developer Solution; 1X Fixing Solution (Ilford)

Section 2.9.5 Electrophoretic transfer of proteins

Protein samples (1-20 μ g) were first resolved by SDS-PAGE on a 12% gel and then transferred onto the nitrocellulose filter for immunoblotting according to the modified method of Towbin *et al* (1979). The gel was first soaked in transfer buffer for 10 minutes and then placed onto two sheets of whatman paper pre-wetted with transfer buffer. An appropriate sized PVDF membrane (millipore), pre-soaked in methanol for 2 minutes and then in transfer buffer for 10 minutes, was placed on top of the gel, carefully removing any air bubbles. Two more sheets of pre-wetted whatman paper were placed on the membrane to sandwich the gel and the membrane. The sandwiched gel was placed into a blotting cassette and electrotransfer of protein to the membrane was carried out in a Transblot cell containing transfer buffer at 4 °C for 1 hour at a constant voltage of 90V.

Section 2.9.6 Probing of transferred protein with antibody

After transfer of protein, the membrane was placed in blocking solution and incubated at room temperature overnight. The blot was then incubated with primary antibody: rabbit anti-mouse PPAR α antibody (1:20000 dilution with 1X TTBS containing 10% Marvel) for 2 hours with continuous agitation. The blot was washed four times with ample amounts of 1X TTBS, 5 minutes for each wash. After washing in TTBS the blot was incubated with secondary antibody: goat anti-rabbit IgG-HRP antibody (1:40000 dilution with 1X TTBS containing 10% Marvel) for 1 hour with continuous agitation. The blot was then washed with TTBS as before and developed using the ECL kit as instructed by the manufacturer. The blot was exposed to Hyperfilm (Amersham Life Science) and then developed.

Section 2.9.7 Expression of bacterially expressed recombinant protein

Mouse PPAR α -LBD, also termed LBD^{wt}, encoding the region from amino acid residue 194 to 468, and subcloned into pET15b vector and transformed in BL21[DE3]PLysS bacterial strain was a kind gift from Dr Colin Palmer (Dundee); Additionally, a mutant version of this LBD protein was also obtained, named G-mutant or LBD^{mut} (where glycine is substituted for glutamine at residue 282) (Hsu *et al.*, 1995). Two types of negative control were used for the expression study: one control was the non-transformed bacterial strain BL21(DE3)PLysS, while the other was bacterial strain BL21(DE3)PLysS transformed with the same expression plasmid but without the insert.

Section 2.9.8 Induction of His-tagged Protein**Composition of reagents:**

IPTG: [1M]

Antibiotics: [50 μ M Ampicillin and 30 μ M Chloramphenicol]

LBD transformed BL21(DE3)pLysS

SDS-PAGE Loading Buffer[5X]: [250mM Tris-HCl (pH 6.8), 0.5M DTT, 10% SDS (w/v), 0.5%

Bromophenol blue (w/v), 50% Glycerol (v/v)]

Tris-EDTA: [50mM Tris-HCl, 5mM EDTA]

Small scale culture was used to determine the inducibility and solubility of the recombinant protein. Fifty μ l of overnight culture (from a single colony) was used to inoculate 15ml of LB-broth, containing appropriate concentration of antibiotics (Amp+Cm), and cultured at room temperature (shaking at 100 rpm/min) for ~15 hours or at 37 $^{\circ}$ C for 4 to 5 hours to reach the log phase of growth. LBD protein expression was induced by adding an appropriate concentration of IPTG and incubated for further 4 hours. Duplicate samples were taken at various time points of induction. Samples were centrifuged for 1 minutes at 14 000g, and one set of pellets were resuspended in 50 μ l of 1X SDS-PAGE Loading Buffer (SDS-PAGE LB) and incubated at 100 $^{\circ}$ C for 3 minutes. The protein samples were resolved on a 12% SDS-PAGE gel. Protein solubility was determined using the other set of samples. To each pellet 50 μ l of Tris-EDTA (pH 8.0) buffer was added and the resuspended cells were freeze-thawed 3/4 times, sonicated and centrifuged for 5 minutes at 14 000g. The pellets were resuspended in 25 μ l of 1X SDS-PAGE LB, and the supernatant was transferred to a fresh tube and mixed with equal volume of 5X SDS-PAGE LB. Samples were resolved in 12% polyacrylamide gels and the resolved protein bands were visualised by Coomassie blue staining.

Section 2.9.9 Affinity Chromatography

Composition of reagents:

IPTG-induced his-tagged LBD protein (500ml culture)

The following buffers were diluted to 1X prior to use in the Ni²⁺ affinity chromatography

Component	Binding Buffer [8X]	Elute Buffer [4X]	Wash Buffer [8X]	Strip Buffer [4X]	Charge Buffer [8X]
Imidazole	40mM	4M	480mM		----
NaCl	4.0M	2M	4M	2M	----
Tris-HCl (pH 7.9)	160mM	80mM	160mM	80mM	----
EDTA	----	----	----	400mM	----

Component	Binding Buffer [8X]	Elute Buffer [4X]	Wash Buffer [8X]	Strip Buffer [4X]	Charge Buffer [8X]
NiSO ₄	----	----	----	----	400mM

Nickel affinity column chromatography was used to purify histidine tagged mPPAR α LBD protein. IPTG induced cultures (500ml) were harvested by centrifugation at 4000g for 20 minutes and the cell pellet was resuspended in 10ml ice-cold binding buffer (1X). The Novagen PET purification system using a Ni²⁺ resin was followed according to the manufacturer instructions. Using a sonicator, resuspended cells were sonicated (50% power output) 5 times (30 seconds for each pulse) with a cooling period of 30 seconds between pulses. To prevent overheating, sample tubes were kept on ice during sonication and the sonicator probe was cooled in sterile ice-cold water following each pulse. Soluble proteins were separated from cell debris by centrifugation at 20 000g for 20 minute at 4 °C. Affinity columns were prepared prior to purification using His.Bind resin (Novagen) charged with the divalent cation Ni²⁺. Supernatant containing soluble proteins was filtered through a 0.45 micron membrane and then loaded on to the column. The column was washed with 10 volumes of 1X binding buffer followed by 6 volumes of 1X wash buffer. Bound proteins were eluted from the column with 6 volumes of 1X elution buffer. All wash and eluant fractions were collected as small volumes for analysis by SDS-PAGE. Following the last elution step the column was washed with 3 volumes of 1X strip buffer and then recharged with 5 volumes of 1X charge buffer. The proteins eluted from the soluble fraction were dialysed to remove any small molecular weight proteins and to reduce the concentration of solutes such as salt and imidazole. Dialysis was carried out in a dialysis tube (with exclusion limit of 6,000 MW) for ~15 hours at 4 °C with five changes of 0.1M Tris-HCl (pH 8.0). Protein samples were then run on ion-exchange column chromatography, by FPLC (Fast Protein Liquid Chromatography).

Section 2.9.10 FPLC Chromatography

Composition of reagents:

Buffer A: [0.1M Tris-HCl, pH 8.0]

Buffer B: [1M NaCl in 0.1M Tris-HCl, pH 8.0]

Eluted his-tagged LBD protein samples from the Ni²⁺ column were further purified from contaminating proteins and solutes and concentrated using ion-exchange FPLC chromatography. Dialysed proteins were passed through a weak cation exchanger (Econo-S, pH range 2-10) using Buffer A and Buffer B at a pH just over one unit above the isoelectric point of the LBD protein (pH 6.6). Protein samples (1 ml per run) were separated using isocratic flow conditions of 0-50% Buffer B for 10 minutes with a flow rate of 1ml/min. Protein separation were monitored using UV detector and eluted fractions (protein peaks) were collected according to their retention time on the chromatogram.

Section 2.10 Data Presentation and Analysis

Section 2.10.1 Illustration

Tissue sections on which *in situ* hybridisation was carried out were analysed using a Carl Zeiss light microscope. For illustrative purposes images were captured using Media Grabber software on an Apple Mac computer and then manipulated in Photoshop (Adobe, version 5.5) for presentation using the frame maker capability(Adobe, version 5.5). Pictures presented for peroxisome proliferation and DNA synthesis studies were photographed directly from the tissue culture flasks using Fuji-Sensia film. Pictures presented for apoptosis was viewed using a fluorescence microscope and photographed using Fuji-Sensia film.

Section 2.10.2 Statistical Analysis

Data presented for hamster CYP4A induction and mouse, hamster and guinea pig PPAR α expression were analysed using Student's t-test with a confidence limit of 95% using the computer package Sigma Plot (version 5.0). Values are considered significant if $p < 0.05$ (i.e. the null hy-

pothesis was rejected at $p < 0.05$).

Chapter 3 Results

Section 3.1 *In vitro* study of peroxisomal events

The pleiotropic responses to peroxisome proliferators are mediated by the steroid receptor PPAR α (Lee *et al.*, 1990). It is intriguing that this phenomenon of peroxisome proliferation is observed in species such as mouse and rat but not in guinea pig or human even though they all express PPAR α in the liver. If peroxisome proliferation is mediated by PPAR α then such species differences could reflect either variation in the level or the function of PPAR α . It was hoped to develop an *in vitro* system to study the physiological responses induced by PPAR α from species displaying varying level of responsiveness to peroxisome proliferators. Following their transfection, the response of different forms of exogenous PPAR α (mouse, guinea pig and two variants of human PPAR α) could be studied in such a system by studying their effects on DNA synthesis as a marker of peroxisome proliferation.

Section 3.2 Primary rat hepatocyte culture system

Hepatocytes from male Wistar rats were isolated by an *in situ*, two-step collagenase perfusion assay as described in Section 2.2. This isolation procedure, originally described by Mitchell *et al.*, 1984, has been established in our laboratory as described by NJ Horley and NJ Plant (PhD theses). Although the cell viability varied between individual isolation procedures, the typical viability was greater than 86% as determined by Trypan blue exclusion method. A typical isolation procedure yielded 4×10^8 viable hepatocytes from a 200-250g male rat. A uniform monolayer of hepatocytes was formed 24 hours after seeding 2×10^6 cells per flask (25 cm^2 growth area), and the hepatocytes were cultured and maintained as described previously by NJ Plant (PhD thesis).

Section 3.2.1 DNA synthesis in primary hepatocyte culture

A high level of DNA synthesis has been observed in rats and mice exposed to peroxisome pro-

liferators that act in a dose dependent manner and represent a good marker of peroxisome proliferation (Styles *et al.*, 1988). Previous studies have demonstrated that rat primary hepatocyte cultures respond well to peroxisome proliferators, especially in the induction of specific microsomal and peroxisomal genes and their enzymic activities (Mitchell *et al.*, 1984; Bell and Elcombe 1991). This hepatocyte culture system has been shown to respond well to peroxisome proliferator-induced DNA synthesis to a level that is comparable to *in vivo* studies (Plant *et al.*, 1998). Using this system, it was hoped to study further aspects of peroxisome proliferation, in particular DNA synthesis. Initially, induction of DNA synthesis has been studied in an attempt to reproduce such data.

Section 3.2.1.1 Mitogenic stimulation by epidermal growth factor

Primary hepatocytes are known to respond well to the hepatic mitogen epidermal growth factor (EGF) (Michalopoulos 1990), and thus EGF was used in the first instance to demonstrate that the cultured hepatocytes were responsive to mitogens, that is they were capable of undertaking

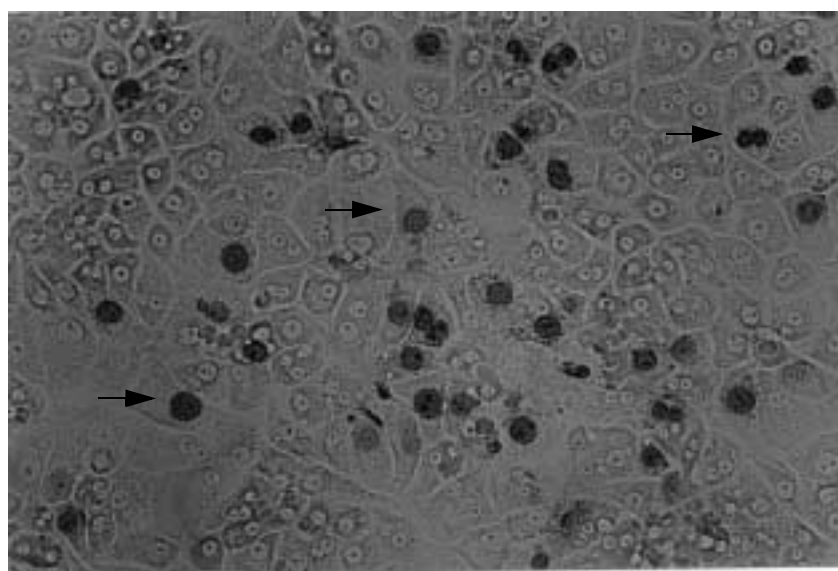


Figure 3.1 Immunochemical detection of BrdUrd labelled cells. Hepatocytes were seeded at a plating density of 2×10^6 cells per 25-cm^2 flask and cultured for 24 hours before EGF (10ng/ml) was added in the medium. DNA synthesis was measured by incorporation of BrdUrd at 24-48 hours after the addition of EGF. Incorporated BrdUrd was detected by immunochemistry as described in methods. Labelled cells stain their nuclei as dark-brown (as shown by solid arrow)

DNA synthesis. This replicative DNA synthesis was measured by incorporation of BrdUrd into DNA during S-phase, which was then visualised by immunocytochemistry. EGF, at a concentration of 10ng/ml, caused a large increase in the number of labelled cells as demonstrated in Figure 3.1. Induction of DNA synthesis was expressed as the labelling index (%), and the quantified data shows that the EGF gave a labelling index of 9.8% (+/- 1.9) while the control gave a 0.95% (+/- 0.3). A labelling index of 10-fold above control ($p < 0.01$) was observed with EGF (Figure 3.3). This demonstrates that the cell culture system is capable of supporting high level induction of DNA synthesis.

Section 3.2.1.2 PP-induced DNA synthesis in primary rat hepatocyte culture

Peroxisome proliferators have been shown to induce liver DNA synthesis in a dose dependent manner both *in vitro* and *in vivo* (Styles *et al.*, 1988; Plant *et al.*, 1998) which reflects their potency in causing peroxisome proliferation. Having found that EGF caused a high level of induc-

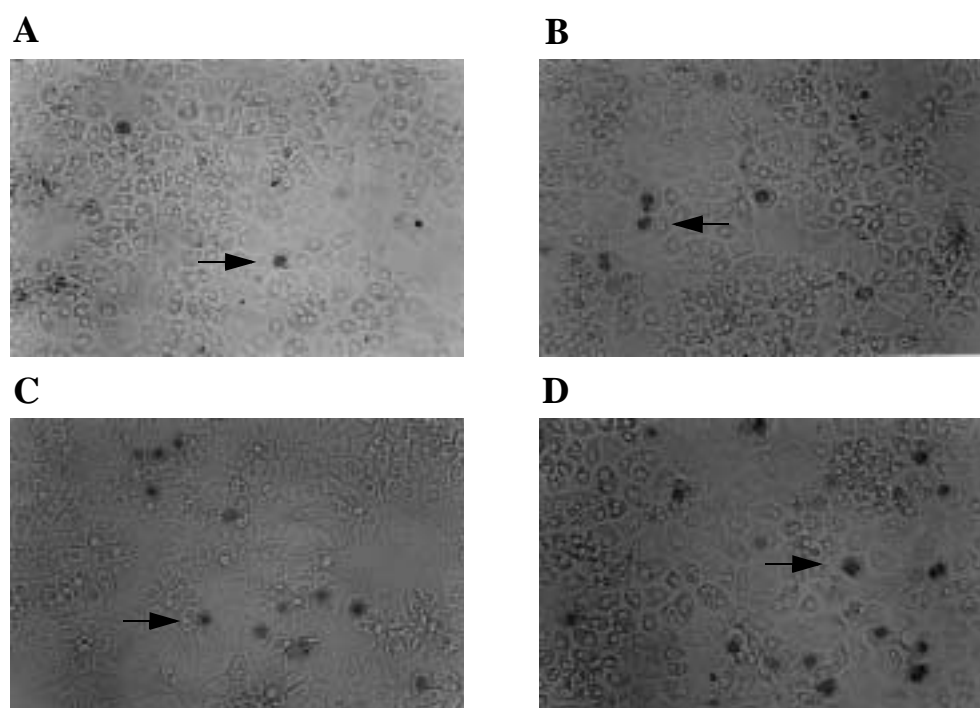


Figure 3.2 Peroxisome proliferator-induced DNA synthesis in rat hepatocytes. Hepatocytes were seeded at a plating density of 2×10^6 cells/flask and cultured for 24 hours. Cells were then exposed to (a) control medium, (b) vehicular control DMSO, (c) 100µM MCP and (d) 100µM Wy-14,643. DNA synthesis was measured by incorporation of BrdUrd 6-30 hours after dosing. Incorporated BrdUrd was detected by immunocytochemistry as described in methods. Labelled cells stain their nuclei as dark-brown (as shown by solid arrow).

tion of DNA synthesis (Figure 3.1 and Figure 3.3), the system was then tested with two potent peroxisome proliferators MCP and Wy-14,643 for their ability to induce DNA synthesis. Figure 3.2 shows the effect of MCP and Wy-14,643 on DNA synthesis, as measured by BrdUrd labelled cells.

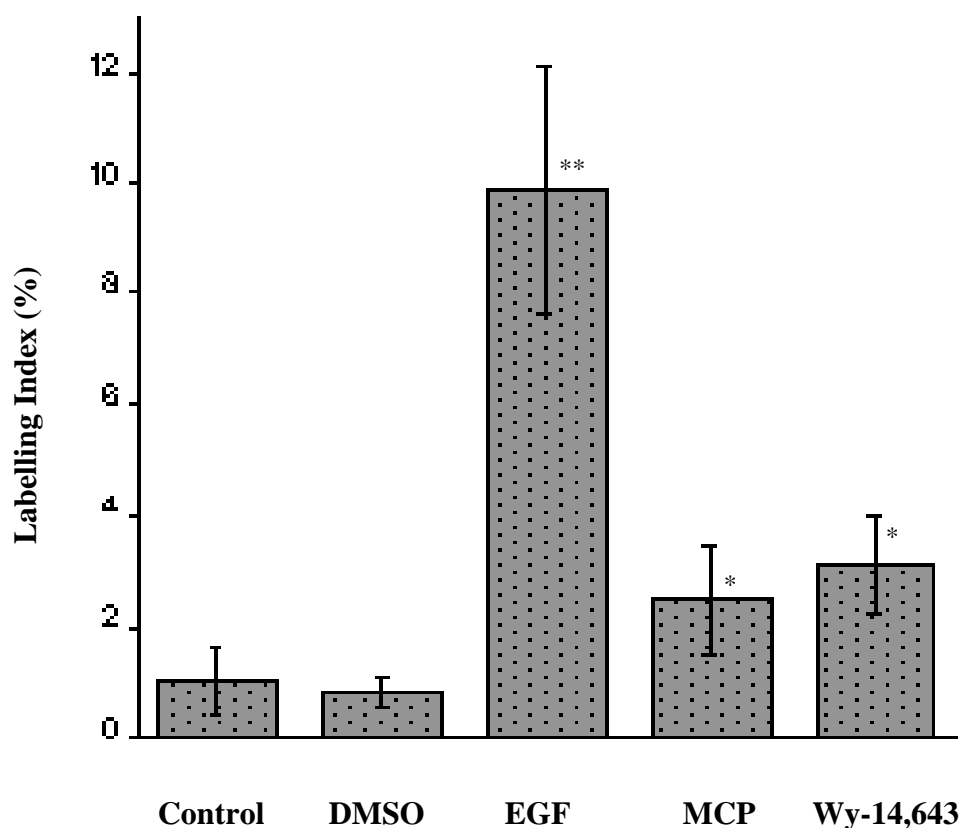


Figure 3.3 Induction of DNA synthesis in primary rat hepatocyte cultures. Twenty-four hours after seeding hepatocytes were exposed to the test chemicals 10ng/ml EGF, 100 μ M MCP, 100 μ M Wy-14,643 or 10 μ l DMSO. DNA synthesis was measured by the incorporation of BrdUrd between 6-24 or 24-48 hours after dosing with peroxisome proliferators MCP and Wy-14,643, and EGF, respectively. DNA synthesis was determined by immunocytochemical localization of BrdUrd as described in methods. Data are expressed as labelling index where four fields (~1200 cells) were counted for two flasks and the experiment was repeated on at least on three occasions. Statistical significance was determined by Student's t-test, and values significantly different from control are indicated by ** = $p < 0.001$ and * = $p < 0.01$. Error bars shown represents the standard deviation from the mean.

The labelling indices from the experiments shown in Figure 3.2 were quantified, as shown in Figure 3.3. The basal level of DNA synthesis of the culture (i.e. untreated control) was 0.95% (+/- 0.3) while both MCP and Wy-14,643 induced this DNA synthesis to 2.4% (+/- 0.56) and 3.1 (+/- 0.55), respectively. A maximum of 3-fold induction ($p < 0.01$) was observed with Wy-14,643, while MCP gave a 2.5-fold induction ($p < 0.01$) in DNA synthesis. These experiments

were repeated on more than five occasions with no success in obtaining higher levels of induction. This level of induction of DNA synthesis by peroxisome proliferators is much lower than previously reported (Plant *et al.*, 1998). Therefore the culture conditions were varied in order to obtain higher levels of DNA synthesis.

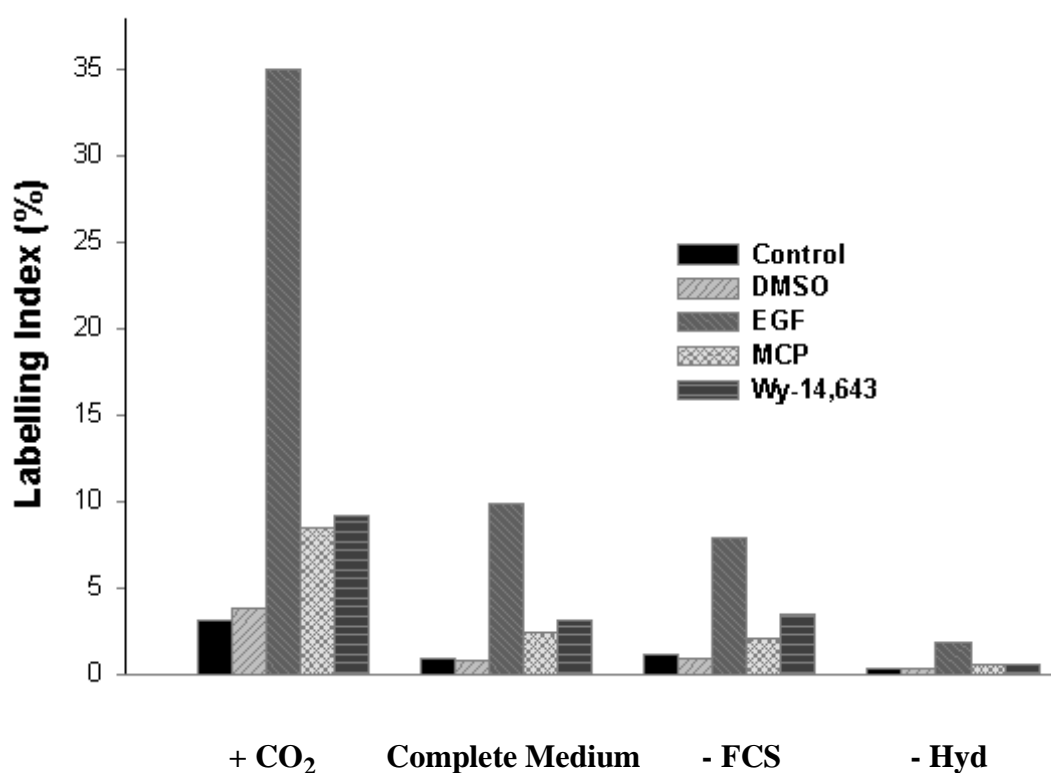


Figure 3.4 Effect of medium components and culture conditions on DNA synthesis. Hepatocytes were seeded at a plating density of 2×10^6 /flask, and cultured for 24 hours in complete CL-15 medium or medium with components removed as indicated. Generally, hepatocytes were cultured in a humidified non-CO₂ conditions unless otherwise indicated. Cells were exposed to the test chemicals 10ng/ml EGF, 100 μ M MCP, 100 μ M Wy-14,643 or 10 μ l DMSO. DNA synthesis was measured by the incorporation of BrdUrd between 6-24 or 24-48 hours after dosing with peroxisome proliferators MCP and Wy-14,643, and EGF, respectively. DNA synthesis was determined by immunocytochemical localization of BrdUrd as described in methods. Data are expressed as labelling index where four fields (~1200 cells) were counted for two flasks and the experiment was repeated on at least two occasions.

The influence of media components such as fetal calf serum and hydrocortisone on the level of DNA synthesis was investigated. When these components were omitted individually from the medium there was a general reduction in the total number of cells undergoing DNA synthesis observed (Figure 3.4). However, the level of induction of DNA synthesis by MCP and Wy-14,643 was not affected. In the case of EGF, there was a slight reduction in the level of induction

of DNA synthesis. When cells were cultured in humidified conditions with 5% CO₂, there was a general increase in the total number of cells undergoing DNA synthesis with up to 35 % of cells in S-phase when exposed to EGF. Since this culture condition also caused an increase in control values, the level of induction of DNA synthesis by peroxisome proliferators remained unaffected. In view of the low induction of DNA synthesis by PPs, it would not be possible to perturb expression of PPAR α and then measure the effect on DNA synthesis.

Section 3.2.2 Effect of peroxisome proliferators on apoptosis

In addition to mitogenic stimulation, suppression of apoptosis by peroxisome proliferators has been observed in hepatocytes (James and Roberts 1996). If the level of suppression is large in

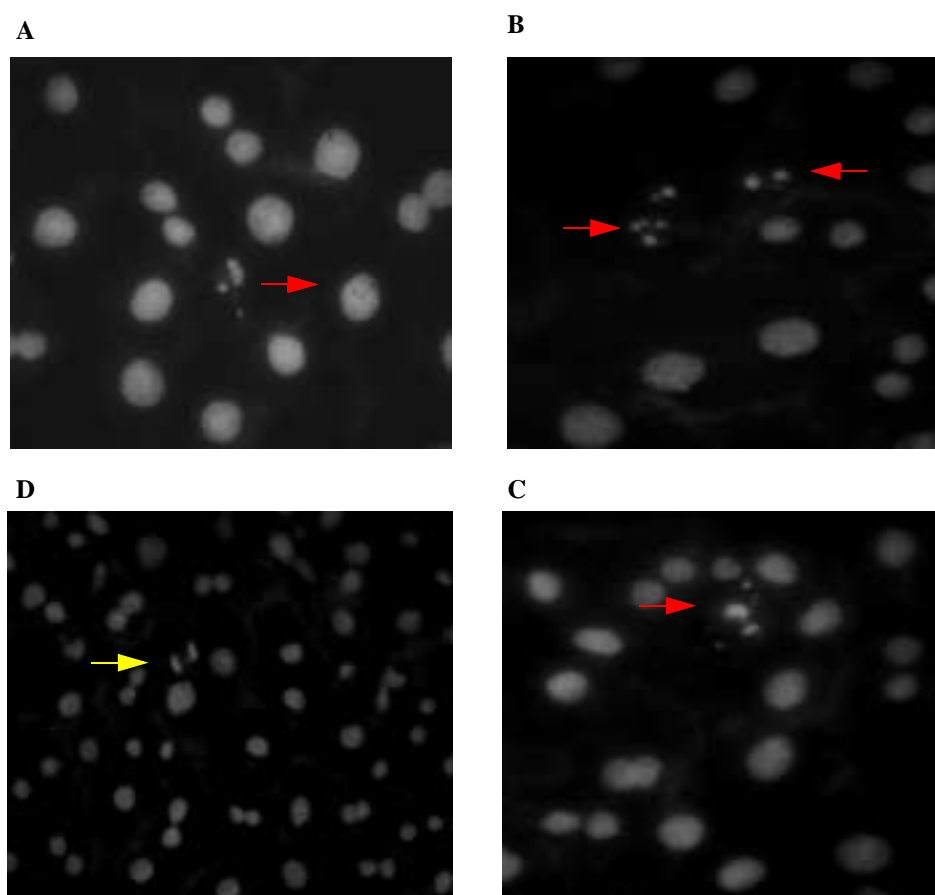


Figure 3.5 Suppression of apoptosis by peroxisome proliferators. Hepatocytes were seeded at a plating density of 2×10^6 cells per 25-cm² flask and cultured for 24 hours before MCP (100 μ M) was added to the medium. Cells were exposed to MCP for 48 hours, and then fixed as described in methods. Fixed cells were stained with Hoescht 33258 for the detection of apoptosis. A, B and C represent control hepatocytes, showing apoptotic cells (red arrow) as viewed under fluorescent microscopy, and D represent MCP treated hepatocytes, showing mitosis (yellow arrow).

primary hepatocytes then apoptosis could be used as a marker of peroxisome proliferation when investigating the effects of PPAR α by peroxisome proliferators. Figure 3.5 shows the effect of the peroxisome proliferator MCP on apoptosis in primary rat hepatocytes. A low basal level of apoptosis was found in rat primary hepatocytes, which was suppressed by the peroxisome proliferator MCP. The quantified data, using two independent experiments, shows that there was a 40% reduction in apoptosis (control= 1.5%, MCP= 0.59%) observed following the treatment of hepatocytes with 100 μ M MCP. Thus, rat primary hepatocyte culture underwent peroxisome proliferator-induced suppression of apoptosis. However, this level of suppression is not big enough to use apoptosis as a marker of peroxisome proliferation in the study of PPAR α function.

Section 3.2.3 Induction of CYP4A1 in primary rat hepatocyte culture

Cytochrome P450A1 (CYP4A1) is an early marker of peroxisome proliferation which is highly induced in rats following administration of peroxisome proliferators (Bell *et al.*, 1991). The level of induction of CYP4A1 is much higher than DNA synthesis and apoptosis, and therefore offers an alternative system to study how PPAR α induces physiological responses. Therefore the induction of CYP4A1 by peroxisome proliferators was investigated in rat primary hepatocyte culture maintained in normal and hydrocortisone-deficient media.

Section 3.2.3.1 Extraction of *in vitro* and *in vivo* RNA

Total RNA was isolated from untreated rat liver and kidney using the method of Chomczynski and Sacchi as described in Methods. The approximate yields of total RNA from one gram of liver and kidney were 1.2 and 0.5mg, respectively. RNA from primary rat and mouse hepatocytes was isolated using the method of Rothblum *et al.* and gave a typical yield of 50 μ g of total RNA per flask initially seeded with 2×10^6 cells for rats, while for mouse 30 μ g of RNA was obtained per flask seeded with 1×10^6 cells.

Total RNA from PPAR α wild-type and knock-out mice treated with corn oil, MCP and Wy-14,643 were extracted using the LiCl/urea method. After three days of treatment with peroxisome proliferators MCP and Wy-14,643 hepatomegaly was observed only in wild type mice. Approximately 1.5-1.8mg of RNA was extracted from one gram of liver tissue processed.

RNA from hamster liver was a generous gift from S Chahal (Nottingham University) and was used in the RNase protection assay. Hamster total liver RNA and guinea pig liver RNA were extracted using the method of Cathala *et al.* (1983). Hepatomegaly was observed in hamsters dosed with peroxisome proliferators, with up to 20% increase in liver weight (see Choudhury *et al.*, 2000). An RNA yield of 1.5mg per gram of liver was obtained using the Cathala purification protocol. RNA used in PCR cloning of hamster CYP4A and PPAR α was purified with a commercial kit (Advanced Biotechnology) with a yield of 1mg per gram of liver tissue. Figure 3.6 shows the integrity of RNA as analysed by agarose gel electrophoresis. .

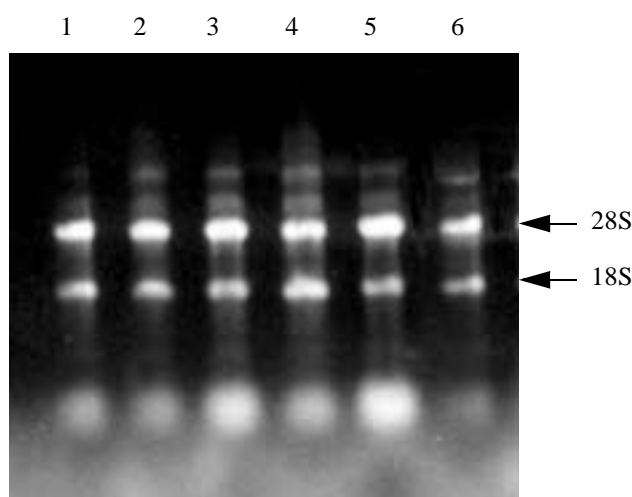


Figure 3.6 Agarose gel electrophoresis of total liver RNA. Analysis of a typical RNA extraction from mouse liver. RNA was extracted from 1g of tissue using the method of Chomczynski and Sacchi as described in methods, and resuspended in 500 μ l DEPC-treated water. One μ l of sample from each preparation (samples 1-6) was run on a 0.8% agarose gel (containing 0.1% SDS) at 70v for 2 hours using 1xTBE. Intact 28S and 18S rRNA bands are shown by the arrow.

Section 3.2.3.2 Expression and induction of rat CYP4A1 in liver and kidney

Expression of CYP4A1 mRNA was investigated in male rat liver and kidney using a ribonu-

clease protection assay (RNase protection). Initially, RNase protection assay was developed and optimised using RNA extracted from tissue samples as CYP4A1 is easily detectable *in vivo* due to its high level of expression. Cloning vector pGEM7 containing a CYP4A1 cDNA insert was used as a template to generate the riboprobe encompassing the 3' end of the RNA, and an anti-sense riboprobe was generated by transcribing from the T7 promoter using an NcoI restriction digested template as shown in Figure 3.7. This results in a 230bp transcript of which 190bp corresponds to the CYP4A1 cDNA insert.

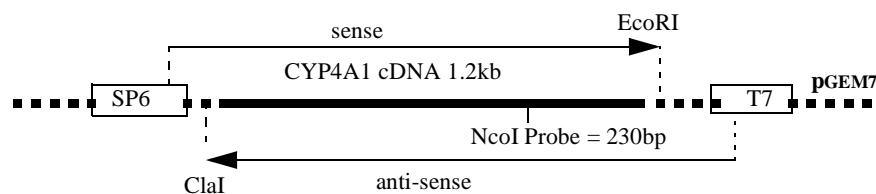


Figure 3.7 Diagrammatic representation of CYP4A1 template. A 1.2kb fragment corresponding to the 3' untranslated region of the rat CYP4A cDNA (residues 965-2157) was subcloned into the EcoRI/ClaI site of the polylinker region of pGEM7 cloning vector. Anti-sense riboprobe can be generated by *in vitro* transcription of NcoI cut template from T7 promoter, resulting in a 232bp length probe of which 190bp corresponds to CYP4A1 insert.

Hybridisation of riboprobe to total tissue RNA resulted in a specific protected fragment which is detected in a denaturing urea/polyacrylamide gel. The specificity of the fragment was shown by hybridisation of the riboprobe to yeast tRNA in the absence (RNase -ve) and presence (RNase +ve) of RNase A. No protected fragment is present after treatment of yeast tRNA hybridised to the probe with RNase A. As expected, the expression of CYP4A1 was detected in both liver and kidney, and the constitutive level of expression of CYP4A1 in liver was higher compared to kidney (Figure 3.8). CYP4A1 was induced in both liver and kidney, however the level of induction was much greater in liver when compared to kidney. The temperature of hybridisation and amount of RNase A was varied: optimal conditions for hybridisation and the detection of the protected fragment were found to be 30 μ g of RNA hybridised to the probe at 42

$^{\circ}\text{C}$ and $10\mu\text{g/ml}$ RNase A treatment following hybridisation (data not shown). Using these optimised conditions, expression of CYP4A1 was detected in primary rat hepatocyte culture in control and MCP treated RNA samples (Figure 3.8). Induction of CYP4A1 mRNA by MCP was evident in primary rat hepatocyte culture when compared to control. Therefore this system shows a highly inducible response (induction of CYP4A1) to peroxisome proliferators *in vitro*.

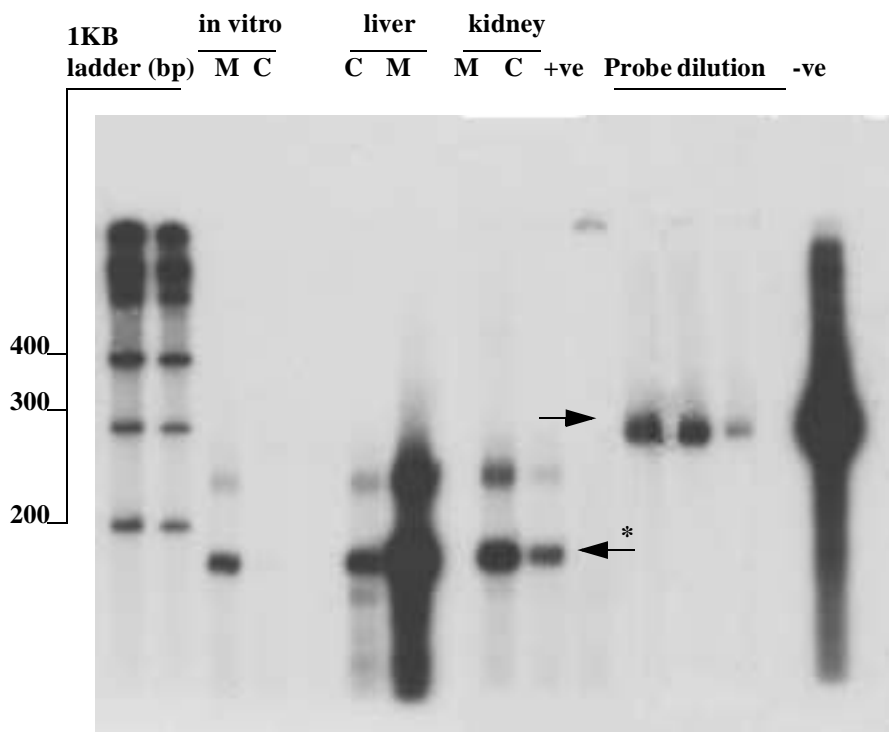


Figure 3.8 Expression of and induction of CYP4A1 gene in rat tissue. RNase protection assay was performed on control (C) and MCP (M) treated total RNA of rat liver and kidney (25 mg/kg for 24hrs) and primary hepatocytes (48hrs exposure to $100\mu\text{M}$ MCP). Anti-sense riboprobe were generated as described in the text. A 230bp length probe (solid arrow) was generated which gave a 190bp protected fragment (solid arrow with an asterisk) representing the CYP4A1 sequence. Total RNA was extracted as described in methods, and $30\mu\text{g}$ of RNA of each sample was used to hybridise [α - ^{32}P] CTP labelled probe. The specificity of the probe was determined by inclusion of two control yeast tRNA samples hybridised to the probe. One sample was treated without RNase A (-ve), while the other was treated with RNase A (+ve). Following hybridisation and RNase A treatment, precipitated RNA samples were resolved in a 6% denaturing urea/acrylamide gel by running in 1xTBE for 2 hours at 120v. Gels were fixed, dried and exposed to Hyperfilm at -80°C for 15 hours.

Section 3.2.3.3 Effects of hydrocortisone on the induction of CYP4A1 in hepatocytes

Glucocorticoid hormone has been shown to modulate PPAR α at the transcriptional level in a primary rat hepatocyte culture system (Lamberger *et al.*, 1996). Since peroxisome proliferators induce the expression of CYP4A gene through transcriptional activation of PPAR α , reducing

the level of PPAR α may affect the transcriptional induction of CYP4A by peroxisome proliferators. Thus the induction of CYP4A1 mRNA in primary hepatocytes, maintained in normal CL-15 medium and in hydrocortisone deficient medium, was investigated following exposure to MCP for 48 hours. Figure 3.9 demonstrates that the level of induction of CYP4A1 following treatment with MCP is reduced in cells cultured in hydrocortisone-deficient medium when compared to cells maintained in medium containing hydrocortisone. Quantification of the protected fragment on a phosphor imager shows that MCP caused up to 14-fold induction of CYP4A1 compared to control in hepatocytes maintained in normal medium (Figure 3.10). This level of induction was reduced to 2.3-fold when cultured in hydrocortisone deficient media, and the experiment was repeated on more than two occasions. The culture conditions were varied, with a view to maximising the difference in induction of CYP4A1 between cultures with and without

hydrocortisone.

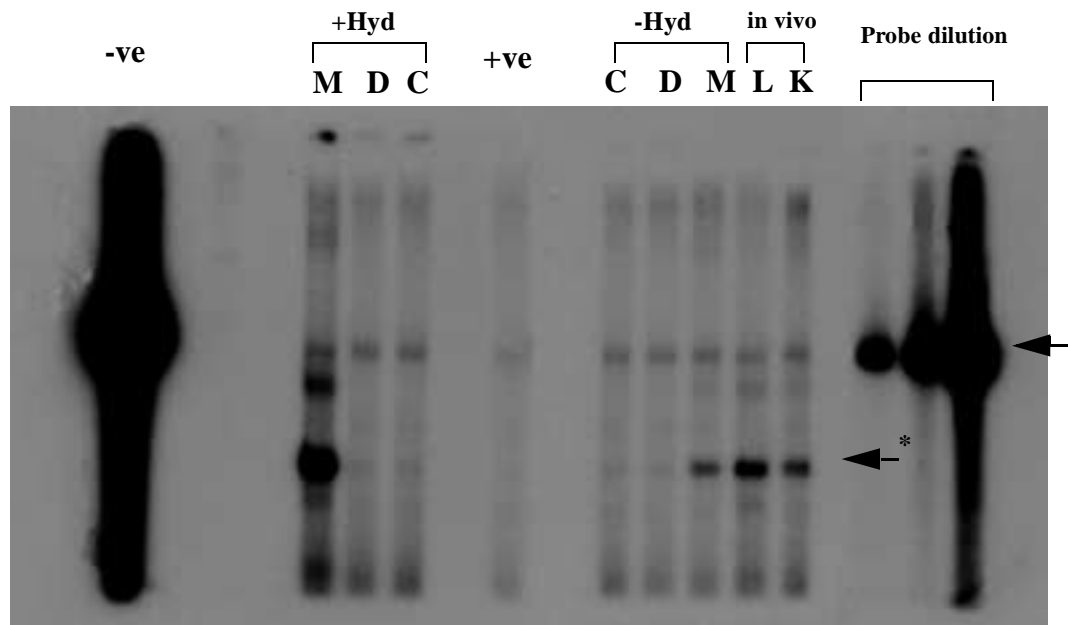


Figure 3.9 Effects of hydrocortisone on induction of CYP4A1. Isolated hepatocytes were seeded at a density of 2×10^6 cells per flask in CL-15 medium containing hydrocortisone. Four hours after seeding the medium was replaced with fresh medium containing either hydrocortisone (+Hyd) or no hydrocortisone (-Hyd) as indicated. Twenty-four hours after seeding cells were dosed with 100 μ M MCP or DMSO and cultured for a further 48 hours. RNase protection were carried out using a CYP4A1 antisense riboprobe as described in methods. Total RNA was extracted as described in methods, and 30 μ g of RNA of each sample was hybridised to the CYP4A1 probe. The specificity of the probe was determined by inclusion of two control yeast tRNA samples and hybridised to the probe. One sample was treated without RNase A (-ve), while the other was treated with RNase A (+ve). Following hybridisation and RNase A treatment, precipitated RNA samples were resolved on a 6% denaturing urea/acrylamide gel by running in 1xTBE for 2 hours at 120v. Gels were fixed, dried and exposed to Hyperfilm at -80 $^{\circ}$ C for 12 hours. Full-length probe is indicated by arrow while protected fragment is shown by arrow with asterisk placed next to it.

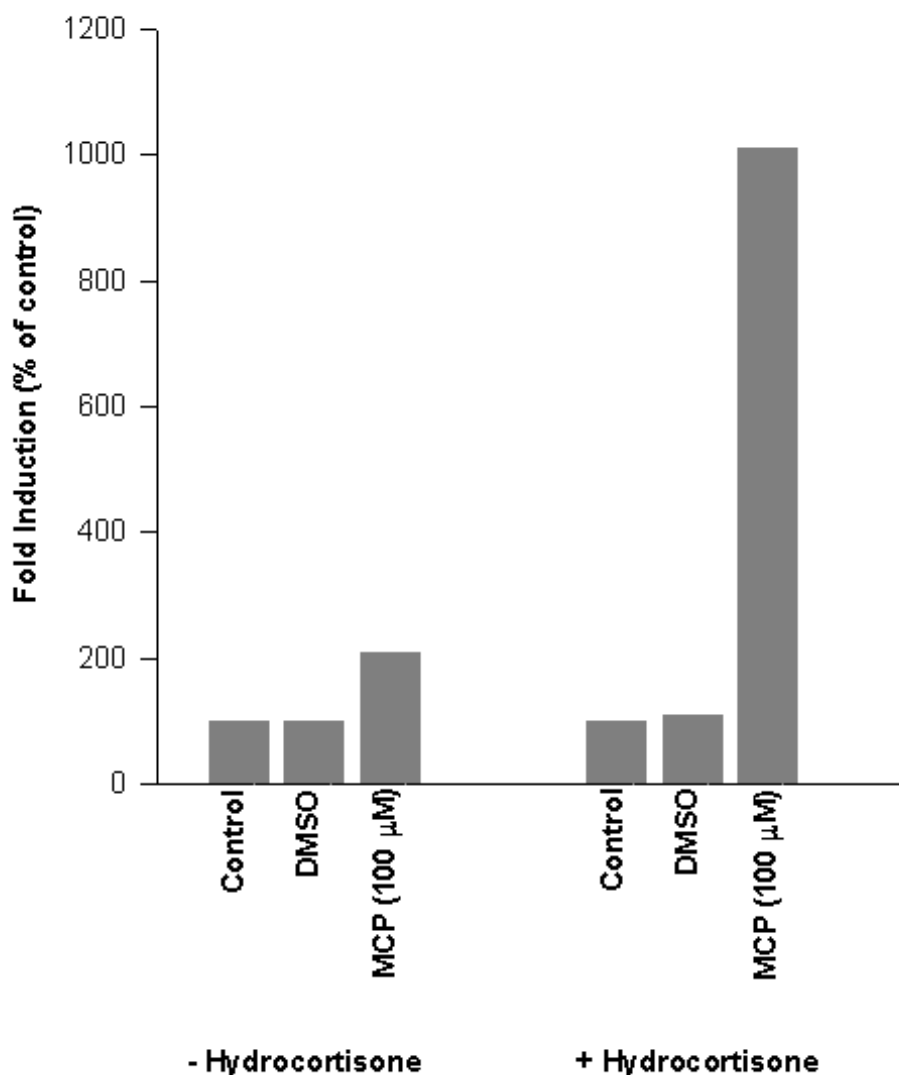


Figure 3.10 Induction of rat CYP4A1. Isolated hepatocytes were seeded at a density of 2×10^6 cells/flask in CL15 medium containing hydrocortisone. Four hours after seeding the medium was replaced with fresh medium containing either hydrocortisone or no hydrocortisone as indicated. Twenty-four hours after seeding cells were dosed with MCP or DMSO and cultured for a further 48 hours. RNase protection were carried out using a CYP4A1 antisense riboprobe as described in methods. Thirty micrograms of RNA was used for each sample. Protected bands were quantified using a phosphor imager and the results are expressed as percentage induction over control, and represent mean value of a least two separate experiments.

Section 3.2.3.4 Effects of culture conditions on the induction of CYP4A1

Induction of CYP4A1 in primary hepatocyte culture was investigated following exposure to MCP for 24, 48 and 72 hours. MCP (10-100μM) induced CYP4A1 in a dose dependent manner and 100μM MCP was found to give high levels of CYP4A1 induction (data not shown) which

was used for subsequent studies. Twenty-four hours of dosing resulted in a 40-fold induction of

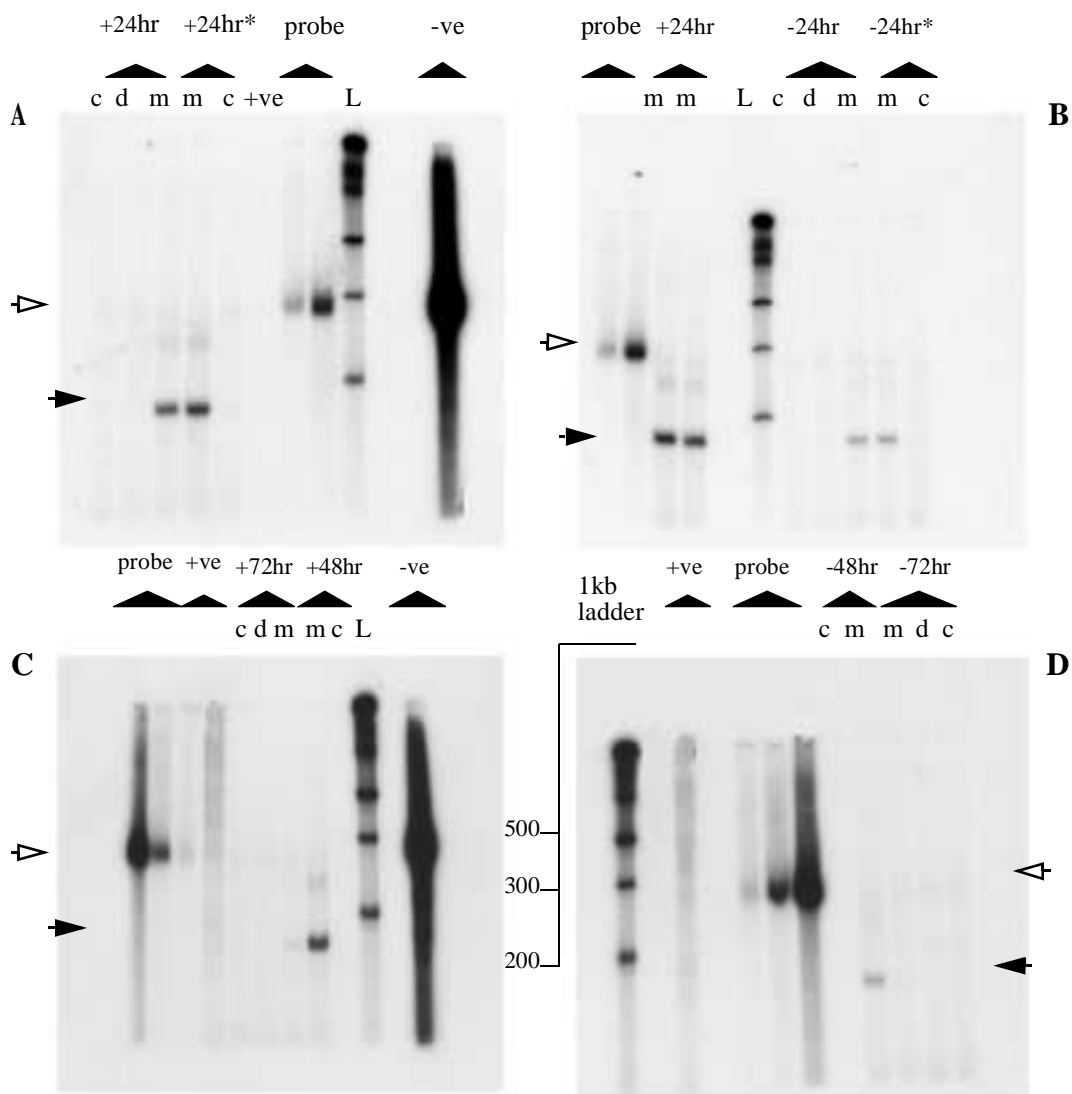


Figure 3.11 Effects of dosing period in the induction of CYP4A1. Isolated hepatocytes were seeded in normal CL-15 medium at a density of 2×10^6 cells/flask. Four hours after seeding the medium was replaced with fresh medium containing either hydrocortisone (A, C) or no hydrocortisone (B, D) as indicated by + and -, respectively. Twenty-four hours after seeding cells were dosed with $100 \mu\text{M}$ MCP or $10 \mu\text{l}$ DMSO and cultured for a further 24 (A, B), 48 or 72 hours (C, D) as indicated. For 24hr dosing study, one sets of flasks were cultured for 48 hours following seeding before being exposed to MCP or DMSO (indicated by asterisk). RNase protection were carried out using a CYP4A1 anti-sense riboprobe as described in methods. Total RNA was extracted as described in methods, and $30 \mu\text{g}$ of RNA of each sample was hybridised to the probe overnight. The specificity of the probe was determined by inclusion of two control yeast tRNA samples hybridised to the probe. One sample was treated without RNase A (-ve), while the other was treated with RNase A (+ve). Following hybridisation and RNase A treatment, precipitated RNA samples were resolved in a 6% denaturing urea/acrylamide gel by running in 1xTBE for 2 hours at 120v. Gels were fixed, dried and exposed to hyperfilm at -80°C for 15 hours. Protected bands were quantified using a phosphor imager and the results are expressed as fold induction. L = 1kb ladder shown in base pair. Full-length probe is indicated by unfilled arrow while protected band is shown by filled arrow.

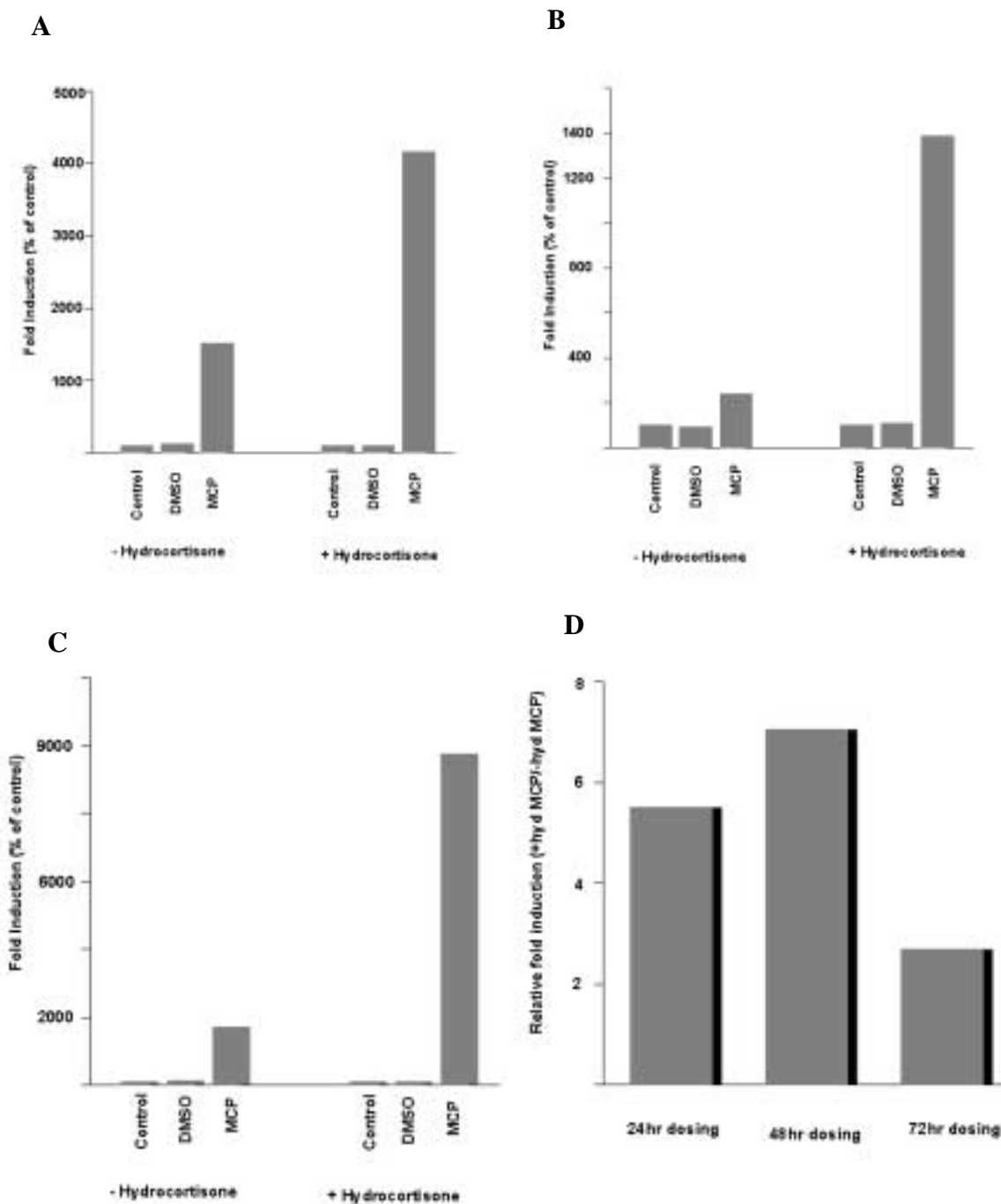


Figure 3.12 Induction of CYP4A1 after different dosing periods. Isolated hepatocytes were seeded at a density of 2×10^6 cells/flask in CL-15 medium containing hydrocortisone. Four hours after seeding the medium was replaced with fresh medium containing either hydrocortisone or no hydrocortisone as indicated. Twenty-four hours after seeding cells were dosed with $100 \mu\text{M}$ MCP or $10 \mu\text{l}$ DMSO and cultured for a further (A) 48 (B) or 72 (C) hours. RNase protection were carried out using a CYP4A1 antisense riboprobe as described in methods. Thirty micrograms of RNA was used for each sample. Protected bands were quantified using a phosphor imager and the results are expressed as fold induction as percentage of control, and represent mean value of a least two separate experiments. The ratio of the fold induction by MCP in normal : hydrocortisone-deficient media is shown in (D).

CYP4A1 in medium containing hydrocortisone (Figure 3.11 and Figure 3.12). However, there was also an increase in CYP4A1 induction observed in hydrocortisone-deficient medium (16-

fold induction), which resulted overall in a differential induction of 2.8-fold by MCP between normal and hydrocortisone-deficient media. Exposure of hepatocytes, 48 hours after seeding, with MCP for 24 hours, resulted in no increase in the overall CYP4A1 induction when compared between normal and hydrocortisone-deficient media for the same dosing period (Figure 3.11, quantified data not shown). Dosing periods of 48 and 72 hours reduced the level of induction seen in hydrocortisone-deficient medium. Although a reduction in CYP4A1 induction was observed in hepatocytes maintained in normal medium after dosing with MCP for 48 hours (14-fold) and 72 hours (9-fold), there was an increase in the overall induction by MCP between normal and hydrocortisone-deficient media. A maximum 7-fold overall induction of CYP4A1 was achieved in hepatocytes dosed with MCP for 48 hours in normal medium when compared to CYP4A1 induction in hydrocortisone-deficient medium for the same exposure period. Exposure of hepatocytes to different dosing periods did not significantly improve the ratio of induction by MCP in normal versus hydrocortisone deficient media (Figure 3.12 D).

It was hoped that the induction of CYP4A1 could be used as a more sensitive measure of peroxisome proliferation (compared to DNA synthesis) that could be related to the activity of PPAR α from various species following their transfection of primary hepatocytes maintained in hydrocortisone-deficient media. Although the measurement of induction of CYP4A1 is more sensitive than DNA synthesis, the difference in induction of this marker gene by MCP between normal and hydrocortisone-deficient media is only 7-fold. However, this level of differential induction between the presence and absence of hydrocortisone was insufficient for further study. Thus, making the hypothesis that the decreased expression of PPAR α in hydrocortisone deficient cells was responsible for the reduced induction of CYP4A1, it follows that transient transfection of 100% of hepatocytes with mouse PPAR α would return all cells to inducibility i.e. 9-

fold above control levels, versus 2.5-fold above control levels in the hydrocortisone deficient group. Since transfection efficiencies are routinely 5-20%, the highest possible level of expression anticipated would be 3.6-fold above control- which is very close to the background level of 2.3-fold above control. It would be difficult to draw significant conclusions about any difference in induction of this scale.

Section 3.3 Expression of *Cyp4a* genes in PPAR α wild-type and -/- mice

The availability of PPAR α knock-out mice offers an alternative system to study the activity of PPAR α . This system is ideal due to the zero level of PPAR α in hepatocytes, and therefore offers a more sensitive system to study peroxisome proliferation following transient transfection of PPAR α from different species. So far three members of the *Cyp4a* family have been identified in mouse (Henderson *et al.*, 1994; Bell *et al.*, 1993; Heng *et al.*, 1997), some of which are inducible by peroxisome proliferators. Initially, the expression and induction of *Cyp4a* gene family members, such as *Cyp4a10*, *12* and *14*, were studied in S129 PPAR α wild type and knock-out mice *in vivo*. This will determine which members of the *Cyp4a* family in this mouse strain are highly inducible by PPs, and so could be utilised as a marker of peroxisomal events in primary hepatocytes.

After three consecutive days of dosing with peroxisome proliferators MCP and Wy-14,643 (25mg/kg) in male S129 PPAR α wild-type mice, hepatomegaly was observed in all animals. This suggests that peroxisome proliferation has occurred in these animals, which was absent in similarly treated PPAR α knock-out mice. RNase protections were performed on total RNA using riboprobes for each member of the *Cyp4a* gene family (*4a10*, *12* and *14*).

Cyp4a10, *12* and *14* cDNA clones were cloned in the pGEM7 cloning vector (Figure 3.13). Probes were designed from the 3' half of each gene and were shown to be specific for their respective genes (Bell *et al.*, 1993). To demonstrate specificity, the RNase protection assay was

evaluated which successfully discriminated between the *Cyp4a10* and *12* transcripts under the conditions used (Bell *et al.*, 1993). *Cyp4a10* and *12* anti-sense probes were transcribed from the SP6 promoter of EcoRI digested templates, which gave 200 bp and 487 bp full length probe, and 155 bp and 401 bp protected fragments, respectively. The antisense probe for *Cyp4a14* was transcribed from the T7 promoter, producing a full length transcript of 220 bp and a protected fragment of 200 bp.

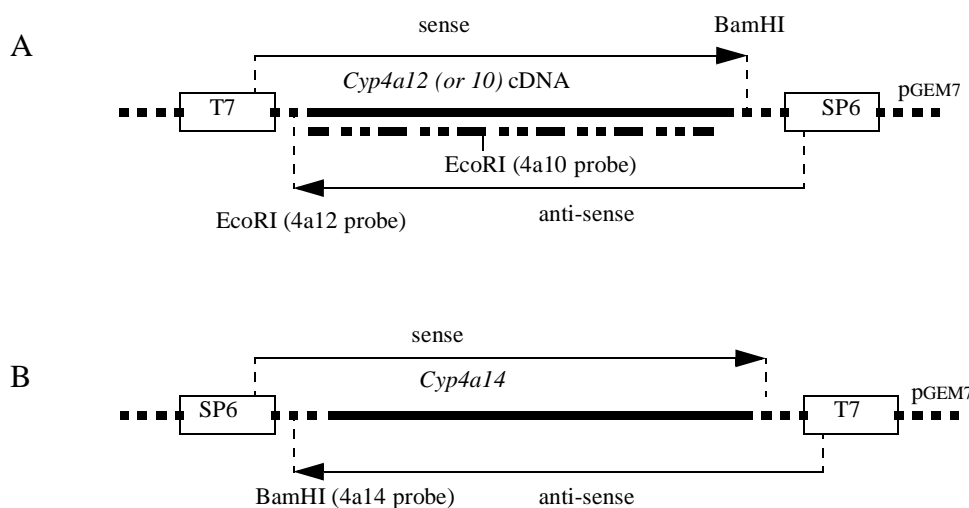


Figure 3.13 Cartoon of *Cyp4a10*, *12* (A) and *14* (B) templates. Fragments corresponding to the 3' ends of the *Cyp4a* cDNAs were cloned into the polylinker region of pGEM7 cloning vector. Anti-sense riboprobe of *Cyp4a10* is generated by *in vitro* transcription of *EcoRI* cut template from SP6 promoter, resulting in 200 bp length probe of which 150bp corresponds to *Cyp4a10* insert. Anti-sense riboprobe of *Cyp4a12* is generated by *in vitro* transcription of *EcoRI* cut template from SP6 promoter, resulting in 487 bp length probe of which 401 bp corresponds to *Cyp4a12* insert. Anti-sense riboprobe of *Cyp4a14* is generated by *in vitro* transcription of *BamHI* cut template from T7 promoter, resulting in 220 bp length probe of which 200 bp corresponds to *Cyp4a14* insert

Section 3.3.1 Induction of murine *Cyp4a* gene family

Section 3.3.1.1 Effects of PPs on *Cyp4a10* expression

Expression of *Cyp4a10* gene has been studied previously in male and female mice, and shown to be highly induced (Bell *et al.*, 1993). Here, the expression and induction of this gene was studied in male S129 PPAR α wild-type and knock-out mice. Using the *Cyp4a10* probe, RNase protection was carried out on total liver RNA from control and MCP treated mice. The RNase protection assay detected a protected fragment in the liver RNA which was specific, since no protected band was present in the RNase A-treated yeast tRNA. RNase protection assays were

performed using the *Cyp4a10* probe on liver RNA of control and MCP treated male PPAR α wild-type and knock-out mice (Figure 3.14). Constitutive expression of *Cyp4a10* mRNA was detected in the liver of control wild-type mice. However, *Cyp4a10* was expressed at very low levels in the liver of knock-out mice treated with the vehicular control corn oil. This level was detected only after prolonged exposure of autoradiographs, and as a result, this level of expression could not be quantified and compared against the control level of wild-type mice. Treatment of wild-type mice with MCP and Wy-14, 643 (25mg/kg) led to a large induction of up to 31 and 41.3-fold, respectively, of *Cyp4a10* in the liver RNA (Figure 3.17). There was no change in the expression of *Cyp4a10* in knock-out mice following treatment with either MCP or Wy-14,643.

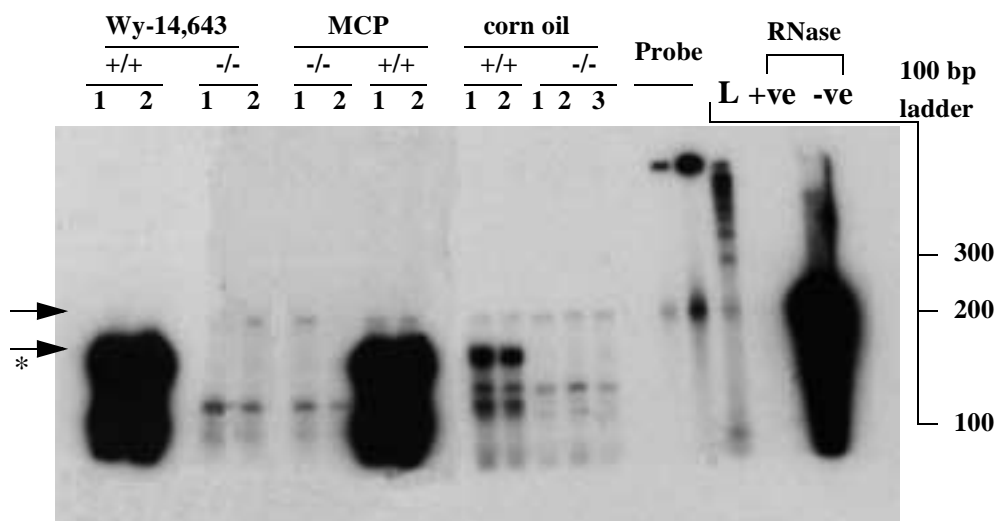


Figure 3.14 *Cyp4a10* expression in PPAR α wild-type and knock-out mice. Male S129 PPAR α wild-type and knock-out mice were treated with either MCP, Wy-14,643 (25mg/kg) or corn oil for three consecutive days, and their liver RNA extracted as detailed in methods. Either 2 or 3 animals are used per treatment group (numbered). RNase protection assay were performed on 30 μ g of RNA using *Cyp4a10* probe. Yeast tRNA treated with (+ve) or without (-ve) RNase A is also included in the assay. Protection assays were run on a 6% gel and visualised by autoradiography. The position of full-length probe is indicated by filled arrow, and the position of the protected fragment by an arrow with an asterisk placed next to it. +/+ and -/- represents wild-type and knock-out mouse liver RNA, respectively. The position of 100bp ladder (L) fragments and their sizes are shown in base pairs.

Section 3.3.1.2 Effects of PPs on *Cyp4a14* expression

Expression of the *Cyp4a14* gene has been studied previously in male and female mice, and shown to be highly inducible (Bell *et al.*, 1993). Here, the expression and induction of this gene

was studied in male S129 PPAR α wild-type and knock-out mice. Using the *Cyp4a14* probe, RNase protection was carried out on liver RNA from control and MCP treated mice. The RNase protection assay detected a protected fragment in the liver RNA which was specific to the probe since no protected band was present in the RNase A-treated yeast tRNA. Expression of *Cyp4a14*, as with *Cyp4a10*, was detectable in the control male liver of wild-type mice, and was detectable in knock-out mice only after prolonged exposure of autoradiographs (Figure 3.15). Therefore the constitutive level of expression of *Cyp4a14* in the liver RNA of knock-out mice is low when compared to control wild-type mice. Administration of MCP and Wy-14,643 led to no change in the level of *Cyp4a14* in the male liver of knock-out mice, but gave a large induction of *Cyp4a14* (80-fold and 41-fold respectively) in the liver of wild-type mice (Figure 3.17). Thus, *Cyp4a10* and *14* are expressed in PPAR α wild-type mice, and are induced more than 30-fold after treatment with the peroxisome proliferators MCP and Wy-14,643.

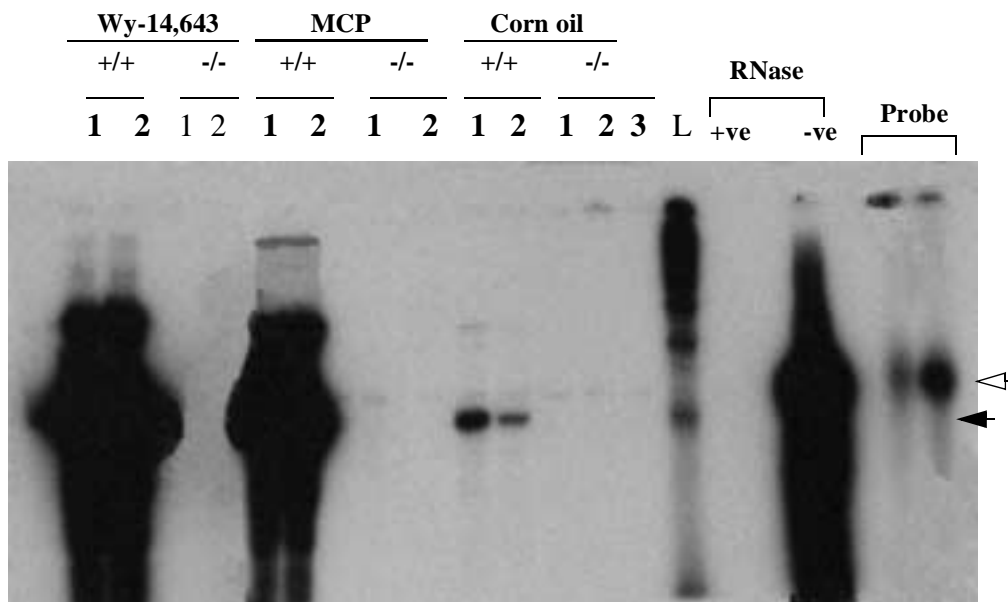


Figure 3.15 *Cyp4a14* expression in PPAR α wild-type and knock-out mice. Male S129 PPAR α wild-type and knock-out mice were treated with either MCP, Wy-14,643 (25mg/kg) or corn oil (100 μ l) for three consecutive days, and their liver RNA extracted as detailed in methods. Either 2 or 3 animals are used per treatment group (numbered). RNase protection assay were performed on 30 μ g of RNA using an anti-sense riboprobe of *Cyp4a14*, labelled with [α ³²P] CTP. Yeast tRNA treated with (+ve) or without (-ve) RNase A are also included in the assay. Protection assays were run on a 6% gel and visualised by autoradiography. The position of full-length probe is indicated by filled arrow, and the position of the protected fragment by an arrow with an asterisk placed next to it. +/+ and -/- represents wild-type and knock-out mouse liver RNA, respectively. L = 100bp ladder. Full-length probe is indicated by unfilled arrow while protected band is shown by filled arrow.

Section 3.3.1.3 Effects of PPs on *Cyp4a12* expression

Expression of *Cyp4a12* has been studied previously in male and female mice, and shown to be regulated in a sex specific manner (Bell *et al.*, 1993). Here, the expression and induction of this gene was studied in male S129 PPAR α wild-type and knock-out mice. Using the *Cyp4a12* probe, RNase protection assay was carried out on liver RNA from control and MCP treated mice. The RNase protection assay detected a protected fragment in the liver RNA which was specific to the probe since no such protected band was present in the RNase A-treated yeast tRNA. *Cyp4a12* was readily detectable in the liver RNA of both control wild-type and knock-out mice. However, there was a four fold reduction in the expression of *Cyp4a12* mRNA in the liver of

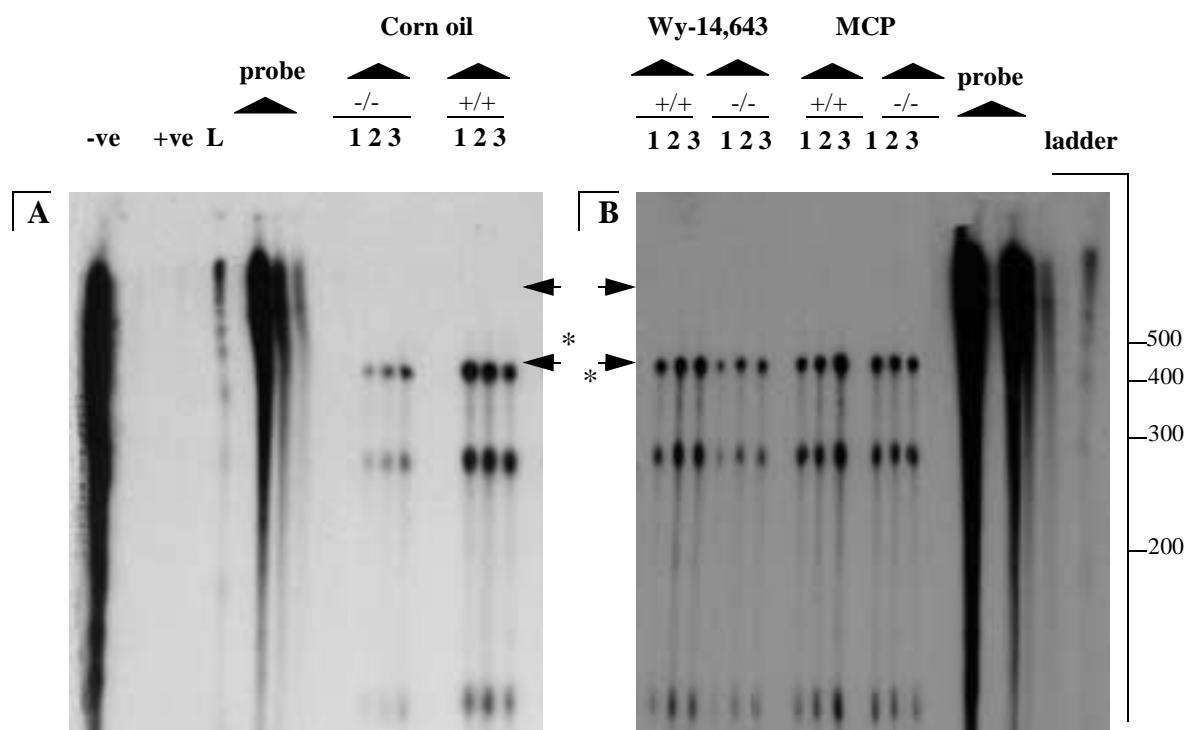


Figure 3.16 *Cyp4a-12* expression in PPAR α +/+ and -/- mice. Male S129 PPAR α wild-type and null mice were treated with either (A) corn oil (100 μ l) or (B) MCP or Wy-14,643 (25mg/kg) for three consecutive days, and their liver RNA extracted as detailed in methods. Three animals are used per treatment group (numbered 1-3). RNase protection assay were performed on 30 μ g of RNA using an anti-sense riboprobe of *Cyp4a12*. The specificity of the probe was determined by inclusion of two control yeast tRNA samples and hybridised to the probe. One sample was treated without RNase A (-ve), while the other was treated with RNase A (+ve). Following hybridisation and RNase A treatment, precipitated RNA samples were resolved in a 6% denaturing urea/acrylamide gel by running in 1xTBE for 3 hours at 320v. Gels were fixed, dried and exposed to hyperfilm at -80 $^{\circ}$ C for 15 hours. Protected bands were quantified using a phosphorimager. The position of full-length probe is indicated by filled arrow, and the position of the protected fragment by an arrow with an asterisk placed next to it. +/+ and -/- represents wild-type and knock-out mouse liver RNA, respectively. The position of 100bp ladder (L) fragments and their sizes are shown in base pairs.

knock-out mice when compared to wild-type (Figure 3.16 and 17). Upon administration of MCP or Wy-14,643, there was no change in the expression of *Cyp4a12* mRNA in both wild-type and knock-out mice.

In vivo studies demonstrated that *Cyp4a10* and *14* were highly inducible by peroxisome proliferators in the liver of male PPAR α wild-type mice. In contrast, PPAR α null mice are refractory to *Cyp4a* induction by peroxisome proliferators, and the constitutive level of expression of these *Cyp4a* genes is much lower in knock-out mice than wild-type mice. Treatment of both wild-type and knock-out mice with peroxisome proliferators had no effect on the expression of *Cyp4a12* in the male liver.

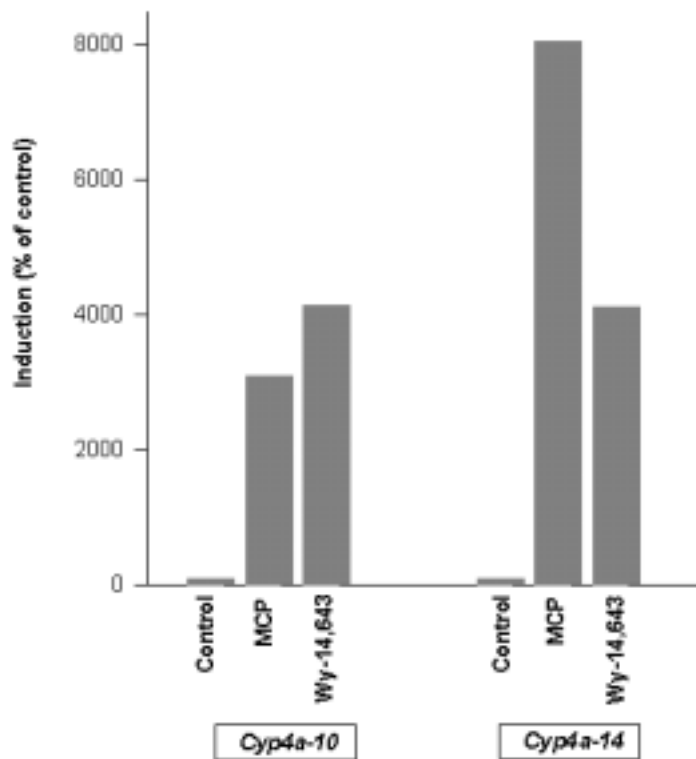


Figure 3.17 Induction of *Cyp4a10* and *14* in *+/+* mice. Groups of two male mice were dosed with either 100 μ l corn oil or 25mg/kg MCP or Wy-14,643 for three consecutive days. RNase protection were performed on the extracted liver RNA from each animal using anti-sense riboprobe derived from *Cyp4a10* and *14* cDNA clone, as detailed in methods. Protected bands were resolved on a 6% gel, and the bands were quantified using a phosphor imager on the linear range of the signal. Mean values of each treatment group were calculated and expressed as percentage of control.

Section 3.3.2 Primary mouse hepatocyte culture system

Hepatocytes from male S129 PPAR α wild-type and knock-out mice were isolated by two-step collagenase perfusion assay as described for rat with slight modifications. Unlike rat, a gall bladder is present in mouse which is ligated during perfusion and removed at the end of perfusion to avoid any contamination. Cell viability of 80% was routinely obtained and was used for subsequent experiments. Mouse hepatocytes are larger in diameter than rat hepatocytes, and it was found that a 1×10^6 cells per flask was optimal for obtaining a uniform monolayer. A typical isolation procedure yielded 3×10^7 viable hepatocytes from 25-30g male S129 mice.

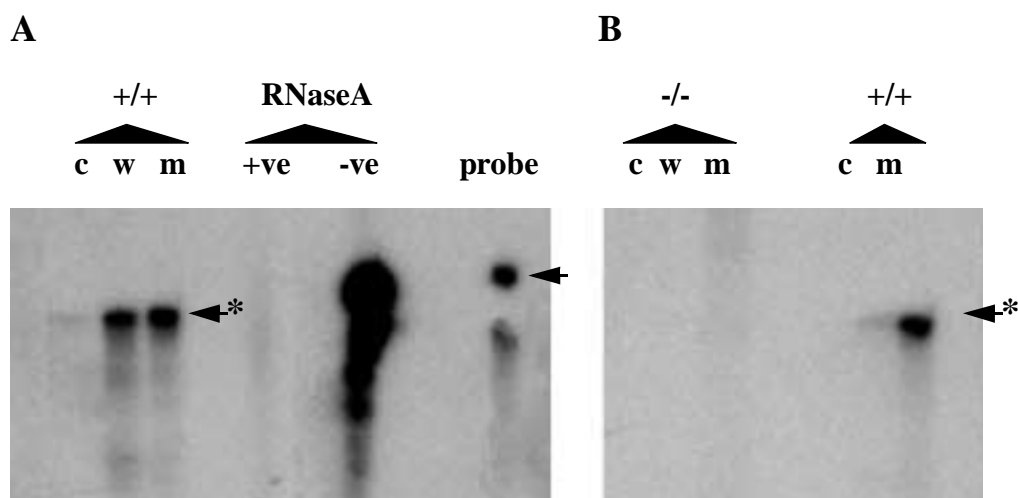


Figure 3.18 Expression of Cyp4a14 in hepatocytes of PPAR α +/+ and -/- mice. Hepatocytes were isolated from PPAR α wild-type (+/+) or knock-out (-/-) mice and seeded at a density of 1×10^6 cells/flask in CL-15 medium. Twenty-four hours after seeding cells were dosed with either 100 μ M MCP (m), 100 μ M WY-14,643 (w), or no chemicals (c), and cultured for a further 48 hours. RNase protection were carried out on extracted RNA using an anti-sense riboprobe of Cyp4a14 as described in methods. The specificity of the probe was determined by inclusion of two control yeast tRNA samples and hybridised to the probe. One sample was treated without RNase A (-ve), while the other was treated with RNase A (+ve). The position of full-length probe is indicated by filled arrow, and the position of the protected fragment by an arrow with an asterisk placed next to it. Following hybridisation and RNase A treatment, precipitated RNA samples were resolved in a 6% denaturing urea/acrylamide gel by running in 1xTBE for 2 hours at 120v. Gels were fixed, dried and exposed to hyperfilm at -80 $^{\circ}$ C for 15 hours. Protected bands were quantified using a phosphor imager. Position of the full-length probe is shown by the solid arrow while the protected fragment is indicated by a solid arrow with an asterisk placed next to it.

Section 3.3.2.1 Induction of Cyp4a genes in primary mouse hepatocytes

Induction of Cyp4a10 and Cyp4a-14 by MCP was determined in primary mouse hepatocyte culture. Hepatocytes were isolated and cultured as detailed in section 2.2. Hepatocytes were ex-

posed to MCP for 48 hours and RNase protection assays were performed on total RNA. Figure 3.18 shows a typical protection gel obtained for *Cyp4a14*. Constitutive expression of *Cyp4a14* was detectable in hepatocytes isolated from wild-type mice, which is induced by 9.5-fold and 6.6-fold after dosing with 100 μ M MCP and Wy-14,643, respectively (Figure 3.19). The vehicular control DMSO had no effect on the expression of *Cyp4a14*, showing that the induction was specifically due to the effects of MCP and Wy-14,643. As with the *in vivo* data, *Cyp4a14* was not detectable in control or MCP treated hepatocytes of PPAR α knock-out mice. Similar results were obtained with a *Cyp4a10* probe in primary hepatocytes isolated from wild-type and knock-out mice (data not shown).

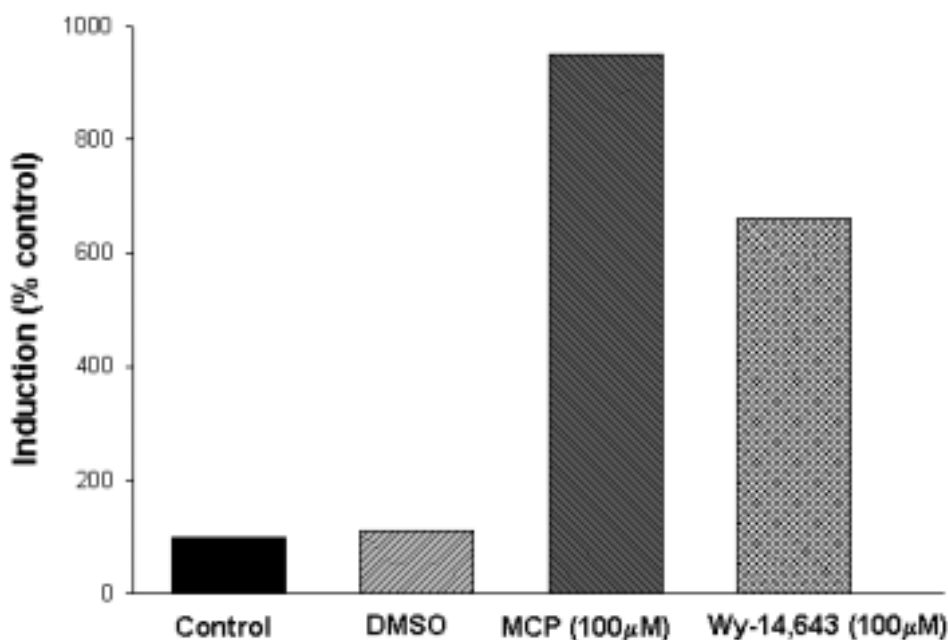


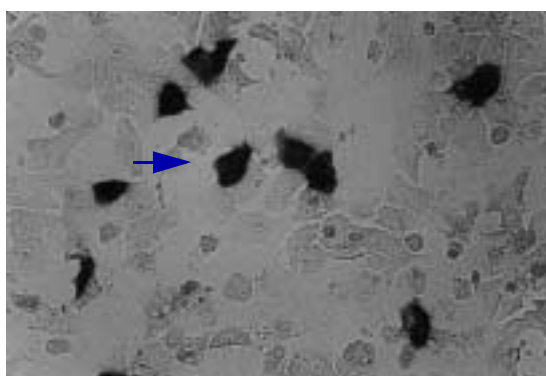
Figure 3.19 Induction of *Cyp4a14* in primary mouse hepatocytes. Isolated hepatocytes were seeded at a density of 1×10^6 cells/flask in CL-15 medium. Twenty-four hours after seeding cells were dosed with 100 μ M MCP, 100 μ M Wy-14,643, 10 μ l DMSO or no chemicals (control) and cultured for a further 48 hours. RNase protection were carried out on extracted RNA using an anti-sense riboprobe of *Cyp4a14* as described in methods. Thirty micrograms of RNA of each sample was used to hybridise [α - 32 P] CTP labelled probe with high specific activity. Protected bands were resolved on a 6% gel, and the bands were quantified using a phosphor imager within the linear range of the signal. Results are expressed as as percentage of control, and represent mean value of a least two independent experiments.

Section 3.3.2.2 Transient transfection of mouse hepatocytes

A liposome-based method of transfection was used for the delivery of the eukaryotic expression vectors containing PPAR α genes into primary hepatocytes. Synthetic cationic lipid was used as a means of transfecting primary hepatocytes with foreign DNA. A non-commercial form of lipofectin termed DOTMA/DOPE (DDP) was prepared in the laboratory, and this formulation has been used successfully before to transfect primary rat hepatocytes and human embryonic kidney 293 cell line (NJ Horley, AR Bell, PhD theses). This established protocol was used as a guideline for further optimisation of transfection of rat and mouse hepatocytes. A plasmid containing a β -galactosidase gene (pRSV- β -gal) was used for the optimization protocol as this plasmid constitutively expresses the β -galactosidase enzyme which can be detected histochemically (Sanes *et al.*, 1986). To determine the optimal transfection conditions, either the amount of DNA or lipofectin were varied while the other was kept constant and the transfection efficiency was determined. Transfection efficiency was expressed as the percentage of cells stained positive blue after histochemical staining with X-gal as shown in Figure 3.20 (chromogenic assay).

Figure 3.21 (A) shows

A Transfected Rat Hepatocytes



B Transfected Mouse Hepatocytes

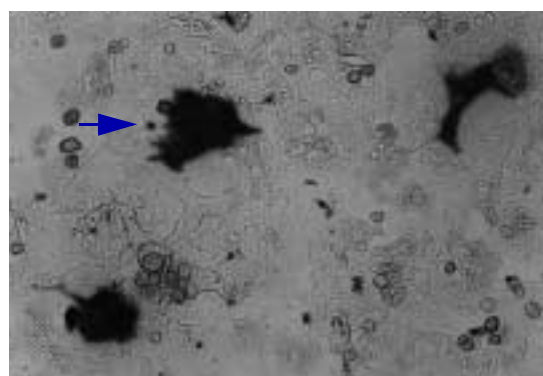


Figure 3.20 Transfection of pRSV- β -GAL in (A) rat and (B) mouse hepatocytes. Isolated hepatocytes were seeded and cultured in CL-15 medium for 24 hours prior to transfection. Hepatocytes were transfected with 6 μ g of DNA (pRSV- β -GAL) complexed with 10 μ g of lipofectin reagent (DDP) for 4 hours by incubating at 37 $^{\circ}$ C in insulin and serum-free CL-15 medium. Cells were cultured for a further 24-30 hours in CL-15 medium before being fixed and stained for β -galactosidase activity. Transfected cells expressing β -galactosidase gene are stained blue after histochemical staining with X-gal chromogenic reagents as indicated by arrow.

the effects of varying the amount of DNA on transfection efficiency, and Figure 3.21 (B) shows the effects of varying the amount of lipofectin on transfection efficiency. Generally, higher transfection efficiency was obtained with rat hepatocytes compared to mouse for the range of concentrations of DNA and lipofectin reagents used. The optimal conditions for transfection

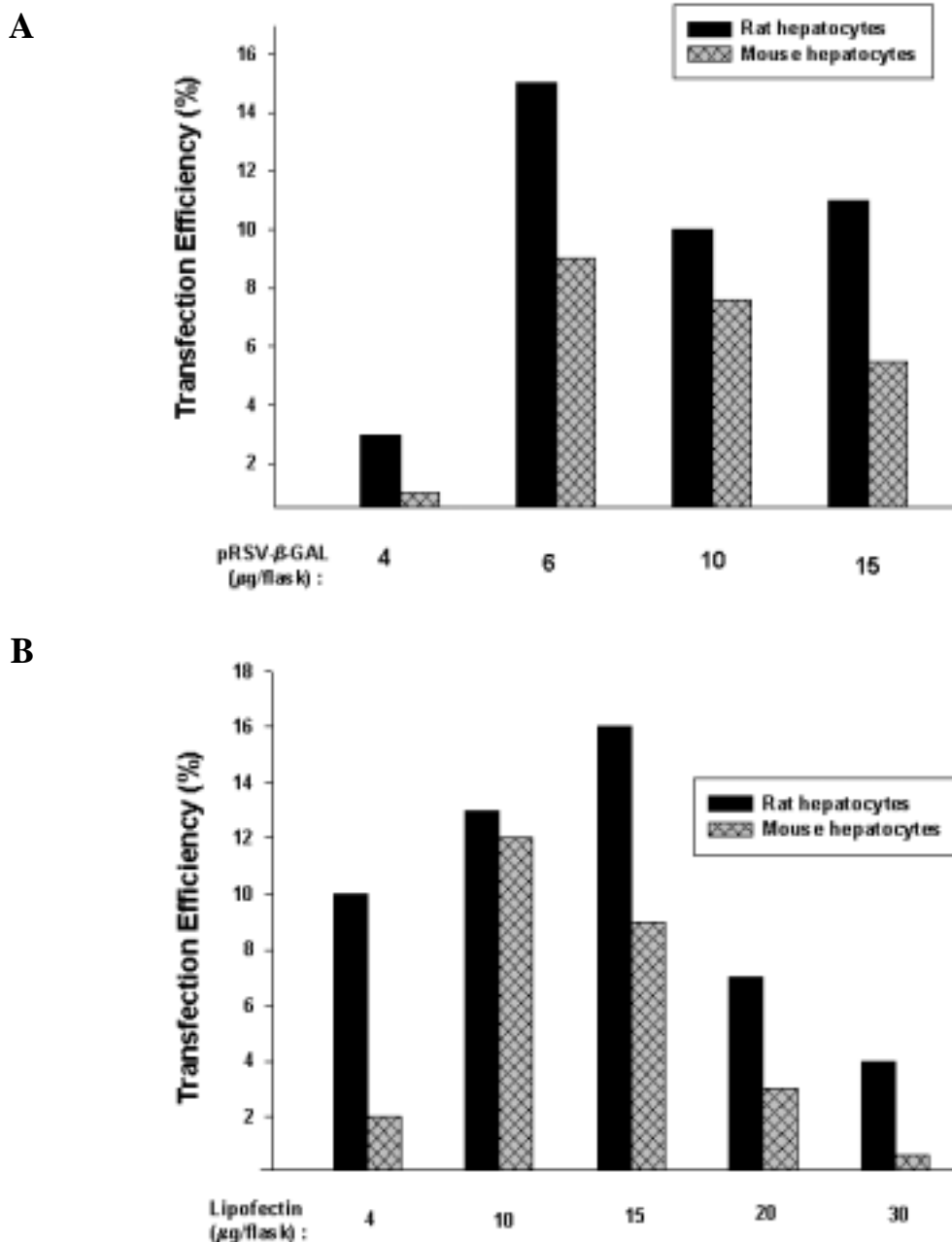


Figure 3.21 Optimisation of transfection efficiency (A) DNA and (B) lipofectin reagent. Isolated hepatocytes were seeded and cultured in CL-15 medium for 24 hours prior to transfection. As indicated, hepatocytes were transfected with either (A) 10μg of lipofectin reagent (DDP) complexed with variable amounts of DNA (pRSV-β-GAL) or (B) 10μg of DNA complexed with variable amounts of lipofectin reagent for 4 hours by incubating at 37 °C in insulin and serum-free CL-15 medium. Cells were cultured for a further 24-30 hours in CL-15 medium before being fixed and stained for β-galactosidase activity. Transfected cells expressing β-galactosidase gene are stained blue after histochemical staining with X-gal. Data are expressed as % transfection efficiency, where four fields were counted for two flasks for each data point, and represents the mean value of two independent experiments.

were found to be 6µg DNA and 6-10µg DDP. Under these conditions transfection efficiencies of 18% and 12% were observed for rat and mouse primary hepatocyte cultures, respectively. Using these optimised conditions, hepatocytes from PPAR α knock-out mice were transfected with eukaryotic expression vector containing PPAR α receptor genes.

Section 3.3.2.3 Transfection of PPAR α in primary mouse hepatocytes

Primary hepatocyte cultures developed from PPAR α knock-out mice have been used to study how different forms of PPAR α induce their physiological responses to peroxisome proliferators. Following their transfection, the trans-activating ability of mouse and guinea pig PPAR α was examined by studying the expression of mouse endogenous *Cyp4a10* and *14* genes in primary hepatocytes of PPAR α knock-out mice. Hepatocytes were transfected with either mouse or guinea pig PPAR α and cultured for a further 48 hours in the presence of peroxisome proliferators MCP or Wy-14,643. RNase protection was performed on total RNA extracted from post-transfected cells using anti-sense riboprobes of *Cyp4a10* or *14*. As expected *Cyp4a14* expression was undetectable in both control and PP-treated non-transfected hepatocytes from PPAR α knock-out mice (-/-). However, there is no evidence of *Cyp4a14* expression when these cells were transfected with either mouse or guinea pig PPAR α and treated with PPs (Figure 3.22). RNA preparations from hepatocytes (*in vitro*) and livers of control and MCP-treated wild-type mice were used as positive controls. As shown in Figure 3.22, expression and induction of *Cyp4a14* was detectable in these control and MCP-treated samples, respectively, using the same probe. No protected bands were detectable in -/- hepatocytes transfected with either mouse or guinea pig PPAR α even when gels were exposed for much longer period (14 days, data not shown). A 4-fold higher amount of probe was used for the protection of MCP and Wy-14,643 treated RNA to look for any evidence of the *Cyp4a14* protected fragment while minimising background level of radioactivity in control samples. As shown in Figure 3.22 C, both control vector and mouse PPAR α transfected hepatocytes, treated with MCP and Wy-14,643

gave similar results; showing a smear of radioactivity in the track, including the position of expected protected fragment. It was concluded that this did not represent a protected fragment since a similar track profile was observed in tRNA samples protected with the same amount of probe. Similar results were also observed with guinea pig PPAR α -transfected $-/-$ hepatocytes with high levels of probes in the treated samples (Figure 3.22 E).

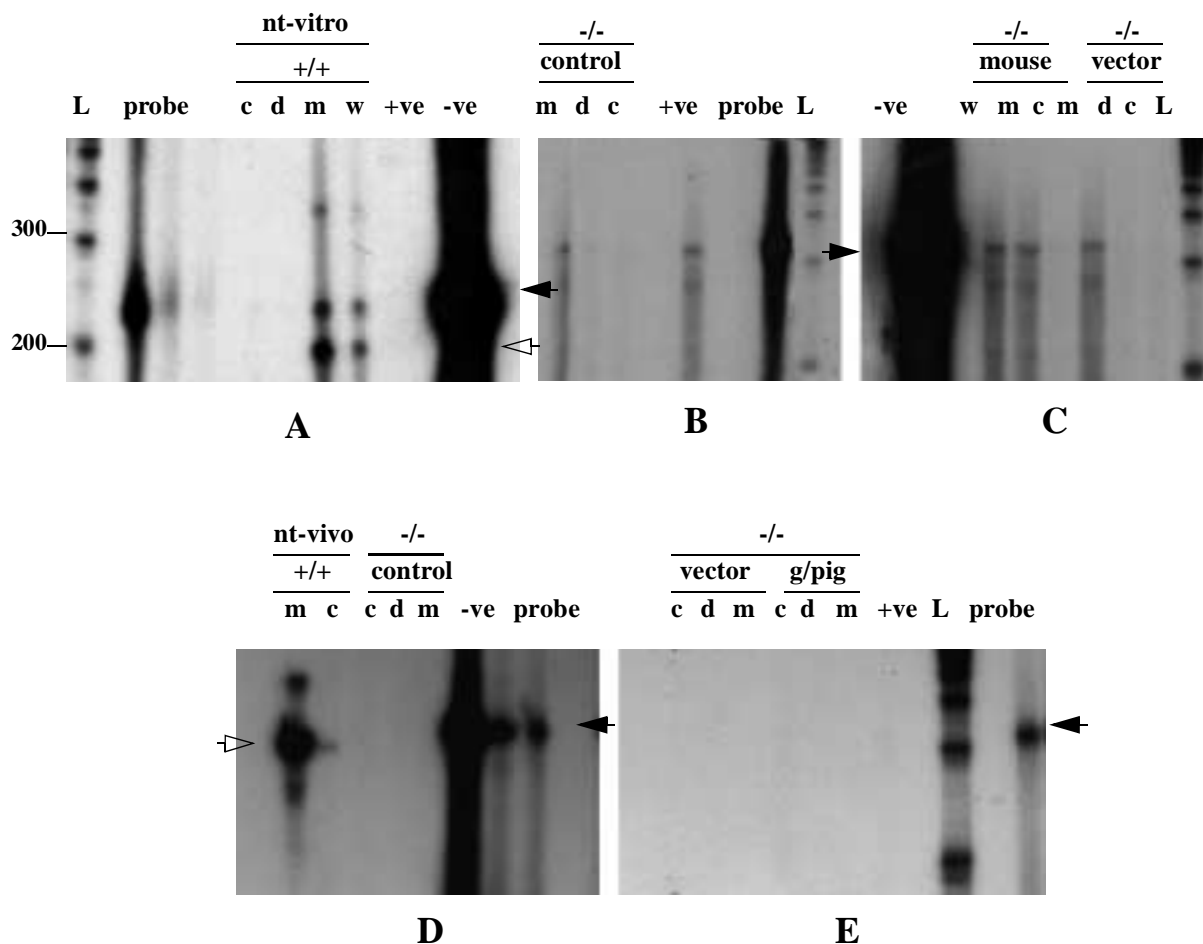


Figure 3.22 Effect of transfected PPAR α on expression of *Cyp4a14* in hepatocytes. Isolated hepatocytes from PPAR α wild-type (+/+) and knock-out mice (-/-) were seeded at a density of 1×10^6 cells/flask. Following seeding, -/- hepatocytes were transfected with no DNA (control) or 3mg of either mouse PPAR α (mouse, B & C), guinea pig PPAR α (g/pig, D & E) or their control vector (vector) complexed with lipofectin reagent as described in methods. pRSET- β plasmid DNA was added to each flask to make the final amount of DNA 6 μ g per flask. Cells were dosed with 100 μ M of MCP (m) or Wy-14,643 (w), 10 μ l of DMSO (d) or no chemicals (c) and cultured for a further 48 hours. RNase protection were carried out on extracted RNA from (+/+) or (-/-) hepatocytes using an anti-sense riboprobe of *Cyp4a14*, and 30 μ g of RNA of was used per protection. In A, B and C, higher amounts of probes (4-fold) were used in MCP and Wy-14,643 than for control and DMSO samples to reduce back ground noise in control samples. The specificity of the probe was determined by inclusion of two control yeast tRNA samples hybridised to the probe and treated with (+ve) or without (-ve) RNase A. Following hybridisation and RNase A treatment precipitated RNA samples were resolved in a 6% denaturing gel and exposed for 15hr (A, D-E) or 48hr (B-C). As a positive control, non-transfected cells treated with MCP (100 μ M) (A, +/+ nt-vitro) and MCP-treated (25mg/kg) in vivo (D, +/+ nt-vivo) were used. The position of 100bp ladder (L) fragments and their sizes are shown in base pairs. The position of full-length probe is indicated by filled arrow, and the position of -ve protected fragment by an unfilled arrow.

Section 3.3.2.4 Expression of transfected PPAR α in mouse hepatocytes

Addition of exogenous PPAR α (mouse and guinea pig) in primary hepatocyte of PPAR α knock-out mice resulted in no detectable changes in the trans-activating activity of PPAR α , as measured by the induction of their responsive genes *Cyp4a10* and 14 (Figure 3.23). To eliminate the possibility that the transfected PPAR α gene is not being expressed, the expression of PPAR α in the post-transfected hepatocytes was examined. Using an anti-sense riboprobe for the guinea pig PPAR α gene, RNase protection was carried out on RNA derived from hepatocytes transfected with guinea pig PPAR α . Figure 3.23 demonstrates that guinea pig PPAR α mRNA is expressed in hepatocytes following their transfection. As expected, no protected bands were observed in the RNA of non-transfected and pBK-CMV vector transfected hepatocytes. As the

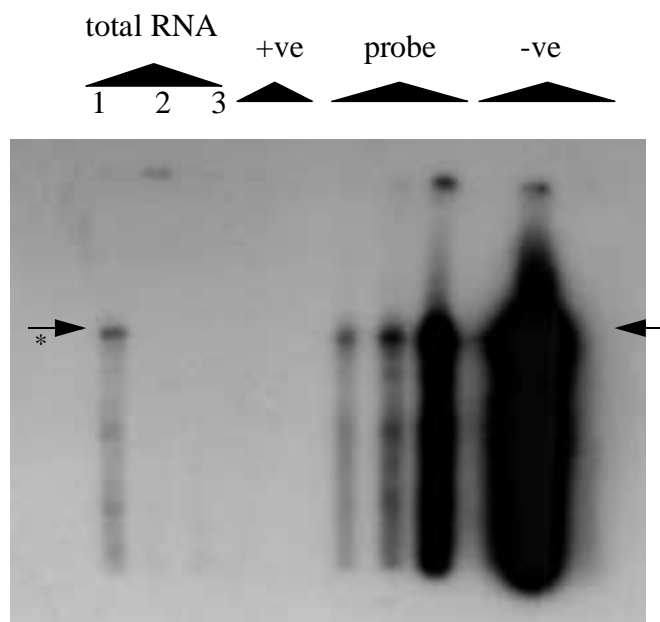


Figure 3.23 Guinea pig PPAR α mRNA after transfection into hepatocytes of +/- mice. Isolated hepatocytes were seeded at a density of 1×10^6 cells/flask in CL-15 medium. Twenty-four hours after seeding cells were transfected with either 3 μ g of gpPPAR α -pBK-CMV expression vector (1) or 3 μ g of pBK-CMV vector alone (2) or no DNA (3) complexed with 10 μ l of lipofectin reagent for 4 hours by incubating at 37 $^{\circ}$ C in insulin and serum-free CL-15 medium. Cells were cultured for a further 48 hours in CL-15 medium. RNase protection were carried out on extracted RNA using an anti-sense riboprobe of gpPPAR α as described in methods. Thirty micrograms of RNA of each sample was used to hybridise [α - 32 P] CTP labelled probe. The specificity of the probe was determined by inclusion of two control yeast tRNA samples and hybridised to the probe. One sample was treated without RNase A (-ve), while the other was treated with RNase A (+ve). The position of full-length probe is indicated by filled arrow, and the position of the protected fragment by an arrow with an asterisk placed next to it. Following hybridisation and RNase A treatment, precipitated RNA samples were resolved in a 6% denaturing urea/acrylamide gel by running in 1xTBE for 2 hours at 120v. Gels were fixed, dried and exposed to Hyperfilm at -80 $^{\circ}$ C for 15 hours.

probe was synthesised from the same expression vector containing guinea pig cDNA insert that was also used for transfection, the protected fragment has the same size as the full-length probe due to the presence of polylinker sequence present both in the full-length probe and in the expressed gpPPAR α mRNA. The protected fragment is specific as shown by its absence in tRNA samples hybridised to the probe and subjected to RNase treatment. The data presented here clearly demonstrate that, at least for guinea pig PPAR α , PPAR α RNA is expressed following transfection into hepatocytes derived from knock-out mice.

Having found that PPAR α is expressed in transfected hepatocytes, the trans-activating activity of PPAR α was assessed by its ability to induce a firefly luciferase reporter gene regulated by a PPRE response element in its promoter region. Two copies of the PPRE response element (recognised by the PPAR α receptor) from rat acyl CoA-oxidase gene were placed in the promoter region of the luciferase gene. Previously this reporter construct has been used successfully to demonstrate the functionality (transcriptional activity) of human and guinea pig PPAR α (Bell *et al.*, 1998). Figure 3.24A demonstrates that luciferase activity is observed only in the presence of co-transfected mouse PPAR α , giving 8-fold induction over control, and its activity is further increased to 14-fold in the presence of MCP. Increasing the amount of transfected PPAR α results in the increased activity of luciferase gene. Control vector pSG5 is unable to increase luciferase activity. Since the luciferase activity is increased in cells transfected with PPAR α , but not with vector, this must be due to expression of PPAR α . Similar results were obtained, albeit at lower levels of activity, with guinea pig PPAR α co-transfected with firefly luciferase reporter gene containing PPRE response elements (Figure 3.24B).

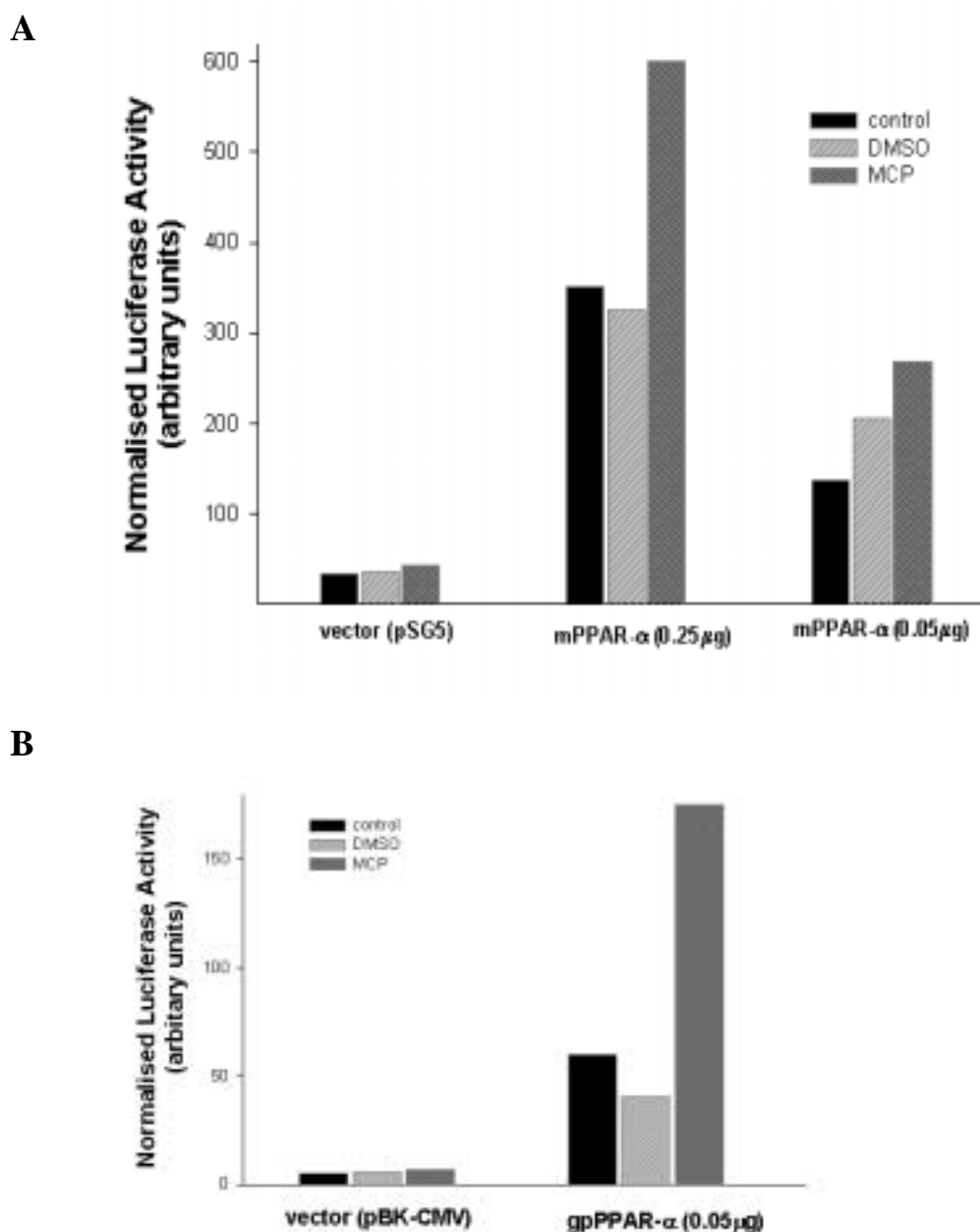


Figure 3.24 Effect of PPAR α on reporter gene in hepatocytes of $-/-$ mice. Hepatocytes were seeded at a density of 1×10^6 cells/flask in CL-15 medium. Twenty-four hours after seeding cells were co-transfected with either (A) mPPAR α -pSG5 (0.05 and 0.25 μ g) expression vector or equal amount of pSG5 vector, or (B) gpPPAR α -pBK-CMV (0.05 μ g) or equal amount of pBK-CMV with 0.1 μ g of (ACO-PPRE) $_2$ -pGL3-Luc and 0.001 μ g pRL-CMV, complexed with 10 μ l of lipofectin reagent. pRSET- β plasmid DNA was added to each flask to make the final amount of DNA 6 μ g per flask, and incubated at 37 $^\circ$ C for 4 hours in insulin and serum-free CL-15 medium. Cells were dosed with 10 μ M MCP, 10 μ l DMSO or no chemicals (control) and cultured for a further 24-30 hours in CL-15 medium. Cell extracts were harvested and assayed for Firefly luciferase activity and *Renilla* luciferase activity. Firefly reporter gene activity was normalised against *Renilla* luciferase activity. Data presented are mean value of two separate experiments.

Section 3.4 Peroxisome proliferation in primary rat hepatocytes

Induction of peroxisome proliferation by MCP was investigated in rat primary hepatocytes using histochemical staining for the peroxisomal enzyme catalase. Hepatocytes were exposed to MCP (100 μ M) for 48 hours and then fixed and prepared for histochemistry. As shown in Figure 3.25, histochemical staining revealed that treatment with MCP (Figure 3.25 C and D) significantly increased the peroxisomal staining when compared to untreated controls (Figure 3.25 A and B). It is possible to utilise this simple histochemical staining of peroxisome as an end point in the study of the effects of exogenous PPAR α following their transfection in primary to hepatocytes. By normalising for transfection efficiency, using β -galactosidase staining, this system may offer an alternative approach to study the effects of transfected PPAR α from different

species.

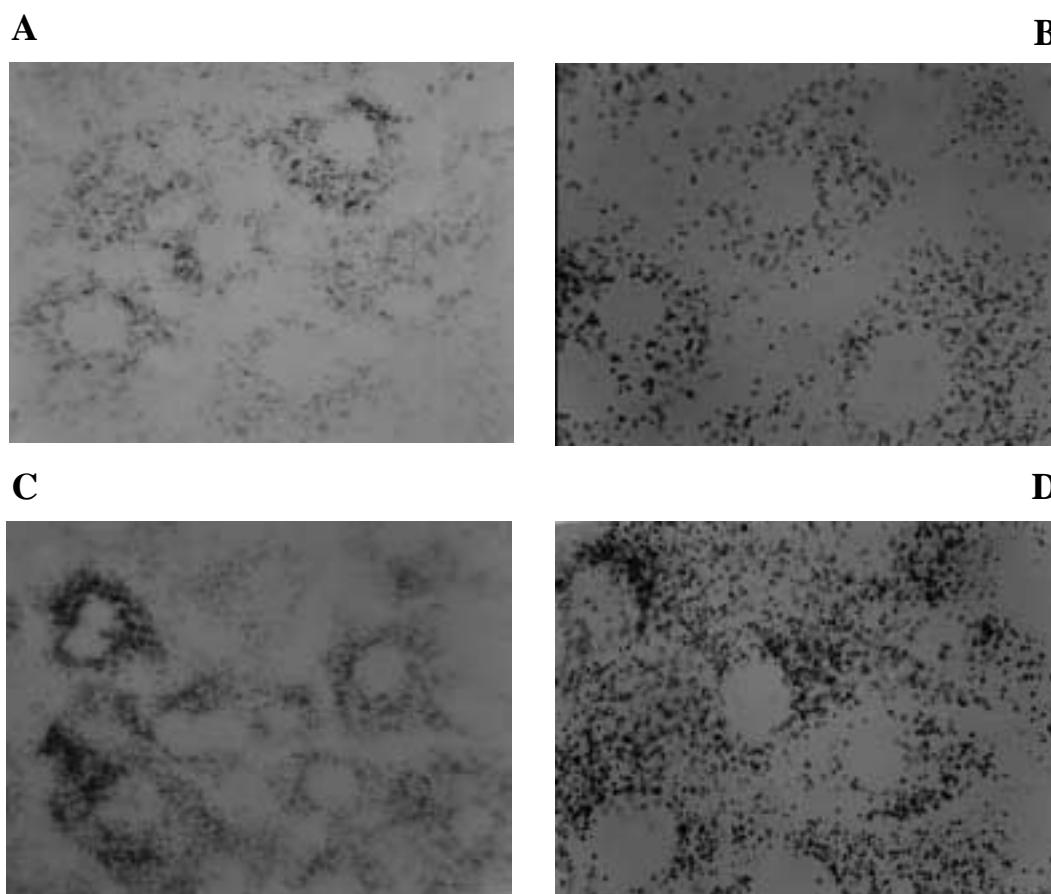


Figure 3.25 Peroxisome proliferation in rat primary hepatocytes. Isolated hepatocytes were seeded at a density of 2×10^6 cells per flask. Twenty-four hours after seeding cells were dosed with either 100 μ M MCP (C, D) or 10 μ l DMSO (A, B) and cultured for a further 48 hours. Cells were then fixed and stained for peroxisomes by histochemical staining of peroxisomal catalase as described in methods. Results are illustrated as viewed under low (A, C) and high (B, D) magnification of light microscopy. Magnification = x400 (A, C), x 800 (B, D).

Section 3.5 PCR cloning of hamster CYP4A genes

Studies in hamster of peroxisomal events such as peroxisome proliferation (Lake *et al.*, 1986; Gray *et al.*, 1984), DNA synthesis (Lake *et al.*, 1993), and induction of peroxisomal and mitochondrial enzyme activity (Lake *et al.*, 1986 and 1989; Sakuma *et al.*, 1992) show that hamster is partially responsive to peroxisome proliferation. There has been no study regarding the inducibility of CYP4A gene(s) by peroxisome proliferators. Induction of CYP4A is an early marker of peroxisome proliferation and offers a more sensitive measure of responsiveness to peroxisome proliferation in hamster. RNase protection assays could be utilised to study the ex-

pression and inducibility of CYP4A genes in hamster. As a prerequisite for such a study, cloning of CYP4A is required since no hamster CYP4A genes have been cloned. Once cloned (partial or full length cDNA), specific probes could be designed for RNase protection assay.

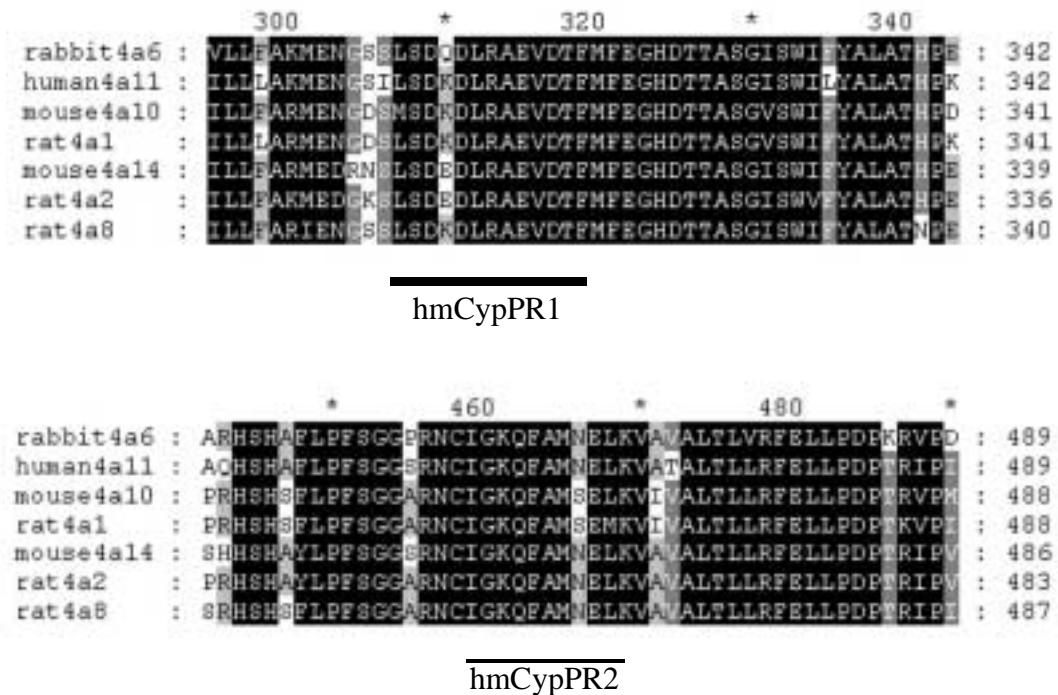


Figure 3.26 Design of PCR primers from alignment of CYP4A proteins. Forward (hmCypPR1) and reverse (hmCypPR2) primers for the cDNA cloning of putative hamster CYP4A genes were designed by aligning the amino acid sequences of rat 4A1, 4A2 and 4A3 (P08516, P20816 and P24464 respectively), mouse 4a10 and 4a14, rabbit 4A6 (P14580) and human 4A11 (Q02928) using the pileup tool within the GCG sequence analysis program, and displayed using GeneDoc. The amino acid position of rabbit 4A6 are shown at the top of the alignment while the amino acid position on the left of the alignment corresponds to individual CYP4A genes. Black shading represent 100%, dark-grey represent 80% and light-grey represent 60% conservation of the aligned region. The regions of amino acid identity used to design PCR primers are underlined.

A

```

1  AAGCTTGGAT CCCATCTCAC TCATAGCAAA TTGTTTCCCA ATGCAGTTCC
51  TTGCTCCTCC CGAGAAGGGC AGGAATGAGT GGCTGTGTGCG GGGAGAATCT
101 GCTGCAAACC TGGAAGGGTC AAACACCTCT GGGTTTGGCC ACACCTTCGG
151 GTTGTGGTGG AGTGCGTAAA TGGAGAGTAC AACTGTGGCA CCTTTGGGTA
201 AAGAGCGCCC ATCAGGGAAG GTGACAGGTG TGCTGAGCTC TCTGACAATG
251 GTTGGGGCAG GTGGGTAGAG CCTCAGGGAC TCCTTGATGC ACATGGTAGT
301 GTAGGGCATC TGGTCCAGGT GATTCCAGGT AATGGAGGAT CCATCTCCCA
351 GGAGGCTCTG AACTTCCTCC CTGCATCTCT GCCGGTATTC AGGGTGAGTG
401 GCCAGAGCAT AGAAGATCCA GGAGACTCCA CTGGCTGTGG TGTCATGTCC
451 CTCAAACATG AATGTGTCCA CCTCAGCACG TAGGTCCTTG TCAGACAAGA
501 ATTCAAGCTT

```

B

```

1  KLEFLSDKDL RAEVDTFMFE GHDTTASGVS WIFYALATHP EYRQRCREEV
51  QSLLDGSSI TWNHLDQMPY TTMCIKESLR LYPPAPTIVR ELSTPVTFPD
101 GRSLPKGATV VLSIYALHHN PKVWPNPEVF DPSRFAADSP RHSHSFLPFS
151 GGARNCIGKQ FAMSEMGSKL

```

Figure 3.27 cDNA (A) and amino acid (B) sequence of hamster CYP4A17. Three independent clones derived from PCR amplification of hamster liver cDNA using hmCypPR1 and hmCypPR2 primers were sequenced on both strands by oligo-primer walking. Full contig of individual clone was obtained using GELMERGE and GEL ASSEMBLE within GCG sequence analysis program. Final consensus sequence was obtained by analysing the full sequence of the three clones using PILE UP, TED and GeneDoc programme. The deduced amino acid sequence was obtained from the cDNA sequence by using TRANSLATE within GCG program.

The CYP4A family has been identified in a number of species including human, mouse and guinea pig, and using this sequence information PCR primers were designed. By aligning the CYP4A proteins, primers CypPR1 and CypPR2 were designed from regions of high identity. Primers CypPR1 correspond to amino acid sequence 305-316 (925-959bp of CYP4A1 mRNA;

accession number M14972) at the 3' end of the gene, while CypPR2 represents amino acid sequence 437-446 (1381-1410bp) at the 5' end of the rat CYP4A1 gene. Figure 3.26 shows the amino acid alignment of the regions of the CYP4A genes used to design the PCR primers.

First strand cDNA was synthesised from total hamster liver RNA using oligo-dT primers. When these cDNA products were subjected to PCR the amplification using CypPR1 and CypPR2 primers, an amplified fragment of the expected size, 500bp, was detected by agarose gel electrophoresis (Figure 3.28, lane 3 and 4). The same PCR reaction conditions also detected a 510bp fragment when rat CYP4A1 cDNA (in pSG5) was used as a template (Figure 3.28, lane 2) and this was absent in the negative control reaction with no template DNA added (lane 1). This

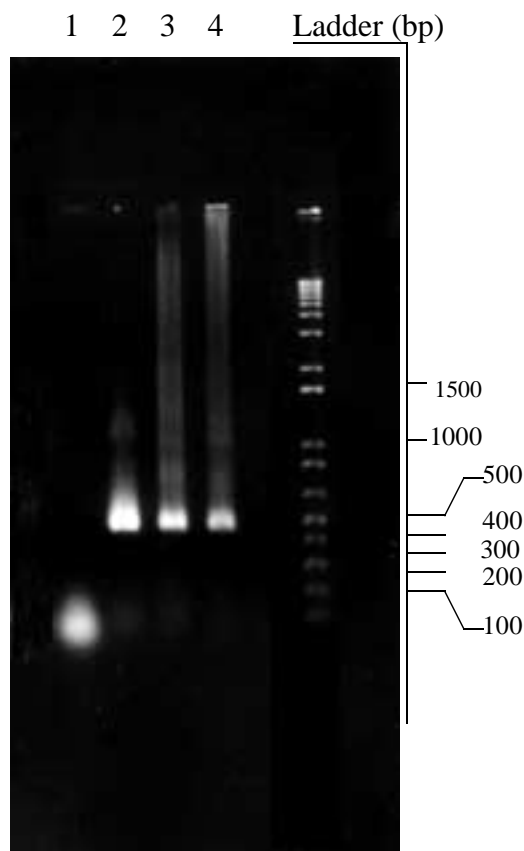


Figure 3.28 PCR of CYP4 genes from hamster liver. PCR reactions were performed using hmCypPR1 and hmCypPR2 primers on hamster liver cDNA, derived from MCP treated total RNA (lane 3-4). All PCR reactions include 1.5mM MgCl₂ (lane 1, 2, 4) except lane 3 where 2.5mM MgCl₂ was used. Lane 1 is negative control in which no template DNA was added. Lane 2 is amplification reaction using of pSG5-mPPAR-a plasmid DNA. Five ml of each reaction was analysed on a 1% agarose gel, run on 1xTBE at 90v for 90 minutes. Syber-Green was added to all samples prior to loading and the resolved DNA bands were visualised using a dark-reader. Molecular size of the DNA ladder are shown in base pairs.

demonstrates that the amplified fragment was specific to the hamster cDNA template. The amplified DNA fragment was purified from the reaction cocktail using a Qiaspin-quick column and subcloned into pGEM-T cloning vector. At least three independent clones containing the 500bp insert were purified and sequenced to obviate the artefacts arising from potential errors arising during the PCR process. Each clone was sequenced on both strands. Initial primers for sequencing were based on the T7 and SP6 promoter sequence of the pGEM-T vector, and the full-length sequence was obtained by oligo-walking process. The complete sequence of 510bp was analysed using the FASTA homology search in gene data bank (SRS) which revealed that the amplified fragment has high sequence similarity, but not identity to rat and mouse CYP4A genes (see later) and CYP4A genes from other species. Figure 3.27 shows the completed nucleic acid sequence and the deduced amino acid of this hamster CYP4A gene.

Section 3.6 Identification of multiple hamster CYP4A genes

Section 3.6.1 Restriction analysis of putative CYP4A clones

The cDNA and deduced amino acid sequence of the hamster CYP4A cDNA is highly similar to rat and mouse CYP4A genes. As there are multiple members of the CYP4A family present in rats and mice, it is possible that other CYP4A genes of CYP4A family may also be present in hamster. This possibility was investigated by restriction analysis of a number of clones containing the 510 bp insert derived from initial PCR reaction of hamster liver cDNA. A total of 50 clones were analysed by restriction digestion using EcoRI and BamHI double digests. These two restriction sites are unique in the primer/polylinker region of the cloning vector, and therefore should release the cloned fragment intact provided that there are no BamHI and EcoRI restriction sites present within the cloned fragment. However, if these restriction sites are present in the cloned fragment then a restriction pattern will be evident which is suggestive of differences of their sequence. Figure 3.29 shows the agarose gel electrophoresis analysis of the restriction pattern of 18 clones obtained using BamHI and EcoRI double digests.



Figure 3.29 Restriction analysis of hamster CYP4A clones. A total of 18 putative CYP4A clones in pGEM-T, derived from PCR of hamster liver cDNA using hmCypPR1 and hmCypPR2 primers, were double restriction digested with BamHI and EcoRI for 1 hour at 37 °C. Products were then phenol:chloroform treated as described in methods and run on 1.2% agarose gel (pre-stained with ethidium bromide) at 90v for 90 minutes. Restriction digested individual clones are numbered from 1 to 18 as shown, and uncut plasmids are represented by an asterisk placed next to the clone number. Uncut pGEM-T vector without the insert is labelled as lane A. Molecular sizes of the 1 Kb⁺ DNA ladder are shown in base pairs.

The restriction pattern obtained can be grouped into five classes of clones as shown in Table 3.1. Three clones from group A (clones 3, 4, & 9), four clones from group B (clones 1, 13, 15 and

Group	Clone number	Genes
A	3, 4, 7, 8, 9, 11	hm4Ai/CYP4A17
B	1, 13, 15 16, 17, 18	hm4Ai/CYP4A18
C	6, 14	hm4Ai/CYP4A19
D	5	mispliced mRNA
E	12	mispliced mRNA

Table 3.1 Grouping of hamster CYP4A clones by restriction digestion. A total of 25 putative hamster CYP4A clones were analysed by restriction digestion using BamHI and EcoRI. According to their restriction pattern clones were placed into five groups. Sequencing of clones from group A, B and C shows that they are different genes. These genes are named for identification purposes as shown. Clones 5 and 12 are mispliced variants of group A clones.

16), two clones from group C (clones 6 & 14), one clone from D and E (clones 5 & 12 respectively) were sequenced once on both strands. Sequence data were analysed using TED, BEST-FIT, SEQED, TRANSLATE tools within GCG programme, and the final sequence of a single contig for each clone was obtained using GELMERGE and GELASSEMBLE PROGRAMME. Sequence analysis of the cDNAs and their deduced amino acids revealed the existence of a further two new genes of CYP4A family in hamster and two mis-spliced RNAs. Group A repre-

A

```

1  AAGCTTGAAT TCTTGTCTGA CAAGGACCTA CGTGCTGAGG TGGACACATT
51  CATGTTTGAA GGTCATGATA CCACAGCCAG TGGAAATATCC TGGATTTTTTT
101 ATGCTCTGGC CACACACCCT GAATACCAAC AGAGATGCAG GGAAGAGGTA
151 CAGAGCATCC TGGGAGATGG AACCTCTGTC ACCTGGGATC ACCTGGACCA
201 GATGCCCTAC ACTACCATGT GCATCAAGGA GGCCCTGAGG CTCTACCCAC
251 CAGTACCAAG TGTGAGTCGA GAGCTCAACA CACCTGTCAC CTTCCCTGAT
301 GGACGCTCCT TACCTAAAGG TATCACAGTT GCAATCTCCA TTTATGGCCT
351 TCACCATAAT CCAAGTTTGT GGCCAAACCC TGAGGTGTTT GACCCATCGA
401 GATTTGCACC AGATTCTTCT CGGCACAGCC ATGCTTTCCT GCCCTTCTCA
451 GGAGGAGCAA GAAACTGCAT TGGGAAACAA TTTGCTATGA GTGAGATGGG
501 ATCCAAGCTT

```

B

```

1  KLEFLSDKDL RAEVDTFMFE GHDTTASGIS WIFYALATHP EYQQRCEEV
51  QSILGDGTSV TWDHLDQMPY TTMCIKEALR LYPPVPSVSR ELNTPVTFPD
101 GRSLPKGITV AISIYGLHHN PSLWPNPEVF DPSRFAPDSS RHSHAFLPFS
151 GGARNCIGKQ FAMSEMGSKL

```

Figure 3.30 cDNA (A) and amino acid (B) sequence of hamster CYP4A18. Four independent clones derived from PCR amplification of hamster liver cDNA using hmCypPR1 and hmCypPR2 primers were sequenced on both strands by oligo-primer walking. Full contig of individual clone was obtained using GELMERGE and GEL ASSEMBLE within GCG sequence analysis program. Final consensus sequence was obtained by analysing the full sequence of the three clones using PILE UP, TED and GeneDoc programmes. The deduced amino acid sequence was obtained from the cDNA sequence by using TRANSLATE within the GCG programme.

sents the first CYP4A gene isolated as discussed previously while group B and C represents another two genes. These two genes are termed hmCYP4Aii/CYP4A18 (group B) and hmCYP4Aiii/CYP4A19 (group C) for descriptive purposes (Table 3.1). Clones in group D and E corresponds to mispliced mRNA as will be discussed later (Section 3.6.3). The cDNA and deduced amino acid sequences of CYP4A18 and CYP4A19 are shown in Figure 3.30 and Figure 3.31, respectively.

A

```

1  AAGCTTGAAT TCTTGTCTGA CAAGGACCTA CGTGCTGAGG TGGACACATT
51  CATGTTTGAG GGCCATGACA CCACAGCCAG TGGAGTCTCC TGGATCTTCT
101 ATGCTCTGGC CACTCACCTT GAATACCAGC AGAGATGCAG GGAAGAAGTT
151 CAGAGCCTCC TGGGAGATGG GTCCTCCATT ACCTGGGATC ACCTGGACCA
201 GATGCCCTAC ACTACCATGT GCATCAAGGA GTCCCTGAGG CTCTACCCAC
251 CTGTCCCAAC CATTGTCAGA GAGCTCAGCA CACCTGTCAC CTTCCCTGAT
301 GGGCGCTCTT TACCAAAGG TATCCAGTC ACACTCTCCA TTTATGCACT
351 CCACCACAAC CCGGAGGTGT GGCCAAACCC AGAGGTGTTT GACCCCTCCG
401 GGTTTGCAGC AGATTCTCCC CGACACAGCC ACTCATTCTC GCCCTTCTCA
451 GGAGGAGCAA GGAAGTGCAT TGGGAAACAA TTTGCTATGA GTGAGATGGG
501 ATCCAAGCTT

```

B

```

1  KLEFLSDKDL RAEVDTFMFE GHDTTASGVS WIFYALATHP EYQQRREEV
51  QSLLDGSSI TWDHLDQMPY TTMCIKESLR LYPPVPTIVR ELSTPVTFPD
101 GRSLPKGIPV TLSIYALHHN PEVWPNPEVF DSPGFAADSP RHSHSFLPFS
151 GGARNCIGKQ FAMSEMGSKL

```

Figure 3.31 cDNA (A) and amino acid (B) sequence of hamster CYP4A19. Two independent clones derived from PCR amplification of hamster liver cDNA using hmCypPR1 and hmCypPR2 primers were sequenced on both strands by oligo-primer walking. Full contig of individual clone was obtained using GELMERGE and GEL ASSEMBLE within GCG sequence analysis program. Final consensus sequence was obtained by analysing the full sequence of the three clones using PILE UP, TED and GeneDoc programmes. The deduced amino acid sequence was obtained from the cDNA sequence by using TRANSLATE within the GCG programme

Section 3.6.2 Sequence analysis of hamster CYP4A genes

The three CYP4A genes in hamster were analysed using the PILEUP tool within the GCG programme. Figure 3.32 shows the aligned amino acid sequences of these genes. It is evident that these genes vary from each other in their amino acid sequences. There are six putative substrate binding sites present in rat CYP2 (Gotoh 1992) which are also found in mouse *Cyp4a14* by sequence comparison. Sequence alignment of hamster CYP4A genes with these rat and mouse genes shows that two of these substrate binding sites are present in the partially-cloned hamster CYP4A genes (Figure 3.32, SRS 4 and 5). The region of conserved cysteine residue present in the haem binding region of the P450 protein family has also been identified in hamster CYP4A genes. The percentage similarity between these partial CYP4A genes were calculated using the BESTFIT programme within GCG, and the results are summarised in Table 3.2. .

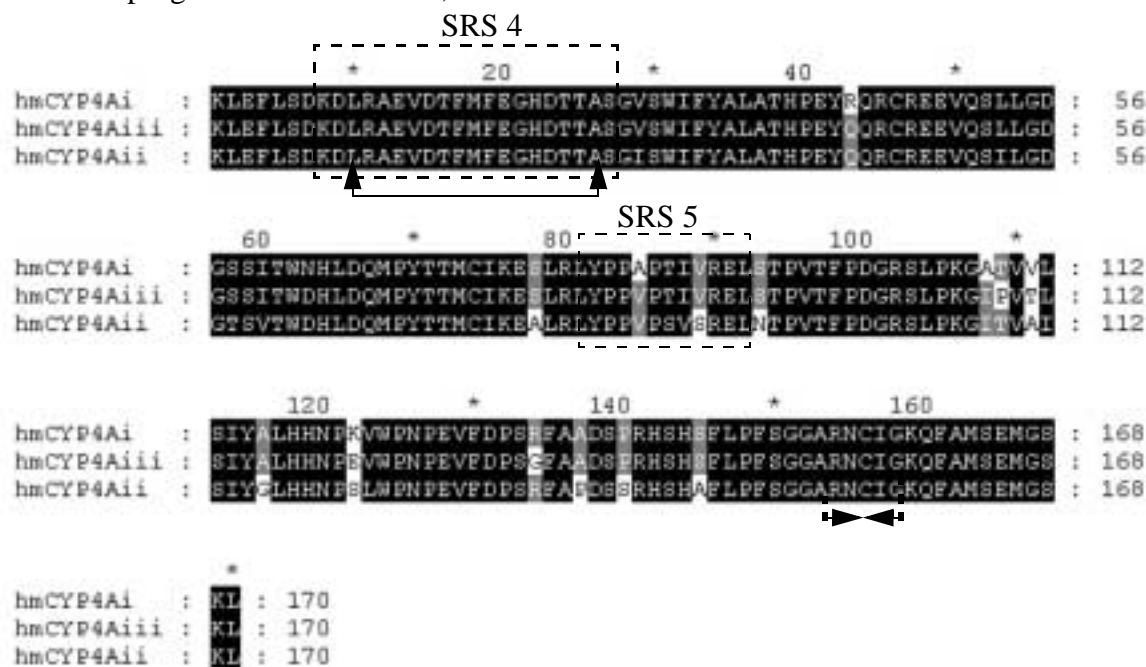


Figure 3.32 Alignment of three CYP4A proteins from hamster. . Deduced amino acid sequences of three hamster CYP4A genes were aligned using PILEUP and highlighted using BOXSHADE. Regions enclosed in a dashed box denote putative substrate binding sites (two out of six) and were inferred from the proposed substrate recognition sites (SRS) in CYP2 (Gotoh, 1992) and *Cyp4a14*. Two facing arrow heads shows the region of conserved Cysteine residue present in haem binding region of the P450 protein family. Also, the stretch of 16 amino acids that has been identified as the signature for CYP4A family are shown by two double arrow-headed line within SRS4. The amino acid positions are shown at the top as well as left of the alignment. Black shading represent 100% conservation of the aligned region. Hamster CYP4A 17, 18 and 19 are represented by hmCYP4Ai, hmCYP4Aii and hmCYP4Aiii, respectively.

The results show that these three CYP4A genes isolated from hamster liver are highly similar to each other but differ in percentage similarity and identity at amino acid level.

hmCYP4A genes	CYP4A17	CYP4A18	CYP4A19
CYP4A17	---	88	95
CYP4A18		---	89
CYP4A19			---

Table 3.2 Identity of hamster CYP4A proteins. The deduced amino acid sequence of hamster CYP4A genes (partial) were compared with each other using BESTFIT tool within GCG sequence analysis programme. These three genes are different from each other as shown by percentage identity at amino acid level.

A comparison was made between rat CYP4A1, CYP4A3 and CYP4A8 against the three CYP4A genes isolated from hamster. Table 3.3 and 3.4 shows the summary of the similarity between hamster CYP4A genes with orthologous sequence of CYP4A genes from other species as analysed by the BESTFIT programme within the GCG package. From this Table, hamster CYP4A17 and CYP4A19 are most similar to rat CYP4A1; but hamster CYP4A18 is equally similar to all three rat genes.

hamster	rat CYP4A genes						mouse CYP4A genes					
	4A1		4A2/3		4A8		4a10		4a12	4a14		
CYP4A17	91	91	80	81	81	83	90	91	82	83	80	81
CYP4A18	88	85	89	87	85	83	86	85	86	83	90	88
CYP4A19	93	93	82	82	83	84	91	92	83	84	81	82

Table 3.3 Comparison of hamster and rat CYP4A genes. Nucleotide sequence and their deduced amino acid sequence of hamster CYP4A genes (partial) were compared with rat CYP4A genes using BESTFIT tool within GCG sequence analysis programme. Because the hamster CYP4A genes were partially cloned, comparison were made using orthologous sequence of rat CYP4A genes: CYP4A1 (m14972), CYP4A3 (m33936), CYP4A8 (m37828). Percentage identity between rat and hamster CYP4A genes both at nucleotide (bold type) and amino acid sequence (normal) are shown in the table.

hamster	rabbit			human	guinea pig
	4A4	4A5/6	4A7	4A11	4A13
4A17	82	83	81	84	79
4A18	83	83	83	84	82
4A19	82	84	83	84	80

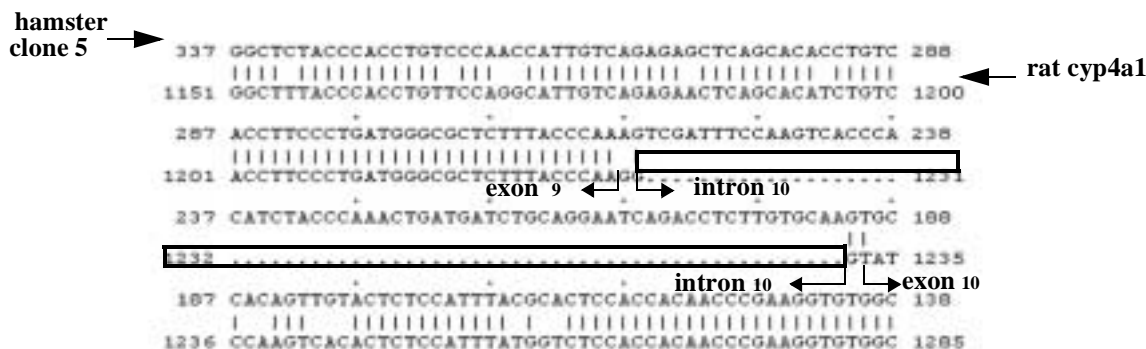
Table 3.4 Comparison of hamster CYP4A proteins with other species. The deduced amino acid sequence of hamster CYP4A genes were compared with rabbit, human and guinea pig CYP4A genes using BESTFIT tool within GCG sequence analysis program. Because the hamster CYP4A genes were partially cloned, comparison were made using orthologous sequence of rabbit, human and guinea pig genes. Percentage identity between these CYP4A genes are shown in the table.

Section 3.6.3 Presence of misspliced CYP4A mRNA species in hamster

As shown in Section 3.6, PCR derived clones from hamster liver cDNA were grouped according to their restriction digest pattern, and sequence analysis of these clones revealed the presence of three CYP4A genes that are expressed in hamster liver. The sequence of clone 5 contains a longer insert while clone 12 contains a shorter insert than the predicted 510bp amplified fragment, but sequence comparison with the three identified hamster CYP4A genes shows that clones 5 and 12 have 100% identity to CYP4A17 and CYP4A19, respectively, suggesting that clones 5 and 12 are derived from hamster CYP4A17 and CYP4A19, respectively. The possibility that these two clones could be the product of misspliced mRNA was investigated by comparing their nucleotide sequence with rat cDNA and genomic CYP4A1 sequence. When the sequence of clone 5 was analysed by comparing with the rat CYP4A1 sequence, an extra 65 bp was found to be present after the intron/exon junction of exon 9 of CYP4A1 (Figure 3.33, A). These 65 nucleotides show over 74% identity with intron 10 of the CYP4A1 gene. However, when the sequence of clone 12 was analysed, a 65 bp region was found to be missing that constitutes the whole of exon 10 (Figure 3.33, B). Therefore the sequence comparison of clones 5 and 12 with

rat CYP4A1 suggests that the mRNAs of clone 5 and 12 were mispliced, resulting in truncated mRNAs which have either an extra intron sequence (intron 10) or a missing exon (exon 10), respectively. These data show the presence of mispliced CYP4A mRNA species in hamster liver treated with MCP.

A



B

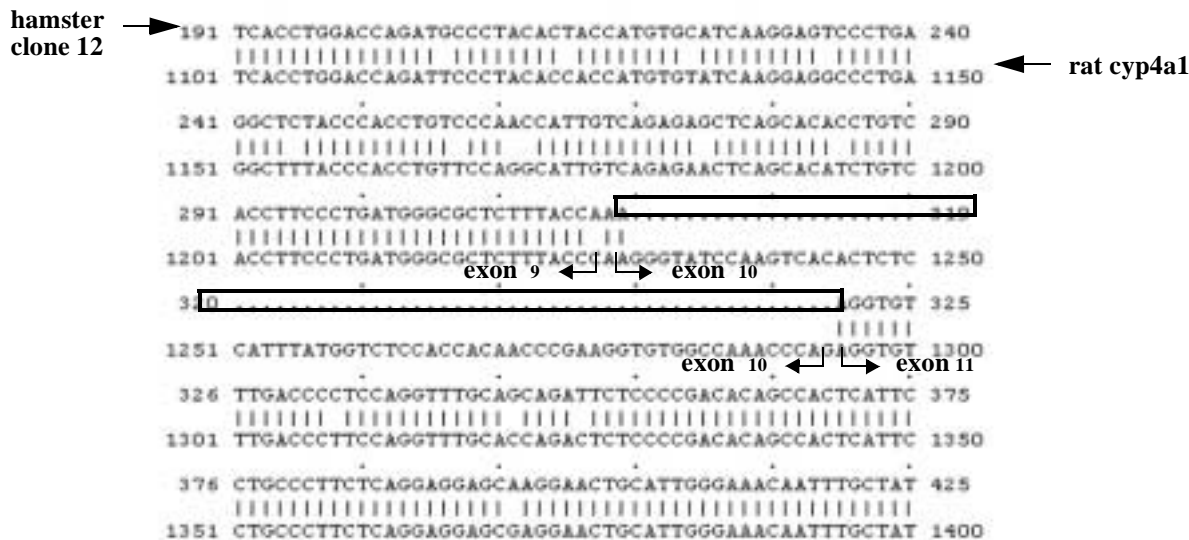


Figure 3.33 Mis-spliced CYP4A mRNA species in MCP-treated hamster liver. Sequence of clone 5 (A), derived from CYP4A17, and Clone 12 (B), derived from CYP4A19 were compared with known rat CYP4A1 genomic and cDNA sequence, respectively, and was found to contain intron sequence in clone 5 and missing exon in clone 12 due to their mispliced mRNA. Extra or missing sequences are shown by the use of solid boxes and the position where misplicing has occurred in intron exon junctions are shown by a solid arrow.

Section 3.6.4 Peroxisome proliferator-induced CYP4A induction in hamster liver

Hamster shows an intermediate level of response to peroxisome proliferators and has been considered to be a partially-responsive species (Lake *et al.*, 1988). These previous studies include peroxisomal events such as induction of microsomal enzyme activities. Having cloned three hamster CYP4A genes, the induction of one such gene by peroxisome proliferators MCP and Wy-14,643 was investigated at mRNA level by means of the RNase protection assay. Dosing of hamster for three consecutive days with either MCP or Wy-14,643 (25mg/kg) resulted in a 20% increase in liver weight (hepatomegaly) as described by Choudhury *et al.* (2000). Total RNA extracted from the liver of these treated animals was investigated for the induction of CYP4A using RNase protection assays with a riboprobe derived from CYP4A17 (Figure 3.34).

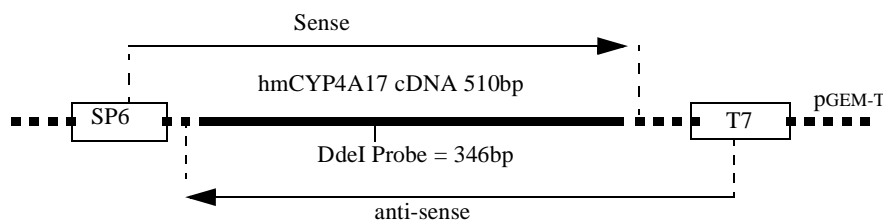


Figure 3.34 Cartoon of hamster CYP4A17 template. A 510bp fragment corresponding to the 3' end of the hamster CYP4A17 cDNA (corresponding to rat CYP4A1 cDNA 925-1410) was cloned into the polylinker region of pGEM-T vector. Anti-sense riboprobe can be generated by in vitro transcription of DdeI cut template from T7 promoter, resulting in 346bp length probe of which 300bp corresponds to CYP4A1 insert.

Figure 3.35 shows a typical protection gel obtained using MCP or Wy-14,643 treated liver RNA hybridised to the riboprobe. A specific protected band of the expected size was detected in hamster liver RNA which was absent in tRNA sample hybridised to the probe and treated with RNase A (+ve lane). Therefore the protected band was due to the presence of CYP4A17 mRNA in hamster liver. The expression of CYP4A17 was detectable in the control liver (corn oil treated) which is induced following exposure to peroxisome proliferators MCP and Wy-14,643 (25mg/kg for 3 days). When these protected bands were quantified on a phosphor imager a 17-

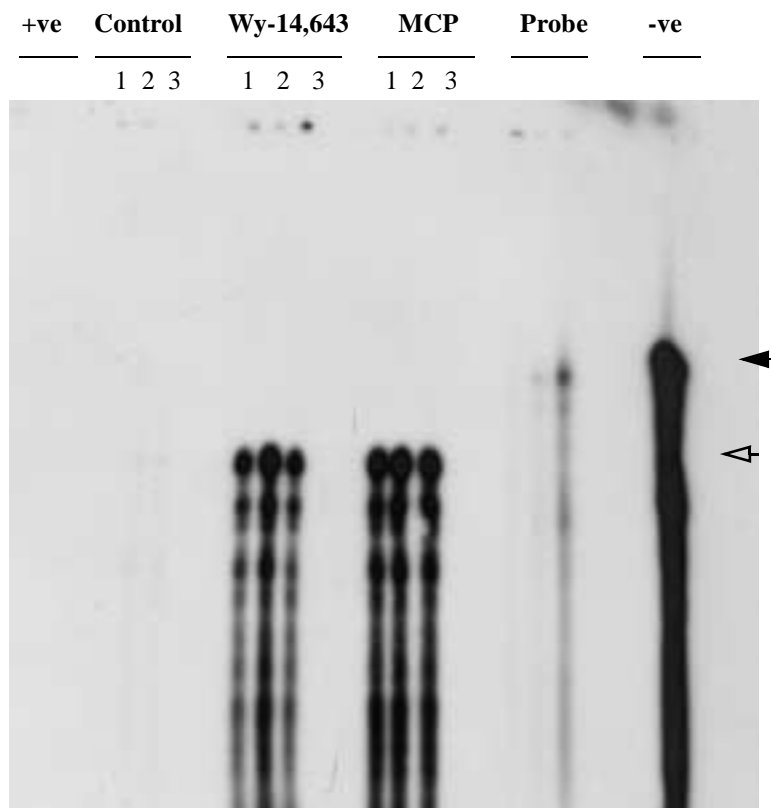


Figure 3.35 CYP4A induction in hamster liver by MCP and Wy-14,643. Male Syrian golden hamster were treated with either MCP, Wy-14,643 (25mg/kg) or corn oil (100 μ l) for three consecutive days, and their liver RNA extracted as detailed in methods. Three animals are used per treatment group (numbered). RNase protection assay were performed on 30 μ g of RNA using an anti-sense riboprobe of CYP4A, labelled with [α - 32 P] CTP. Yeast tRNA treated with (+ve) or without (-ve) RNase A are also included in the assay. Protection assays were run on a 6% gel and visualised by autoradiography. The position of full-length probe is indicated by filled arrow, and the position of the protected fragment by an unfilled arrow.

fold induction ($P < 0.005$) was observed in the Wy-14,643 treated sample. Treatment with MCP resulted in slightly higher induction of CYP4A (21-fold, $P < 0.0005$) compared to Wy-14,643 (Figure 3.36). Therefore CYP4A is constitutively expressed in hamster liver and is induced over 17-fold by treatment with peroxisome proliferators.

Section 3.7 Cloning of hamster PPAR α cDNA

PPAR α is central to peroxisome proliferation and subsequent carcinogenesis as demonstrated by knock-out studies (Lee *et al.*, 1995). Species differences in responsiveness to peroxisome proliferators are well documented and may be a reflection in the level and activity of PPAR α receptors in different species. To determine the correlation between species response to perox-

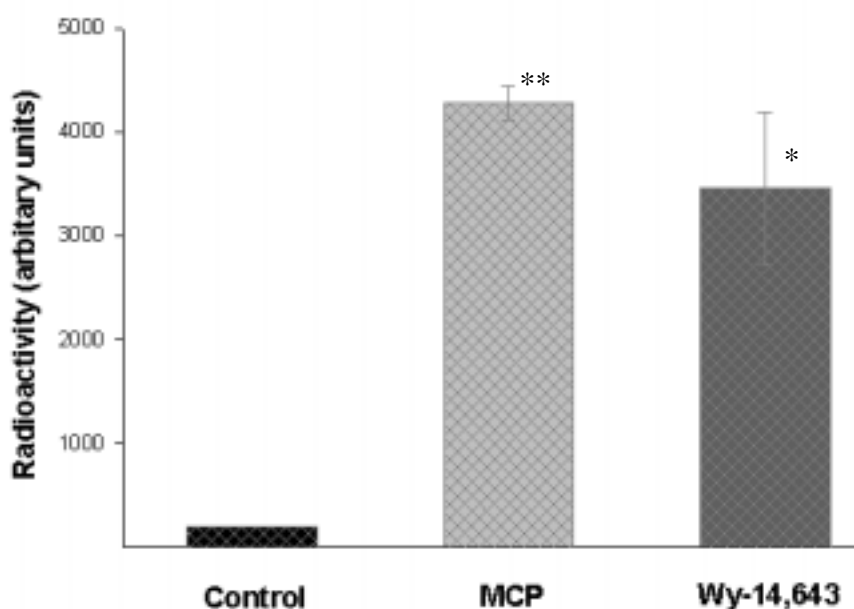


Figure 3.36 Induction of hamster CYP4A by MCP and Wy-14,643. Groups of three male hamsters were dosed with either 100 μ l corn oil or 25mg/kg MCP or Wy-14,643 for three consecutive days. RNase protection were performed on the extracted liver RNA from each animal using anti-sense riboprobe derived from CYP4A cDNA clone, as detailed in methods. Protected bands were resolved on a 6% gel, and the bands were quantified using a phosphor imager on the linear range of the signal. Mean radioactivity values of each treatment group were calculated and expressed as arbitrary units. The error bars shown represent the standard deviation from the mean. Values significantly different from control where * * = $p < 0.0005$ and * = $p < 0.005$.

isome proliferators and the PPAR α level in the liver, a comparative study of the constitutive level of expression of PPAR α mRNA was carried out in species with differing responses to peroxisome proliferators: mouse representing a highly responsive group and guinea pig as non-responsive, while hamster represents the partially responsive group. Since no hamster PPAR α has been cloned previously, it was necessary to clone and sequence PPAR α from this species so that a specific probe could be generated for the RNase protection assay.

PCR cloning of hamster PPAR α was carried out from total liver RNA using primers HMppar-P1 and HMppar-P2. These primers were designed from regions of identity in aligned amino acid sequences of mouse (x57638), rat (M88592), human (L02932), guinea-pig (O35507) and *Xenopus* (M84161) PPAR α . Figure 3.37 shows the amino acid alignment of the regions of the PPAR α receptors used to design the PCR primers. Primer pparP-1 was designed from the DNA-

binding domain, and corresponds to 325-MNKDGML-331, while ppar-P2 was designed from C-terminal end of the receptor that corresponds to 463-IYRDMY-468-XX (X= 3' non-coding triplet). Total liver RNA was used for the synthesis of first-strand cDNA using oligo-dT primers. When this cDNA was used as a template in the PCR reaction, using ppar-P1 and ppar-P2 primers, a 1.5 kb fragment was amplified (Figure 3.38, lanes 1-2).

Using this PCR condition a similar sized fragment was also amplified when mouse PPAR α cDNA (in pSG5 plasmid) was used as a template, but was absent when no template DNA was added in the reaction. This demonstrates that the amplified fragment obtained using hamster liver cDNA is derived from expressed hamster PPAR α gene. Sequencing was undertaken to verify this. The amplified fragment from hamster cDNA was purified from the PCR reaction cocktail and subcloned into pGEM-T cloning vector. DNA fragments from three independent clones containing the insert were sequenced on both strands. Initially sequencing primers were de-

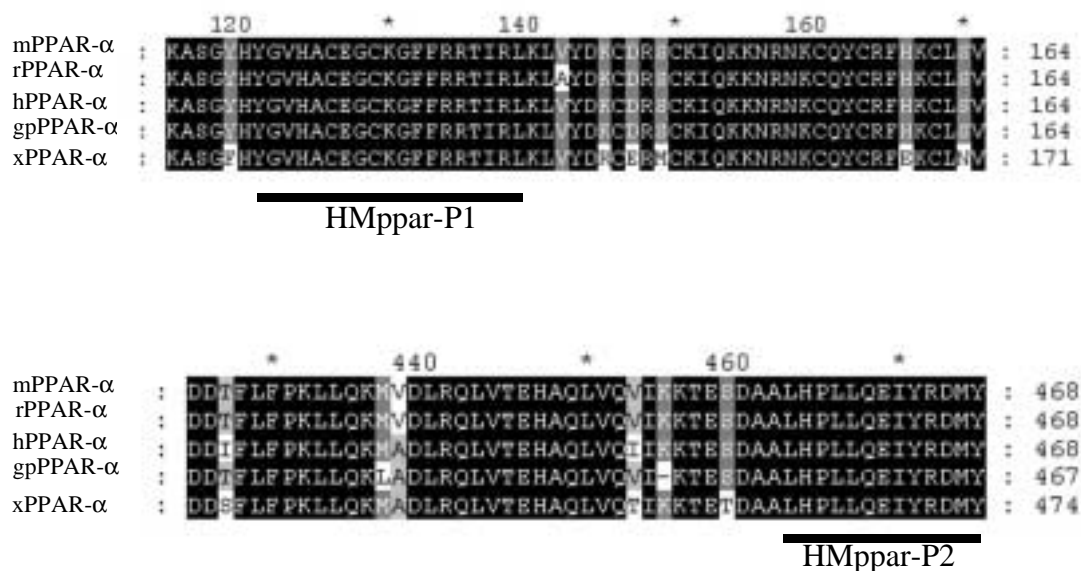


Figure 3.37 Design of PCR primers from alignment of PPAR α proteins. Forward (HMppar-P1) and reverse (HMppar-P2) primers for the cDNA cloning of putative hamster PPAR α genes were designed by aligning the amino acid sequences of mouse, rat, human, guinea-pig and *Xenopus* PPAR α (denoted as m, r, h, gp and x, respectively) using the pileup tool within the GCG sequence analysis program, and displayed using GeneDoc. The amino acid position of mouse PPAR α are shown at the top of the alignment while the amino acid position on the right of the alignment corresponds to individual PPAR α proteins. Black shading represent 100%, dark-grey represent 80% and light-grey represent 60% conservation of the aligned region. The regions of amino acid identity used to design PCR primers are underlined.

signed from the SP6 and T7 promoter sequence of the vector, and subsequent primers were designed for sequencing as the new sequence became available (oligo-walking process). Sequences obtained using multiple primers were assembled into a single contig using the GELMERGE and GELASSEMBLE tool within the GCG programme. The double stranded sequence was analysed for homology to known PPAR α cDNA sequences. DNA sequence analysis of the cloned 1069 bp hamster PCR product demonstrated that it showed sequence similarity but not identity to mouse, rat, human, guinea-pig and *Xenopus* PPAR α cDNA sequences.

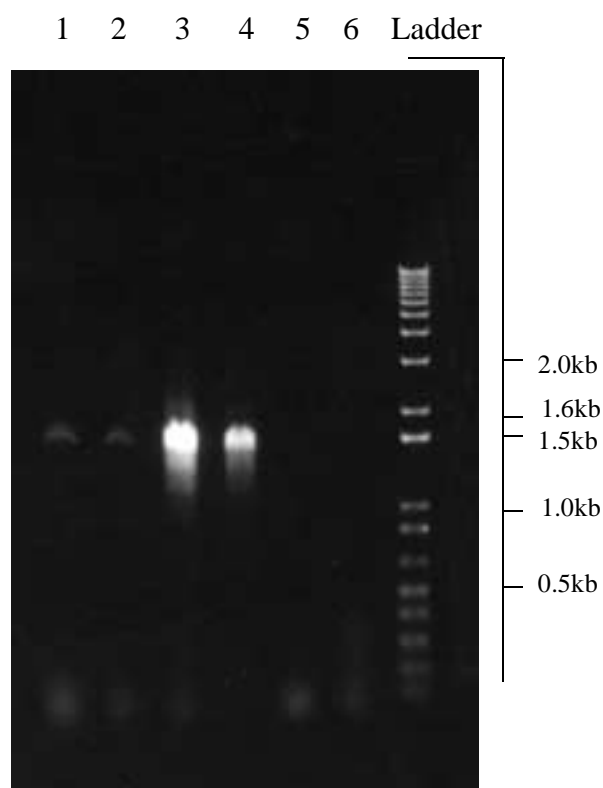


Figure 3.38 PPAR α amplified from hamster liver cDNA. PCR reactions were performed using HMppar-P1 and HMppar-P2 primers on hamster liver cDNA, derived from MCP treated total RNA (lane 1-2). All PCR reactions include 1.5mM MgCl₂ (lane 2-6) except lane 1 where 2.5mM MgCl₂ was used. Lane 5 and 6 are negative controls where, RNA and no template DNA was added, respectively. Lane 3 and 4 are amplification reactions of pSG5-mPPAR α and pBK-CMV-gpPPAR α plasmid DNA, respectively. Five μ l of each reaction was analysed on a 1% agarose gel, run on 1xTBE at 90v for 90 minutes. Syber-Green was added to all samples prior to loading and the resolved DNA bands were visualised using a dark-reader. Molecular size of the DNA ladder are shown in kilobase pairs.

Section 3.7.1 Cloning of 5' end of hamster PPAR α .

The PCR strategy employed using HMpparP-1 and P-2 primers enabled the cloning of a partial hamster PPAR α cDNA that includes complete 3' end of the cDNA, and therefore required ad-

ditional cloning of the 5'-cDNA end for cloning of full-length PPAR α cDNA. A 5'-rapid amplification of cDNA ends (RACE) method was utilised for the cloning of the remainder of the hamster PPAR α cDNA containing the N-terminal coding region. A commercial RACE kit from Gibco BRL was used for the 5'-RACE. Three gene-specific primers, termed RACE 1, RACE 2 and RACE 3, were designed from the completed sequence of the 1069 bp fragment of putative hamster PPAR α as shown in Figure 3.38. First strand cDNA was synthesized from both total and polyA⁺ RNA of hamster liver using the gene-specific primer RACE 1 (corresponding to nucleotides 116-142 of the 1069 bp hmPPAR α clone). The first strand cDNA was dC-tailed by terminal deoxynucleotidyl transferase method and then purified. This putative dC-tailed 5'-cDNA end of hmPPAR α was amplified by using a second gene-specific primer RACE 2 (corresponding to nucleotides 58-89 of the 1069 bp hmPPAR α clone), which is 5' upstream of RACE

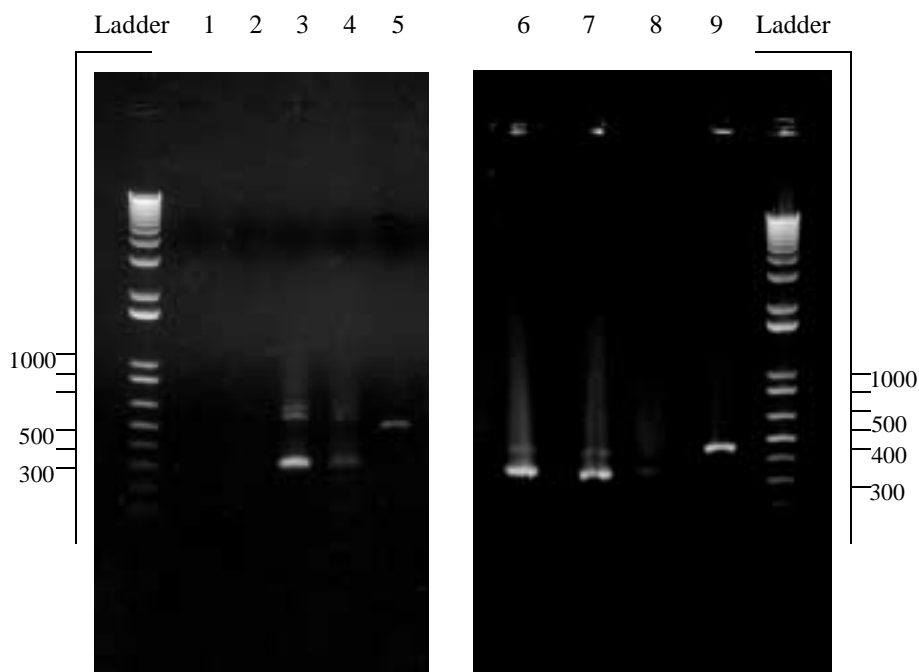
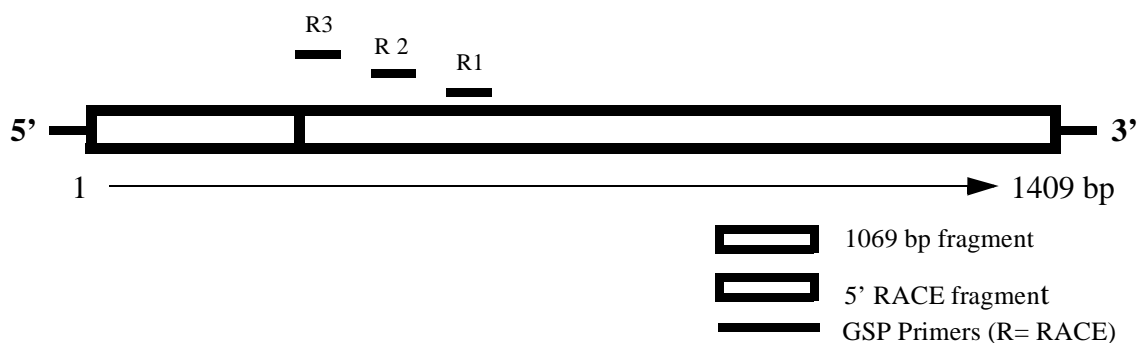


Figure 3.39 5'RACE products from hamster PPAR α cDNA. Gibco, BRL RACE-Kit was used for the cloning of 5'cDNA ends of hamster PPAR α . Both total (lane 3 and 6) and polyA⁺ (lane 4 and 7) RNA were used in the amplification reactions and were performed as described in methods. Gene-specific primer race1 was used for the synthesis of first-strand cDNA which were then subjected to first round of amplification using a second gene-specific primer race2 (lane2). A second round of amplification was performed on the PCR products derived from the first round using either race2 (lane 3-4) or race3 (lane 6-7). Lane 1 and 8 represent negative control where no template DNA was added. Lane 5 and 9 represent positive control for 5'RACE reaction for which template DNA was provided in the kit, and the PCR reaction amplify a 500bp fragment.

1, and 5' RACE anchor primer from the RACE kit. Due to the low levels of products formed, the amplified products were not detectable when analysed by gel electrophoresis (Figure 3.39 lane 2). Reamplification of this reaction product (diluted 50-fold) using RACE 2 and Universal Amplification Primer produced a number of amplified fragments, one of which is 350 bp in size as shown in Figure 3.39, lane 3-4. This reaction products were further reamplified using a third gene-specific primer RACE 3 (corresponding to nucleotides 9-39 of the 1069 bp hmPPAR α clone), 5'upstream of RACE 2, and Universal Amplification Primer. Figure 3.39, lane 6-7 shows the amplified reaction products obtained.

The PCR product obtained using RACE 2 primer was cloned into pGEM-T Easy vector. Restriction digests were performed using EcoRI to release the insert from the plasmid. Analysis of the digest (Figure 3.40) shows that the clones vary in their insert size. Assuming the full-length open reading frame of hamster PPAR α cDNA is approximately 1407 bp, then the predicted RACE product with RACE 2 primer is 400 bp. Therefore, three clones were selected according to their expected insert size for sequencing. These clones had 100% identity to 1069 bp fragments of 5'-end of hamster PPAR α over 100 bp that incorporate GSP primers (RACE 1, 2 and 3) as outlined below.



Analysis of the sequence obtained from these clones shows that they are highly similar but not identical to the 5'-end of rat and mouse PPAR α (90% identity). One of the clones shows identity to the transcription start site of the open reading frame of rat PPAR α while the other two clones

contain sequence 100 bp short of the start site. Therefore full-length hamster PPAR α cDNA has been cloned by two-stage PCR strategy, where the 1069 bp fragment was cloned initially using a primer derived from consensus of known PPAR α sequences and the remaining 5'-end was obtained by employing a 5'-RACE strategy.

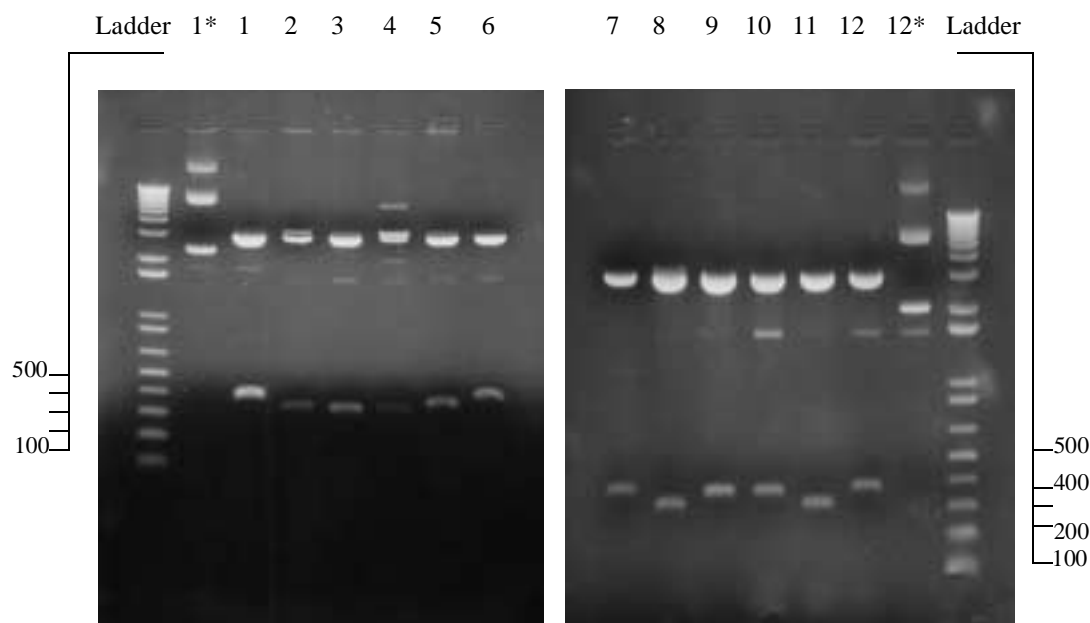


figure 3.40 Restriction analysis of 5'-clones of hamster PPAR α . A total of 12 clones derived from 5'-RACE reaction (cloned in pGEM-T Easy vector) were restriction digested with EcoRI. Products were then phenol:chloroform treated as described in methods and run on 1.2% agarose gel (pre-stained with ethidium bromide) with 1xTBE at 90v for 90 minutes. Restriction digested individual clones are numbered from 1 to 12 as shown, and uncut plasmids are represented by an asterisk laced next to the clone number. Molecular sizes of the 1 Kb⁺ DNA ladder are shown in base pairs.

Section 3.7.2 Hamster PPAR α cDNA and deduced amino acid sequence

The cloned sequence of putative hamster PPAR α was analysed using the TED, BESTFIT, SEQED, TRANSLATE tools within the GCG programme, and the final sequence of single contig was obtained using GELMERGE and GELASSEMBLE programmes. The DNA sequence and deduced amino acid sequence of the assembled cDNA are shown in Figure 3.41 and Figure 3.42, respectively. Translation of the full-length hamster PPAR α (1407 bp) gives an open reading frame of 468 amino acid of predicted molecularweight 52.4 kDa and an isoelectric point 6.95. Comparison of the predicted protein sequence of the cloned hamster cDNA with known PPAR α receptors demonstrates that the cDNA encodes a PPAR α protein.


```

1  ATGGTGGACA CAGAGAGTCC CATCTGTCCC CTCTCCCCAC TTGAAGCGGA
51  TGACCTGGAG AGTCCCTTAT CGGAAGAATT CTTACAAGAA ATGGGAAACA
101 TTCAAGATAT TTCTCAGTCC CTTGAGGAGG AAAGTTCCGG AAGCTTTAGT
151 TTCACGGACT ACCAGTACTT AGGAAGCTGT CCAGGCTCCG AGGGCTCTGT
201 CATCACAGAC ACTCTGTCTC CAGCGTCCAG CCCCTCATCA GTCAGCTGCC
251 CCGTGATCCC CGCCAGCACA GACGAGTCCC CTGGCAGTGC GCTGAACATT
301 GAGTGTGCGA TATGTGGGGA CAAGGCCTCA GGCTACCACT ACGGAGTCCA
351 TGCATGTGAA GGTTGCAAGG GTTTCTTTTCG GCGAACTATT CGGCTAAAGC
401 TGGCGTATGA CAAATGTGAT CGAAGCTGTA AGATTCAAGAA AAAGAACAGG
451 AATAAATGCC AATACTGCCG CTTCCACAAA TGCCTGTCTG TTGGGATGTC
501 ACACAATGCG ATTCGTTTTG GACGCATGCC AAGATCTGAG AAAGCAAAAC
551 TGAAAGCAGA GATTCTCACG TGTGAACACG ATCTGGAAGA TTCGGAAACT
601 GCCGACCTCA AATCTCTGGC CAAGAGAATC CACGAGGCCT ACCTGAAGAA
651 CTTCAACATG AATAAGGTCA AGGCCCGGGT CATCCTGGCA GGAAAGACCA
701 GCAATAACCC GCCCTTCGTT ATACATGACA TGGAGACCTT GTGTATGGCT
751 GAGAAGACGC TTGTGGCCAA GATGGTGGCC AATGGCATCC AAAATAAGGA
801 GGCAGAAGTC CGGATCTTCC ACTGCTGCCA GTGCATGTCT GTGGAGACTG
851 TCACCGAGCT CACAGAATTC GCCAAGGCCA TCCCAGGCTT CGCAAACCTG
901 GACTTAAATG ACCAAGTTAC CTTGCTAAAG TACGGTGTGT ATGAAGCCAT
951 ATTCACAATG CTGTCCTCCT TGATGAACAA AGACGGAATG CTGATCGCGT
1001 ATGGCAATGG CTTTCATCACA AGGGAGTTCC TAAAGAACCT GAGGAAGCCA
1051 TTCTGTGACA TCCTGGAACC GAAGTTTGAT TTTGCTATGA AGTTCAATGC
1101 CCTAGAACTG GATGACAGTG ACATTTCCCT TTTTGTGGCT GCTATAATTT
1151 GCTGTGGAGA TCGGCCTGGC CTTCTAAACA TAGGATACAT TGAGAAGATG
1201 CAGGAGGGTA TCGTGCACGT GCTCAAATC CACCTGCAGA GCAACCATCC
1251 AGATGATACC TTTCTCTTCC CGAAGCTTCT TCAAAAATG GTGGACCTTC
1301 GGCAGCTGGT CACGGAGCAT GCGCAGCTCG TGCAGGTCAT CAAGAAGACC
1351 GAGTCTGACG CAGCGCTGCA CCCGCTTCTG CAGGAGATCT ACAGGGACAT
1401 GTACTGA

```

Figure 3.41 cDNA sequence of hamster PPAR α . Three independent clones derived from PCR amplification of hamster liver cDNA using HMppar-P-1 and P-2 primers were sequenced on both strands by oligo-primer walking. Full contig of individual clone was obtained using GELMERGE and GEL ASSEMBLE within GCG sequence analysis programmes. Final consensus sequence was obtained by analysing the full sequence of the three clones using PILEUP, TED and GeneDoc programme.

```

1  MVDTESPICP LSPLEADDLE SPLSEEFLOE MGNIQDISQS LEEESSGSFS
51  FTDYQYLGSC PGSEGSVITD TLSPASSPSS VSCPVIPAST DESPGSALNI
101  ECRICGDKAS GYHYGVHACE GCKGFFRRTI RLKLAYDKCD RSCKIQKKNR
151  NKCQYCRFHK CLSVGMSHNA IRFGRMPRSE KAKLKAEILT CEHDLEDSET
201  ADLKSLAKRI HEAYLKNFNM NKVKARVILA GKTSNNPPFV IHDMETLCMA
251  EKTLVAKMVA NGIQNKEAEV RIFHCCQCMS VETVTELTEF AKAIPGFANL
301  DLNDQVTLK YGVYEAIFTM LSSLMNKDGM LIAYGNGFIT REFLKnlRKP
351  FCDILEPKFD FAMKFNALEL DDSDISLFVA AIICCGDRPG LLNIGYIEKM
401  QEGIVHVLKL HLQSNHPDDT FLFPKLLQKM VDLRQLVTEH AQLVQVIKKT
451  ESDAALHPLL QEIYRDMY

```

Figure 3.42 Deduced amino acid sequence of hamster PPAR α . Three independent clones derived from PCR amplification of hamster liver cDNA using HMpparP-1 and HMpparP-2 primers were sequenced on both strands by oligo-primer walking. Full contig of individual clone was obtained using GELMERGE and GEL ASSEMBLE within GCG sequence analysis program. Final consensus sequence was obtained by analysing the full sequence of the three clones using PILEUP, TED and GeneDoc programmes. Stop codon in protein sequence is represented by an asterisk. The deduced amino acid sequence was obtained from the cDNA sequence by using TRANSLATE within the GCG program. The predicted amino acid sequence was compared to known PPAR α amino acid sequences and was found to have high similarity, indicating that it encodes a PPAR α receptor.

Section 3.7.3 Sequence analysis of the PPAR α amino acid sequence

The partial amino acid sequence of hamster PPAR α was compared with other known PPARs, including other subtypes β and γ , using BESTFIT within the GCG sequence analysis program. Hamster PPAR α shows high identity to other alpha subtypes, particularly to rat and mouse PPAR α (97%), but has less identity to mouse gamma (65%) and beta (67%) subtypes. Table 3.5 gives a breakdown of the percent amino acid identity between individual protein domains of hmPPAR α and other known isoforms. The DNA binding domain of hmPPAR α is identical to rat PPAR α and also shows very high degree of identity to mouse human and guinea pig PPAR α . The ligand binding domain shows highest identity to rat and mouse, and the hinge region shows high identity to rat, mouse and human PPAR α when compared the corresponding region in hamster PPAR α . The most 5'-end of PPAR α receptor corresponds to the A/B transactivation domain, which is known to show wide variation between species, and the analysis shows that

such is the case for hamster PPAR α when compared to the β and γ isoforms (Table 3.5).

domain (aa region)	A/B (1-101)	DBD (102-166)	Hinge (167-280)	LBD (281-468)
rPPAR α	93	100	97	99
mPPAR α	95	98	95	99
huPPAR α	84	98	95	94
gpPPAR α	79	98	82	93
xPPAR α	53	91	84	87
mPPAR β	41(30)	87	57	71
mPPAR γ	70(10)	83	50	69

Table 3.5 Similarity between hamster PPAR α and other PPARs. The amino acid sequence of cloned hamster PPAR α was compared with other PPARs using BESTFIT tool within GCG sequence analysis program. Percentage identity of putative DBD (DNA binding domain), LBD (ligand binding domain), A/B (transactivation domain) and Hinge region are shown. Sequences of rPPAR α (rat, m88592), mPPAR α (mouse, x57638), huPPAR α (human, y07619), gpPPAR α (guinea pig, aj000222), xPPAR α (xenopus, m84161), mPPAR β (mouse, p35396) and mPPAR γ (mouse, p37238) were obtained from EMBL/SWISSPROT gene databank. The figures in brackets next to the percentage identities are the length of amino acid stretch over which the identity was matched.

The amino acid sequences of hmPPAR α , rPPAR α (m88592), mPPAR α (x57638), huPPAR α (y07619), gpPPAR α (aj000222) and xPPAR α (m84161) have been aligned for comparison using PILEUP within GCG sequence analysis program and displayed using GeneDoc. Figure 3.43 shows this comparative analysis in terms of the differences in the amino acid sequence of hmPPAR α to the aligned sequences. At amino acid positions 50 and 135 (of hamster sequence) the rat and hamster PPAR α differ from the other PPAR α , and there are seven other positions (position in hamster sequence: 8, 44, 53, 64, 83, 90, 95, 195, 211, 258, 279, 324, 332, 396, 431) where hamster, rat and mouse have identical amino acid sequence but are different from rest of the PPAR α . Of these 15 changes, 11 are conserved between human and guinea pig PPAR α , with the remaining 4 being non-conserved. There are 6 amino acid positions (amino acid position of hamster sequence: 52, 196, 263, 264, 272, 400) where the hamster PPAR α differs from rat and mouse PPAR α but the sequences are conserved between human and guinea pig. A com-

parison of the charge properties of these 6 differences reveals that at two positions a change in the charge property has occurred. At position 196 in hmPPAR α , negatively charged glutamine

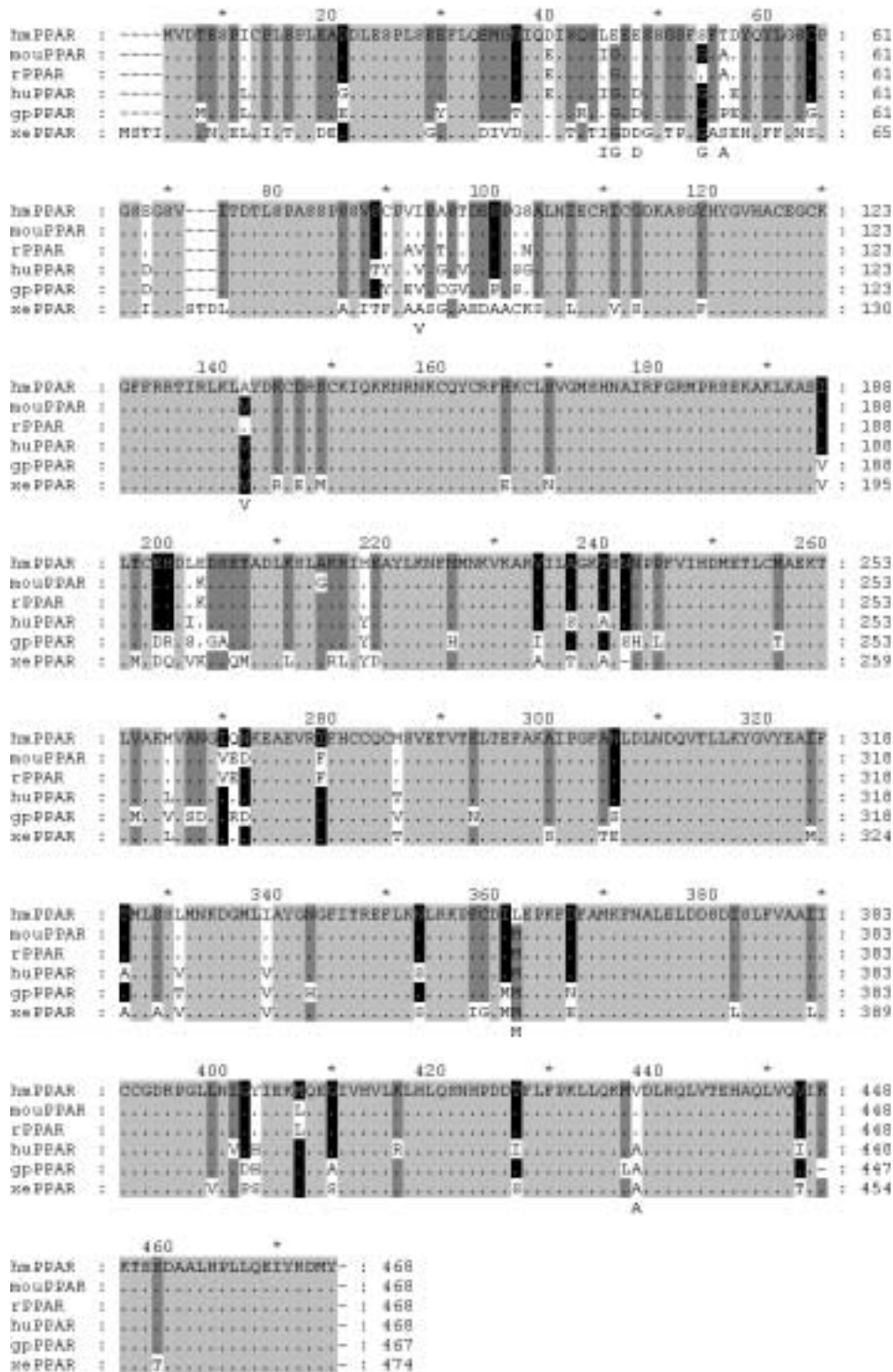


Figure 3.43 Alignment of hamster PPAR α with known PPAR α proteins. PPAR α sequence of rat (rPPAR, m88592), mouse (mouPPAR, x57638), human (huPPAR, y07619), guinea pig (gpPPAR, aj000222) and xenopus (xePPAR, m84161) were compared with hamster PPAR α sequence at amino acid level using PILEUP tool within GCG programme. The alignment were displayed using GeneDoc program. Amino acid conservation are shown by shading where light grey = 100%, dark-grey = 80% and black = 60% conservation. The amino acid position of mouse PPAR α are shown at the top of the alignment while the amino acid position on the right of the alignment corresponds to individual PPAR α proteins.

is present in hamster while positively charged lysine occupies the corresponding position in rat and mouse PPAR α . Negatively charged glutamic acid at position 264 of rat and mouse PPAR α is replaced by the polar uncharged group glutamine in hmPPAR α (position 264).

Section 3.7.4 Phylogenetic analysis of PPAR α genes

The phylogeny of PPAR α genes was analysed by the maximum likelihood method of analysis. All PPAR α protein sequences, including hamster, were aligned using CLUSTALW for input into Puzzle 4 programme. Mouse PPAR β and γ were used as out groups as the divergence of β/γ from α predates the human/*Xenopus* split. Figure 3.44 shows the best tree from this maximum likelihood method. The tree was rooted with PPAR γ and visualised by Treeview. All PPAR α proteins cluster, and β and γ branch outside this clade. Hamster PPAR α is placed between guinea pig and rat/mouse gene, and like rat, mouse and human, hamster PPAR α has a slow rate of evolution compared to guinea pig which is evolving rapidly as shown by a longer branch.

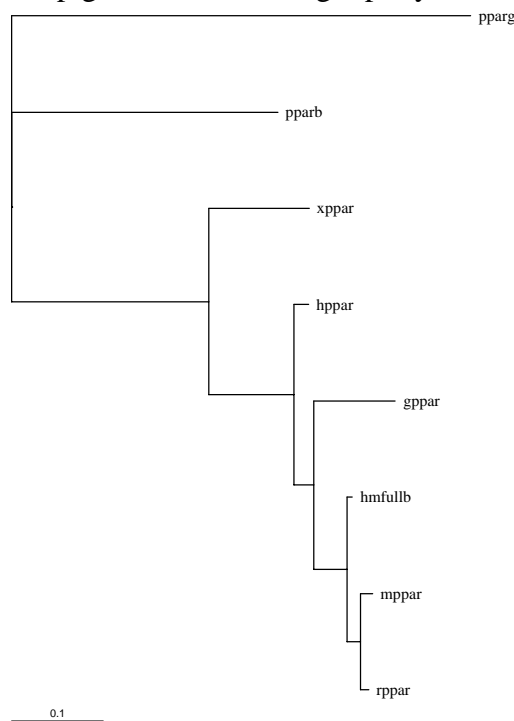


Figure 3.44 Phylogenetic relationship of PPAR α proteins. Deduced amino acid sequences of all PPAR α were aligned and analysed by using CLUSTALW and then converted to phylip format. Phylogenetic tree was produced using Maximum-likelihood method of analysis by puzzle 4 with mouse PPAR β (pparb) and γ (pparg) were added as outgroups. The tree output was visualised with treeview and rooted with PPAR γ as an outgroup. The horizontal length of each branch is proportional to the estimated number of amino acid substitutions (synonymous substitution rate, $K_S = 0.1$). The branches are defined as xppar = xenopus, hppar = human, gppar = guinea pig, hmfull b= hamster, mppar = mouse and rppar = rat PPAR α .

Section 3.7.5 Expression of PPAR α in mouse, hamster and guinea pig Liver

Constitutive expression of PPAR α mRNA in the liver of mouse, hamster and guinea pig was investigated using the RNase protection assay. Total RNA extracted from the liver of untreated control animals (4 animals of each species) was investigated for the expression of PPAR α mRNA using species specific riboprobes. Probes were designed from 3'-end of the gene and synthesised from ApaI cut templates so that they all give roughly similar sized protected fragments in the RNase protection assay (Figure 3.45).

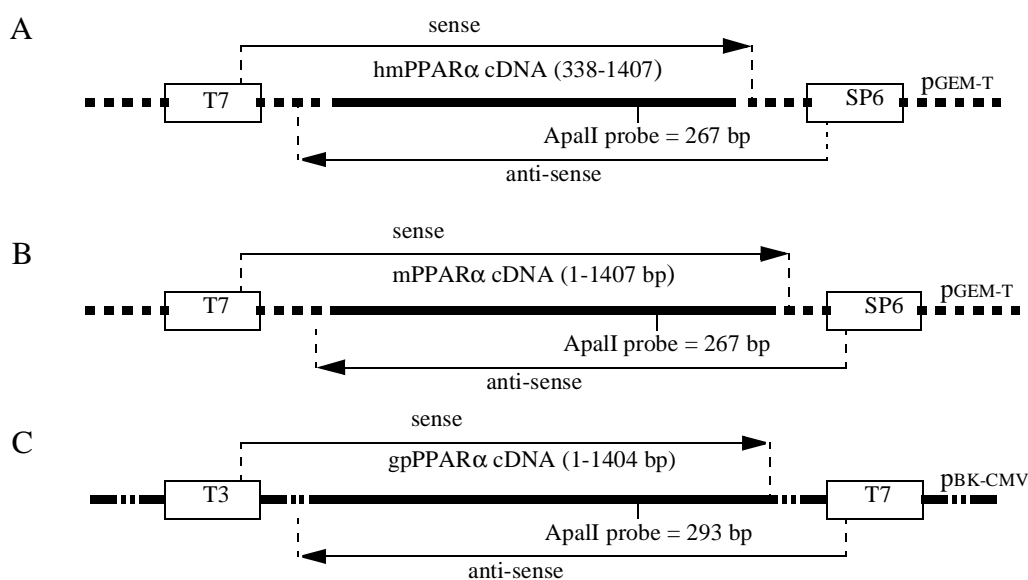


Figure 3.45 Cartoon of hamster (A), mouse (B) and guinea-pig (C) PPAR α templates. A 1.1kb fragment corresponding the 3' end of the hamster and mouse cDNA was subcloned into the polylinker region of pGEM-T vector. Anti-sense riboprobe of mouse and hamster PPAR α was generated by in vitro transcription of ApaI cut template from SP6 promoter, resulting in 267bp length probe of which 196bp corresponds to PPAR α insert. Full-length guinea pig PPAR α in pBK-CMV was used to generate anti-sense riboprobe by transcribing from T7 promoter using ApaI cut template, resulting in 293bp length probe of which 196bp corresponds to PPAR α insert.

RNase protection assays were carried out using anti-sense probes of PPAR α from each species, and probes of equal specific activity was used in the hybridisation reaction so that species comparisons could be made. Figure 3.46 shows a typical protection gel obtained using untreated liver RNA from mouse (Figure 3.46, C), hamster (Figure 3.46, A) and guinea pig (Figure 3.46, B) hybridised to their respective riboprobes. A specific protected band of the expected size was detectable in the liver RNA of each species which was absent in yeast tRNA sample hybridised

to the probe and treated with RNase A (+ve lane). Therefore the protected band was due to the presence of PPAR α mRNA in the liver of each species.

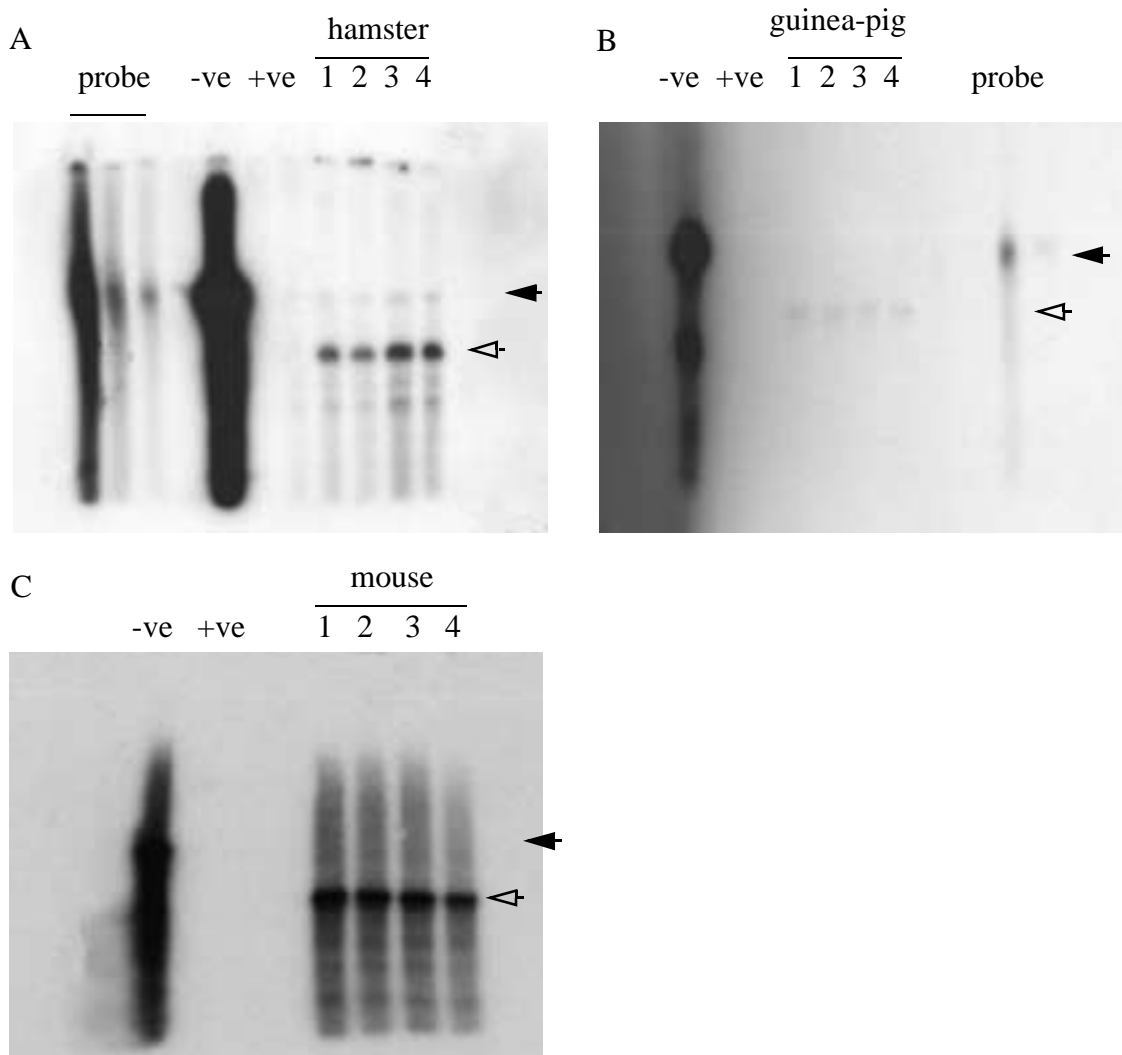


Figure 3.46 PPAR α mRNA in hamster (A), guinea pig (B) and mouse (C) liver. Total RNA was extracted from untreated male hamster, guinea pig and mouse liver as detailed in methods. Four animals of each species are used (numbered) For each species, RNase protection assay were performed on 30 μ g of RNA per animal using an anti-sense riboprobe, labelled with [α - 32 P] CTP, of PPAR α of that species. Mouse, guinea-pig and hamster probes used in the protection were adjusted so that the same specific activity was present for all probes in the hybridisation reactions. Yeast tRNA treated with (+ve) or without (-ve) RNase A are also included in the assay. Protection assays were run on a 6% gel and visualised by autoradiography. All protection gels were exposed together for the same length of exposure on the same autorad film. The position of full-length probe is indicated by filled arrow, and the position of the protected fragment by an unfilled arrow.

The level of PPAR α mRNA expression in mouse, hamster and guinea pig liver was quantified using a phosphor imager. It was possible to make a species comparison on the expression of PPAR α as the mouse, hamster and guinea pig PPAR α probes used in the protection assay had

identical specific activity. All protection gels were exposed together for the same length of exposure on the same cassette, and the bands were quantified using a phosphor imager within the linear range of the signal. As shown in Figure 3.47, a higher level of expression of PPAR α mRNA was found to be present in mouse liver than hamster and guinea pig liver. The level of expression of mouse PPAR α was 14-fold ($P < 0.0005$) and 5-fold ($P < 0.005$) higher when compared to guinea pig and hamster PPAR α , respectively. PPAR α is expressed at a higher level in hamster than in guinea pig (3-fold, $P < 0.005$). Therefore, the constitutive expression of PPAR α in the liver of mouse, hamster and guinea pig shows the same rank order as their response to peroxisome proliferators.

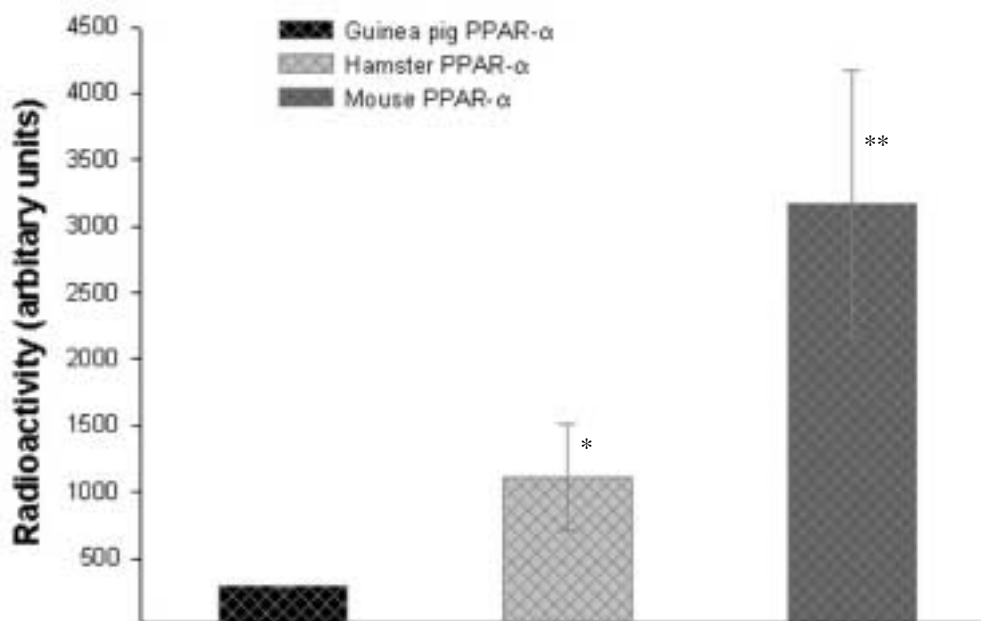


Figure 3.47 Comparative hepatic expression of PPAR α . Total liver RNA was extracted from groups of four untreated male animals from each species (hamster, guinea-pig and mouse). For each species, RNase protection assay were performed on 30 μ g of RNA per animal using an anti-sense riboprobe, labelled with [α - 32 P] CTP, of PPAR α of that species. Mouse, guinea-pig and hamster probes used in the protection were adjusted so that they so that same specific activity were present for all probes in the hybridisation reactions. Protection assays were run on a 6% gel and visualised by autoradiography. All protection gels were exposed together on the same autorad cassette, and the bands were quantified using a phosphor imager on the linear range of the signal. Mean radioactivity values of each group were calculated and expressed as arbitrary units. The error bars shown represent the standard deviation from the mean. Values significantly different from guinea pig where * = $p < 0.005$ and ** = $p < 0.0005$

Section 3.8 The mPPAR α ligand binding domain (mPPAR α -LBD)

PPAR α is a transcription factor and therefore regulates its responsive genes transcriptionally. It is possible that PPAR α , like other steroid receptors, may require specific coactivator protein(s) for its transcriptional activity. The expression of such coactivator proteins in tissue and species specific patterns may be crucial in determining species responsiveness to peroxisome proliferators. As steroid receptors interact with coactivator and other proteins of the transcription machinery via their ligand binding domain it is possible to isolate novel protein(s) that may function as coactivators using the mouse PPAR α ligand binding domain (mPPAR α -LBD) in protein-protein interaction studies. Recombinant expression and purification of mPPAR α -LBD was undertaken so that it could be utilised in protein-protein interaction studies, specifically a nuclear pull-down assay.

Section 3.8.1 Induction of mPPAR α -LBD protein

Mouse PPAR α -LBD (amino acids 194-468), subcloned into pET15b prokaryotic expression vector, was obtained from Dr C. Palmer (Dundee). As well as wild-type LBD (mPPAR α -LBD^{wt}), a mutant version of this LBD protein was also obtained, termed G-mutant where glycine is substituted for glutamine at residue 282 (mPPAR α -LBD^{G-mut}). Mouse PPAR α -LBD (both wild-type and G-mutant) was bacterially expressed following transformation into *E.coli* strain BL21(DE3)pLysS. Small scale cultures of transformed BL21 (DE3) pLysS cells were grown to an optical density (O.D_{600nm}) of 0.5, and the expression of LBD was induced by the addition of 0.5mM IPTG to the medium. Induction of proteins was analysed by SDS-PAGE, and Figure 3.48 shows a typical protein gel obtained using induced and uninduced total cell extracts. Comparison of the protein banding patterns revealed the presence of an induced band only in mPPAR α -LBD transformed cell extracts treated with IPTG. The induced band is easily recognisable one hour after the addition of IPTG, and it appears to be between 30-35 kDa when compared with known molecular size markers. This value is in agreement with the predicted

molecular weight of the LBD protein (33.3 kDa).

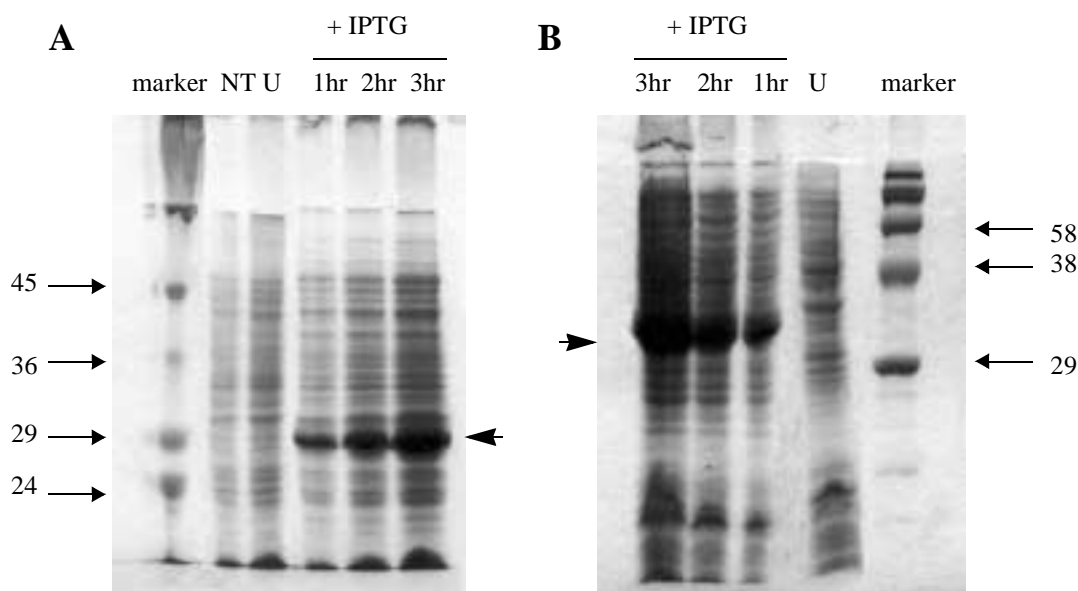


Figure 3.48 Induction of mPPAR α -LBD in *E. coli*. Total cell extracts of induced and uninduced BL21 (DE3) pLysS-pET15b-mPPAR α -LBD^{wt} (A) and BL21 (DE3) pLysS-pET15b-mPPAR α -LBD^{G-mut} (B) were analysed by 12% SDS-PAGE gel, stained with Coomassie blue. Cells were cultured at 37 °C and induced with 0.5mM IPTG. Samples were taken at 0 (U), 1, 2 and 3 hour (+IPTG) time points following induction and analysed as shown. BL21 (DE3) pLysS (non-transformed, NT) was used as negative control. Size of the molecular weight markers are shown in kDa, and the positions of the induced band is shown by the large arrow.

Section 3.8.1.1 Effect of temperature on protein solubility

The solubility of the induced protein was determined using small scale cultures. BL21(DE3) pLysS-pET15b-mPPAR α (both wild-type and G-mutant) were grown at 37 °C and induced with 0.5mM IPTG after the culture had reached the log phase of the growth ($O.D_{600nm} = 0.5$). To separate soluble and insoluble protein fractions, the cell pellet was resuspended in Tris buffer, freeze-thawed several times and then sonicated as detailed in Methods. Soluble and insoluble proteins were separated by centrifugation and then analysed by SDS-PAGE as shown in Figure 3.49. The protein gel shows that most, if not all, of the induced proteins are present in an insoluble form. The effect of lower temperatures (30 °C and 25 °C) on the solubility of the induced protein was investigated using BL21(DE3)pLysS-pET15b-mPPAR α -LBD^{wt}. Cells cultured at

these lower temperatures require longer periods of growth (12-18 hours) to reach the log phase ($O.D_{600nm} = 0.5$). Figure 3.49 demonstrates that at lower temperatures IPTG induction of LBD protein is still achieved, and the soluble fraction of the induced protein is marginally increased when compared to induction at 37 °C.

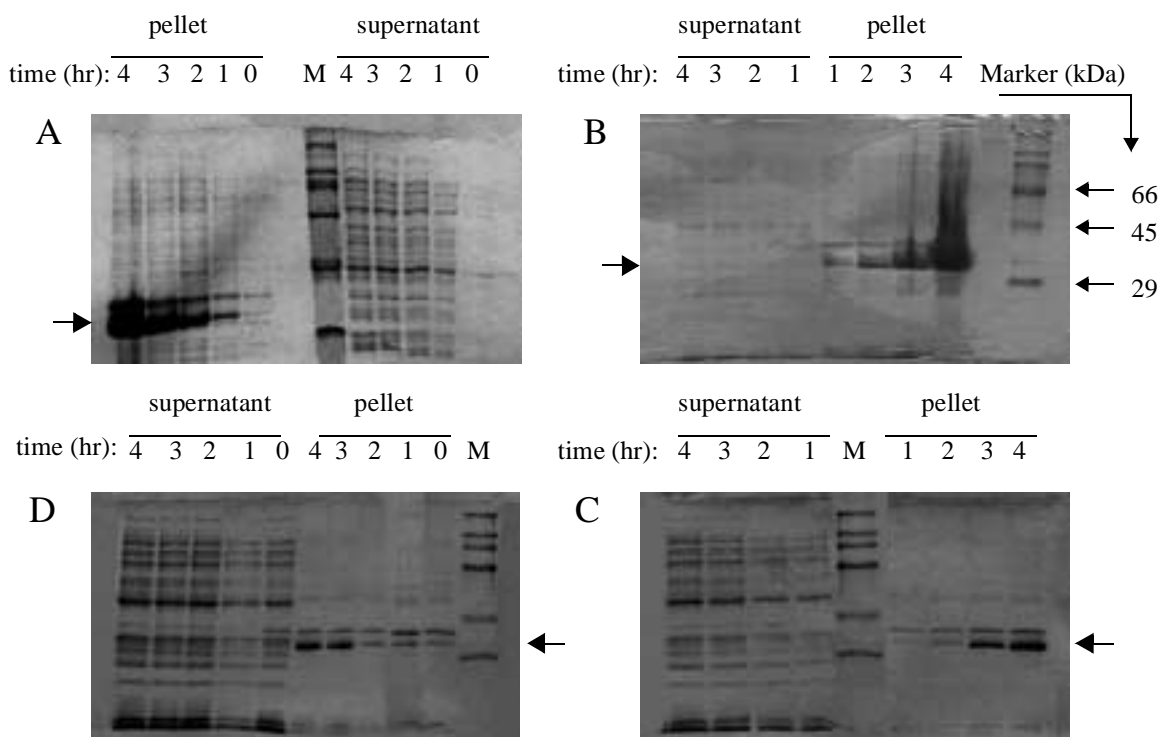


Figure 3.49 Solubility of mPPAR α -LBD; effect of temperature. BL21 (DE3) pLysS carrying the expression plasmid pET15b-mPPAR α -LBD^{wt} (A, C, D) and pET15b-mPPAR α -LBD^{G-mut} (B) were grown and induced at either 37 °C (A, B), 30 °C (C) or 25 °C (D). Cells were collected at different time points (shown in hours) following their induction with 0.1mM IPTG. The soluble (supernatant) and insoluble (pellet) protein fractions were separated by freeze-thaw, sonication and centrifugation as described in methods. Samples were analysed by loading and resolving on a 12% SDS-PAGE gel stained with Coomassie blue. Size of molecular weight markers are shown in kDa, and position of the induced band is shown by the large arrow.

Section 3.8.1.2 Effect of IPTG concentration on protein solubility

Having found that growth at lower temperatures marginally increased the solubility of induced LBD protein, the effect of IPTG concentration on the solubility of induced protein at 25 °C were investigated using mPPAR- α -LBD^{wt}. Figure 3.50a shows that five hours of exposure to 0.5mM IPTG concentration produced a higher induction when compared to 0.05mM and 0.1mM IPTG, for the same induction period. Solubility tests demonstrate that IPTG at 0.5mM improved the solubility of the induced protein marginally, although most of the induced protein still segre-

gates into the insoluble fraction.

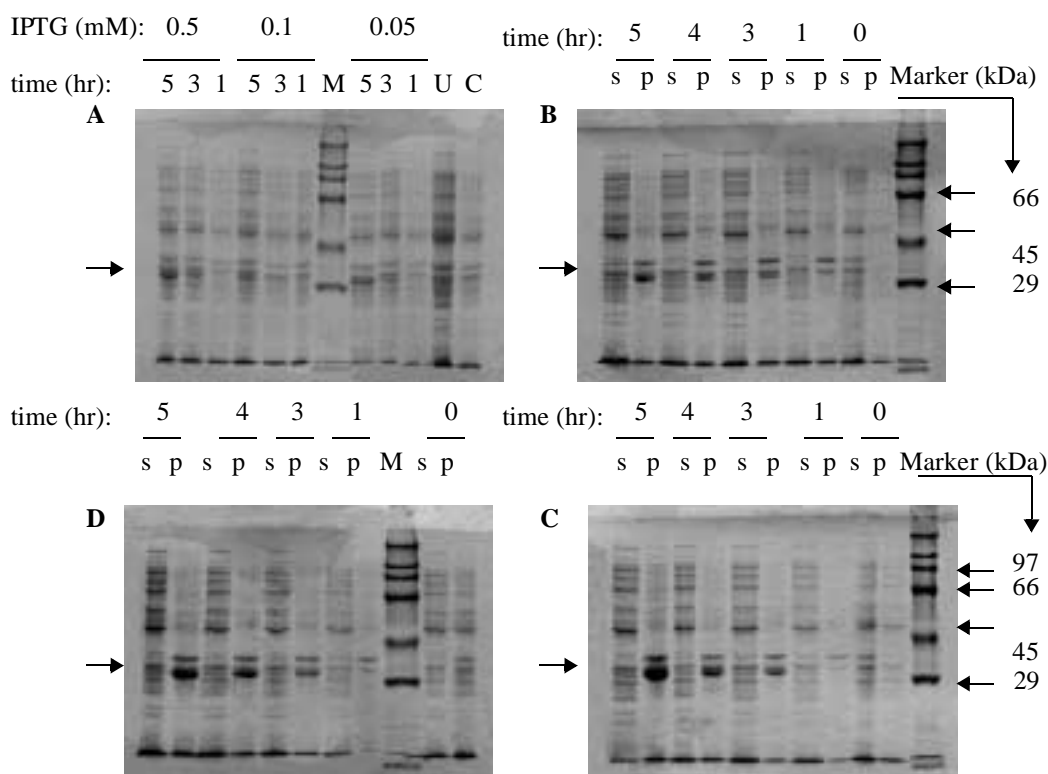


Figure 3.50 Effect of IPTG on induction and solubility of mPPAR α -LBD. BL21 (DE3) pLysS-pET15b-mPPAR α -LBD^{wt} were grown at 25 °C and induced with either 0.05mM (B), 0.1mM (C) or 0.5mM (D) IPTG. Cells were collected at different time points (shown in hours) following their induction with IPTG. The soluble (s) and insoluble (p) protein fractions were separated by freeze-thaw, sonication and centrifugation as described in methods. Samples were analysed by loading and resolving on a 12% SDS-PAGE gel stained with Coomassie blue. Total cell extracts of induced cells are shown in A, where U= uninduced cells and C= non-transformed BL21 (DE3) pLysS. The size of the molecular weight markers are shown in kDa, and position of the induced band is shown by the arrow.

Section 3.8.2 Affinity purification of mPPAR α -LBD protein

Solubility tests demonstrate that cell growth and induction at a lower temperature (25 °C) with 0.5mM IPTG improves the solubility of the induced protein. Using these optimised conditions, the soluble fraction of the induced proteins was purified by affinity purification from a large scale culture (1 litre) of BL21(DE3)pLysS-pET15b-mPPAR α -LBD (wild-type and G-mutant). The cloning strategy included a stretch of six consecutive histidine residues at the N-terminal end of the LBD (his⁶-tagged mPPAR α -LBD), which has been utilised for the affinity purification of the induced protein. The soluble protein fraction was passed through the His⁶Bind metal chelation resin column (with immobilised Ni²⁺) and the fractions collected. Figure 3.51 shows

the SDS-PAGE analysis of the fractions collected at different stages of his-tag purification. Multiple bands were visible in the earlier eluted fractions (fractions E1-E3) but were absent from the final collected fractions where only one band of the expected molecular size (for LBD protein) was detectable as shown in lane E_f/E_f^* .

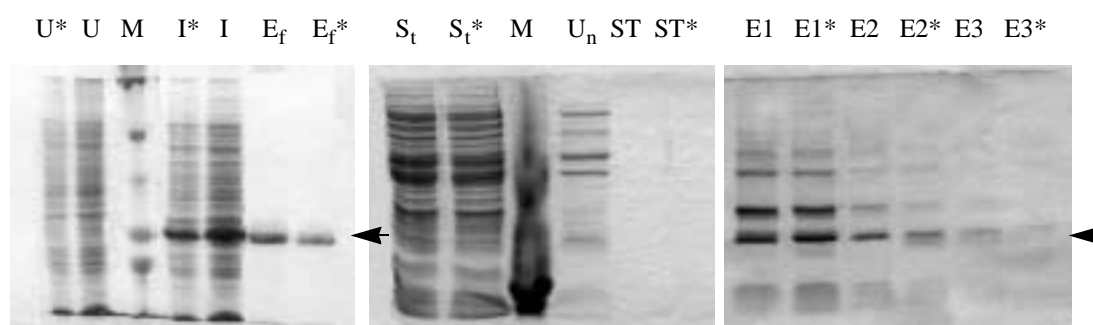


Figure 3.51 Affinity purification of mPPAR α -LBD. Large scale growth and induction of BL21(DE3)pLysS carrying the expression plasmid pET15b-mPPAR α -LBD^{wt} and pET15b-mPPAR α -LBD^{G-mut} (*) were carried out at 25 °C. Cells were grown to log phase and then induced with 0.5mM IPTG. Following freeze-thaw and sonication, soluble and insoluble proteins were separated by centrifugation. Total soluble proteins (supernatant) were passed through the Ni²⁺ column and fractions were collected at various stages of purification. Collected fractions were analysed by 12% SDS-PAGE gel, stained with Coomassie blue. Lanes are: U= uninduced and I= induced total cell extract, E_f = final elute fraction, S_t= total supernatant before passed through the column and U_n= unbound supernatant after passed through the column, E1-3 eluted fractions collected at different stages of purification, where 1 represent the first collected fraction, ST= fraction collected after stripping with high concentration of salt solution, M= molecular marker. The position of the induced band is shown by the arrow.

Using this affinity purification procedure 200 μ g of protein was purified from one litre of culture. Western immunoblotting was performed on the induced total cell extract and on the histidine purified samples of mPPAR α -LBD (both wild-type and G-mutant). Using a polyclonal rabbit-anti-mousePPAR α antibody a protein band was detected both in induced total cell extracts and in the affinity-purified fraction of this induced sample (Figure 3.52). This demonstrates that both mPPAR α -LBD^{wt} and mPPAR α -LBD^{G-mut} proteins were successfully purified by affinity purification using Ni²⁺ immobilised His⁶Bind resin.

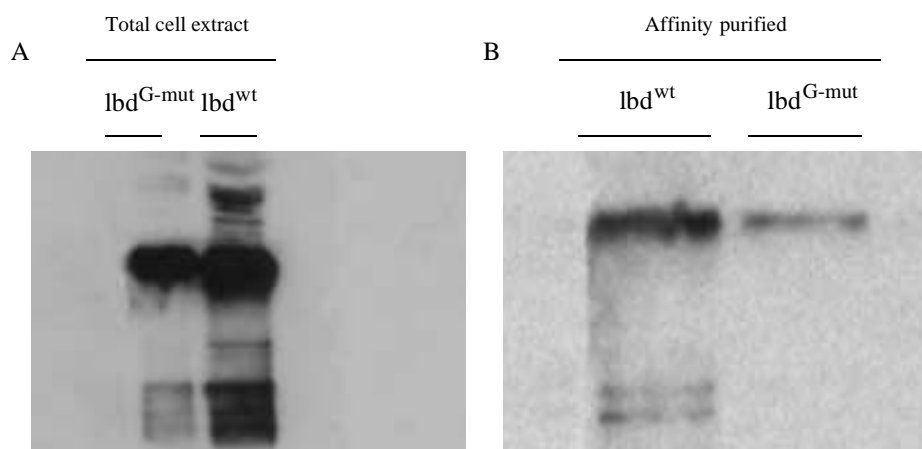


Figure 3.52 Detection of mPPAR α -LBD by Western blotting. Total cell extracts (A) and affinity purified (B) mPPAR α -LBD^{wt} (lbd^{wt}) and mPPAR α -LBD^{G-mut} (lbd^{G-mut}), induced with 0.5mM IPTG, were resolved on a 12% SDS-PAGE gel and then transferred by electroblotting onto PVDF membrane as detailed in methods. Transferred proteins on the membrane were probed with rabbit anti-mousePPAR α antibody (1 : 30,000 dilution). A goat anti-rabbit-IgG, conjugated to horseradish peroxidase, antibody (1 : 40,000) was used to detect anti-mousePPAR α antibody. Immunoreactive mPPAR α -LBD protein bands on the membrane were visualised using ECL chemiluminescent detection kit and exposing to Hyperfilm as described in the methods.

Section 3.8.3 FPLC purification of mPPAR α -LBD protein

Eluted his-tagged LBD protein samples from the Ni²⁺ column were further purified from contaminating proteins and solutes and concentrated using ion-exchange FPLC chromatography. Eluted protein samples from the Ni²⁺ column were first dialysed in 0.1M Tris-HCl (pH 8.0) at 4 °C for 15 hours (five changes). This removed most of the contaminating small molecular weight proteins and solutes such as imidazole and NaCl. Dialysed proteins were passed through a weak cation exchanger (Econo-S, pH range 2-10) using buffer A (0.1M Tris-HCl, pH 8.0) and buffer B (1M NaCl in 0.1M Tris-HCl pH 8.0) at a pH one unit above the isoelectric point of LBD protein (pH 6.6). Using isocratic elution, a single peak was observed as shown in the FPLC chromatogram (Figure 3.53). The identity of this eluted protein fraction could be determined immunochemically but the presence of a single peak suggests that it is most likely to be LBD. Moreover, immunoreactivity towards his-tagged purified LBD protein samples was demonstrated using the anti-mouse PPAR α antibody (Figure 3.52). The eluted protein fractions require desalting and then ligand binding studies to demonstrate functional LBD protein.

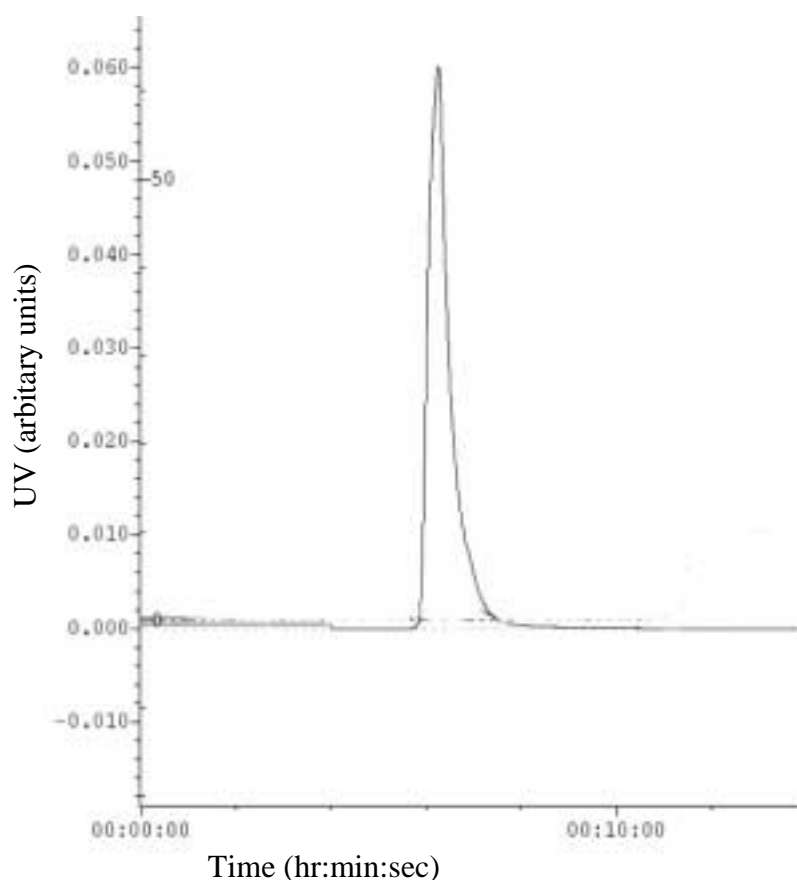


Figure 3.53 FPLC of PPAR α -LBD^{wt}. His-tag purified proteins were dialysed overnight in TRIS-HCl solution to remove contaminating small molecular weight solutes. Protein samples were then run on a weak cation exchanger (Econo-S, Bio-rad) FPLC column with isocratic flow using buffer A (0.1M Tris-HCl, pH 8.0) and buffer B (1M NaCl in 0.1M Tris-HCl, pH 8.0). Samples were eluted from the column using a flow rate of 1ml/min and a gradient of 0-50% buffer B over 10 minutes (from 2 minutes to 12 minutes).

Section 3.9 Localisation of RNA in mouse liver

Recently, using the yeast two-hybrid screening method, a number of coactivator proteins have been identified for the steroid receptor superfamily. Some of them are specific coactivator proteins for a particular receptor as in the case of PPAR- γ , which has a cold-inducible coactivator protein PGC-1 (PPAR gamma coactivator protein-1) (Puigserver *et al.*, 1998). Most coactivator proteins have been shown to interact with a number of steroid receptors. Although PPAR α is typical in this respect, so far no coactivator proteins have been found to be specific for PPAR α . It is possible that some of these coactivators may be important in peroxisome proliferation mediated by PPAR α . Determination of the expression of PPAR α and any such coactivator proteins

in the liver acini may provide a clue as to which, if any, of the coactivators are important in the functioning of PPAR α -mediated peroxisomal events that show zonal distribution. Also the effect of a peroxisome proliferator (MCP) on the local expression of both PPAR α and “general” coactivator proteins for steroid receptors has been examined by *in situ* hybridisation.

Section 3.9.1 Region-specific distribution of mPPAR α mRNA

Expression and spatial distribution of mPPAR α in the liver acini has been investigated using *in situ* hybridisation. To determine the expression of each gene, sense and anti-sense oligo-nucleotides (45 nucleotides in length) were designed from the 5'-end of the gene and were synthesized using automated sequencer (Biomedical Synthesis and Analysis unit, QMC, Nottingham). Using a FASTA search on Genbank, the probe for each gene was checked to ensure that the designed probe shows only 100% homology to the particular mouse gene of interest.

Cryostat sections of frozen liver were treated with ^{35}S ATP labelled sense and anti-sense probes and hybridised at 42 $^{\circ}\text{C}$ overnight. Hybridized probes were detected by coating the tissue sections (for appropriate length of time) with emulsion and then developed as detailed in Methods. Hybridization to α - ^{35}S -labelled probes was visualized by bright-field microscopy, revealing positive signals as black silver grains. Expression of glutamine synthase was used as a reliable positive control which is highly expressed in the liver and shows distinct centrilobular distribution pattern (Moorman *et al.*, 1994). Figure 3.54 shows the distribution of glutamine synthase expression in the liver which is illustrated at high and low power magnification as observed under bright-field microscopy. As expected, sense control was unable to detect any mRNA messages while anti-sense probe specifically detected the expression of GS-mRNA in the centrilobular region (Figure 3.54 A,C, labelled C) of the liver acini. Expression of mPPAR α mRNA was detected in the liver, and due to its low abundance, the radioactive signal was observed under high magnification only (Figure 3.55). The expression of mPPAR α mRNA was localised in the nu-

clei but showed no specific pattern of distribution, i.e. mouse PPAR α has panlobular distribution. Dosing of mouse with MCP caused no observable change in the expression of liver PPAR α when compared to untreated liver (not shown).

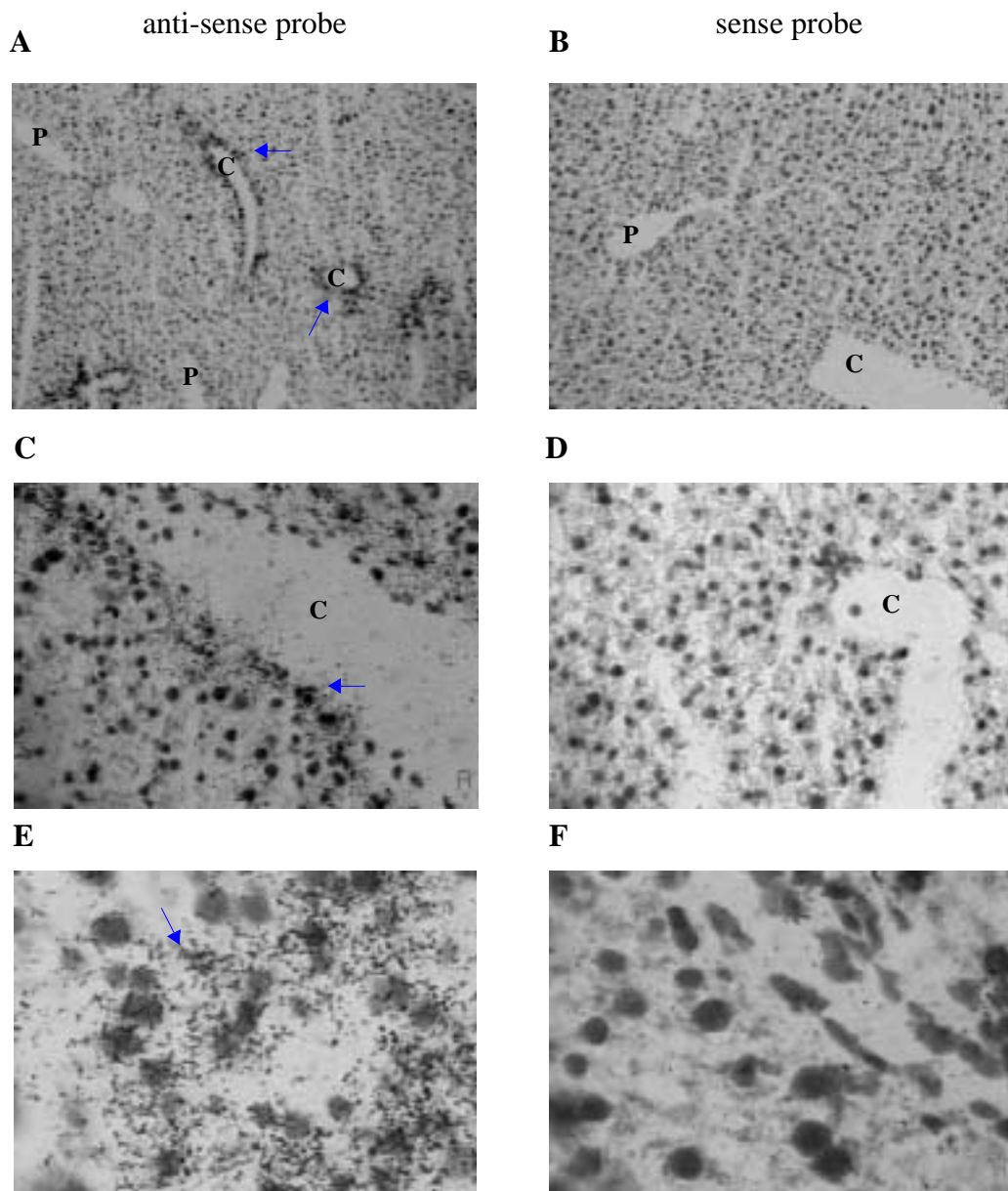


Figure 3.54 Distribution of glutamine synthase mRNA in mouse liver. Specific centrilobular distribution of glutamine synthase mRNA in the mouse liver were determined using in situ hybridisation. Radiolabelled anti-sense (A, C, E) and sense (B, D, F) probes were prepared as detailed in methods and hybridised to frozen liver sections of untreated mice. Hybridised probes in the tissue sections were localised by overlaying the sections with emulsion and then developed after 6 weeks of exposure in the dark at 4 0C. Hybridisation to a-35S-labelled probe was visualised by bright-field microscopy, revealing positive signals as black silver grain (shown by the use of an arrow). For illustration purposes, results are presented in the picture format as viewed under light microscope using magnification: x200 (A, B); x800 (C, D); x2000 (E, F).

Section 3.9.2 Expression of co-activator proteins in the liver

The expression and distribution, at the mRNA level, of a number of coactivator proteins which have been shown to interact and enhance or modulate transcriptional activity of PPAR α *in vitro* has been investigated in the mouse liver. These coactivators include PBP (peroxisome proliferator binding protein), SRC-1 (steroid receptor coactivator-1), CBP/p300 (CREB binding protein), PGC-1 (PPAR gamma binding protein-1) and RIP-140 (receptor interacting protein). Anti-sense probes for each gene were used for the detection of their mRNAs using *in situ* hybridisation while sense probe was used as a control. As shown in Figure 3.56, using anti-sense probes, low level expression of PBP, SRC-1 and CBP/300 was detectable in the liver but their expression was not confined to a particular pattern in the liver acini. As expected no signal was obtained using sense controls (not shown). Dosing of mouse with MCP caused no observable change in the expression of liver PBP, SRC-1 and CBP/300 mRNA when compared to untreated liver (not shown). The expression of the coactivator PGC-1 and RIP-140 mRNAs were not detectable in either untreated and MCP treated mouse liver.

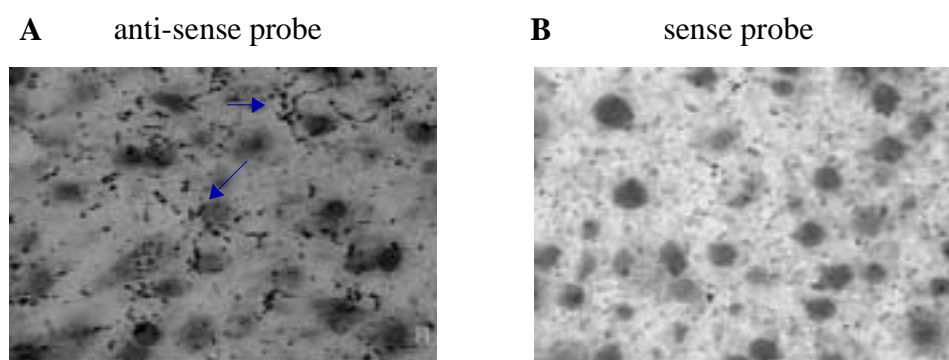


Figure 3.55 *In situ* hybridisation with anti-sense (A) and sense (B) PPAR α . Radiolabelled anti-sense probes were prepared as detailed in methods and hybridised to frozen liver sections of untreated mice. Hybridised probes in the tissue sections were localised by overlaying the sections with emulsion and then developed after 6 weeks of exposure in the dark at 4 $^{\circ}$ C. Hybridisation to α - 35 S-labelled probe was visualised by bright-field microscopy, revealing positive signals as black silver grain (shown by the use of an arrow). For illustration purposes, results are presented in the picture format as viewed under light microscope (x2000 magnification).

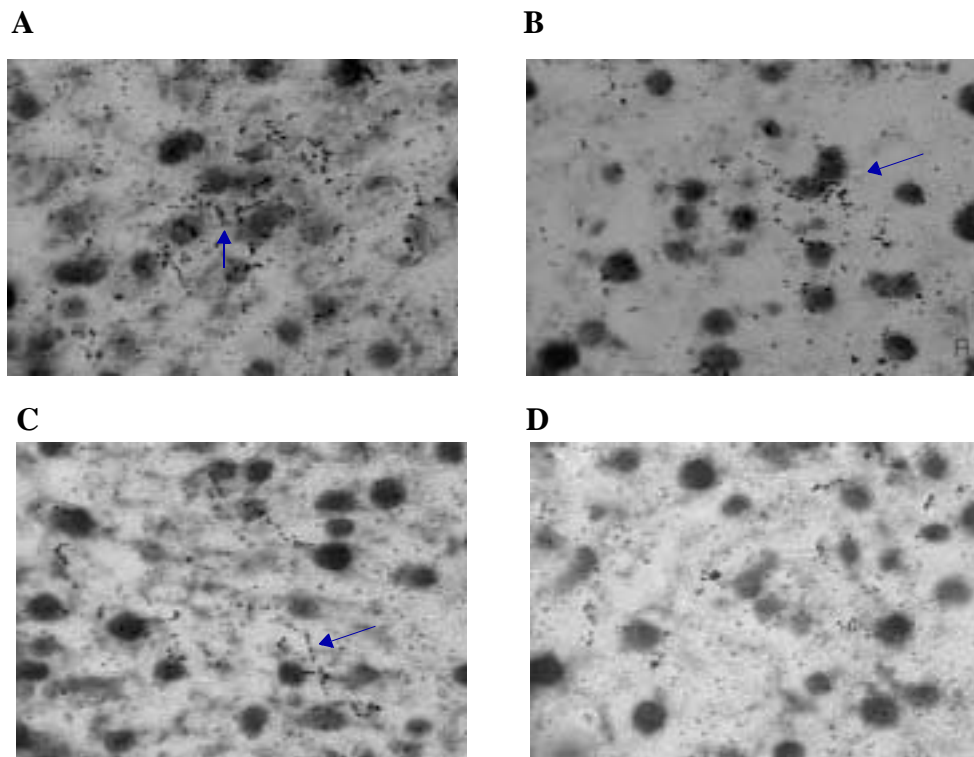


Figure 3.56 Localisation of coactivator mRNA expression in mouse liver. *In situ* hybridisation for the localisation of mRNAs for coactivator protein (A) PBP, (B) CPB/300, (C) SRC-1 and (D) PGC-1. Radiolabelled anti-sense probes were prepared as detailed in methods and hybridised to frozen liver sections of untreated mice. Hybridised probes in the tissue sections were localised by coating the sections with emulsion and then developed after 6 weeks of exposure in the dark at 4 °C. Hybridisation to α -³⁵S-labelled probe was visualised by bright-field microscopy, revealing positive signals as black silver grains (shown by the use of an arrow). For illustration purposes, results are presented in the picture format as viewed under light microscope (x2000 magnification).

Chapter 4 Discussion

Section 4.1 The role of PPAR α in peroxisome proliferation

Understanding species differences in response to peroxisome proliferators at the molecular level is fundamental to the evaluation of human risk from peroxisome proliferator-induced hepatocarcinogenesis. The discovery of the steroid receptor PPAR α (Isseman and Green, 1990) and subsequent demonstration that the pleiotropic effects of PPs are mediated by PPAR α (Lee *et al.*, 1995; Cattley *et al.*, 1991) has greatly increased our understanding of the molecular mechanisms of peroxisome proliferation and subsequent carcinogenesis. It is perplexing to find that functional PPAR α is expressed in both responsive and non-responsive species (Gottlicher *et al.*, 1992; Bell *et al.*, 1998) since it was originally considered that species non-responsiveness to PPs may be due to the lack of PPAR α . This suggests that there are other factors involved in determining species response to PPs.

To investigate if an intrinsic property of PPAR α is a determining factor in species response, the effects of PPAR α from different species on peroxisome proliferation could be studied in an *in vitro* system following their transfection. Primary hepatocytes from responsive species such as rat or mouse are a useful model system to study such PPAR α induced effects. These primary hepatocytes have all the necessary components to respond to PPs fully. However, since the endogenous level of PPAR α is sufficient for the process of peroxisome proliferation to occur in rat hepatocytes, perturbation (reduction) of the PPAR α level is required to study the effects of transfected PPAR α in the system. Therefore the rat primary hepatocyte system was investigated first for a highly inducible marker of peroxisome proliferation and then evaluated as a potential model system to study the effects of transfected PPAR α .

Section 4.1.1 Peroxisome proliferation in rat primary hepatocytes

Primary hepatocyte culture provides a powerful investigative tool to study peroxisome prolifer-

ation. Many studies have used rat primary hepatocytes to investigate the effects of PPs due to their responsive nature. These studies have shown that PPs causes an increase in peroxisome number and increase in peroxisomal β -oxidation (Lake *et al.*, 1984; Gray *et al.*, 1982; Foxworthy and Eacho, 1986) and DNA synthesis (Plant *et al.*, 1998). A rat primary hepatocyte culture system has been developed in our laboratory that is shown to respond well to PPs. In particular, increase in peroxisomal β -oxidation enzyme activities (Mitchell *et al.*, 1994), and induction of acyl-CoA oxidase and CYP4A1 mRNA (Bell *et al.*, 1991) have been observed in response to PPs at levels comparable to *in vivo* data. Therefore this primary hepatocyte culture system is capable of modeling the increase in specific enzyme levels by PPs and could be used to study other aspects of peroxisome proliferation.

Section 4.1.2 Induction of DNA synthesis in rat primary hepatocytes

The hyperplastic response to PPs has been shown to result in liver enlargement and is important in PP-induced hepatocarcinogenesis (Lock *et al.*, 1988). This hyperplastic response is due to transient or sustained increase in of cell replication. PPs induce cell replication, as measured by DNA synthesis, in a dose dependent manner (Styles *et al.*, 1988), and up to 16-fold induction in DNA synthesis has been observed *in vivo* (Price *et al.*, 1992). This high level of DNA synthesis has been reproduced in primary rat hepatocytes, and PPs are found to act in a dose dependent manner (Plant *et al.*, 1998). Using this replicative DNA synthesis as a marker of peroxisome proliferation, it would be desirable to study the effect of exogenously added PPAR α in hepatocyte cultures. Rat primary hepatocytes were investigated to see if such high levels of DNA synthesis could be reproduced. As shown in Figure 3.1, rat primary hepatocytes undergo DNA synthesis following exposure to the mitogen EGF, thus demonstrating that primary cultures are capable of undergoing mitogenic stimulation. EGF has been shown to cause a high level of replicative DNA synthesis both *in vitro* and *in vivo* (Michalopoulos, 1990) and the results obtained here are consistent with these observations.

Section 4.1.3 Peroxisome proliferator-induced DNA synthesis

The ability of two potent PPs MCP and Wy-14,643 to cause hepatic DNA synthesis has been investigated in primary rat hepatocytes. As can be seen from Figure 3.3, between 2 and 3 fold induction of DNA synthesis was observed following exposure to these chemicals. In agreement with previous studies the labelling period (BrdUrd incorporation) used for studying the stimulation of DNA synthesis by PPs (6-30 hour) was different from that used for EGF (24-48 hour). PPs stimulate DNA synthesis rapidly and therefore may use a different pathway from EGF-induced DNA synthesis. This difference in response may be due to the type of receptor they bind to and activate. Since PPAR α is a transcription factor, its activation by PPs may result in rapid expression of genes involved in mitogenesis. The EGF receptor, on the other hand, is a cell surface receptor that, upon binding to its ligand, transduces the signal through a cascade of secondary messenger pathways that eventually result in nuclear localisation of the signal and altered gene expression.

Although MCP and Wy-14,643 have been shown to be mitogenic in primary hepatocytes, a maximum of 3-fold induction of DNA synthesis was observed for Wy-14,643, and this level of induction is lower than *in vivo*. Using both BrdU and ^3H labelling, a high level of DNA synthesis has been observed in rat liver dosed with potent PPs (Marsman *et al.*, 1988). Previously, this primary hepatocyte culture system has been used to show a ten-fold induction in DNA synthesis by Wy-14, 643 (Plant *et al.*, 1998). However, the lower level of induction observed in this study has been reported by most studies of primary rat hepatocytes (Bieri *et al.*, 1994; Marsman *et al.*, 1993; James and Roberts, 1994). In conclusion, the rat primary hepatocyte system used in this study is responsive to mitogenic stimulation by both EGF and PPs, but the levels of DNA synthesis observed are much lower than those seen in *in vivo* studies.

Section 4.1.4 Influence of culture components on DNA synthesis

A number of factors have been shown to influence the level of DNA synthesis in primary rat

hepatocyte culture. Insulin for example has been shown to augment DNA synthesis in fetal hepatocytes (Gruppuso *et al.*, 1994), and calcium has been shown to influence both peroxisome proliferator and EGF-induced DNA synthesis in cultured rat hepatocytes (Zhang and Farrell, 1995; Bennett and Willams, 1993). In this study hepatocytes were cultured in complex CL-15 medium which may contain components that can affect the response of hepatocytes to PP-induced DNA synthesis. For example, the fetal calf serum used in CL15 medium may contain growth inhibitory as well as stimulatory factors and therefore may affect PP-induced DNA synthesis. However, removal of serum from the media marginally decreased the level of DNA synthesis caused by PPs and EGF. This is not surprising since previous studies have demonstrated that in the presence of chemically defined serum-free media human hepatocytes can proliferate following exposure to EGF (Runge *et al.*, 1999). Moreover, Plant *et al.* (1998) found that PPs exert their mitogenic stimulation in primary rat hepatocytes cultured in chemically-defined (serum-free) media.

Previously it has been shown that EGF-induced DNA synthesis in primary hepatocytes requires the presence of CO₂ (Mitaka *et al.*, 1991). Maintenance of cells in 5% CO₂ resulted in a higher percentage of cells undergoing DNA synthesis induced by EGF or the PPs MCP or Wy-14,643. This increase in cell replication was not confined to EGF and PP-treated cells, as there was a rise in DNA synthesis in untreated control hepatocytes. The pH of the CL-15 medium drops when hepatocytes are maintained in 5% CO₂ which drastically reduces cell viability and response to mitogens. Thus, addition of 20mM sodium bicarbonate is required to buffer the drop in pH caused by CO₂. However, bicarbonate has been shown to cause DNA synthesis in primary hepatocytes maintained in the presence of CO₂ (Mitaka *et al.*, 1991). Therefore the increase in DNA synthesis under CO₂ conditions found in this study is likely to be due to the effect of bicarbonate.

Removal of hydrocortisone from the media dramatically reduces EGF and PP-induced DNA synthesis (Figure 3.4). Hydrocortisone has been shown to be necessary for PP-induced mitogenesis (Plant *et al.*, 1998). These authors showed that PP-induced DNA synthesis was prevented in hydrocortisone-deficient medium and this effect was reversed when dexamethasone was added to the medium. As PPAR α is regulated by glucocorticoids (Lamberger *et al.*, 1984) and since PPAR α mediates PP-induced DNA synthesis (Holden *et al.*, 2000), it is not surprising to see that the induction of DNA synthesis by PPs is inhibited in hydrocortisone-deficient medium.

Varying the culture conditions and the media components did not result in a higher level of induction of DNA synthesis caused by PPs (Figure 3.4). Other parameters such as cell density may play an important role in PP-induced DNA synthesis. Cell density is important for cell-cell interaction and communication. At high cell density (confluent) proliferative responses to HGF and EGF in rat and human hepatocytes, respectively, were inhibited (Greuet *et al.*, 1997; Takehara *et al.*, 1992). However, the cell density used in this study has been determined previously to be optimal for DNA synthesis. Further, the same culture conditions have been used to demonstrate suppression of apoptosis (Section 3.2.2) and peroxisome proliferation (Section 3.4) and a high level of CYP4A1 induction (Section 3.2.3) by MCP.

Section 4.1.5 Suppression of apoptosis by MCP

PPs have been shown to suppress the basal level of apoptosis in rat hepatocytes (Roberts *et al.*, 1995) and this suppression of apoptosis has been proposed as a complement to the induction of DNA synthesis in the mechanism of PP-induced hepatocarcinogenesis. Since PPAR α mediates the effects of PPs, suppression of apoptosis could be used as a marker of peroxisome proliferation to study the effects of transfected PPAR α from different species. Therefore, the effects of MCP on rat primary hepatocyte cultures was investigated for their ability to suppress apoptosis. Using Hoechst 33258 staining, the basal (spontaneous) level of apoptosis was found to be 1.3%

(Figure 3.5). MCP reduced this incidence of apoptosis by as much as 40%. This level of suppression is lower than previously reported both in primary rat hepatocytes and in hepatoma cell lines (Bayly *et al.*, 1994; Plant *et al.*, 1998; James and Roberts, 1996). For example, Plant *et al.* (1998) found a 70% reduction in apoptosis induced by 100 μ M MCP and James and Roberts (1996) found even greater reduction (4-fold) by nafenopin. However, the basal rate of apoptosis was much higher in the primary rat hepatocytes used by James and Roberts (1996) in their study. This could be attributable to the difference in culture media used which may have a significant effect on the ability of hepatocytes to respond to PPs. In view of such low a level of suppression induced by PPs it is not possible to perturb the PPAR α level and then study the effects of exogenously added PPAR α on apoptosis as a marker of peroxisome proliferation. Although the primary hepatocytes used in this study are capable of undergoing peroxisome proliferation (Figure 3.25), it is not clear why they respond poorly to PP-induced induction of DNA synthesis and suppression of apoptosis.

Section 4.1.6 Induction of CYP4A1 mRNA as marker of peroxisome proliferation

Treatment of rats with PPs has been shown to cause an increase in the activity of lauric acid hydroxylase in the liver (Kimura *et al.*, 1989), which was later demonstrated to be preceded by an increase in the amount of CYP4A1 mRNA produced (Bell *et al.*, 1991; Bell and Elcombe, 1991). This transient induction of CYP4A1 is early, rapid and occurs at a high level (Bell *et al.* 1991). Therefore PP-induced induction of CYP4A1 represents an early marker of peroxisome proliferation. Induction of CYP4A1 mRNA is mediated by PPAR α which trans-activates the CYP4A gene by interacting with a response element PPRE found upstream of the gene (Tugwood *et al.*, 1992). High level induction of CYP4A1 was demonstrated in primary hepatocytes, and the early and rapid induction seen *in vivo* has also been reproduced *in vitro* (Bell and Elcombe, 1991). In the absence of high levels of induction of DNA synthesis or suppression of apoptosis, the study of CYP4A1 induction in primary hepatocytes represented a better proposi-

tion to study the functionality of PPAR α . A highly specific and sensitive RNase protection assay was used to detect the expression and induction of CYP4A1. As well as CYP4A1, other CYP4A members are expressed in rat liver (Hardwick *et al.*, 1987; Kimura *et al.*, 1989a and 1989b; Aoyama *et al.*, 1990). Therefore, a probe was designed from the 3' end of the mRNA that contains non-coding sequences so that it will be more likely to discriminate CYP4A1 from other members of the CYP4A subfamily in the liver. Using such a probe, a protected fragment of 190bp was detected which was specific to rat liver RNA (Figure 3.8). Initially the RNase protection assay was optimised using *in vivo* MCP-treated liver and kidney RNA samples as CYP4A1 is highly induced in animal studies. Using the optimised conditions, constitutive expression of CYP4A1 was detected in both liver and kidney, although liver has a higher level of CYP4A1 mRNA. CYP4A1 mRNA was induced in both liver and kidney following exposure to MCP (25mg/kg), and higher level expression was seen in the liver compared to kidney (Figure 3.8). Although the level of induction was not quantified it is evident from the autoradiograph that CYP4A1 is highly induced, in agreement with previous findings (Hardwick *et al.*, 1987; Bell *et al.*, 1991 and 1992). Therefore induction of CYP4A1 was demonstrated in rat liver and kidney using the specific RNase protection assay.

Section 4.1.7 CYP4A1 induction in primary hepatocytes

Expression of CYP4A1 was examined in RNA extracted from cultured rat hepatocytes using the RNase protection assay. Expression of CYP4A1 was very low in control hepatocytes and was detectable only after prolonged exposure to autoradiographic film, whereas CYP4A1 was readily detectable in liver RNA (Figure 3.8). This low steady-state level of CYP4A1 in primary hepatocytes has been reported previously (Bell and Elcombe, 1991). However, CYP4A1 was induced in primary hepatocytes following 48-hours of exposure to 100 μ M MCP. This level of induction was readily detectable and was comparable to *in vivo* control liver and kidney (Figure 3.8). MCP induced the expression of CYP4A1 mRNA by as much as 14-fold (Figure 3.8 and

Figure 3.10). This high-level response is suitable for further study. However, it is necessary to lower, or eliminate, the expression of the endogenous PPAR α in order to study the effect of added PPAR α . The requirement for a low level of endogenous PPAR α is proposed due to the observation that during peroxisome proliferation PPAR α levels are not induced and therefore the constitutive level of PPAR α is sufficient to promote peroxisome proliferation. Thus it is unlikely that additional transfected PPAR α , in the presence of a normal constitutive level of PPAR α , will have any additive effects on the marker of peroxisome proliferation (in this case CYP4A1) or indeed the process of peroxisome proliferation itself.

Section 4.1.8 Modulation of CYP4A1 expression

Administration of the synthetic glucocorticoid hormone dexamethasone has been shown to result in an increase in PPAR α mRNA expression in rat liver (Steineger *et al.*, 1994). Using rat hepatocyte culture, Lamberger *et al.* (1994) demonstrated that glucocorticoids dexamethasone and hydrocortisone can modulate PPAR α level by stimulating PPAR α mRNA synthesis in a dose dependent manner. Further, the level of PPAR α protein has been found to be down-regulated in primary hepatocytes cultured in hydrocortisone-deficient medium (Plant *et al.*, 1998). These data show that the level of PPAR α can be reduced in primary hepatocytes maintained in hydrocortisone-deficient medium, and this, in theory, could affect the induction of CYP4A1 based on the assumption that in rat hepatocytes PPAR α regulates the transcriptional induction of this gene. Thus, induction of CYP4A1 by PPs was investigated in rat hepatocytes maintained in normal CL-15 and hydrocortisone-deficient media. Figure 3.9 demonstrates that the level of induction of CYP4A1 is reduced in hepatocytes cultured in hydrocortisone-deficient medium, although hepatocytes in the absence of hydrocortisone are still capable of responding to PP-induced CYP4A1 induction. These data demonstrate that hydrocortisone is required for the maximal induction of CYP4A1 in primary rat hepatocyte cultures. This requirement of hydrocortisone for the maximal induction of CYP4A1 seen in primary hepatocytes may be due

to the indirect effect of hydrocortisone which is required for maximal expression of PPAR α (Lamberger *et al.*, 1994), as PPAR α is known to mediate the transcriptional induction of CYP4A (Lee *et al.*, 1995).

Forty-eight hours of dosing with MCP resulted in a maximum of 14-fold induction of CYP4A1 in the presence of hydrocortisone. However, the level of induction was reduced to 2.5-fold in hydrocortisone-deficient medium (Figure 3.9). This low level of induction of CYP4A1 seen in hydrocortisone-deficient medium probably reflects the presence of residual PPAR α still present in hepatocytes. Effects of culture conditions, namely duration of seeding period before dosing and duration of MCP exposure on CYP4A1 induction, were investigated with a view to maximizing the difference in induction of CYP4A1 between cultures with and without hydrocortisone. Initially cells were seeded for four hours in the presence of hydrocortisone which was later replaced with either normal or hydrocortisone-deficient medium as appropriate. This initial requirement of hydrocortisone in the medium was necessary for the maintenance of cell monolayer, and therefore hydrocortisone may still be present in hepatocytes at residual levels even when cells are incubated in hydrocortisone-deficient media. Culturing cells for two days before being exposed to MCP for twenty-four hours did not increase the difference in induction between cultures with and without hydrocortisone when compared to the induction seen in one day old cultures with same dosing period (Figure 3.11 A and B). CYP4A1 induction was elevated to greater than 40-fold following 24 hours of exposure of MCP (Figure 3.12 A). Similar levels of induction of CYP4A1 have been observed previously in primary hepatocyte cultures (Bell and Elcombe 1991). However, induction of CYP4A1 in hydrocortisone-deficient medium was also significantly high (16-fold) so that the induction ratio by MCP in normal as compared to hydrocortisone-deficient media did not improve significantly. A comparison of dosing periods of 24, 48 and 72 hours of hepatocytes (cultured for 24 hours prior to dosing) found that 48 hours of

dosing gives a maximal 7-fold increase in overall induction of by MCP between normal and hydrocortisone-deficient media (Figure 3.11 and Figure 3.12D), i.e. MCP induced CYP4A1 in normal medium by 14.2-fold but by only to 2.3-fold in hydrocortisone-deficient medium. It was hypothesised that decreased expression of PPAR α in hydrocortisone-deficient cells is responsible for the reduced induction of CYP4A1.

This differential induction between normal and hydrocortisone-deficient media is insufficient for the study of the effects of transfected PPAR α using induction of CYP4A1 as a marker of peroxisome proliferation. This is simply because a transfection efficiency of 100% hepatocytes with PPAR α is required to produce maximal inducibility (14-fold) of CYP4A1. Since transfection efficiencies of 5-20% (Figure 3.20) are routinely observed, the highest possible level of expression would be very close to the background level. For example, a 20% transfection efficiency of hepatocytes that give 2.3 and 14-fold induction, respectively, of CYP4A1 in normal and hydrocortisone-deficient media would result in 3.6-fold above control, which is very close to the background level of 2.3-fold control. It would be very difficult to draw significant conclusions about any difference in induction of this scale.

Section 4.1.9 Endogenous versus reporter gene activation to study of PPAR α function

One possibility is that species differences in peroxisome proliferation may be due to differences in the level of PPAR α as there is evidence that mouse has a higher level of PPAR α compared to guinea pig (Bell *et al.*, 1998). The functionality of guinea pig or human PPAR α has been demonstrated in transient transfection studies where the trans-activating ability of transfected PPAR α was measured by the expression of a reporter gene containing a minimal PPRE response element in its promoter region. Although this simple *in vitro* study demonstrates basic functionality of PPAR α , its usefulness as a measure of true trans-activating ability in the context of peroxisome proliferation is incomplete. This is because the majority of the studies have found

a low level, in most cases roughly equal, of induced reporter activity for all studied PPAR α (whether from responsive or non-responsive species) using a minimal PPRE (see Table 4.1). However, such genes are known to be highly inducible only in responsive species. As can be seen from Table 4.1 most studies have reported only low-level induction of reporter gene expression under the control of minimal rat acyl-CoA PPRE (2-4 fold) whereas the induction of acyl-CoA gene in rat liver is over 13-fold (Bell *et al.*, 1991) Similarly rat CYP4A1 and rabbit CYP4A4 genes are highly induced in liver as opposed to a small induction of reporter gene expression under the control of their respective PPRE (Table 4.1). This probably reflects the complex nature of the regulatory regions (promoter) of PPAR responsive genes whose activity may also be influenced by the interaction of *cis* and *trans* acting elements.

Receptor	PPRE used	Induction (n-fold over control)	Reference
mPPAR α	ACO-PPRE	2.5	Marcus <i>et al.</i> , 1993
	ACO-PPRE	2	McNae <i>et al.</i> , 1994
	ACO-PPRE	100	Kliwer <i>et al.</i> , 1994
	ACO-PPRE	14	Issemann <i>et al.</i> , 1993
mPPAR α	HD-PPRE	2	Marcus <i>et al.</i> , 1993
	CYP4A6-PPRE	2	Johnson <i>et al.</i> , 1996
rPPAR α	ACO-PPRE	4	Marcus <i>et al.</i> , 1993
	HD-PPRE	4.5	Marcus <i>et al.</i> , 1993
hPPAR α	ACO-PPRE	9	Mukerjee <i>et al.</i> , 1994
	ACO-PPRE	5	Pineau <i>et al.</i> , 1996
hPPAR α	CYP4A6z-PPRE	3.7	Pineau <i>et al.</i> , 1996
xPPAR α	ACO-PPRE	3	Krey <i>et al.</i> , 1993
	HD-PPRE	6.4	Krey <i>et al.</i> , 1993
	CYP4A6z-PPRE	4.7	Krey <i>et al.</i> , 1993
gpPPAR α	ACO-PPRE	6	Bell <i>et al.</i> , 1998
	ACO-PPRE	6	Tugwood <i>et al.</i> , 1998

Table 4.1 Induction of reporter genes. A literature review of various PPAR α mediated induction of reporter containing minimal PPRE in the promoter region of reporter genes. Maximum induction of reporter genes obtained with a number of peroxisome proliferator responsive genes are shown. Mouse (m), rat (r), human (h), xenopus (x) and guinea pig (gp) PPAR α are shown. Genes containing PPRE are shown by ACO (acyl-CoA oxidase), HD (hydratase dehydrogenase), CYP4A6 (cytochrome P450 4A6).

Mouse *Cyp4a* genes are physically linked on chromosome 4 (Henderson *et al.*, 1994; Kimura *et al.*, 1989; Heng *et al.*, 1997). Although these genes are inducible by peroxisome proliferators, they show different levels of regulation and inducibility and therefore are under complex control within the same locus. The influence of a *cis*-acting regulatory region called the LCR (locus control region), in addition to promoters and enhancers, on the expression of β -globin genes is well studied in the case of the β -globin multigene locus (Dillon and Grosveld, 1993). Using transgenic and stable cell line transfection approaches they showed that the LCR is required for the expression of the β -globin genes at close to physiological levels (Collis *et al.*, 1990; Grosveld *et al.*, 1987). The fact that mouse *Cyp4a* genes are physically linked at a single chromosomal locus suggests that their regulation may be complex and may include large flanking sequences (both 5' and 3'). It is therefore of interest to study the induction of PP-responsive endogenous genes (*Cyp4a*) as opposed to minimal PPRE-reporter genes to determine the true activity of PPAR α .

Transient transfection has been shown to give variable results, however stable transfection has been found to express genes reproducibly at physiological levels which are directly proportional to transgene copy number (Collis *et al.*, 1990). Also, the mode of transfection has been shown to influence the stability of ectopically expressed mRNA (Nanbu and Nagamine, 1997). Thus, to study the functionality/activity of PPAR α on a comparative basis it will be more informative to study the induction/expression of endogenous genes as a marker of peroxisome proliferation. Transfection of PPAR α in primary hepatocytes from responsive species provides an ideal system for this study.

Section 4.2 Characterization of the induction of murine *Cyp4a* genes

In rat primary hepatocytes, it proved to be difficult to perturb endogenous PPAR α level and then examine the effects of transfected PPAR α . The availability of PPAR α knock-out mice has pro-

vided an ideal system in which to study PPAR α function, since there is a zero background level of PPAR α in the hepatocytes of knock-out mice. Therefore any induction of marker *Cyp4a* genes would be due to the activity of transfected PPAR α . Members of the murine *Cyp4a* subfamily show different levels of inducibility by PPs and some are induced in a tissue and sex specific manner. In addition, strain differences in peroxisome proliferation have been observed (Hiratsuka *et al.*, 1996). Since induction of *Cyp4a* has been postulated to be the primary event during peroxisome proliferation it is important to determine which members of the *Cyp4a* gene family in S129 mice liver are highly inducible by PP treatment as high inducibility of that particular enzyme is most likely to play an important role in their tissue specific responses to peroxisome proliferation.

Section 4.2.1 Induction of murine *Cyp4a* family

Expression and induction of the *Cyp4a* gene family has been determined in male S129 mice using control, MCP and Wy-14,643 treated liver RNA. Since members of *Cyp4a* subfamily show high sequence similarity to each other, RNase protection was employed which has high specificity (Myers *et al.*, 1985) and is therefore likely to discriminate between the *Cyp4a10*, *12* and *14* genes. Probes used for the protection of *Cyp4a10* and *12* have been shown to be specific for their respective genes (Bell *et al.*, 1993). For the protection of *Cyp4a14* mRNA, probes were synthesised from the untranslated region of the gene which is highly divergent from other *Cyp4a* genes and therefore is most likely to be specific for the *Cyp4a14* gene.

Constitutive expression of *Cyp4a10* and *14* was detectable in the liver RNA of control PPAR α wild-type mice (Figure 3.14, Figure 3.15). In contrast, constitutive expression of *Cyp4a10* and *14* mRNA was reduced in the control liver of PPAR α knock-out mice such that it was only detectable only after prolonged exposure of autoradiographs. This reduction seen in knock-out mice was below the limit of accurate measurement, and, as a result, it was not possible to quan-

titatively compare against the control level in wild-type mice. *Cyp4a10* mRNA was highly induced following treatment with MCP (31-fold) and Wy-14,643 (41-fold) in the liver of PPAR α wild-type mice (Figure 3.17), but their expression was unaffected by PPs in the knock-out mice. As with *Cyp4a10*, *Cyp4a14* was highly induced by MCP and Wy-14,643 in the liver of wild-type mice but was unaffected in the liver of PPAR α knock-out mice (Figure 3.15). MCP and Wy-14,643 gave greater induction of *Cyp4a14*, 80 and 41 fold respectively, when compared to *Cyp4a10* induction (Figure 3.17). These observations have been reported by Barclay *et al.* (1999) where, using Northern blot analysis, *Cyp4a10* and *14* were found to be highly induced in wild-type mice following treatment with clofibrate, while expression was non-inducible in knock-out mice. Other studies have also demonstrated high level induction by PPs of hepatic CYP4A1 in rat (Bell *et al.*, 1991) and *Cyp4a10* and *14* in other mouse strains (Bell *et al.*, 1993; Heng *et al.*, 1997). The reduced expression of *Cyp4a10* and *14* seen in the liver of male knock-out mice suggests that some involvement of PPAR α in the constitutive expression of these two genes in the male liver of this mouse strain. The high inducibility of *Cyp4a10* and *14* by PPs in PPAR α wild-type mice and their lack of inducibility in knock-out mice strongly suggest that PPAR α mediates the transcriptional induction of these two members of the murine *Cyp4a* family.

Constitutive expression of *Cyp4a12* was found to be high in the male liver of both PPAR α wild-type and knock-out mice (Figure 3.16). However compared to wild-type control mice, a 4-fold reduction of *Cyp4a12* was observed in knock-out mice. MCP and Wy-14,643 had no effect on the hepatic expression of *Cyp4a12* in male PPAR α wild-type and knock-out mice. These findings confirm a previous report where *Cyp4a12* was shown to be regulated differently from other *Cyp4a* isoforms (Bell *et al.*, 1993). This study demonstrated that *Cyp4a12* is expressed constitutively at high levels in male liver and kidney and is non-inducible by MCP. By contrast, the

Cyp4a12 gene is expressed at low levels in both liver and kidney of female mice and treatment of these animals with MCP induced *Cyp4a12* mRNA to levels comparable with those in the male. Similarly, sex differences in the expression of murine renal *Cyp4a* proteins and lauric acid hydroxylase activity have been described (Henderson *et al.*, 1990; Henderson and Wolf, 1992), as well as in the expression of CYP4A2 in rat that shows sex specific regulation similar to *Cyp4a12* (Sundseth and Waxman, 1992). Generally, the observed low constitutive expression of all three murine *Cyp4a* genes in PPAR α knock-out mice (compared to control wild-type) suggest that PPAR α may play a significant role in the constitutive expression of these genes. High level inducibility of *Cyp4a10* and *14* by PPs in wild-type mice and their lack of inducibility in knock-out mice demonstrates that PPAR α is involved in the transcriptional regulation of these two murine genes. Although the enzymatic activity of *Cyp4a14* has not been determined yet, the high inducibility of both *Cyp4a10* and *14* by PPs and their low constitutive expression tend to suggest that they may play an important role in peroxisome proliferation in the mouse liver. In contrast, the lack of inducibility of *Cyp4a12* in the liver and its high constitutive level suggest that *Cyp4a12* may have a house keeping function and is less important in peroxisome proliferation in the liver.

In vivo studies demonstrated that *Cyp4a14* is highly inducible by PPs in the liver of S129 mice. This high level of induction of *Cyp4a14*, compared to other member of *Cyp4a* family suggest that *Cyp4a14* would be a better marker to study peroxisome proliferation. To study *Cyp4a14* as a marker of peroxisome proliferation, its level of induction was determined in mouse primary hepatocyte cultures. As with the *in vivo* study, *Cyp4a14* was inducible (Figure 3.17 and Figure 3.18) by MCP and Wy-14,643 in hepatocytes isolated from PPAR α wild-type mice and its expression was undetectable in both control and PP-treated hepatocytes from knock-out mice.

Section 4.2.2 Effects of transfected PPAR α in the hepatocytes knock-out mice

To study the function of PPAR α from different species in the context of peroxisome proliferation, a primary hepatocyte culture system has been developed using S129 PPAR α knock-out mice. This system is ideal to study the effects of exogenously added PPAR α since mouse (being a responsive species) contains all the molecular components required for peroxisome proliferation but lacks functional PPAR α in this strain. Therefore, in theory, any induction of *Cyp4a14* by transfected PPAR α (in the presence of PPs) would be detectable so long as transfection efficiency is at a reasonable level. A maximum transfection efficiency of 15% was observed in mouse hepatocytes (Figure 3.21) which is high enough to detect PPAR α induced *Cyp4a14* induction, at least for mouse PPAR α , provided that it has similar activity to the endogenous receptor.

However, any expression of *Cyp4a14* observed after transfection of PPAR α would simply identify the activity of the receptor and would not discriminate whether the observed effect is due to the basal or induced activity of the PPAR α . This is particularly relevant in the case of PPAR α from non-responsive species such as guinea pig. If the non-responsive nature of guinea pig is due to the lack of high levels of PPAR α in the liver (quantitative differences) then transfected gpPPAR α would also produce *Cyp4a14* induction. This is also consistent with the possibility that the guinea pig lacks other component(s) required for *Cyp4a14* induction which are present in mice but absent in guinea pig hepatocytes.

Primary hepatocytes of PPAR α knock-out mice were transfected with either mouse or guinea pig PPAR α and then treated with PPs to induce the expression of *Cyp4a* genes. Expression of *Cyp4a14* was investigated in the total RNA of PPAR α post transfected hepatocytes by the RNase protection assay. As expected, *Cyp4a14* expression was undetectable in both control and PP-treated non-transfected hepatocytes from PPAR α knock-out mice (-/-). However, there is no

evidence of *Cyp4a14* expression when these cells were transfected with either mouse or guinea pig PPAR α and treated with PPs (Figure 3.22). These experiments were repeated on several occasions but with similar findings, i.e. transfected mouse or guinea pig PPAR α had no effect on the expression of *Cyp4a14* in the hepatocytes of knock-out mice. It was envisaged that the induction of *Cyp4a14* would be attainable following the addition of mPPAR α in the hepatocytes of knock-out mice, since hepatocytes from the wild-type mice (i.e. in the presence of endogenous PPAR α) are capable of responding to PP-induced *Cyp4a14* induction.

The possibility that transfected PPAR α is not being expressed from the expression vector was investigated in the case of gpPPAR α by RNase protection assays using a specific probe. Figure 3.23 demonstrates that the expression of gpPPAR α mRNA was detectable in RNA from gpPPAR α -transfected hepatocytes but not in the case of non-transfected or vector alone. Although the expression of mPPAR α mRNA was not determined in mPPAR α post-transfected hepatocytes, it is likely that PPAR α is expressed following their transfection. This vector has previously been used in transfection studies (Isseman and Green, 1990). Having established that the transfected PPAR α (at least for guinea pig) is being expressed it is still a possibility that non-functional PPAR α protein is being synthesised. Trans-activating ability of PPAR α was assessed by co-transfection of a luciferase reporter gene containing a PPRE response element linked to the promoter region. This reporter assay demonstrates that transfected mouse and guinea pig PPAR α are capable of inducing the expression of this luciferase gene, thus providing evidence of trans-activating ability on episomal DNA (Figure 3.24).

Having found that transfected PPAR α is being expressed and has trans-activating ability active in the PPRE reporter assay it is tempting to speculate that the functioning of the exogenous receptor (from the expression vector) may differ from that of the endogenous receptor in such a way as to account for the induction of *Cyp4a14* by endogenous PPAR α and lack of induction

by the transfected PPAR α . However, there is no such report of whether transiently expressed PPAR α from expression vector differs in its functioning from chromosomally expressed PPAR α . The other possibility is that the transfection efficiency of primary hepatocytes may have a major influence in the outcome of such studies. This is simply because transfection of all the hepatocytes (100% transfection efficiency) from knock-out mice would be required to achieve the maximum 9.5-fold induction of *Cyp4a14* observed in the hepatocytes from the wild-type mice, assuming that transfected PPAR α are equally as transcriptionally active as endogenous receptors. However, although the transfection efficiency varied between experiments, a transfection efficiency of between 10 and 15% has been achieved in primary hepatocytes. It is quite possible that transfected PPAR α (at least from mouse) had resulted in the induction of *Cyp4a14*, but due to the low number of hepatocytes being transfected, this level of induction is rather low and below the sensitivity of the detection by RNase protection assay. However, the level of induction of *Cyp4a14* seen in wild-type hepatocytes suggests that even low-level induction by transfected PPAR α (due to low transfection efficiency), would produce an easily detectable *Cyp4a14* protected fragment in knock-out hepatocytes. It may be more appropriate to study the function of PPAR α by stable transfection since stable transfection has been found to express genes reproducibly at physiological levels (Collis *et al.*, 1990). PPAR α could be stably transfected in to cell lines responsive to PPs with low levels of endogenous PPAR α or into immortalised hepatocytes from PPAR α knock-out mice. Oncogene immortalisation of rat hepatocytes has been successfully used in other applications (MacDonald and Willett, 1997).

PPAR α mediated activation of PPRE-containing reporter genes in transient transfection assay should be treated with caution. This is because the minimal PPRE used in this assay is in a total artificial system that lacks its normal milieu, and the results obtained with minimal PPRE are contentious. Episomal DNA (transiently transfected plasmid DNA) is considered to be in a 'na-

ked' conformation since the packaging of DNA within the confines of the cell nucleus require chromatin which represents the natural environment of regulated genes in eukaryotic cells. Moreover, there may be other flanking regions important in determining the physiological level of expression of PP-responsive genes. One case where this has been shown to be important is the cluster of β -like globin genes. A locus control region (LCR), containing a number of separate regulatory element, present in the β -globin locus (Grosveld *et al.*, 1987), is important for high level, developmental, and tissue specific expression of the β -globin like genes (Dillon and Grosveld, 1991; BlomVan Assendelft *et al.*, 1989; Talbot *et al.*, 1989). Furthermore, in the absence of complete LCR elements, "position effects" are observed in transgenic experiments (Townes *et al.*, 1985; Kollias *et al.*, 1986).

It is unclear why reintroduction of PPAR α into knock-out hepatocytes, in the presence of PPs, did not result in any observable changes in *Cyp4a14* expression, since it was assumed that, like wild-type cells, hepatocytes of knock-out mice would respond to PPs following the addition of functional PPAR α . It is tempting to speculate that gene silencing of the *Cyp4a* locus may have occurred in the PPAR α knock-out mice such that constitutive expression of *Cyp4a* is permissible (e.g. *Cyp4a12*) but PPAR α -mediated induction by PPs is non-permissible. This scenario may be envisaged if PPAR α is important developmentally for maintaining *Cyp4a* in an active expressible/inducible configuration. Absence of PPAR α in $-/-$ mice during ontogeny may have resulted in the modification of the PPPE-containing promoter region of *Cyp4a* genes. Chromatin-mediated regulation of gene expression has been well studied in the case of homeotic selector genes (Akram, 1987) and gene silencing has been shown to be repressed by an evolutionarily conserved chromodomain protein-group of genes called the polycomb group (Jurgens, 1985; for review see Jones *et al.*, 2000). Reversible histone acetylation and DNA methylation are important in the regulation of mammalian gene expression, and their activity on expressible genes re-

sults in DNase I hypersensitive sites in their promoter regions (for reviews see Kingston and Narliker, 1999; Bird and Wolffe, 1999). It would be interesting to examine DNaseI hypersensitive sites in the *Cyp4a* locus in both PPAR α knock-out and wild-type mice to see if both are in an active conformation.

Another possible mechanism for the inability of transfected PPAR α to induce endogenous *Cyp4a* in the hepatocytes of PPAR α knock-out mice may be due to the binding of truncated PPAR α in the *Cyp4a* promoter. This truncated protein may be produced in the knock-out mice with a C-terminal deletion (LBD) but has intact DBD. Therefore, truncated protein has the ability to bind PPRE containing PP-responsive genes but lacks trans-activating function, as a result, it may act in a dominant negative manner by excluding added PPAR α (full-length) from binding to its responsive genes. This might resemble v-erbA/thyroid hormone receptor (THR) interaction. Expression of viral oncogene v-erbA, an altered THR, abolishes the responsiveness to thyroid hormone since v-erbA can bind to thyroid hormone response element but unlike THR is unable to bind thyroid hormone (Sap *et al.*, 1989; Wahlstrom *et al.*, 1996).

Section 4.3 Hamster response to peroxisome Proliferators

Based on biochemical and morphological studies of the liver, hamster is regarded as less or partially-responsive to peroxisome proliferating chemicals when compared to rats and mice (Lake *et al.*, 1989; Price *et al.*, 1992; Grey *et al.*, 1984 and references therein). Comparative studies using potent PPs show a small level of induction of β -oxidation and ω -hydroxylation activities (2-fold) in syrian hamster, compared to high level induction in rat (Lake *et al.*, 1989 and 1993; Price *et al.*, 1992). However, while several groups have reported an induction of peroxisomal β -oxidation (Lake *et al.*, 1989; Lhuguenot *et al.*, 1988), other groups have found no such increase in β -oxidation activity in hamster liver caused by PPs (Sakuma *et al.*, 1992). Similarly, conflicting results have been reported in relation to PP-induced DNA synthesis in hamster. For

example, Styles *et al.* (1988) observed induction of DNA synthesis while Price *et al.* (1992) found no such induction even though both groups used potent peroxisome proliferators in their study. In addition, varying levels of induction of ω -hydroxylase activity have been observed in hamster treated with nafenopin, where one reports a 3-fold (Lake *et al.*, 1989) induction while another have found up to 10-fold induction in lauric acid 12-hydroxylase activity (Price *et al.*, 1992). It is therefore not clear to what extent hamster are responsive to PPs. Where studied, PP-induced transcriptional induction of CYP4A correlates well with species response to peroxisome proliferation. For example, high level induction of CYP4A mRNA occurs in rat and mouse liver (Bell *et al.*, 1991 and 1993; Henderson *et al.*, 1994; Heng *et al.*, 1997) while it is non-inducible by PPs in non-responsive guinea pig (Bell *et al.*, 1993), reflecting the species response to peroxisome proliferation. Thus, transcriptional induction of CYP4A represents a good marker of peroxisome proliferation. To study hamster response to PPs, a cloning project was undertaken to isolate expressed CYP4A genes (cDNA) from hamster liver so that specific probes could be used to determine CYP4A induction.

Section 4.3.1 Cloning of hamster CYP4A cDNA

To date no CYP4A genes have been cloned from hamster, although hamster has inducible lauric acid hydroxylase activity in liver microsomes. For the cloning of putative hamster CYP4A gene(s), two primers, HMCyp-P1 and HMCyp-P2, were designed from the aligned protein sequences of known rat, mouse, human and rabbit CYP4A genes (Figure 3.26). These primers were designed from high regions of identity and include the haem-binding region (HMCyp-P2) and the highly conserved 13 amino acids of the I-helix in the CYP4A family (HMCyp-P1). These primers were expected to amplify a cDNA fragment of around 500bp if hamster has expressed CYP4A genes. Figure 3.28 shows that a 500bp amplified fragment was obtained from MCP-treated hamster liver cDNA using the forward HMCyp-P1 and the reverse HMCyp-P2 primers. Sequence analysis of the complete double strand of this amplified fragment confirmed

the cloning of partial hamster hepatic CYP4A cDNA since they showed >80% identity to rat and mouse CYP4A genes as well as other species at the nucleic acid level (Table 3.3).

Section 4.3.2 Cloning of three CYP4A cDNAs in hamster

Three members of the CYP4A family in mouse (*Cyp4a10*, 12 and 14) and four members in rat (CYP4A1, 2, 3 and 8) have been identified. Phylogenetic analysis suggests that in rat and mouse these multiple members are the result of a recent gene duplication event (Heng *et al.*, 1997). The possibility that multiple members of the CYP4A family may also exist in hamster was investigated. Following the initial cloning of 500bp amplified hamster cDNA product, 18 recombinant transformed colonies were picked at random and their plasmid DNAs were analysed by double restriction digests with *EcoRI* and *BamHI*, since these sites are present in the primers (Figure 3.29). These clones were grouped as shown in Table 3.1. Three clones from group A (clones 3, 4 and 9) and B (clones 1, 13 and 16) and two clones from group C (clones 6 and 14) have been sequenced on both strands. The consensus sequences from all these groups show that they have high similarity with other known CYP4A genes at the cDNA and amino acid level (>80%). Consensus sequences of group A, B and C were compared with each other and, as shown in Table 3.2, they are highly similar to each other but differ in percentage identity at amino acid level. This demonstrate that the three groups represent three different cDNA clones and were designated CYP4A17, CYP4A18 and CYP4A19 relating to clones of groups of A, B and C respectively (Dr Nelson, personal communication).

Section 4.3.3 Sequence analysis of hamster CYP4A genes

CYP4A17, CYP4A18 and CYP4A19 are highly similar to each other, but CYP4A18 is equally similar to all rat and mouse CYP4A genes at both cDNA and amino acid level, while CYP4A17 and 19 (which are highly similar to each other) are most similar to rat CYP4A1 (91% and 93% identity, respectively) and its mouse homologue *Cyp4a10* (90% and 91%, respectively). However, CYP4A17, 18 and 19 are equally similar to rabbit, human and guinea pig (>80% identity)

(Table 3.3, Table 3.4). Thus, the high identity of hamster CYP4A genes with other members of CYP4A subfamily demonstrates that they are also members of this subfamily. The high similarity between rat CYP4A1 and the hamster CYP4A17 and 19 suggest that the common ancestor to CYP4A1 and CYP4A17 and 19 must have existed before hamster and rat split in the evolutionary tree. Furthermore, the high similarity of CYP4A17 with CYP4A19 suggests that CYP4A17 may have evolved from CYP4A19 by a gene duplication event after the separation of rat/mouse and hamster from their common ancestor. Phylogenetic analysis of rat and mouse CYP4A genes shows a similar relationship between mouse *Cyp4a14* and rat CYP4A2 and CYP4A3. Phylogeny of rat and mouse CYP4A shows that both CYP4A3 and its homologue *Cyp4a14* existed before speciation, and in rat gene duplication of CYP4A3 has given rise to CYP4A2 after the formation of the rat and mouse lineages. Approximately equal similarity of hamster CYP4A18 to all rat and mouse CYP4A genes indicates that the duplication event giving rise to all rat and mouse genes must have happened after the common ancestor of rat and mouse CYP4A and hamster CYP4A split up.

Since all hamster genes were partial clones it was not appropriate to assess the phylogenetic tree of the evolutionary relationship to rat and mouse CYP4A genes. From Table 3.4, Table 3.3 it can be seen that rat, mouse and hamster CYP4A genes are approximately equally similar to the rabbit, human and guinea pig CYP4A genes. Unlike rat and mouse, guinea pig CYP4A13 gene is equally similar to all hamster genes. Guinea pig CYP4A13 shares much lower identity (80%) to rat and mouse CYP4A genes when compared to the high identity of hamster CYP4A genes (up to 93%) with rat and mouse genes. The guinea pig CYP4A13 gene shows similar identity with all three hamster CYP4A genes as do rabbit CYP4A genes. This is interesting since rat, mouse, guinea pig and hamster belong to the same mammalian order Rodentia yet guinea pig appears similar to rabbit. Taxonomic classification, based on comparative morphology, places

guinea pig in the order Rodentia (Novacek, 1992) while molecular analysis of mitochondrial DNA has argued in favour of the inclusion of guinea pig in a new mammalian order distinct from myomorphs (such as rat mouse) of the order Rodentia (D'Erica *et al.*, 1996, Cao *et al.*, 1997).

Mouse *Cyp4a* genes have been localized to chromosome 4 (Bell *et al.*, 1993; Handerson *et al.*, 1994) which also contains the *Cyp4b* subfamily (Heng *et al.*, 1997). Moreover, all three mouse *Cyp4a* genes are shown to be physically linked and are phylogenetically related to the *Cyp4b* subfamily (Heng *et al.*, 1997). A comparison of amino acid identity of all members of CYP4A subfamilies shows that the members of CYP4A subfamily are considerably less conserved across species (as low as 72%) compared to the CYP4B gene subfamily despite being in tandem on the same chromosome (data not shown). This implies that the evolution of the CYP4A genes is particularly rapid compared with the neighbouring CYP4B subfamily. It would be interesting to see if all hamster CYP4A genes are co-localised on the same chromosome and are physically linked.

Section 4.3.4 Functions of putative hamster P4504A proteins

Amino acid sequences of the three identified partial hamster CYP4A genes were compared with each other and with rat CYP4A1 (Figure 3.32). PCR primers used to amplify CYP4A genes from hamster liver cDNA were designed from highly conserved exons (8 and 11/12) of the CYP4A family. Exons 11 and 12 encode the well-known RNCIG motif which is characteristic of P450 proteins. The conserved cysteine residue is involved in the binding of an iron atom present in the prosthetic group as evident from the crystal structure of the bacterial CYP101 protein (Poulos *et al.*, 1986). The RNCIG motif is a crucial feature in the P450 protein and has been proposed to be a signature for the cytochrome P450 superfamily of enzymes (Gonzalez, 1989). This motif is present in all partial hamster CYP4A proteins, indicating that they are P450 pro-

teins. Further, comparison of CYP2 with partial hamster CYP4A proteins reveal the existence of two of the six substrate recognition motifs (SRS4 and 5, Figure 3.32) proposed by Goto (1992) based on analysis of amino acid and coding nucleotide sequences. Previously a stretch of 13 amino acids present in exon 8 was identified among CYP4 family and was proposed as a signature motif for the CYP4 family (Bradley *et al.*, 1991). Exon 8 of each of the three hamster CYP4A genes putatively encodes this motif present within a stretch of 16 amino acids: LRAEVDTFMFEGHDTT. Therefore the presence of this CYP4 motif further identified the putative hamster genes as members of the CYP4 family, and their high similarity with other CYP4A genes indicates that they are members of CYP4A the subfamily. It is likely that these putative hamster P450A proteins are capable of ω -hydroxylating fatty acids as do other members of this subfamily (Hardwick *et al.*, 1987; Johnson *et al.*, 1990; Kimura *et al.*, 1989a and b). The inducibility of ω -hydroxylase activity in hamster liver microsomes (Lake *et al.*, 1989; Price *et al.*, 1992), together with the fact that hamster CYP4A gene(s) are induced by PPs (Figure 3.34), suggests that P450s encoded by these genes are responsible for this fatty acid oxidation.

Section 4.3.5 Evidence of mis-spliced CYP4A mRNA in MCP-treated hamster liver

While screening putative hamster cDNA clones for the presence of multiple CYP4A genes two clones (clone 5 and 12) showed different restriction patterns from the clones of groups A, B and C (Table 3.1). Clone 5 is derived from CYP4A17 but contains an extra 65bp sequence. Bestfit analysis of clone 5 with rat CYP4A1 cDNA places this extra sequence between exon 9 and 10 of CYP4A1 cDNA. This suggested the possibility that the mRNA from which clone 5 is derived is likely to be a mis-spliced variant of CYP4A17, i.e. the extra sequence starts in the exon 9/intron 10 boundary and ends at the intron 10/exon 10 boundary. Translation of clone 5 with all possible reading frames shows that premature termination of the protein sequence will occur and therefore the extra 65bp results in the open reading frame going out of frame. While the sequence of clone 5 shows 91% identity with CYP4A1, the extra 65bp sequence has 73% identity

(over 25bp) with intron 10 of the CYP4A1 sequence. Poor intron identity for corresponding gene positions in different species is expected since there is less functional constraint, and as a result less conservation of the nucleotide sequences is expected to occur during evolution (Van Den Berg *et al.*, 1978). On the evidence of this sequence analysis it is proposed that clone 5 is a mis-spliced derivative of the hamster CYP4A17 gene. Clone 12 is derived from the CYP4A19 gene but is shorter than the expected 510 bp nucleotides. Sequence comparison with rat CYP4A1 indicates that this missing sequence comprises 65 nucleotides, representing the whole of exon 10. It is proposed that clone 12 represents a mis-spliced mRNA derived from hamster CYP4A19 where the whole of exon 10 is missing.

It is not clear why CYP4A17 and 19 are being wrongly processed. For the cloning of hamster genes, the cDNA that was used for the amplification reactions was derived from MCP treated hamster liver RNA and it was subsequently shown that CYP4A17 is induced over 30-fold in the hamster liver following treatment with MCP (Figure 3.36). The removal of introns from pre-mRNA is catalysed by the spliceosome, a dynamic complex composed of numerous small nuclear RNA and protein components (Kramer, 1996). Splicing and 3' end processing appear to be rate limiting for the release of mRNA from the site of transcription (Custodio *et al.*, 1999). Thus it could be speculated that mis-splicing of CYP4A17 and 19 pre-mRNA into mature mRNA may be due to the constraints placed on the post-transcriptional processing machinery as a result of the high level of transcriptional induction of these genes. Spliceosome assembly occurs on each substrate pre-mRNA *de novo* and requires conserved recognition sequences located at the exon-intron boundaries. Mutated splice sites in MCAD (medium-chain acyl-CoA) genes, as with a number of other genes in disease conditions, have been found to result in exon skipping and intron insertion (Zhang *et al.*, 1992). To examine if any alteration has occurred at the intron-exon boundaries (especially around intron 10) in CYP4A genes, the genomic sequence of ham-

ster CYP4A is required.

A member of CYP2A gene subfamily (CYP2A7) has been found to be alternatively spliced in human liver (Ding *et al.*, 1995). This variant of CYP2A7 clone was shown to have the whole of exon 2 missing but contains a 10 bp sequence from intron 1, resulting in a truncated protein. Although in some human liver RNAs this aberrantly spliced P450 was the predominant species expressed, it is not known whether this may affect the functioning of the normal CYP2A7 protein. Alternative splicing of CYP2B6 has been reported (Miles *et al.*, 1990). Thus mis-splicing is a relatively common event in CYP RNA processing. In relation to the normal transcripts, the relative levels of CYP4A17 and 19 variants were not determined. However, they are expressed at much lower levels compared to the normal transcripts since these two variants were identified following screening of 50 initial PCR derived clones. If CYP4A induction by PPs is important in the mechanism of peroxisome proliferation then the relative expression of mis-spliced species may be relevant in species response to PPs. In the case of PPAR α , a truncated form of the receptor (lacking exon 6) has been detected in human liver (Palmer *et al.*, 1998; Roberts *et al.*, 1998; Gervois *et al.*, 1999) but this has not been reported in rodent species responsive to peroxisome proliferators (Gervois *et al.*, 1999). If the truncated PPAR α competes with wild-type PPAR α then it may have an important bearing on species response to peroxisome proliferators. It is interesting to note that so far there have only been reports of mis-spliced variants of PPAR α and CYP4A in non-responsive species and partially-responsive species (in this study), respectively. Whether this has any bearing on species response to peroxisome proliferators remains to be determined.

Section 4.3.6 Induction of hamster CYP4A by peroxisome proliferators

Induction of CYP4A1 precedes the induction of other genes, especially those of the peroxisomal β -oxidation pathway, during peroxisome proliferation (Bell *et al.*, 1991). The concomitant rise

in lauric acid hydroxylase activity in rat and mouse liver has been associated with an increase in dicarboxylic acids, metabolites of fatty acids that are ω -hydroxylated by the CYP4A proteins. Dicarboxylated fatty acids have been implicated in peroxisome proliferation. It has been postulated that CYP4A induction represents a primary event in peroxisome proliferation (Lock *et al.*, 1989), and therefore the level of CYP4A mRNA represents a good marker of peroxisome proliferation as it is easily measured and occurs as a primary event in the response to peroxisome proliferators. Hamsters have been described as partially responsive to PPs (Lake, 1995 and references therein). However, variable levels of induced ω -hydroxylase activity in the hamster liver microsome has been reported (Lake *et al.*, 1989; Price *et al.*, 1992). It is therefore not clear from enzymatic studies to what extent hepatic P4504A genes are induced by PPs. From enzymatic activity it is not possible to deduce whether this increase in activity is due to the activation of nascent protein, production of protein from stable mRNA pools, transcription of new mRNA, or indeed, if a CYP4A protein is involved. However, studies on rat show that treatment of PPs causes an increase in lauric acid hydroxylase activity in the liver (Kimura *et al.*, 1989) which is preceded by an increase in the amount of CYP4A mRNA. It could be speculated that in hamster liver the increase in lauric acid hydroxylase activity is similarly associated with increase in the level of CYP4A mRNA.

Expression and induction of CYP4A mRNA was investigated in RNA from MCP and Wy-14,643 treated male hamster liver. Constitutive expression of CYP4A17 was detectable in the hamster liver RNA using a CYP4A17 riboprobe (Figure 3.35). Following three consecutive days of treatment (25mg/kg), high level induction of CYP4A17 was observed in the liver by both MCP (21-fold) and Wy-14,643 (17-fold) (Figure 3.36). This level of induction at the mRNA level is much higher than the reported induction of lauric acid hydroxylase activity (Price *et al.*, 1992) by PPs. If the increase in enzymic activity is caused by the CYP4A17 level

then it is possible that differences between the induction of CYP4A17 mRNA and its protein activity are due to the better specificity of the RNase protection assay.

CYP4A genes in non-responsive species, such as guinea pig, have been shown to be non-inducible by PPs (Bell *et al.*, 1993) while over 1000-fold induction of *Cyp4a14* has been reported in mouse liver, a highly responsive species (Heng *et al.*, 1997). Therefore when compared with the level of induction of PP-induced CYP4A genes in other species, CYP4A17 in hamster shows an intermediate level of induction by PPs. Further, in this study CYP4A has also been shown to be highly inducible in rat hepatocyte culture (Figure 3.8) and mouse liver (Figure 3.17), and their level of induction is much higher than hamster CYP4A17.

Multiple members of the CYP4A subfamily have been identified in rats and mice, and some of them are expressed in a tissue specific manner while others are regulated in a sex specific manner. For example, rat CYP4A1 and 3 are expressed at low constitutive levels in liver and kidney and are highly induced in the liver by PPs. CYP4A2 on the other hand is expressed at low levels in the liver but at a higher level in the male kidney and is induced by PPs. In female rats, CYP4A2 is undetectable. It would be interesting to see if hamster CYP4A genes show similar tissue specific expression especially in liver and kidney and if any such genes are regulated in a sex specific manner.

Section 4.4 Cloning of hamster PPAR α .

The response of hamster to peroxisome proliferators suggests that hamster is likely to have expressed and functional PPAR α . To study the level of expression of hamster PPAR α (hmPPAR α) on a comparative basis with other responsive and non-responsive species, cloning of hmPPAR α was undertaken. By aligning rat, mouse, human, guinea pig and *Xenopus* PPAR α amino acid sequences forward (HMppar-P1) and reverse (HMppar-P2) primers, representing DNA-binding domain and C-terminal end respectively, were designed from regions of absolute

identity. Using these primers, a fragment of around 1.2kb long was amplified from hamster liver cDNA derived from total RNA (Figure 3.38). Analysis of the complete double strand DNA sequence of this fragment confirmed that a partial hmPPAR α cDNA of 1069bp had been cloned. In order to clone the remaining 5'-end of the PPAR α cDNA, a 5'-rapid amplification of cDNA ends (RACE) system was used. Using gene specific primers and universal amplification primers several 5'-cDNA fragments were amplified (Figure 3.39). Several independent clones derived from the amplified cDNA fragment were sequenced. One of the clones was found to contain the full-length of the 5'-cDNA end that includes the initiation codon, while two other clones were found to contain most but not all of the 5'-cDNA end, terminating about 100bp from the putative initiation codon (Figure 3.41).

Section 4.4.1 Sequence analysis of hamster PPAR α .

The complete cDNA sequence of putative hmPPAR α , like rat and mouse PPAR α cDNA, is 1404bp long. The predicted molecular weight of this 468 amino acid hmPPAR α was determined to be 52.4 kDa with an isoelectric point of 6.95. Comparison of the hmPPAR α protein sequence with other known PPAR α shows that it has high similarity to rat (97% identity) and mouse (96%) PPAR α and has 95% identity to human and guinea pig PPAR α . The high similarity of putative hmPPAR α with other PPAR α from different species, and the lower similarity (70%) to PPAR β and γ isoforms shows that the cloned cDNA is a PPAR α isoform. This finding is further supported by a detailed modular domain comparison of known PPAR α , β and γ sequences with that of hmPPAR α (Table 3.5). The DBD of hmPPAR α is identical to rat PPAR α and has very high identity (98%) to mouse, human and guinea pig PPAR α . The corresponding amino acid sequence of PPAR β and γ isoforms has much less similarity to the PPAR α isoform. A characteristic feature of PPAR receptors, which places them as a distinct subfamily from other steroid hormone receptors, is that PPARs have only three amino acids in the D box of the zinc finger of the DNA binding domain while others have five amino acids in the D box (Laudet *et*

al., 1992; Motojima *et al.*, 1993). The identity of hmPPAR α with other PPAR member in the D box region provides further evidence that the cloned hamster cDNA is a member of the PPAR subfamily. Although α and γ overlap for some ligand/activator, both receptors have distinct high specificity ligands, a feature which is reflected in their LBD regions that share much lower identity (69%). The LBD of hmPPAR α is almost identical (99%) to the rat and mouse PPAR α LBD sequences, which provides strong evidence that the cloned cDNA is PPAR α isoform.

The hinge domain and the A/B domain of PPAR α are less conserved and show the greatest amount of variation between receptors from different species. A similar trend is observed when hmPPAR α is compared with PPAR α from other species, i.e. the DBD and LBD region show high levels of similarity while the hinge and A/B domain share much lower similarity.

Alignment of hamster amino acid sequence with rat, mouse, hamster and guinea pig has identified a number of amino acid positions where the hamster sequence differs from human and guinea pig (Figure 3.43). The importance of conservation of key amino acids in the functioning PPAR α has been reported by cloning of a naturally occurring variant form of PPAR α from human liver, termed hPPAR α -6/29 (Tugwood *et al.*, 1996). This human receptor has a number of amino acid changes from published hPPAR α sequences, including a threonine to methionine change at position 71, a lysine to methionine change at position 123 and a valine to alanine change at position 444. Although this human variant is able to bind to a PPRE, it is unable to transcriptionally activate PPRE-regulated reporter gene in response to PPs (Roberts *et al.*, 1998). Further, hPPAR α -6/29 can act as dominant negative regulator of mouse PPAR α -mediated transcription *in vitro* and prevent PP-induced suppression of apoptosis in rat primary hepatocytes. Myers *et al.* (1997) found that restoration of methionine 123 and alanine 444 in hPPAR α -6/29 to the wild-type amino acids restored PP-induced trans-activation. However, these amino acid polymorphisms are not present in hmPPAR α .

A change in the charge properties of hmPPAR α has been found at amino acid position 196 in r/mPPAR α , where a positively charged lysine is replaced by a negatively charged glutamic acid in hmPPAR α while a negatively charged glutamic acid at 264 of r/mPPAR α is replaced by the polar uncharged group glutamate in hmPPAR α (Figure 3.43). Changes in charge properties may affect the tertiary structure of the receptor and may have important consequences in its functioning. For example, changes in tertiary structure may affect the interaction of PPAR α with other proteins such as its heterodimerisation partner RXR α or proteins of the transcription machinery or coactivators. Alteration of a single amino acid at position 282 of mPPAR α (glutamate to glycine) has been found to alter the trans-activation ability of this receptor in response to PPs (Hsu *et al.*, 1995; Muerhoff *et al.*, 1992). This glutamate to glycine substitution in mPPAR α (mPPAR $\alpha^{\text{G-mut}}$) does not effect its binding to PPRE but, unlike the wild-type receptor, it displayed lower intrinsic transactivation (in the absence of added PPs) in a reporter assay. This difference in transactivation may be due to the lower affinity of G-mutant receptor for endogenous ligands since the mPPAR $\alpha^{\text{G-mut}}$ displayed higher EC50s for prixinic acid and eicosatetraenoic acid than the wild-type mPPAR α (Hsu *et al.*, 1995).

Comparison of all available PPAR α sequences shows that, unlike rat, mouse and human PPAR α , guinea pig PPAR α has a single amino acid deletion at position 448 which lies in the ligand binding domain. This loss of a charged group may affect ligand binding by the receptor (weaker interaction) as well as changes in transactivation resulting in weaker interactions with other proteins in the transcriptional complex. Investigation into mPPAR α function has found that the last C-terminal 20 amino acids are not necessary for heterodimerisation with RXR α but could add to the stability of the heterodimeric complex when bound to DNA (Dowell *et al.*, 1997). Since only guinea pig PPAR α has this lysine deletion residing within the C-terminal region it is likely that such a deletion may affect gpPPAR α rather than rat, mouse, human or hamster PPAR α .

Section 4.4.2 Hamster PPAR α function

Cloning of full-length PPAR α cDNA from total hamster liver RNA demonstrates that hamster expresses PPAR α in liver. However, this does not demonstrate that hamster has functional PPAR α . Following the cloning of PPAR α from other species, transcriptional activation of a reporter gene (e.g. luciferase) containing a PPRE response element in its promoter region has been used to demonstrate PPAR α functionality *in vitro* (Bell *et al.*, 1998). However, in the absence of functional studies for the cloned hamster PPAR α , several lines of evidence suggest that hamster has a functional PPAR α . Hypolipidaemic actions of PPs have been observed in hamster where MCP and Wy-14,643 have been found to lower blood lipid and cholesterol levels (Choudhury *et al.*, 2000). Since knock-out studies demonstrate that the hypolipidaemic action of PPs is mediated by PPAR α in mice and is associated with peroxisome proliferation (Peters *et al.*, 1997), it is likely that the observed PP-induced hypolipidaemia in hamster is also mediated by PPAR α . Induction of *Cyp4a10* and *14* transcription and their enzymic activities has been shown to be highly induced in mouse liver by PP treatment (Bell *et al.*, 1993; Heng *et al.*, 1997), which is again mediated by PPAR α since mouse lacking functional PPAR α are resistant to this effect (Barclay *et al.*, 1999). An increase in lauric acid ω -hydroxylase activity has been observed in hamster liver treated with PPs (Lake *et al.*, 1989; Price *et al.*, 1992). Rat CYP4A1 has been shown to encode this enzymic activity (Hardwick *et al.*, 1987; Kimura *et al.*, 1989), suggesting that the PP-induced ω -hydroxylase activity in hamster liver is due to the induction of CYP4A. In this study (Figure 3.36) CYP4A transcriptional induction by PPs has been demonstrated in hamster liver. Finally, peroxisome proliferation has been observed in hamster liver (Gray *et al.*, 1984; Lake *et al.*, 1986), an effect that require functional PPAR α (Lee *et al.*, 1990). These lines of evidence together indicate that hamster is likely to have a functional PPAR α .

Section 4.4.3 Molecular phylogeny of PPAR α genes

A molecular phylogenetic tree of all known PPAR α was constructed to gain insight into the

evolution of hamster PPAR α in relation to rat, mouse, human and guinea pig PPAR α . The tree was constructed using the maximum likelihood method: since there is evidence that orthologous genes for rodents evolve faster than man (Wu and Li, 1985), it was important to choose a method for phylogenetic analysis which is robust to genes evolving at different rates. Thus, for phylogenetic inferences based on a small data set, maximum likelihood is the method of choice since it has solid statistical background and maximum-parsimony method has been found to behave badly in some situations (Felsenstein, 1978; Hasegawa and Fujiware, 1993). In this study clustalW (NJ method) has been found to give a different tree as it can not take account of the rapid evolution of the guinea pig (data not shown).

Alignment of mammalian PPAR α protein sequences was done in tandem with evolutionarily distant *Xenopus* PPAR α , and mouse PPAR β and γ as well. PPAR γ and β were included in the analysis as they are related to PPAR α but have diverged early in evolution. Therefore PPAR γ and β were used as out groups to root the analysis and give it phylogenetic perspective. The phylogenetic tree presented in Figure 3.44 shows that rat, mouse and hamster form a clade where hamster has branched off first from the muroid lineage (i.e. diverged early in evolution from rat and mouse) but the rate of evolution is small as shown by the branch length. Guinea pig diverged before the branching of hamster and rat-like rodents and guinea pig PPAR α between human (primate) and other members of rodentia family (rat, mouse and hamster). A similar branching order of rat, mouse, human, hamster and guinea pig has been observed with the 11- β hydroxylase gene using neighbour-joining method (Bulow *et al.*, 1996), and with α -1 antiproteinase (Nakatani *et al.*, 1995). Figure 3.44 demonstrates that mouse, rat, hamster and guinea pig form a clade after early splitting from human lineage. From the molecular evolutionary point of view, the guinea pig is unique among mammals, since a number of proteins such as insulin, lipoprotein lipase and glucagon have evolved several fold faster than their respective ortholo-

gous proteins in other mammals (Li *et al.*, 1992). Comparison of the branch lengths indicates that guinea pig PPAR α is also evolving more rapidly than human, mouse or rat PPAR α genes.

The phylogenetic position of guinea pig is rather controversial. Traditional views of the phylogenetic relationship of caviomorph and myomorph forming a rodentia clade (monophyla) is based on comparative morphology (Luckell and Haortaby 1985). However, biochemical comparisons suggest that guinea pig is distant from other rodents (Nogachi *et al.*, 1994), and on the basis of molecular phylogenetic analysis of a number of proteins, Graur *et al.* (1991) suggested that the mammalian order rodentia is polyphyletic and guinea pig-like rodents may be an out-group with evolutionary origin separate from that of rat-like rodents. However, using maximum-likelihood method of analysis (as opposed to maximum-parsimony by Graur), Cao *et al.* (1994) and Kuma and Miyata (1994) re-examined the same phylogeny and demonstrated weakness in the analysis of Graur and coworkers. Further, phylogenetic analysis of partial mitochondrial DNA using several method of analysis shows strong support for rodent monophyly (Frye and Hedge, 1995). Recently, however, D'Erica and coworkers (1996) have challenged the traditional view of rodent monophyly using complete guinea pig mitochondrial genome in their analysis, which supports rodent polyphyly and places guinea pig closer to lagomorph (rabbit)/primates than to myomorphs. Although their tree was supported by all three major methods of protein phylogeny (i.e ML, MP and NJ), the statistical significance of the ML tree was not evaluated as pointed out by Cao *et al.* (1997). On the basis of these lines of evidence, rodent monophyly could not be dismissed and inclusion of a larger gene database in the phylogeny may provide a better answer.

Section 4.4.4 Hepatic expression of PPAR α in species with differing responses to PPs

In view of the finding that functional PPAR α is present in both species responsive and non-responsive to peroxisome proliferators and since PPAR α is non-inducible by PPs, it was suggest-

ed that their differing responses may be due to the relative level of PPAR α present in the liver. That is, quantitative differences in PPAR α levels may be responsible for species responsiveness to peroxisome proliferators. Although previous studies have reported low levels of PPAR α transcript in guinea pig liver as compared to higher in mouse liver (Palmer *et al.*, 1998; Tugwood *et al.*, 1998), there is no direct comparison with hamster. In the absence of a specific hamster PPAR α probe it was not possible to compare the level of hepatic PPAR α transcript in various species. Following the cloning of hmPPAR α cDNA it was possible for the first time to investigate the expression of PPAR α mRNA level in the livers of different species displaying varying levels of response to peroxisome proliferators. As shown in Figure 3.46, PPAR α mRNA is constitutively expressed in the liver of mouse, hamster and guinea pig. Mouse has a higher level of expressed PPAR α mRNA than hamster and guinea pig, and guinea pig has the lowest level, as shown quantitatively in Figure 3.47. Hamster has an intermediate level of PPAR α i.e. higher than guinea pig but lower than mouse. Thus, these data demonstrate that the level of expressed PPAR α transcript in the liver correlates well with the species sensitivity to PPs; high levels of expression are found in the highly responsive species mouse, intermediate levels in the partially responsive species hamster and low levels in the non-responsive species guinea pig.

In reporter assays (using the minimal rat Acyl-CoA PPRE) human, mouse and guinea pig PPAR α have been found to have comparable trans-activation abilities in liver cells. In human, in addition to functional PPAR α , another inactive variant has been cloned from hepatic cDNA. Therefore, in human at least, the quantity of functional PPAR α may be a critical factor in determining species responsiveness since the active pool of PPAR α may be depleted due to expression of an inactive competing form. Recently it has been observed that over expression of both human and guinea pig PPAR α (transient transfection) results in increased activity of cyanide-insensitive palmitoyl-CoA oxidation in guinea pig hepatocytes to levels similar to those

from transfected mouse PPAR α in the same system (MacDonald *et al.*, 1999), suggesting that the quantity of PPAR α may play a significant role in the lack of response to PPs especially in guinea pigs. It remains to be seen if transfected gpPPAR α is also able to induce CYP4A13 mRNA and peroxisome proliferation in guinea pig primary hepatocytes, given that induction of CYP4A is highly induced in responsive species by PPs.

Compared to other tissues, PPAR α is highly expressed in the liver where PPs have their greatest effects (Jones *et al.*, 1995; Braissant *et al.*, 1996). Studies on rat and mouse demonstrated that PPAR α is the predominating subtype present in the liver with β and γ present at very low levels (Jones *et al.*, 1995). Although knock-out studies demonstrated that the process of peroxisome proliferation is mediated by PPAR α , the relative amounts of other subtypes in the liver may be an important determinant in species responsiveness to PPs. For example, Kliewer and coworkers (1994) have shown that, like PPAR α , β and γ are also capable of heterodimerisation with RXRa and coexpression of α with either β or γ has resulted in repression of PPAR α -mediated transactivation (Klewer *et al.*, 1994; Jow and Mukerjee *et al.*, 1995). Thus, in addition to lower levels of PPAR α , higher levels of either γ or β or both relative to α may be present in species that are less sensitive to PPs. If such is the case then this may also be responsible for observed species differences in peroxisome proliferation. Therefore the relative levels of all isoforms need to be determined in responsive and non-responsive species.

PPAR α 's ability to mediate peroxisome proliferation may assume greater significance when comparing between responsive and non-responsive species. Keller *et al.* (1997) found that by changing a number of amino acids in the ligand binding domain of human PPAR α to the corresponding sequence of mouse PPAR α resulted in a transactivation profile similar to mPPAR α when induced by Wy-14,643 in a reporter assay. In addition, substitution of critical amino acid(s) in PPAR α has been found to give either weaker (Shu *et al.*, 1995) or no transactivation of

PPRE-regulated reporter genes even though these PPAR α s are capable of binding to the PPRE as heterodimers with RXR α . Since PPAR α sequences differ between responsive and non-responsive species, such differences in critical amino acids may result in weaker interaction and/or functioning of PPAR α in non-responsive species. However, *trans*-activation assays reveal no apparent difference in the ability to drive ligand-dependent gene activation between PPAR α from different species.

The nature of the PPRE may also be responsible for species differences in peroxisome proliferation. Human Acyl-CoA oxidase gene contains an inactive PPRE in its promoter region (Woodyatt *et al.*, 1999) as opposed to an active PPRE in rat (Tugwood *et al.*, 1992). Differences in PPRE sequence between rat and human apolipoprotein A-I gene is also responsible for species-specific regulation of their expression where, in contrast to rat, human apo-PPRE is active and is inducible by fibrates. In addition, the repression of rat apo-PPRE was characterized to be due to the presence of a negative regulatory element close to PPRE that are regulated by RevRa. This type of receptor cross-talk may have influence on PPAR α functioning in the case of HNF4 and COUP-TF. HNF4, a liver enriched transcription factor, is able to bind the rat Acyl-CoA PPRE and suppress PP-dependent gene activation (Nishiyama *et al.*, 1998).

Having found an inactive PPRE in Acyl-CoA genes, encoding an enzyme highly induced during peroxisome proliferation, it will be interesting to see if other PP-responsive genes in human have active PPRE. It may be that PPAR α regulated genes in humans that are relevant to peroxisome proliferation have lost (or inactivated) their functional PPREs whereas those relevant for hypolipidaemic actions have retained them. If this is the case then it would easily explain why PPs induce hypolipidaemia and at the same time do not promote peroxisome proliferation in humans and guinea pigs. Therefore a better understanding of the promoter regions (including PPREs) of all PP-responsive genes in human is important and completion of human genome

project will provide some insight into whether such genes contain PPREs in their promoter region. Thus it seems that species responsiveness to peroxisome proliferation is a complex process which may be an interplay between a number of factors including the nature of the response element (PPRE), qualitative and quantitative differences in PPAR α , and the presence of cross-talking proteins (receptors and coactivators) in the liver.

Section 4.5 Distribution of PPAR α and interacting coactivator proteins

Within the liver lobule or acinus, the functional unit of liver, a number of metabolic functions have been found to be distributed in a gradient manner which may be a reflection of their metabolic activity (Oinonen and Lindros, 1998). Zonation of some functions is confined mainly to the periportal cells while others are restricted to the centrilobular region of the acini. The effects of PPs are also known to be expressed differentially across the liver lobule: PP-induced DNA synthesis occurs predominantly in the periportal region of the liver lobule (Barrass *et al.*, 1993) whereas induction of CYP4A1 and acyl-CoA oxidase occurs in the perivenous region. Since the expression of PPAR α was determined using RNA extracted from homogenised liver tissue it is not known if PPAR α expression is restricted to certain populations of hepatocytes (region-specific distribution). Distribution of PPAR α transcripts was determined in the liver of both control and MCP-treated mice, and was found to be homogenous through out the liver lobule and was unaffected by MCP treatment (Figure 3.55). This lack of association between PPAR α expression and the regional distribution of peroxisome proliferation events suggests that cell specific factors may be involved in PPAR α -mediated effects such as induction of DNA synthesis or CYP4A by PPs in distinct regions of the liver acini.

Coactivator proteins are important in the functional association between nuclear receptors and general transcription machinery, and their presence has been found to modulate receptor activity (Chakravarti *et al.*, 1996). This integrator function for a number of coactivator proteins has

been found to enhance the transcriptional activity of PPAR α as well as other nuclear receptors (Dowell *et al.*, 1997; Zhu *et al.*, 1997). Although no specific coactivators for PPAR α have been identified, there is a possibility that some of these general coactivators may influence PPAR α function in the liver and their high level expression and co-localisation with PPAR α in responsive species may be the determining factor in species response to PPs. Distribution of mRNAs encoding a panel of coactivators that are known to interact with PPAR α has been studied in the liver of control and MCP treated mice. Coactivator protein PBP was identified using PPAR γ as a bait in yeast two-hybrid assay (Zhu *et al.*, 1997) and was found to be expressed in the liver. In this study, compared to other studied coactivators, PBP was found to be the most abundantly expressed coactivator. However, as with PPAR α , its distribution is not confined to a particular region of the liver acini i.e. uniform distribution. Expression of both CBP/p300 and SRC-1 was found to be low compared to PBP and did not show region-specific distribution. Recently knock-out studies demonstrated that SRC-1 is not essential for PPAR α -regulated gene expression and indeed the whole process of peroxisome proliferation (Qui *et al.*, 1999). It will be interesting to see how the disruption of PBP gene effects PPAR α functioning given that PBP is the most abundantly expressed coactivator amongst those studied here. Expression of RIP-140 and PGC-1 was undetectable in the liver, and like PBP, SRC-1 and CBP/p300, their expression was unaffected by MCP treatment. Although MCP shows no effect at the mRNA level, the possibility that it could affect coactivator expression post-transcriptionally cannot be ruled out. Previous studies found that PGC-1 is undetectable in the mouse liver but expressed in heart, kidney, brain and brown fat, and is highly induced in the brown fat following cold exposure of mouse (Puigserver *et al.*, 1998). PGC-1 has been shown to interact with PPAR γ but there is no report of whether it also can interact with PPAR α . Given that PGC-1 is not expressed in the liver even after PP treatment it is unlikely that this coactivator is physiologically important in the function of PPAR α . RIP-140 has been found to be expressed in a number of cell lines including the liver

derived HepG2 using Northern analysis (Cavailles *et al.*, 1995). The failure to detect this coactivator in the liver sections may be due to its low abundance and lack of sensitivity of the *in situ* hybridisation techniques. Although a number of coactivators are known to interact with and enhance the transcriptional activity of PPAR α *in vitro*, their biological significance in PPAR α functioning and in peroxisome proliferation has yet to be determined.

Section 4.6 Heterologous expression and purification of mPPAR α -LBD

PPAR α is a ligand-dependent transcription factor, and like other nuclear receptor-family displays a modular structure including a central DBD and a carboxy terminal domain that mediates ligand binding, dimerisation and transactivation functions. Ligand-dependent transcription requires a highly conserved motif, termed activating function-2 (AF-2), located at the C-terminus of the LBD (Evans *et al.*, 1988). The structure of the LBD of RXR α , RAR γ , TR and ER has been solved (Bourguet *et al.*, 1995; Wagner *et al.*, 1995; Renaud *et al.*, 1995; Brzozowski *et al.*, 1997), and has provided evidence of their high degree of conformational similarity and identified regions involved in ligand binding and transactivation functions. Recently the crystal structure of PPAR γ LBD has been solved, providing important insights into the functioning of the receptor (Nolte *et al.*, 1998). For example, the structure revealed a large binding pocket which may explain the diversity of ligands for γ , and also glutamate and lysine residues are found to form a 'charge clamp' that are involved in the interaction of coactivator proteins. To understand how these various functions of the PPAR α -LBD operate and interact at molecular level requires both functional and structural analysis. Therefore purification of functional PPAR α -LBD will be useful to study the structural and functional aspects of this domain.

PPAR α -LBD was expressed from prokaryotic expression vector pET5b in BL21 (DE3)pLysS cells. A stretch of six histidine residues was placed at one end of the LBD so that the expressed protein can be purified by one step affinity chromatography on Ni²⁺ containing resins. As well

as wild-type LBD (PPAR α -LBD^{wt}) a mutant form of the protein, termed G-mutant (PPAR α -LBD^{G-mut}) was also expressed from pET5b vector. Both wild-type and G-mutant LBD proteins were inducible by IPTG (Figure 3.48), however almost all of the induced proteins were found in the insoluble fraction when induced at 37 °C (Figure 3.49 A and B). To increase the solubility of the induced protein, effects of IPTG concentration and growth temperature of the culture were investigated. Altering the growth temperature of the culture may affect the physicochemical properties of the induced protein such that low temperature may increase the fraction of soluble protein. Figure 3.49 shows that induction at lower temperature (25 °C) marginally increased the solubility of the induced protein. LBD of PPAR γ has been expressed similarly from pRSET vector transformed in BL21(DE3) cells (Nolte *et al.*, 1998). IPTG concentration of 0.5mM also marginally improved the solubility of the induced protein cultured at 25 °C (Figure 3.50). The soluble fraction of his-tagged LBD protein was purified successfully using Ni²⁺ containing resin (Figure 3.51). SDS-PAGE shows that a single purified band of expected size (~30kDa) was eluted from the column. A single band of expected molecular size was also detected in Western blotting analysis using a polyclonal rabbit anti-mouse PPAR α antibody (Figure 3.52). Thus, using affinity chromatography, soluble his-tagged PPAR α -LBD (wild-type and G-mutant) were purified. For further purification of the LBD, eluted proteins were dialysed to remove imidazole and then FPLC purified using a Econ-S column (Pharmacia). A single peak (of protein) was eluted from the FPLC run as shown in the chromatogram (Figure 3.53). Although the identity of this peak was not further characterised, the presence of a single peak suggest that it is likely to be LBD protein. To demonstrate that the purified LBD protein is still functionally active, ligand binding studies could be performed with high-affinity radiolabelled ligand a in classical ligand binding assay (Kliwer *et al.*, 1997) or a scintillation proximity assay (Nichols *et al.*, 1998).

Functionally active PPAR α -LBD in pure form could be utilised to study the structure and function of this domain. In addition to solving crystal structure, LBD protein could be used to search for a *bona fide* cellular ligand using recently identified high-affinity ligands (with K_d in the nanomolar range) that have been shown to bind and activate PPAR α but are not themselves true physiological ligands (Forman *et al.*, 1997; Kliewer *et al.*, 1997; Devchand *et al.*, 1996). Yeast two-hybrid assays have been used to identify cofactors (such as PBP, SRC-1 and PGC-1) for PPAR receptors using PPAR γ as a bait (Zhu *et al.*, 1996 and 1997; Puigserver *et al.*, 1998). However, these coactivators have also been shown to interact with other nuclear receptors, including PPAR α , and, therefore, may represent coactivators for the steroid receptor family in general. PPAR α -LBD protein could be used to search for a novel, specific coactivator(s) in nuclear pull-down assay (protein-protein interaction assay or far-Western blot). This may be a better approach since the LBD region differs considerably between all three PPAR isoforms, and inclusion of a mutant receptor LBD in the assay may aid in assessing the potential significance of any interactions. Also, coactivators have been found to contain the signature motif LXXLL (where L is leucine and X is any amino acids) that specifically interact with nuclear receptors via the LBD. RIP-140 has been isolated as an ER interacting protein using the ER-hormone binding domain in nuclear pull-down assay (Cavailles *et al.*, 1994).

Section 4.7 Conclusions

The pleiotropic effects of PPs are mediated by PPAR α as demonstrated by global PPAR α knock-out studies. Since PPAR α is expressed in species both responsive and non-responsive to PPs, it is likely that the functional activity of PPAR α may play a significant role in determining species response. In the present study, primary hepatocyte culture has been used as an investigative tool to examine the functionality of PPAR α from different species. Although rat hepatocytes were found to be responsive to PPs, their usefulness for studying of the effects of added PPAR α (exogenous) is hampered by the presence of endogenous level of PPAR α protein.

Hepatocytes from PPAR α knock-out mice has been used to overcome this problem, since they lack any background activity of PPAR α . This hepatocyte system clearly demonstrates that the transcriptional induction of *Cyp4a* genes require PPAR α . However, addition of PPAR α back into the system did not result in the induction of endogenous *Cyp4a* marker genes. This may be a consequence of gene silencing effects which may have occurred in the absence of PPAR α during development. Examining the promoter activity of *Cyp4a* in PPAR α wild-type and knock-out mice-for example, by locating DNaseI hypersensitive sites- may provide a clue as to whether this is the case. The PPAR α knock-out has been generated by disruption of the protein's ligand binding domain, and, therefore, truncated PPAR α is still present in the cell. Since these truncated proteins possess DNA binding domain, it is possible that they may act as a dominant negative manner by binding to PPRE elements in the promoters of the PP-responsive genes such as *Cyp4a*. This type of interference may explain why the addition of full-length mouse PPAR α back into the hepatocytes of knock-out mice did not induce *Cyp4a* mRNA in the presence of PPs. This could be demonstrated by binding of nuclear proteins, isolated from knock-out hepatocytes, to PPRE using electromobility gel shift and supershift assays.

In this study, level of hepatic PPAR α transcripts has been found to correlate with species sensitivity to PPs, where high levels were associated with responsive species and lower levels with non-responsive species. However, the relative levels of other PPAR α isoforms in the liver may also be an important determinant factor of species response to PPs, since there is evidence that both PPAR β and γ represses PPAR α activity *in vitro*. Therefore, it is important to determine the relative levels of all three isoforms in the livers of both responsive and non-responsive species. In addition, an improved understanding of such complex receptor "cross-talk" may be achieved through the generation of tissue specific knock-outs of these isoforms, and assessing their contribution to PPAR α -mediated peroxisome proliferation.

Investigation of hamster response to PPs demonstrated the presence of expressed PPAR α and PPAR α -responsive CYP4A genes in the liver; both the hepatic PPAR α level and the inducibility of CYP4A correlate well with hamster's partial responsiveness to PPs. The presence of multiple CYP4A genes in rat, mouse and hamster, and the selective induction of some of these genes in the liver by PPs, together suggest that the induction of these genes may be important in the process of peroxisome proliferation. Regulatory regions of these and other PP-responsive genes are mainly studied in rat and, and it is therefore important to understand the nature of the response elements of the corresponding genes in other species such as mouse, hamster and guinea pig. Constitutive and tissue-specific expression patterns vary between the CYP4A genes, and therefore it is likely that they may have different physiological functions. For example, renal CYP4A has been implicated in inflammation and maintenance of vascular tone. Therefore greater understanding of the catalytic functions of their protein products is required. In future studies, generation of knock-out mice for these genes will be important to delineate their role in tissue physiology.

As well as the level of PPAR α activity, there may be other factors that determine species response to PPs. Therefore it is necessary to explore other possibilities such as factors affecting the PPAR α trans-activating function as well as PPAR α expression. In the latter case, PPAR α expression has been shown to be hormonally regulated but was largely unaffected by PP treatment, as shown in this study. A number of coactivators have been shown to enhance PPAR α activity but so far no specific coactivator has been implicated as critical for PPAR α function or peroxisome proliferation. Therefore, it is still possible that specific coactivator(s), as yet unidentified, may exist for PPAR α which could be critical determinants of species response to PPs. The PPAR α ligand binding domain purified in this study should serve as a useful bait for the isolation of any novel coactivator(s) of PPAR α in protein-protein interaction studies.

Finally, there remains the problem of clarifying the exact mechanism by which treatment with PPs in rodents results in peroxisome proliferation and ultimately in liver cancer. There may be further, as yet uncharacterised, molecular components that could be critical for species sensitivity to PPs. Using microarray technology, the expression pattern of genes in the liver of both PPAR α wild-type and knock-out (treated with and without PPs) should identify target genes (both novel and previously characterised) that may be implicated in peroxisome proliferation.

Chapter 5 References

Akam, M. (1987). The molecular basis for metamerism in the *Drosophila* embryo. *Development* **101** : 1-22.

Aldridge, T.C., Tugwood, J.D. and Green, S. (1995). Identification and characterization of DNA elements implicated in the regulation of the CYP4A1 transcription. *Biochemical Journal* **306** : 473-479.

Amri, E.Z., Bonino, F., Aihaud, G., Abumrad, N.A. and Grimaldi, P.A. (1995). Cloning of a protein that mediates transcriptional effects of fatty acids in preadipocytes. *Journal of Biological Chemistry* **270** (5) : 2367-2371.

Aoyama, T., Hardwick, J.P., Imaoka, S., Funae, Y., Gelboin, H.V. and Gonzalez, F.J. (1990). Clofibrate-inducible rat hepatic P450s IVA1 and IVA3 catalyze the ω - and (ω -1)-hydroxylation of fatty acids and the ω -hydroxylation of prostaglandins E1 and F2a. *Journal of Lipid Research* **31** : 1477-1481.

Aoyama, T., Peters, J.M., Iritani, N., Nakajima, T., Furihata, K., Hashimoto, T. and Gonzalez, F.J. (1998). Altered constitutive expression of fatty acid-metabolizing enzymes in mice lacking the peroxisome proliferator-activated receptor- α (PPAR α). *Journal of Biological Chemistry* **273** (10) : 5678-5684.

Aperlo, C., Pognonec, P., Saladin, R., Auwerx, J. and Boulukos, K.E. (1995). cDNA cloning and characterization of the transcriptional activities of the hamster peroxisome proliferator-activated receptor haPPAR γ . *Gene* **162** : 297-302.

Arany, Z., Sellers, W.R., Livingston, D.M. and Eckner, R. (1994). E1A-associated p300 and

CREB-associated CBP belong to a conserved family of coactivators. *Cell* **77** (6) : 799-800.

Ashby, J., Brady, A., Elcombe, C.R., Elliott, B.M., Ishmael, J., Odum, J., Tugwood, J. and Purchase, I.F.H. (1994). Mechanistically based human hazard assessment of peroxisome proliferator induced hepatocarcinogenesis. *Human and Experimental Toxicology* **13** (suppl.2) : S19-S33.

Auwerx, J., Schoonjans, K., Fruchart, J.C., Staels, B. (1996). Transcriptional control of triglyceride metabolism: Fibrates and fatty acids change the expression of the LPL and apo C-III genes by activating the nuclear receptor PPAR. *Atherosclerosis* **124** : S29-S37.

Baes, M., Castelein, H., Desmet, L. and Declercq, P.E. (1995). Agonism of COUP-TF and PPAR α /RXR α on the activation of the malic enzyme gene promoter: modulation by 9-*cis* RA. *Biochemical and Biophysical Research Communications* **215** (1) : 338-345.

Barclay, T.B., Peters, J.M., Sewer, M.B., Ferrari, L., Gonzalez, F.J. and Morgan, E.T. (1999). Modulation of cytochrome P-450 gene expression in endotoxemic mice is tissue specific and peroxisome proliferator-activated receptor- α dependent. *Journal of Pharmacology and Experimental Therapeutics* **290** (3) : 1250-1257.

Bardot, O., Aldridge, T.C., Latruffe, N. and Green, S. (1993). PPAR-RXR heterodimer activates a peroxisome proliferator response element upstream of the bifunctional enzyme gene. *Biochemical and Biophysical Research Communications* **192** (1) : 37-45.

Barettino, D., Vivanco Ruiz, M.M. and Stunnenberg, H.G. (1994). Characterisation of the ligand-dependent transactivation domain of thyroid-hormone receptor. *EMBO Journal* **13** (13) : 3039-3049.

Barrass, N.C., Price, R.J., Lake, B.G. and Orton, T.C. (1993). Comparison of the acute and

chronic mitogenic effects of the peroxisome proliferators methylclofenapate and clofibric acid in rat liver. *Carcinogenesis* **14** (7) : 1451-1456.

Baudhuin, P., Beaufay, H. and De Duve, C. (1965). *Journal of Cell Biology* **26** : 219-43.

Baumgart, E., Volkl, A., Pill, J. and Fahimi, H.D. (1990). Proliferation of peroxisomes without simultaneous induction of the peroxisomal fatty acid β -oxidation. *FEBS Letters* **264** (1) : 5-9.

Bayly, A.C., French, N.J., Dive, C. and Roberts, R.A. (1993). Nongenotoxic hepatocarcinogenesis *in vitro* - the FaO hepatoma line responds to peroxisome proliferators and retains the ability to undergo apoptosis. *Journal of Cell Science* **104** (2) : 307-315.

Bayly, A.C., Roberts, R.A. and Dive, C. (1994). Suppression of liver cell apoptosis *in vitro* by the nongenotoxic hepatocarcinogen and peroxisome proliferator nafenopin. *Journal of Cell Biology* **125** (1) : 197-203.

Bell, A.R., Saovory, R., Horley, N.J., Choudhury, A.I., Dickens, M., Gray, T.J.B., Salter, A.M. and Bell, D.R. (1998). Molecular basis of non-responsiveness to peroxisome proliferators: the guinea pig PPAR α is functional and mediates peroxisome proliferator-induced hypolipidaemia. *Biochemical Journal* **332** : 689-693.

Bell, D.R. and Elcombe, C.R. (1991). Induction of acyl-CoA oxidase and cytochrome P450IVA1 RNA in rat primary hepatocyte culture by peroxisome proliferators. *Biochemical Journal* **280** (1) : 249-253.

Bell, D.R., Bars, R.G. and Elcombe, C.R. (1992). Differential tissue-specific expression and induction of cytochrome P450 4A1 and acyl-CoA oxidase. *European Journal of Biochemistry* **206** (3) : 979-986.

Bell, D.R., Bars, R.G., Gibson, G.G. and Elcombe, C.R. (1991). Localization and differential induction of cytochrome P450IVA and acyl-CoA oxidase in rat liver. *Biochemistry Journal* **275** : 247-252.

Bell, D.R., Plant, N.J., Rider, C.G., Na, L., Brown, S., Ateitalla, I., Acharya, S.K., Davies, M.H., Elias, E., Jenkins, N.A., Gilbert, D.J., Copeland, N.G. and Elcombe, C.R. (1993). Species specific induction of cytochrome P450 4A RNAs: PCR cloning of partial guinea pig, human and mouse CYP4A cDNAs. *Biochemical Journal* **294** : 173-180.

Bennett, A.M. and Williams, G.M. (1993). Calcium as a permissive factor but not an initiation-factor in DNA-synthesis induction in cultured rat hepatocytes by the peroxisome proliferator ciprofibrate. *Biochemical Pharmacology* **46** (12) : 2219-2227.

Bentley, P., Bieri, F., Mitchell, F., Waechter, F. and Staubli, W. (1987). Investigations on the mechanism of liver tumour induction by peroxisome proliferators. *Archives of Toxicology* **10** : S157-161.

Bentley, P., Calder, I., Elcombe, C., Grasso, P., Wiegand, H.G. and Stringer, D.A. (1993). Hepatic peroxisome proliferation in rodents and its significance for humans. *Food and Chemical Toxicology* **31** : 857-907.

Bird, A.P. and Wolffe, A.P. (1999). Methylation-induced repression-Belts, Braces and Chromatin. *Cell* **99** : 451-454.

Blaauboer, B.J., Van Holsteijn, C.W.M., Bleumink, R., Mennes, W.C., Van Pelt, F.N.A.M., Yap, S.H., Van Pelt, J.F., Van Iersel, A.A.J., Timmerman, A. and Schmid, B.P. (1990). The effect of becloric acid and clofibrilic acid on peroxisomal β -oxidation and peroxisomal prolifera-

tion in primary cultures of rat, monkey and human hepatocytes. *Biochemical Pharmacology* **40** (3) :521-528.

Blumcke, S., Schwartzkopft, W., Lobeck, H., Edmondson, N.A., Prentice, D.E. and Blane, G.F. (1983). Influence of fenofibrate on cellular and subcellular liver structure in hyperlipidaemic patients. *Atherosclerosis* **46** : 105-116.

Bocos, C., Gottlicher, M., Gearing, K., Banner, C., Enmark, E., Teboul, M., Crickmore, A. and Gustafsson, J.A. (1995). Fatty acid activation of peroxisome proliferator-activated receptor (PPAR). *Journal of Steroid Biochemistry and Molecular Biology* **53** (1-6) : 467-473.

Bogazzi, F., Hudson, L.D. and Nikodem, V.M. (1994). A novel heterodimerisation partner for thyroid hormone receptor. *Journal of Biological Chemistry* **269** (16) : 11683-11686.

Bourguet, W., Ruff, M., Chambon, P., Gronemeyer, H. and Moras, D. (1995). Crystal structure of the ligand binding domain of the human nuclear receptor RXR α . *Nature* **375** : 377-382.

Braissant, O., Foufelle, F., Scotto, C., Dauca, M. and Wahli, W. (1996). Differential expression of peroxisome proliferator activated receptors (PPARs):Tissue distribution of PPAR- α , - β , - γ in the adult rat. *Endocrinology* **137** : 354-366.

Brzozowski, A.M., Pike, A.C.W., Dauter, Z., Hubbard, R.E., Bonn, T., Engstrom, O., Ohman, L., Greene, G.L., Gustafsson, J.A. and Carlquist, M. (1997). Molecular basis of agonism and antagonism in the oestrogen receptor. *Nature* **389** (6652) : 753-758.

Butterworth, B.E., Smith-Oliver, T., Earle, L., Loury, D.J., White, R.D., Doolittle, D.J., Working, P.K., Cattely, R.C., Jirtle, R., Michalopoulos, G. and Strom, S. (1989). Use of primary cultures of human hepatocytes in toxicology studies. *Cancer research* **49** : 1075-1084.

Camp, H.S. and Tafuri, S.R. (1997). Regulation of peroxisome proliferator activated receptor- γ activity by mitogen-activated protein kinase. *Journal of Biological Chemistry* **272** (16) : 10811-10816.

Cao, Y., Adachi, J., Yano, T. and Hasegawa, M. (1994). Phylogenetic place of guinea pigs: no support of the rodent-polyphyly hypothesis from maximum-likelihood analyses of multiple protein sequences. *Molecular Biology and Evolution* **11** (4) : 593-604.

Cao, Y., Okada, N. and Hasegawa, M. (1997). Phylogenetic position of the guinea pigs revisited. *Molecular Biology and Evolution* **14** (4) : 461-464.

Castelein, H., Gulick, T., Declercq, P.E., Mannaerts, G.P., Moore, D.D. and Baes, M.I. (1994). The peroxisome proliferator activated receptor regulates malic enzyme gene expression. *Journal of Biological Chemistry* **269** (43) : 26754-26758.

Cattley, R.C. and Glover, S.E. (1993). Elevated 8-hydroxydeoxyguanosine in hepatic DNA of rats following exposure to peroxisome proliferators : relationship to carcinogens and nuclear localization. *Carcinogenesis* **14** : 2495-2499.

Cattley, R.C. and Popp, J.A. (1989). Differences between the promoting activities of the peroxisome proliferator WY-14,643 and phenobarbital in rat liver. *Cancer Research* **49** **12** : 3246-3251.

Cattley, R.C., Conway, J.G. and Popp, J.A. (1987). Association of persistent peroxisome proliferation and oxidative injury with hepatocarcinogenicity in female F344 rats fed di(2-ethyl-hex-yl) phthalate for 2 years. *Cancer Letters*. **38** (1-2) : 15 - 22.

Cattley, R.C., Marsman, D.S. and Popp, J.A. (1991). Age-related susceptibility to the carcino-

genic effect of the peroxisome proliferator WY-14,643 in rat liver. *Carcinogenesis* **12** (3) : 469-473.

Cattley, R.C., Richardson, K.K., Popp, J.A. and Butterworth, B.E. (1986). Effects of peroxisome proliferator carcinogens (PPC) on unscheduled DNA synthesis (UDS) in primary rat hepatocytes as monitored by quantitative autoradiography. *Proceedings of the American Association for Cancer Research* **27** : 106.

Cavailles, V., Dauvois, S., Danielian, P.S., Parker, M.G. (1994). Interaction of proteins with transcriptionally active estrogen receptors. *Proceedings of the National Academy of Sciences (USA)* **91** (21) : 10009-10013.

Cavailles, V., Dauvois, S., Danielian, P.S. and Parker, M.G. (1994). Interaction of proteins with transcriptionally active estrogen receptors. *Proceedings of the National Academy of Sciences (USA)* **91** (21) : 10009-10013

Cavailles, V., Dauvois, S., L'Horset, F., Lopez, G., Hoare, S., Kushner, P.J. and Parker, M.G. (1995). Nuclear factor RIP40 modulates transcriptional activation by the estrogen receptor. *EMBO Journal* **14** (15) : 3741-3751.

Chakravarti, D., LaMorte, V.J., Nelson, M.C., Nakajima, T., Schulman, I.G., Juguilon, H., Montminy, M. and Evans, R.M. (1996). Role of CBP/P300 in nuclear receptor signaling. *Nature* **383** (6595) : 99-103.

Chance, D.,S., Wu, S.M., and McIntosh, M.K. (1995). Inverse relationship between peroxisomal and mitochondrial β -oxidation in HepG2 cells treated with dehydroepiandrosterone and clofibric acid. *Proceedings of the Society for Experimental Biology and Medicine* **208** : 378-384.

Chen, H., Huang, C-Y., Wilson, M.W., Lay, L.T., Robertson, L.W., Chow, C.K. and Glauert, H. (1994). Effect of the peroxisome proliferators ciprofibrate and perfluorodecanoic acid on hepatic cell proliferation and toxicity in sprague-dawley rats. *Carcinogenesis* **15** (12) : 2847-2850.

Chen, D, Lepar, G., Kemper, B. (1994). A transcriptional regulatory element common to a large family of hepatic cytochrome P450 genes is a functional binding site of the orphan receptor HNF4. *Journal of Biological Chemistry* **269** : 5420-5427.

Choudhury, A.I, Chahal, S., Bell, A.R., Tomlinson, S.R., Roberts, R.A., Salter, A.M. and Bell, D.R. (2000). Species differences in peroxisome proliferation; mechanisms and relevance. *Mutation Research-fundamental and molecular mechanisms of mutagenesis* **448** (2) : 201-212.

Chrivia, J.C., Kwok, R.P.S., Lamb, N., Hagiwara, M., Montminy, M.R. and Goodman, R.H. (1993). Phosphorylated CREB binds specifically to the nuclear protein CBP. *Nature* **365** (6449) : 855-859.

Chu, R., Lin, Y., Rao, S. and Reddy, J.K. (1995). Cooperative formation of higher order peroxisome proliferator activated receptor and retinoid X receptor complexes on the peroxisome proliferator responsive element of the rat hydratase-dehydrogenase gene. *Journal of Biological Chemistry* **270** (50) : 29636-29639.

Ciriolo, M.R., Mavelli, I., Rotilio, G., Borzatta, V., Cristofari, M. and Stanzani, L. (1982). Decreased superoxide dismutase and glutathione peroxidase in liver of rats treated with hypolipidaemic drugs. *FEBS Letters* **144** : 264-268.

Clayson, D.B., Mehta, R. and Iverson, F. (1994). Oxidative DNA damage- The effects of certain genotoxic and operationally non-genotoxic carcinogens. *Mutation Research* **317** : 25-42.

Cohen, A.J. and Crasso, P. (1981). Review of hepatic response to hypolipidaemic drugs in rodents and its toxicological significance to man. *Food and Cosmetic Toxicology* **19** : 585-605.

Cole, T.J., Blendy, J.A., Monaghan, A.P., Krieglstein, K., Schmid, W., Aguzzi, A., Fantuzzi, G., Hummler, E., Unsicker, K. and Schutz, G. (1995). Targeted disruption of the glucocorticoid receptor gene blocks adrenergic chromaffin cell development and severely retards lung maturation. *Genes & development* **9** (13) : 1608-1621.

Collis, P., Antoniou, M. and Grosveld, F. (1990). Definition of the minimal requirements within the human beta globin gene and the dominant control region for high-level expression. *EMBO Journal* **9** (1) : 233-240.

Coni, P., Simbula, G., Deprati, A.C., Menegazzi, M., Suzuki, H, Sarma, D.S.R. Leddacolumbano, G.M. and Columbano, A. (1993). Differences in the steady-state levels of *c-fos*, *c-jun* and *c-myc* messenger RNA during mitogen-induced liver growth and compensatory regeneration. *Hepatology* **17** (6) : 1109-1116.

Cornu, M.C., Lhuguenot, J.C., Brady, A.M., Moore, R. and Elcombe, C.R. (1992). Identification of the proximate peroxisome proliferators derived from di(2-ethylhexyl)adipate and species differences in response. *Biochemical Pharmacology* **43** (10) : 2129-2134.

Custodio, N., CarmoFonseca, M., Geraghty, F., Pereira, H.S., Grosveld, F. and Antoniou, M. (1999). Inefficient processing impairs release of RNA from the site of transcription. *EMBO Journal* **18** (10) : 2855-2866.

D'Erchia, A.M., Gissi, C., Pesole, G., Saccone, C. and Arnason, U. (1996). The guinea pig is not a rodent. *Nature* **381** : 597-600.

Danielian, P.S., White, R., Lees, J.A. and Parker, M.G. (1992). Identification of a conserved region required for hormone dependent transcriptional activation by steroid-hormone receptors. *EMBO Journal* **11** (3) : 1025-1033.

De Duve, C. and Baudhuin, P. (1966). *Physiology Review* **46** : 323-57.

De La Inglesia, F.A., Lewis, J.E., Buchanan, R.A., Marcus, E.L. and McMahon, G. (1982). Light and electron microscopy of liver in hyperlipoproteinemic patients under long term gemfibrozil treatment. *Atherosclerosis* **43** : 19-37.

Devchand, P.R., Keller, H., Peters, J.M., Vazques, M., Gonzalez, F.J. and Wahli, W. (1996). The PPAR α -leukotriene B₄ pathway to inflammation control. *Nature* **384** : 39-43.

Dillon N. and Grosveld, F. (1993). Transcriptional regulation of multigene loci multi level control. *Trends in Genetics* **9** (4) : 134-137.

Dirven, H.A.A.M., Van Den Broek, P.H.H., Peeters, M.C.E., Peters, J.G.P., Mennes, W.C., Blaauboer, B.J., Noordhoek, J. and Jongeneelen, F.J. (1993). Effects of the peroxisome proliferator mono(2-ethylhexyl)phthalate in primary hepatocyte cultures derived from rat, guinea pig, rabbit, and monkey. *Biochemical Pharmacology* **45** (12) : 2425-2434.

Dowell, P., Peterson, V.J., Zabriskie, M., and Leid, M. (1997). Ligand-induced Peroxisome Proliferator-Activated Receptor α conformational change. *Journal of Biological Chemistry* **272** (3) : 2013-2020.

Dreyer, C., Keller, H., Mahfoudi, A., Laudet, V., Krey, G. and Wahli, W. (1993). Positive regulation of the peroxisomal beta-oxidation pathway by fatty acids through activation of peroxisome proliferator-activated receptors (PPAR). *Biol. Cell* **77** (1) : 67-76.

Dreyer, C., Krey, G., Keller, H., Givel, F., Helftenbein, G. and Wahli, W. (1992). Control of the peroxisomal β -oxidation pathway by a novel family of nuclear hormone receptors. *Cell* **68** : 879-887.

Duclos, S., Bride, J., Ramirez, L.C. and Bournot, P. (1997). Peroxisome proliferation and β -oxidation in FaO and MH₁ C₁ rat hepatoma cells, HepG2 human hepatoblastoma cells and cultured human hepatocytes: effect of ciprofibrate. *European Journal of Cell Biology* **72** : 314-323.

Eacho, P.I., Lanier, T.I. and Brodhecker, C.A. (1991). Hepatocellular DNA synthesis in rats given peroxisome proliferating agents- comparison of WY-14,643 to clofibrac acid, nafenopin and LY171883. *Carcinogenesis* **12** (9) : 1557-1561.

Eacho, P.I., Lanier, T.I. and Brodhecker, C.A. (1991). Hepatocellular DNA synthesis in rats given peroxisome proliferating agents- comparison of WY-14,643 to clofibrac acid, nafenopin and LY171883. *Carcinogenesis* **12** (9) : 1557-1561.

Elbrecht, A., Chen, Y., Cullinan, C.A., Hayes, N., Leibowitz, M.D., Moller, D.E. and Berger, J. (1996). Molecular cloning, expression and characterization of human peroxisome proliferator-activated receptors γ 1 and γ 2. *Biochemical and Biophysical Research Communications* **224**: 431-437.

Elcombe, C.R. (1985). Species differences in carcinogenicity and peroxisome proliferation due to trichloroethylene: a biochemical human hazard assessment. *Archives of Toxicology* (suppl.) **8** : 6-17.

Elcombe, C.R. and Mitchell, A.M. (1986). Peroxisome proliferation due to di(2-ethylhexyl)phthalate (DEHP): species differences and possible mechanisms. *Environmental health perspec-*

tives **70** : 211-219.

Eldridge, S.R., Tilbury, L.F., Goldsworthy, T.L. and Butterworth, B.E. (1990). Measurement of chemically-induced cell-proliferation in rodent liver and kidney- a comparison of 5-bromo-2'-deoxyuridine and [³H] thymidine administered by injection or osmotic pump. *Carcinogenesis* **11** (12) : 2245-2251.

Elholm, M., Bjerking, G., Knudsen, J., Kristiansen, K and Mandrup, S. (1996). Regulatory elements in the promoter region of the rat gene encoding the acyl-CoA-binding protein. *Gene* **173** : 233-238.

Elliott, B.M. and Elcombe, C.R. (1987). Lack of DNA damage or lipid peroxidation measured *in vivo* in the rat following treatment with peroxisome proliferators. *Carcinogenesis* **8** : 1213-1218.

Evans, R.M. (1988). The steroid and thyroid hormone receptor superfamily. *Science* **240** (4854) : 889-895.

Felgner, P.L. and Ringold, G.M. (1989). Cationic liposome-mediated transfection. *Nature* **337** : 387-388.

Felgner, P.L., Gadek, T.R., Holm, M., Roman, R., Chan, H.W., Wenz, M., Northrop, J.P., Ringold, G.M. and Danielsen, M. (1987). Lipofection - A highly efficient, lipid-mediated DNA-transfection procedure. *Proceedings of the National Academy of Sciences (USA)* **84** (21) : 7413-7417.

Felsenstein, J. (1978). Cases in which parsimony and compatibility methods will be positively misleading. *Systematic Zoology* **27** : 401-410.

Fitzpatrick, F.A. and Murphy, R.C. (1988). Cytochrome P-450 metabolism of arachidonic acid-

formation and biological actions of epoxygenase-derived eicosanoids. *Pharmacological Reviews* **40** (4) : 229-241.

Foerster, E.C., Fahrenkemper, T., Rabe, U., Graf, P. and Sies, H. (1981). Peroxisomal fatty acid oxidation as detected by H₂O₂ production in intact perfused rat liver. *Biochemical Journal* **196** (3) : 705-172.

Foliot, A., Touchard, D and Mallet, L. (1986). Inhibition of liver glutathione S-transferase activity in rats by hypolipidaemic drugs related to or unrelated to clofibrate. *Biochemical Pharmacology* **35** : 1685-1690.

Forman, B.M., Chen, J. and Evans, R. (1997). Hypolipidaemic drugs, polyunsaturated fatty acids, and eicosanoids are ligands for peroxisome proliferator-activated receptors α and γ . *Proceedings of the National Academy of Science (USA)* **94** : 4312-4317.

Forester, E., Fahrenkemper, T., Rabe, U., Graf, P. and Sies, H. (1981). Peroxisomal fatty acid oxidation as detected by H₂O₂ production in rat liver. *Biochemical Journal* **196** : 705.

Foxworthy, P.S. and Eacho, P.I. (1986). Conditions influencing the induction of peroxisomal beta-oxidation in cultured rat hepatocytes. *Toxicology Letters* **30** (2) : 189-196.

Foxworthy, P.S. and Eacho, P.I. (1994). Culture hepatocytes for studies of peroxisome proliferation: methods and applications. *Journal of Pharmacological and Toxicological Methods* **31** : 21-30.

Foxworthy, P.S., White, S.L., Hoover, D.M. and Eacho, P.I. (1990). Effect of ciprofibrate, bezafibrate and LY171883 on peroxisomal β -oxidation in cultured rat, dog and rhesus monkey hepatocytes. *Toxicology and applied pharmacology* **104** : 386-394.

Frick, H., Elo Haapa, K. and Heinonen, O.P. (1987). Helsinki Heart Study: Primary-prevention trial with gemfibrozil in middle aged men with dyslipidemia. *New England Journal of Medicine* **317** : 1235-1247.

Furukawa, K., Numoto, S., Furuya, K., Furukawa, N.T. and Williams, G.M. (1985). Effects of the hepatocarcinogen nafenopin, a peroxisome proliferator on the activities of rat liver glutathione requiring enzymes and catalase in comparison to the action of phenobarbital. *Cancer Research* **45** : 5011-5019.

Gariot, P., Barrat, P., Drouin, P., Genton, P., Pointer, B., Foliguet, B., Kolopp, M. and Debry, G. (1987). Morphometric study of human hepatic cell modifications induced by fenofibrate. *Metabolism* **36** : 203-210.

Gaunitz, F., Papke, M. and Gebhardt, R. (1996). Transient transfection of primary cultured hepatocytes using CaPO₄/DNA precipitation. *Biotechniques* **20** : 826-832.

Gearing, K.L., Gottlicher, M., Teboul, M., Widmark, E. and Gustafsson, J.A. (1993). Interaction of the peroxisome-proliferator-activated receptor and retinoid x receptor. *Proceedings of the National Academy of Sciences (USA)* **90** (4) : 1440-1444.

Gebel, T., Arand, M. and Oesch, F. (1992). Induction of the peroxisome proliferator activated receptor by fenofibrate in the rat liver. *FEBS Letters* **309** (1) : 37-40.

Gervois, P., Torra, I.P., Chinetti, G., Grotzinger, T., Dubois, G., Fruchart, J.C., FruchartNajib, J., Leitersdorf, E, Staels, B. (1999). *Molecular Endocrinology* **13** (9) : 1535-1549.

Gibson, G. and Lake, B. (1993). Peroxisomes: Biology and Importance in Toxicology and Medicine. Taylor and Francis Ltd.

Gibson, G.G., Orton, T.C. and Tamburini, P.P. (1982). Cytochrome P-450 induction by clofibrate. *Biochemical Journal* **203** : 161 - 1678.

Ginot, J., Decaux, J.F., Cognet, M., Berbar, T., Levrat, F., Khan, A. and Weber, A. (1989). Transfection of hepatic genes into adult rat hepatocytes in primary culture and their tissue specific expression. *European Journal of Biochemistry* **180** : 289-294.

Glauert, H.P. and Clark, T.D. (1989). Lack of initiating activity of the peroxisome proliferator ciprofibrate in 2-stage hepatocarcinogenesis. *Cancer Letters* **44** (2) : 95-100.

Goldsworthy, T.L., Goldsworthy, S.M., Sprankle, C.S. and Butterworth, B.E. (1994). Expression of *myc*, *fos* and *ha-ras* associated with chemically-induced cell-proliferation in the rat-liver. *Cell Proliferation* **27** (5) : 269-278.

Gonzalez, F.J. (1989). The Molecular Biology of Cytochrome P450s. *Pharmacology Reviews* **40** (4) : 243-288.

Gonzalez, F.J. (1997). Recent update on the PPAR alpha-null mouse. *Biochimie* **79** (2-3) : 139-144.

Gotoh, O. (1992). Substrate Recognition Sites in Cytochrome P450 Family 2 (CYP2) Proteins Inferred from Comparative Analyses of Amino Acid and Coding Nucleotide Sequences. *Journal of Biological Chemistry* **267** (1) : 83-90

Gottlicher, M., Widmark, E., Li, Q. and Gustafsson, J.A. (1992). Fatty acids activate a chimera of the clofibric acid-activated receptor and the glucocorticoid receptor. *Proceedings of the National Academy of Sciences (USA)* **89** : 4653-4657.

Graur, D., Hide, W.A. and Li, W.H. (1991) Is the guinea pig a rodent ? *Nature* **351** : 649-652.

Gray, R.H. and De La Iglesia, F.A. (1984). Quantitative microscopy comparison of peroxisome proliferation by the lipid regulating agent gemfibrozil in several species. *Hepatology* **4** (3) : 520-530.

Gray, T.J.B., Beamand, J.A., Lake, B.G., Foster, J.R. and Gangolli, S.D. (1982). Peroxisome proliferation in cultured rat hepatocytes produced by clofibrate and phthalate ester metabolites. *Toxicology Letters* **10** (2-3) : 273-279.

Green, S. (1992). Peroxisome proliferators: a model for receptor mediated carcinogenesis. *Cancer Surveys* **14** : 221-232.

Green, S., Tugwood, J.D. and Issemann, I. (1992). The molecular mechanism of peroxisome proliferator action: a model for species differences and mechanistic assessment. *Toxicology Letters* **64/65** : 131-139.

Greuet, J., Pichard, L., Ourlin, J.C., Bonfils, C., Domergue, J., LeTreur, P. and Maurel, P. (1997). Effect of cell density and epidermal growth factor on the inducible expression of CYP3A and CYP1A genes in human hepatocytes in primary culture. *Hepatology* **25** (5) : 1166-1175.

Grosveld, F., Blom van Assendelft, G., Greaves, D.R. and Kollias, G. (1987). Position-independent, high-level expression of the human b-globin gene in transgenic mice. *Cell* **51** : 975-985.

Gruppuso, P.A., Boylan, J.M. and Bienicki, T.C. (1994). The fetal hepatic mitogens transforming growth factor alpha (TGF-alpha) and hepatocyte growth-factor (HGF) signal through a common pathway redundancy in fetal growth-regulation. *Pediatric Research* **35** (4) : 100.

GuardiolaDiaz, H.M., Rehnmark, S., Usuda, N., Albrektsen, T., Feltkamp, D., Gustafsson, J.A.

and Alexson, S.H.E. (1999). Rat peroxisome proliferator-activated receptors and brown adipose tissue function during cold acclimatization *Journal of Biological Chemistry* **274** (33) : 23368-23377.

Gupta, R.C., Goel, S.K., Earley, K., Singh, B. and Reddy, J.K. (1985). P-32-postlabeling analysis of peroxisome proliferator-DNA adduct formation in rat liver *in vivo* and hepatocytes *in vitro*. *Carcinogenesis* **6** (6) : 933-936.

Handler, J. and Thurman, R. (1988). Catalase dependent ethanol oxidation in perfused rat liver, requirement for fatty acid stimulated H₂O₂ production in peroxisomes. *European Journal of Biochemistry* **176** : 477.

Hanefeld, M., Kemmer, C. and Kadner, E. (1983). Relationship between morphological changes and lipid lowering action of p-chlorophenoxyisobutyric acid (CPIB) on hepatic mitochondria and peroxisomes in man. *Atherosclerosis* **46** : 239-246.

Hardwick, J.P, Song, B.-J., Huberman, E. and Gonzalez, F.J. (1987). Isolation, Complementary DNA Sequence, and Regulation of Rat Hepatic Lauric Acid ω-Hydroxylase (Cytochrome P-450_{LAW}). *Journal of Biological Chemistry* **262** (2) : 801-810.

Hasmall, S.C., Pyrah, I.T.G., Soames, A.R. and Roberts, R.A. (1997). Expression of the immediate-early genes, *c-fos*, *c-jun*, and *c-myc*: A comparison in rats of Nongenotoxic hepatocarcinogens with noncarcinogenic liver mitogens. *Fundamental and Applied Toxicology* **40** (1) : 129-137.

Hawkins, J., Jones, W., Bonner, F. and Gibson, G. (1987). The effect of peroxisome proliferators on microsomal, peroxisomal and mitochondrial enzyme activities in liver and kidney. *Drug Metabolism Reviews* **18** : 441.

Heery, D.M., Kalkhoven, E., Hoare, S. and Parker, M.G. (1997). A signature motif in transcriptional co-activators mediates binding to nuclear receptor. *Nature* **387** (6634) : 733-736.

Henderson, C.J. Wolf, C.R. (1991). Evidence that the androgen receptor mediates sexual-differentiation of mouse renal cytochrome-p450 expression. *Biochemical Journal* **278** : 499-503.

Henderson, C.J., Bammler, T. and Wolf, C.R. (1994). Deduced amino acid sequence of a murine cytochrome P450 *Cyp4a* protein : developmental and hormonal regulation in liver and kidney. *Biochimica et Biophysica Acta* **1200** : 182-190.

Henderson, C.J., Bammler, T. and Wolf, C.R. (1994). Deduced amino-acid-sequence of a murine cytochrome-p-450 *cyp4a* protein- developmental and hormonal-regulation in liver and kidney. *Biochimica et Biophysica Acta* **1200** (2) : 182-190.

Henderson, C.J., Scott, A.S., Yang, C.S. and Wolf, C.R. (1990). Testosterone-mediated regulation of mouse renal cytochrome P-450 enzymes. *Biochemical Journal* **206** : 675-681.

Heng, Y.M, Kuo, S.C.-W., Jones, P.S., Savory, R., Schultz, R.M., Tomlinson, S. R., Gray, T.J.B. and Bell, D.R. (1997). A Novel Murine P450 Gene, *Cyp4a14*, is Part of a Cluster of *Cyp4a* and *Cyp4b*, but not CYP4F, Genes in Mouse and Man. *Biochemical Journal* **325** (3) : 741-749.

Hertz, R., Bishara-Shieban, J. and BarTana, J. (1995). Mode of action of peroxisome proliferators as hypolipidaemic drugs: suppression of apolipoprotein C-III. *Journal of Biological Chemistry* **270** (22) : 13470-13475.

Hertz, R., Magenheimer, J., Berman, I. and BarTana, J. (1998). Fatty acyl-CoA thioesters are ligands of hepatic nuclear factor-4 alpha. *Nature* **392** (6675) : 512-516.

Hertz, R., Seckbach, M., Zakin, M.M. and Bar-Tana, J. (1996). Transcriptional suppression of the transferrin gene by hypolipidaemic peroxisome proliferators. *Journal of Biological Chemistry* **271** (1) : 218-224.

Hiratsuka, M., Matsuura, T., Watanabe, E., Sato, M. and Suzuki, Y. (1996). Sex and Strain Difference in Constitutive Expression of Fatty Acid ω -Hydroxylase (CYP4A-Related Proteins) in Mice. *Journal of Biochemistry* **119** : 340 -345.

Holden, P.R., Hasmall, S.C., James, N.H., West, D.R., Brindle, R.D., Gonzalez, F.J., Peters, J.M. and Roberts, R.A. (2000). Tumour necrosis factor alpha (TNF alpha): Role in suppression of apoptosis by the peroxisome proliferator nafenopin. *Cellular and Molecular Biology* **46** (1) : 29-39.

Holmen, S.L., Vanbrocklin, M.W., Eversole, R.R., Stapleton, S.R. and Ginsberg, L.C. (1995). Efficient lipid-mediated transfection of DNA into primary rat hepatocytes. *In Vitro Cell Developmental Biology* **30** : 347-351.

Horwitz, K.B., Jackson, T.A., Rain, D.L., Richer, J.K., Takimoto, G.S. and Tung, L. (1996). Nuclear receptor coactivators and corepressors. *Molecular Endocrinology* **10** (10) : 1167-1177

Hsu, M.H., Palmer, C.N.A., Griffin, K.J. and Johnson, E.F. (1995). A single amino-acid change in the mouse peroxisome proliferator-activated receptor-alpha alters transcriptional responses to peroxisome proliferators. *Molecular Pharmacology* **48** (3) : 559-567.

Huang, C-Y., Wilson, M.W., Lay, L.T., Chow, C.K., Robertson, L.W. and Glauert, P. (1994). Increased 8-hydroxydeoxyguanosine in hepatic DNA of rats treated with the peroxisome proliferators ciprofibrate and perfluorodecanoic acid. *Cancer Letters* **87** : 223-228.

Hunter, J., Kassam, A., Winrow, C.J., Rachubinski, R.A. and Capone, J.P. (1996). Cross-talk between the thyroid hormone and peroxisome proliferator-activated receptors in regulating peroxisome proliferator-responsive genes. *Molecular and Cellular Endocrinology* **116** (2) : 213-221.

Ijpenberg, A., Jeannin, E., Wahli, W. and Desvergne, B. (1997). Polarity and specific sequence requirements of peroxisome proliferator-activated receptor (PPAR) retinoid X receptor heterodimer binding to DNA- A functional analysis of the malic enzyme gene PPAR response element. *Journal of Biological Chemistry* **272** (32) : 20108-20117.

Imaoka, S., Ogawa, H., Kimura, S. and Gonzalez, F.J. (1993). Complete cDNA sequence and cDNA-directed expression of CYP4A11, a fatty acid ω -hydroxylase expressed in human kidney. *DNA and Cell Biology* **12** (10) : 893-899.

Issemann, I. and Green, S. (1990). Activation of a member of the steroid hormone receptor superfamily by peroxisome proliferators. *Nature* **347** : 645-650.

Issemann, I., Prince, R., Tugwood, J. and Green, S. (1992). A role for fatty acids and liver fatty acid binding protein in peroxisome proliferation. *Biochemical Society Transactions* **20** (4) : 824-827.

Issemann, I., Prince, R.A., Tugwood, J.D. and Green, S. (1993). The peroxisome proliferator activated receptor:retinoid X receptor heterodimer is activated by fatty acids and fibrate hypolipidaemic drugs. *Journal of Molecular Endocrinology* **11** : 37-47.

James, N.H. and Roberts, R.A. (1996). Species differences in response to peroxisome proliferators correlate *in vitro* with induction of DNA synthesis rather than suppression of apoptosis. *Carcinogenesis* **17** (8) : 1623-1632.

Janknecht, R. and Hunter, T. (1996). Transcription- A growing coactivator network. *Nature* **383** (6595) : 22-23.

Johnson, E.F. , Walker, D.W. Griffin, K.J., Clark, J.E., Okita, R.T., Muerhoff, A.S. and Masters, B.S.S. (1990). Cloning and expression of three rabbit kidney cDNAs encoding lauric acid omega hydroxylases. *Biochemistry* **29** (4) : 873-879.

Johnson, E.F., Palmer, C.N.A., Griffin, K.J. and Hsu, M.H. (1996). Cytochromes P450 .7. Role of the peroxisome proliferator-activated receptor in cytochrome P450 4A gene regulation. *FASEB Journal* **10** (11) : 1241-1248.

Jones, P.S., Savory, R., Barratt, P., Bell, A.R., Gray, T.J.B., Jenkins, N.A., Gilbert, D.J., Copeland, N.G. and Bell, D.R. (1995). Chromosomal localization, inducibility, tissue specific expression and strain differences in three murine peroxisome proliferator activated receptor genes. *European Journal of Biochemistry* **233** : 219-226.

Jones D.O., Cowell, I.G. and Singh, P.B. (2000). Mammalian chromodomain proteins: Their role in genome organization and expression. *BioEssay* **22** : 124-137.

Jow, L. and Mukherjee, R. (1995). The human peroxisome proliferator-activated receptor (PPAR) subtype NUC1 represses the activation of hPPAR α and thyroid hormone receptors. *Journal of Biological Chemistry* **270** (8) : 3836-3840.

Jugeaubry, C.E., Gorlabajszczak, A., Pernin, A., Lemberger, T., Wahli, W., Burger, A.G. and Meier, C.A. (1995). peroxisome proliferator-activated receptor mediates cross-talk with thyroid-hormone receptor by competition for retinoid-x receptor - possible role of a leucine zipper-like heptad repeat. *Journal of Biological Chemistry*. **270** (30) : 18117-18122.

Jurgens, G. (1985). A group of genes controlling the spatial expression of the biothorax complex in *Drosophila*. *Nature* **316** : 153-155.

Kaikaus, N.M., Chan, W.K., Lysenko, N., Ray, R., Ortiz de Montellano, P.R. and Bass, N.M. (1993). Induction of peroxisomal fatty acid β -oxidation and liver fatty acid-binding protein by peroxisome proliferators- mediation via the cytochrome P450A1 ω -hydroxylase pathway. *Journal of Biological Chemistry* **268** : 9593-9603.

Kaku, M., Ichihara, K., Kusunose, E., Ogita, K., Yamamoto, S., Yano, I. and Kusunose, M. (1984). Purification and characterization of cytochrome P-450 specific for prostaglandin and fatty acid hydroxylase activities from the microsomes of rabbit small intestinal mucosa. *Journal of Biochemistry* **96** (6) : 1883-1891.

Kamei, Y., Xu, L., Heinzl, T., Torchia, J., Kurokawa, R., Gloss, B., Lin, S.C., Heyman, R.A., Rose, D.W., Glass, C.K. and Rosenfeld, MG. (1996). A CBP integrator complex mediates transcriptional activation and AP-1 inhibition by nuclear receptors. *Cell* **85** (3) : 403-414.

Kasai, H., Okada, Y., Nishimura, S., Rao, M.S. and Reddy, J.K. (1989). Formation of 8-hydroxyguanosine in liver DNA of rats following long term exposure to a peroxisome proliferator. *Cancer Research* **49** : 2603-2605.

Kawashima, H., Kusunose, E., Kikuta, Y., Kinoshita, H., Tanaka, S., Yamamoto, S., Kishimoto, T. and Kusunose, M. (1994). Purification and cDNA cloning of human liver CYP4A fatty acid omega-hydroxylase. *Journal of Biochemistry* **116** (1) : 74-80.

Kawashima, H., Kusunose, E., Kubota, I., Maekawa, M. and Kusunose, M. (1992). Purification and NH₂-terminal amino acid sequences of human and rat kidney fatty acid ω -hydroxylases. *Biochimica Biophysica Acta* **1123** : 156-162.

Keller, H., Devchand, P.R., Perroud, M. and Wahli, W. (1997). PPAR α structure-function relationships derived from species specific differences in responsiveness to hypolipidaemic agents. *Biological Chemistry* **378** : 651-655

Keller, H., Dreyer, C., Medin, J., Mahfoudi, A., Ozato, K. and Wahli, W. (1993). Fatty-acids and retinoids control lipid-metabolism through activation of peroxisome proliferator-activated receptor retinoid-x receptor heterodimers. *Proceedings of the National Academy of Sciences (USA)* **90** (6) : 2160-2164.

Kimura, S., Hanioka, N., Matsunaga, E. and Gonzalez, F.J. (1989a). The rat clofibrate-inducible CYP4A gene subfamily I. Complete intron and exon sequence of the CYP4A1 and CYP4A2 genes, unique exon organization, and identification of a conserved 19-bp upstream element. *DNA* **8** (7) : 503-516.

Kimura, S., Hardwick, J.P., Kozak, C.A. and Gonzalez, F.J. (1989b). The Rat Clofibrate-Inducible CYP4A subfamily II. cDNA Sequence of IVA3, Mapping of the *Cyp4a* Locus to Mouse Chromosome 4, and Coordinate and Tissue-Specific Regulation of the CYP4A genes. *DNA* **8** (7) : 517-525.

Kingston, R.E. and Narlikar, G.J. (1999). ATP-dependent remodelling and acetylation as regulators of chromatin fluidity. *Genes and Development* **13** : 2339-2352.

Kliewer, S.A., Forman, B.M., Blumberg, B., Ong, E.S., Borgmeyer, U., Mangelsdorf, D.J., Umesono, K. and Evans, R.M. (1994). Differential expression and activation of a family of murine peroxisome proliferator-activated receptors. *Proceedings of the National Academy of Sciences (USA)* **91** : 7355-7359.

Kliewer, S.A., Sundseth, S.S., Jones, S.A., Brown, P.J., Wisely, G.B., Koble, C.S., Devchand,

P., Wahli, W., Willson, T.M., Lenhard, J.M. and Lehmann, J.M. (1997). Fatty acids and eicosanoids regulate gene expression through direct interactions with peroxisome proliferator-activated receptors α and γ . *Proceedings of the National Academy of Sciences (USA)* **94** : 4318-4323.

Kluwe, W.M., Haseman, J.K., Douglas, J.F. and Huff, J.E. (1982). The carcinogenicity of dietary di(2-ethylhexyl) phthalate (DEHP) in Fischer 344 rats and b6c3f1 mice. *Journal of Toxicology and Environmental Health* **10** : 797-815.

Kramer, A. (1996). The structure and function of proteins involved in mammalian pre-mRNA splicing. *Annual Review of Biochemistry* **65** : 367-409.

Kraupp-Grasl, B., Huber, W., Taper, H. and Schulte-Hermann, R. (1991). Increased susceptibility of aged rats to hepatocarcinogenesis by the peroxisome proliferator nafenopin and the possible involvement of altered liver foci occurring spontaneously. *Cancer Research* **51** (2) : 666-671.

Krey, G., Braissant, O., L'Horset, F., Kalkhoven, E., Perroud, M., Parker, M.G. and Wahli, W. (1997). Fatty acids, eicosanoids, and hypolipidemic agents identified as ligands of peroxisome proliferator-activated receptors by coactivator-dependent receptor ligand assay. *Molecular Endocrinology* **11** : 779-791.

Krey, G., Keller, H., Mahfoudi, A., Medin, J., Ozato, K., Dreyer, C. and Wahli, W. (1993). *Xenopus* peroxisome proliferator activated receptors: genomic organization, response element recognition, heterodimer formation with retinoid X receptor and activation by fatty acids. *Journal of Steroid Biochemistry and Molecular Biology* **47** (1-6) : 65-73.

Kuma, K. and Miyata, T. (1994). Mammalian phylogeny inferred from multiple protein data. *Japanese Journal of Genetics* **69** (5) : 555-566.

Lake, B.G., Evans, J.G., Gray, T.J.B., Korosi, S.A. and North, C.J. (1989a). Comparative studies on nafenopin-induced hepatic peroxisome proliferation in the rat, Syrian hamster, guinea pig and marmoset. *Toxicology and Applied and pharmacology* **99** : 148-160.

Lake, B.G. (1995). Mechanisms of hepatocarcinogenicity of peroxisome proliferating drugs and chemicals. *Annual Review of Pharmacology and Toxicology* **35** : 483-507.

Lake, B.G., Evans, J.G., Cunninghame, M.E. and Price, R.J. (1993). Comparison of the hepatic effects of nafenopin and Wy-14,643 on peroxisome proliferation and cell replication in the rat and Syrian hamster. *Environmental Health Perspectives* **101** (suppl. 5) : 241-248.

Lake, B.G., Gray, T.J.B. and Gangolli, S.D. (1986). Hepatic effects of phthalate esters and related compounds- *in vivo* and *in vitro* correlations. *Environmental Health Perspectives* **67** : 283-290.

Lake, B.G., Gray, T.J.B., Korosi, S.A. and Walters, D.G. (1989b). Nafenopin, a peroxisome proliferator depletes hepatic vitamin E content and elevates plasma oxidised glutathione levels in rats. *Toxicology Letters* **45** : 221-229.

Lake, B.G., Gray, T.J.B., Rijcken, W.R.P., Beamand, J.A. and Gangolli, S.D. (1984). The effect of hypolipemic agents on peroxisomal beta-oxidation and mixed-function oxidase activities in primary cultures of rat hepatocytes-relationship between induction of palmitoyl-CoA oxidation and lauric acid hydroxylation. *Xenobiotica* **14** (3) : 269-276.

Lalwani, N.D., Alvares, K., Reddy, M.K., Reddy, M.N., Parikh, I. and Reddy, J.K. (1987). Peroxisome proliferator-binding protein: identification and partial characterization of nafenopin, clofibric acid, and ciprofibrate-binding proteins from rat liver. *Proceedings of the National Academy of Sciences (USA)* **84** (15) : 5242-5246.

Lalwani, N.D., Dethloff, L.A., Haskins, J.R., Robertson, D.G. and De La Iglesia, F.A. (1997). Increased nuclear ploidy, not cell proliferation, is sustained in the peroxisome proliferator treated rat liver. *Toxicologic Pathology* **25** (2) : 165-176.

Lalwani, N.D., Fahl, W.E. and Reddy, J.K. (1983). Characterization of hypolipidemic peroxisome proliferator nafenopin binding-protein in rat liver cytosol. *Federation Proceedings* **42** (4) : 876.

Lambe K.G. and Tugwood, J.D. (1996). A human peroxisome proliferator-activated receptor- γ is activated by inducers of adipogenesis, including thiazolidinedione drugs. *European Journal of Biochemistry* **239** : 1-7.

Latruffe, N., Pacot, C., Passily, P., Petit, M., Bardot, O., Caira, F., Cherkaoui Malki, M., Jannin, B., Clemencet, M.C. and Deslex, P. (1995). Peroxisomes and Hepatotoxicity. *Comparative Haematology International* **5** : 189-195.

Laudet, V., Hanni, C., Coll, J., Catzeflis, F. and Stehelin, D. (1992). Evolution of the nuclear receptor gene superfamily. *EMBO Journal* **11** (3) : 1003-1013.

Lazarow, P.B. (1978). Rat liver peroxisomes catalyze the β -oxidation of fatty acids. *Journal of Biological Chemistry* **253** (5) : 1522-1528.

Lazarow, P.B. and De Duve, C. (1976). A fatty acyl-CoA oxidising system in rat liver peroxisomes: enhancement by clofibrate, a hypolipidaemic drug. *Proceedings of the National Academy of Science (USA)* **73** : 2043-2046.

Lazarow, P.B. and Moser, H.W. (1989). The metabolic basis of inherited disease. Sixth edition (ed C.R. Scriver, A.L. Beaudet, W.S. Sly, and D. Valle) New York: McGraw-Hill, pp1479-1509.

Lazo, O., Contreras, M., Hashmi, M., Stanley, W., Irazu, C. and Singh, I. (1988). Peroxisomal lignoceroyl-CoA ligase deficiency in childhood adrenoleukodystrophy and adrenomyeloneuropathy. *Proceedings of the National Academy of Sciences (USA)* **85** (20) : 7647-7651.

Lee, S.S.T., Pineau, T., Drago, J., Lee, E.J., Owens, J.W., Kroetz, D.L., Fernandez-Salguero, P.M., Westphal, H. and Gonzalez, F.J. (1995). Targeted disruption of the α isoform of the peroxisome proliferator activated receptor gene in mice results in abolishment of the pleiotropic effects of peroxisome proliferators. *Molecular and Cellular Biology* **15** (6) : 3012-3022.

Lemberger, T., Saladin, R., Vazquez, M., Assimacopoulos, F., Staels, B., Desvergne, B., Wahli, W. and Auwerx, J. (1996). Expression of the peroxisome proliferator- activated receptor α gene is stimulated by stress and follows a diurnal rhythm. *The Journal of Biological Chemistry* **271** (3) : 1764-1769.

Lemberger, T., Staels, B., Saladin, R., Desvergne, B., Auwerx, J. and Wahli, W. (1994). Regulation of the peroxisome proliferator activated receptor α gene by glucocorticoids. *Journal of Biological Chemistry* **269** (40) : 24527-24530.

Leone, T.C., Weinheimer, C.J. and Kelly, D.P. (1999). A critical role for the peroxisome proliferator-activated receptor-alpha (PPAR alpha) in the cellular fasting response: The PPAR alpha-null mouse as a model of fatty acid oxidation disorders. *Proceedings of the National Academy of Sciences (USA)* **96** (13) : 7473-7478.

Lhuguenot, J.C., Mitchell, A.M. and Elcombe, C.R. (1988). The metabolism of mono-(2-ethylhexyl)phthalate (MEHP) and liver peroxisome proliferation in the hamster. *Toxicology and Industrial Health* **4** (4) : 431-441.

Lock, E.A., Mitchell, A.M. and Elcombe, C.R. (1989). Biochemical mechanisms of induction

of hepatic peroxisome proliferation. *Annual Review of Pharmacology and Toxicology* **29** : 145-163.

Luckett, W.P. and Hartenberger, J.L. (eds.) (1985). Evolutionary relationships among rodents. A multidisciplinary analysis. Plenum Press, New York.

Ma, Y.H., Debebe, G., Schwartzman, M.L., Flack, J.R., Clark, J.E., Masters, B.S., Harder, D.R. and Roman, R.R. (1993). 20-hydroxyicosatetraenoic acid is an endogenous vasoconstrictor of canine renal arteries. *Circulation Research* **72** : 126-136.

Macdonald, N., Holden, P.R. and Roberts, R.A. (1999). Addition of Peroxisome Proliferator-Activated Receptor α to guinea pig hepatocytes confers increased responsiveness to peroxisome Proliferators. *Cancer Research* **59** : 4776-4780.

MacDonald, C. and Willet, B. (1997). The immortalisation of rat hepatocytes by transfection with SV40 sequences. *Cytotechnology* **23** : 161-170.

Manglesdorf, D.J. and Evans, R.M. (1995). The RXR heterodimers and orphan receptors. *Cell* **83** : 841-850.

Marcus, S.L., Capone, J.P. and Rachubinski, R.A. (1996). Identification of COUP-TFII as a peroxisome proliferator response element binding factor using genetic selection in yeast: COUP-TFII activates transcription in yeast but antagonises PPAR signaling in mammalian cells. *Molecular and Cellular Endocrinology* **120** : 31-39.

Marcus, S.L., Miyata, K.S., Zhang, B., Subramani, S, Rachubinski, R.A. and Capone, J.P. (1993). Diverse peroxisome proliferator activated receptors bind to the peroxisome proliferator-responsive elements of the rat hydratase/dehydrogenase and fatty acyl-CoA oxidase genes but

differentially induce expression. *Proceedings of the National Academy of Science (USA)* **90** : 5723-5727.

Marilley, D., Mahfoudi, A. and Wali, W. (1994). Gene transfer into *Xenopus* hepatocytes: transcriptional regulation by members of the nuclear receptor superfamily. *Molecular Endocrinology* **101** : 227-236.

Marsman, D.S., Cattley, R.C., Conway, J.G. and Popp, J.A. (1988). Relationship of hepatic peroxisome proliferation and replicative DNA synthesis to the hepatocarcinogenicity of the peroxisome proliferators di(2-ethylhexyl)phthalate and [4-chloro-6-(2,3-xylylidino)-2-pyrimidinylthio]acetic acid (WY-14,643) in rats. *Cancer Research* **48** (23) : 6739-6744.

Marsman, D.S., Swansonpfeiffer, C.L. and Popp, J.A. (1993). Lack of comitogenicity by the peroxisome proliferator hepatocarcinogens, WY-14,643 and clofibrac acid. *Toxicology and Applied Pharmacology* **122** (1) : 1-6.

Masters, C. and Crane, D. (Eds.) (1995). The peroxisome: a vital organelle. Cambridge University Press

Mastes, C. (1996). Cellular signalling: The role of the peroxisome. *Cellular Signalling* **8**, (3) : 197-208.

Matsubara, S., Yamamoto, S., Sogawa, K., Yokotani, N., Fujii-Kuriyama, Y., Haniu, M., Shively, J.E., Gotoh, O., Kusunose, E. and Kusunose, M. (1987). cDNA cloning and inducible expression during pregnancy of the mRNA for rabbit pulmonary prostaglandin ω -hydroxylase (cytochrome P-450p-2). *Journal of Biological Chemistry* **262** (27) : 13366-13371.

McGuire, E.J, Gray, R.H. and De La Iglesia, F.A. (1992). Chemical structure-activity relation-

ships: peroxisome proliferation and lipid regulation in rats. *Journal of the American College of Toxicology* **11** (3) : 353-361.

McNae, F., Sharma, R. and Gibson, G.G. (1994). Molecular toxicology of peroxisome proliferators. *European Journal of drug Metabolism and Pharmacokinetics* **3** : 219-223.

Melchiorri, C., Chieco, P., Zedda, A.I., Coni, P., Ledda-Columbano, G.M. and Columbano, A. (1993). Ploidy and nuclearity of rat hepatocytes after compensatory regeneration or mitogen-induced liver growth. *Carcinogenesis* **14** (9) : 1825-1830.

Michalopoulos, G.K. (1990). Liver regeneration: molecular mechanisms of growth control. *FASEB Journal* **4** (2) : 176-187.

Miller, R.T., Glover, S.E., Stewart, W.S., Corton, J.C., Popp, J.A. and Cattley, R.C. (1996). Effect on the expression of *c-met*, *c-myc* and PPAR α in liver and liver tumours from rats chronically exposed to the hepatocarcinogenic peroxisome proliferator Wy-14,643. *Carcinogenesis* **17** (60) : 1337-1341.

Milton, M.N., Elcombe, C.R. and Gibson, G.G. (1990). On the mechanism of induction of microsomal cytochrome P450IVA1 and peroxisome proliferation in rat-liver by clofibrate. *Biochemical Pharmacology* **40** (12) : 2727-2732.

Mitaka, T., Sattler, G.L. and Pitot, H.C. (1991). The bicarbonate ion is essential for efficient DNA-synthesis by primary cultured rat hepatocytes. *In Vitro Cellular and Developmental Biology* **27** (7) : 549-556.

Miyamoto, T., Kaneko, A., Kakizawa, T., Yajima, H., Kamijo, K., Sekine, R., Hiramatsu, K., Nishii, Y., Hashimoto, T. and Hashizume, K. (1997). Inhibition of peroxisome proliferator sig-

nalling pathways by thyroid hormone receptor. *Journal of Biological Chemistry*, **272** (12) : 7752-7758.

Miyata, K.S. McCaw, S.E., Patel, H.V., Rachubinski, R.A. and Capone, J.P. (1996). The orphan nuclear hormone receptor LXR α interacts with the peroxisome proliferator-activated receptor and inhibits peroxisome proliferator signalling. *Journal of Biological Chemistry* **271** (16) : 9189-9192.

Mochizuki, Y., Furukawa, K. and Sawada, N. (1983). Effect of simultaneous administration of clofibrate with diethylnitrosamine on hepatic tumourigenesis in the rat. *Cancer Letters* **19** : 99-105.

Moody, D.E., Reddy, J.K., Lake, B.G., Popp, J.A. and Reese, DH. (1991). Peroxisome proliferation and nongenotoxic carcinogenesis. *Symposium Fundamental and Applied Toxicology* **16** (2) : 233-248.

Moody, D. and Reddy, J. (1978). The hepatic effects of hypolipidaemic drugs (clofibrate, nafenopion, fibric acid and Wy-14,643) on hepatic peroxisomes and peroxisome-associated enzyme. *Journal of Pathology* **90** : 291.

Moser, H.W. (1987). New approaches in peroxisomal disorders. *Developmental Neuroscience* **9** : 1-18.

Moser, H.W. (1993). Peroxisomal Disorders. Advances in human genetics (ed H.Harris and K.Hirschhorn). Plenum Press New York, vol. 21, pp 1-106.

Motojima, K. (1993). Peroxisome Proliferator-Activated Receptor (PPAR): Structure, Mechanisms of Action and Diverse Functions. *Cell Structure and Function* **18** : 267-277.

Muerhoff, A.S., Griffin, K.J. and Johnson, E.F. (1992). Characterization of a rabbit gene encoding a clofibrate-inducible fatty acid ω -hydroxylase:CYP4A6. *Archives of Biochemistry and Biophysics* **296** (1) : 66-72.

Muerhoff, A.S., Griffin, K.J. and Johnson, E.F. (1992a). The peroxisome proliferator-activated receptor mediates the induction of CYP4A6, a cytochrome P450 fatty acid omega-hydroxylase, by clofibric acid. *Journal of Biological Chemistry* **267** (27) : 19051-19053.

Muerhoff, A.S., Griffin, K.J. and Johnson, E.F. (1992b). Characterization of a rabbit gene encoding a clofibrate-inducible fatty acid ω -hydroxylase: CYP4A6. *Archives of Biochemistry and Biophysics* **296** (1) : 66-72.

Mukherjee, R., Jow, L., Croston, G.E. and Paterniti, J.R. (1997). Identification, characterization and tissue distribution of human peroxisome proliferator-activated receptor (PPAR) isoforms PPAR γ 2 versus PPAR γ 1 and activation with retinoid X receptor agonists and antagonists. *Journal of Biological Chemistry* **272** (12) : 8071-8076.

Mukherjee, R., Jow, L., Noonan, D. and McDonnell, D.P. (1994). Human and rat peroxisome proliferator activated receptors (PPARs) demonstrate similar tissue distribution but different responsiveness to PPAR activators. *Journal of Steroid Biochemistry and Molecular Biology* **51** (3-4) : 157-166.

Mukherjee, R., Jow, L., Noonan, D. and McDonnell, D.P. (1994). Human and rat peroxisome proliferator activated receptors (PPARs) demonstrate similar tissue distribution but different responsiveness to PPAR activators. *Journal of steroid Biochemistry and Molecular Biology* **51** (3-4) : 157-166.

Myers, K.A., Lambe, K.G., Aldridge, T.C., MacDonald, N. and Tugwood, J.D. (1997). Amino

acid residues in both the DNA-binding and ligand-binding domains influence transcriptional activity of the human peroxisome proliferator-activated receptor alpha. *Biochemical and Biophysical Research Communications* **239** : 522-526.

Myers, R.M., Larin, Z. and Maniatis, T. (1985). Detection of single base substitutions by ribonuclease cleavage at mismatches in RNA-DNA duplexes. *Science* **230** (4731) : 1242-1246.

Nakatani, T., Suzuki, Y., Yoshida, K. and Sinohara, H. (1995). Molecular cloning and sequence analysis of cDNA encoding plasma α -1-antiproteinase from Syrian hamster: implications for the evolution of rodentia. *Biochimica and Biophysica Acta* **1263** : 245-248.

Nanbu, R. and Nagamine, Y. (1997). Mode of transfection influences the stability of ectopically expressed mRNA. *Biochimica et Biophysica Acta* **1350** (2) : 221-228.

Nebert, D.W., Adesnik, M., Coon, M.J., Estabrook, R.W., Gonzalez, F.J., Guengerich, F.P., Gunsalus, I.C., Johnson, E.F., Kemper, B., Levin, W., Phillips, J.R., Sato, R. and Waterman, M.R. (1987). The P-450 gene superfamily: Recommended nomenclature. *DNA* **5** : 1-11.

Nelson, D.R., Koymans, L., Kamataki, T., Stegeman, J.J., Feyereisen, R., Waxman, D.J., Waterman, M.R., Gotoh, O., Coon, M.J., Estabrook, R.W., Gunsalus, I.C. and Nebert, D.W. (1996). P450 superfamily: update on new sequences, gene mapping, accession numbers and nomenclature. *Pharmacogenetics* **6** (1) : 1-42.

Nemali, M.R., Usuda, N., Reddy, M.K., Oyasu, K., Hashimoto, T., Osumi, T., Rao, M.S. and Reddy, J.K. (1988). Comparison of constitutive and inducible levels of expression of peroxisomal beta-oxidation and catalase genes in liver and extrahepatic tissues of rat. *Cancer Research* **48** (18) : 5316-5324.

Nichols, J.S., Parks, D.J., Consler, T.G. and Blanchard, S.G. (1998). Development of a scintillation proximity assay for peroxisome proliferator-activated receptor gamma ligand binding domain. *Analytical Biochemistry* **112** (126): 257-263.

Noguchi, T., Fujiwara, S., Hayashi, S. and Haruhiko, S. (1994). Is the guinea pig (*Cavia porcellus*) a rodent? *Computational Biochemistry and Physiology* **107B** (2) : 179-182.

Nolte, R.T., Wisely, G.B., Westin, S., Cobb, J.E, Lambert, M.H., Kurokawa, R., Rosenfeld, M.G., Willson, T.M., Glass, C.K. and Milburn, M.V (1998). Ligand binding and co-activator assembly of the peroxisome proliferator-activated receptor-gamma. *Nature* **395** (6698) : 137-143.

Norseth, J. and Thomassen, M.S. (1983). Stimulation of microperoxisomal beta-oxidation in rat heart by high fat diets. *Biochimica et Biophysica Acta* **751** (3) : 312-320.

Novacek, M.J. (1992). Mammalian phylogeny: shaking the tree. *Nature* **356** : 121 - 125.

Nunez, S.B., Medin, J.A., Braissant, O., Kemp, L., Wahli, W., Ozato, K. and Segars, J.H. (1997). Retinoid X Receptor and Peroxisome Proliferator Activated Receptor activate an estrogen responsive gene independent of the Estrogen receptor. *Molecular and Cellular Endocrinology* **127** : 27-40.

Ohmura, T., Ledda-Columbano, G.M., Piga, R., Columbano, A., Glemba, J., Katyal, S.L., Locker, J. and Shinozuka, H. (1996). Hepatocyte proliferation induced by a single dose of a peroxisome proliferator. *American Journal Pathology* **148** 3 :815-824.

Oinonen, T. and Lindros, K.O. (1998). Zonation of hepatic cytochrome P-450 expression and regulation. *Biochemical Journal* **329** : 17-35.

Oliver, M.F., Heady, J.A., Morris, J.N. and Cooper, J. (1978). A cooperative trial in the primary prevention of ischemic heart disease using clofibrate. *Heart* **40** : 1069-1118.

Onate, S.A., Tsai, S.Y., Tsai, M-J. and O'Malley, B.W. (1995). Sequence and characterization of a coactivator for the steroid hormone receptor superfamily. *Science* **270** : 1354-1357.

Orton, T.C. and Parker, G.L. (1982). The effect of hypolipidaemic agents on the hepatic microsomal drug-metabolizing enzyme system of the rat. *Drug Metabolism and Disposition* **10** : 110-115.

Osada, S., Tsukamoto, T., Takiguchi, M., Mori, M. and Osumi, T. (1997). Identification of an extended half-site motif required for the function of peroxisome proliferator-activated receptor α . *Genes to cells* **2** : 315-327.

Osumi, T., Ozasa, H. and Hashimoto, T. (1984). Molecular-cloning of cDNA for rat acyl-CoA oxidase. *Journal of Biological Chemistry* **259** (4) : 2031-2034.

Osumi, T., Wen, J-K. and Hashimoto, T. (1991). Two cis-acting regulatory sequences in the peroxisome proliferator-responsive enhancer region of rat acyl-CoA oxidase gene. *Biochemical and Biophysical Research communications* **175** (30) : 866-871.

Pacot, C., Petit, M., Caira, F., Rollin, M., Behecti, N., Gregoire, S., Cherkaoui Malki, M., Cavatz, C., Moisant, M., Moreau, C., Thomas, C., Descotes, G., Gallas, J-F., Deslex, P., Althoff, J., Zahnd, J-P., Lhuguenot, J.C. and Latruffe, N. (1993). Response of genetically obese Zucker rats to ciprofibrate, a hypolipidaemic agent, with peroxisome proliferation activity as compared to Zucker lean and sprague-dawley rats. *Biol. Cell* **77** : 27-35.

Pacot, C., Petit, M., Rollin, M., Behecti, N., Moisant, M., Deslex, P., Althoff, J., Lhuguenot,

J.C. and Latruffe, N. (1996). Difference between guinea pig and rat in the liver peroxisomal response to equivalent plasmatic level of ciprofibrate. *Archives of Biochemistry and Biophysics*, **327** (1) : 181-188.

Palmer, C.N.A., Griffin, K.J. and Johnson, E.F. (1993a). Rabbit prostaglandin omega-hydroxylase (CYP4A4) : gene structure and expression. *Archives of Biochemistry and Biophysics* **300** (2) : 670-676.

Palmer, C.N.A., Hsu, M.H., Griffin, K.J., Raucy, J.L. and Johnson, E.F. (1998). Peroxisome proliferator activated receptor-alpha expression in human liver. *Molecular Pharmacology* **53** (1) : 14-22.

Palmer, C.N.A., Hsu, M-H., Muerhoff, A.S, Griffin, K.J. and Johnson, E.F. (1994). Interaction of the peroxisome proliferator-activated receptor α with the retinoid X receptor a unmasks a cryptic peroxisome proliferator response element in the CYP4A6 promoter. *Journal of Biological Chemistry*, **269** (27) : 18083-18089.

Palmer, C.N.A., Richardson, T.H., Griffin, K.J., Hsu, M.H., Muerhoff, A.S., Clark, J.E. and Johnson, E.F. (1993b). Characterization of a cDNA encoding a human kidney, cytochrome P-450 4A fatty acid ω -hydroxylase and the cognate enzyme expressed in *Escherichia coli*. *Biochimica et Biophysica Acta* **1171** : 161-166

Palosaari, P.M. and Hiltunen, J.K. (1990). Peroxisomal bifunctional protein from rat liver is a trifunctional enzyme possessing 2-enoyl-CoA hydratase, 3-hydroxylacyl-CoA dehydrogenase, and D₃, D₂-enoyl-CoA isomerase activities. *Journal of Biological Chemistry* **265** (5) : 2446-2449.

Peters, J.M., Hennuyer, N., Staels, B., Fruchart, J.C., Fievet, C., Gonzalez, F.J. and Auwerx,

J. (1997). Alterations in lipoprotein metabolism in peroxisome proliferator-activated receptor alpha-deficient mice. *Journal of Biological Chemistry* **272** (43) : 27307-27312.

Pineau, T., Hudgins, W.R., Liu, L., Chen, L.C., Sher, T., Gonzalez, F.J. and Samid, D. (1996). Activation of a human peroxisome proliferator-activated receptor by the anti-tumour agent phenylacetate and its analogues. *Biochemical Pharmacology* **52** : 659-667.

Plant, N.J., Horley, N.J., Savory, R.L., Elcombe, C.R., Gray, T.J.B. and Bell, DR. (1998). The peroxisome proliferators are hepatocyte mitogens in chemically-defined media: glucocorticoid-induced PPAR alpha is linked to peroxisome proliferator mitogenesis. *Carcinogenesis* **19** (5) : 925-931.

Price, R.J. Evans, J.G. and Lake, B.G. (1992). Comparison of the effects of nafenopin on hepatic peroxisome proliferation and replicative DNA synthesis in the rat and Syrian hamster. *Food and Chemical Toxicology* **30** (11) : 937-944.

Puigserver, P., Wu, Z.D., Park, C.W., Graves, R., Wright, M. and Spiegelman, B.M. (1998). A cold-inducible coactivator of nuclear receptors linked to adaptive thermogenesis. *Cell* **92** (6) : 829-839.

Qi, C., Zhu, Y.J., Pan, J., Yeldandi, A.V., Rao, M.S., Maeda, N., Subbarao, V., Pulikuri, S., Hashimoto, T. and Reddy, J.K. (1999). Mouse steroid receptor coactivator-1 is not essential for peroxisome proliferator-activated receptor alpha-regulated gene expression. *Proceedings of the National Academy of Sciences (USA)* **96** (4) : 1585-1590.

Rao, M.S. and Reddy, J.K. (1987). Peroxisome proliferation and hepatocarcinogenesis. *Carcinogenesis* **8** (5) : 631-636.

Rao, M.S. and Reddy, J.K. (1991). An overview of peroxisome proliferator induced hepatocarcinogenesis. *Environmental Health Perspectives* **93** : 205-209.

Rao, M.S., Lalwani, N.D., Watanabe, T.K. and Reddy, J.K. (1984). Inhibitory effect of antioxidants ethoxyquin and 2(3)-tert-butyl-4-hydroxyanisole on hepatic tumourigenesis in rats fed ciprofibrate, a peroxisome proliferator. *Cancer Research* **44** : 1072.

Rao, M.S., Lalwani, N.D. and Reddy, J.K. (1984). Sequential histologic study of rat liver during peroxisome proliferator [4-chloro-6-(2,3-xylidino)-2-pyrimidinylthio]-acetic acid (WY-14,643)-induced carcinogenesis. *Journal of the National Cancer Institute* **73** (4) : 983-990.

Reddy, J.K. and Lalwani, N.D. (1983). Carcinogenesis by hepatic peroxisome proliferators: Evaluation of the risk of hypolipidaemic drugs and industrial plasticizers to humans. *CRC Critical Reviews in Toxicology* **12** : 1-58.

Reddy, J.K. and Rao, M.S. (1989). Oxidative DNA damage caused by persistent peroxisome proliferation- its role in hepatocarcinogenesis. *Mutation Research* **214** (1) : 63-68.

Reddy, J.K., Azarnoff, D.L. and Hignite, C.E. (1980). Hypolipidaemic hepatic peroxisome proliferators form a novel class of chemical carcinogens. *Nature* **283** : 397 - 398.

Reddy, J.K., Goel, S.K., Nemali, M.R., Carrino, J.J., Laffler, T.G., Reddy, M.K., Sperbeck, S.J., Osumi, T., Hashimoto, T, Lalwani, N.D. and Rao, M.S. (1986). Transcriptional regulation of peroxisomal fatty acyl-CoA oxidase and enoyl-CoA hydratase/3-hydroxyacyl-CoA dehydrogenase in rat liver by peroxisome proliferators. *Proceedings of the National Academy of Sciences (USA)* **83** (6) : 1747-1751.

Reddy, J.K., Lalwani, N.D., Qureshi, S.A., Reddy, M.K. and Moehle, C.M. (1984). Induction

of hepatic peroxisome proliferation in non-rodent species, including primates. *American Journal of Pathology* **114** : 171-183.

Reddy, P.G., Nemali, M.R., Reddy, M.K., Reddy, M.N., Yuan, P.M., Yuen, S., Laffler, T.G., Shiroza, T., Kuramitsu, H.K., Usuda, N., Chisholm, R.L., Rao, M.S. and Reddy, J.K. (1988). Isolation and sequence determination of a cDNA clone for rat peroxisomal urate oxidase- liver-specific expression in the rat. *Proceedings of the National Academy of Sciences (USA)* **85** (23) : 9081-9085.

Ren, B., Thelen, A. and Jump, D.B. (1996). Peroxisome proliferator-activated receptor alpha inhibits hepatic S14 gene transcription: Evidence against the peroxisome proliferator-activated receptor alpha as the mediator of polyunsaturated fatty acid regulation of S14 gene *Journal of Biological Chemistry* **271** (29) : 17167-17173.

Renaud, J.P., Rochel, N., Ruff, M., Vivat, V., Chambon, P., Gronemeyer, h. and Moras, D. (1995) crystal-structure of the ret- γ ligand-binding domain bound to all-trans-retinoic acid. *Nature* **378** (6558) : 681-689.

Richter, C., Park, J.W. and Ames, B.N. (1988). Normal oxidative damage to mitochondrial and nuclear DNA is extensive. *Proceedings of the National Academy of Sciences (USA)* **85** (17) : 6465-6467.

Roberts, R.A., James, N.H., Woodyatt, N.J., MacDonald, N. and Tugwood, J.D. (1998). Evidence for the suppression of apoptosis by the peroxisome proliferator activated receptor alpha (PPAR alpha). *Carcinogenesis* **19** (1) : 43-48.

Roberts, R.A., Soames, A.R., Gill, J.H., James, N.H and Wheeldon, E.B. (1995). Nongenotoxic hepatocarcinogens stimulate DNA-synthesis and their withdrawal induces apoptosis, but in dif-

ferent hepatocyte populations. *Carcinogenesis* **16** (8) : 1693-1698.

Roberts, R.A., James, N.H., Hasmall, S.C, Holden, P.R., Lambe, K, Macdonald, N., West, D, Woodyatt, N.J. and Whitcombe, D. (2000). Apoptosis and proliferation in nongenotoxic carcinogenesis: species differences and role of PPAR α . *Toxicology Letters* **112-113** : 49-57.

Rodriguez, J.C., Gilgomez, G., Hegardt, F.G. and Haron, D. (1994). Peroxisome proliferated activated receptor mediates induction of the mitochondrial 3-hydroxy-3-methylglutaryl-CoA synthase gene by fatty acids. *Journal Biological Chemistry* **269** (29) : 18767-18772.

Roman, L.J., Palmer, C.N.A., Clark, J.E., Muerhoff, A.S., Griffin, K.J., Johnson, E.F. and Masters, B.S.S. (1993). expression of rabbit cytochromes P4504A which catalyze the ω -hydroxylation of arachidonic acid, fatty acids, and prostaglandins. *Archives of Biochemistry and Biophysics* **307** (1) : 57-65.

Runge, D.M., Runge, D., Dorko, K., Pizarov, L.A., Leckel, K., Kostrubsky, V.E., Thomas, D., Strom, S.C. and Michalopoulos, G.K. (1999). Epidermal growth factor- and hepatocyte growth factor-receptor activity in serum-free cultures of human hepatocytes. *Journal of Hepatology* **30** (2) : 265-274.

Sakuma, M., Yamada, J. and Suga, T. (1992). Comparison of the inducing effect of dehydroepiandrosterone on hepatic peroxisome proliferation-associated enzymes in several rodent species. *Biochemical Pharmacology* **43** (6) : 1269-1273.

Samuelsson, B. (1983). Leukotrienes - mediators of immediate hypersensitivity reactions and inflammation. *Science* **220** (4597) : 568-575.

Samuelsson, B., Dahlen, S.E., Lindgren, J.A., Rouzer, C.A. and Serhan, C.N. (1987). Leukot-

rienes and lipoxins - structures, biosynthesis, and biological effects. *Science* **237** (4819) : 1171-1176.

Sap, J., Munoz, A., Schmitt, J., Stunnenberg, H. and Vennstrom, B. (1989). Repression of transcription mediated at a thyroid hormone response element by the v-erbA oncogene product. *Nature* **340** (6230) : 242-244.

Sato, T., Murayama, N., Yamazoe, Y. and Kato, R. (1995). Suppression of clofibrate-induction of peroxisomal and microsomal fatty acid-oxidising enzymes by growth hormone and thyroid hormone in primary cultures of rat hepatocytes. *Biochimica et Biophysica Acta* **1256** : 327-333.

Sausen, P.J., Lee, D.C., Rose, M.L. and Cattley, R.C. (1995). Elevated 8-hydroxydeoxyguanosine in hepatic DNA of rats following exposure to peroxisome proliferators: relationship to mitochondrial alterations. *Carcinogenesis* **16** 8 : 1795-1801.

Schladt, L., Hartmann, R., Timms, C., Strolinbenedetti, M., Dostert, P., Worner, W. and Oesch, F. (1987). Concomitant induction of cytosolic but not microsomal epoxide hydrolase with peroxisomal beta-oxidation by various hypolipidemic compounds. *Biochemical Pharmacology* **36** (3) : 345-351.

Schmezer, P., Pool, B.L., Klein, R.G., Komitowski, D. and Schmahl, D. (1988). Various short-term assays and 2 long-term studies with the plasticizer di(2-ethylhexyl)phthalate in the Syrian golden-hamster. *Carcinogenesis* **9** (1) : 37-43.

Schmidt, A., Endo, N., Rutledge, S.J., Vogel, R., Shinar, D. and Rodan, G.A. (1992). Identification of a new member of the steroid hormone receptor superfamily that is activated by a peroxisome proliferator and fatty acids. *Molecular Endocrinology* **6** (10) : 1634-1641.

Schoonjans, K., Peinado-Onsurbe, J., Lefebvre, A-M, Heyman, R.A., Briggs, M., Deeb, S., Staels, B. and Auwerx, J. (1996). PPAR α and PPAR γ activators direct a distinct tissue-specific transcriptional response via a PPRE in the lipoprotein lipase gene. *EMBO Journal* **15** (190) : 5336-5348.

Schoonjans, K., Watanabe, M., Suzuki, H., Mahfoudi, A., Krey, G., Wahli, W., Grimaldi, P., Staels, B., Yamamoto, T. and Auwerx, J. (1995). Induction of the acyl-coenzyme A synthetase gene by fibrates and fatty acids is mediated by a peroxisome proliferator response element in the C-promoter. *Journal of Biological Chemistry*, **270** (33) : 19269-19276.

Schultz, H. (1991). Beta oxidation of fatty acids. *Biochimica and Biophysica Acta* **1081** : 109-120.

Schutgens, R.B.H., Heymans, H.S.A., Wanders, R.J.A., Van den Bosch, H. and Tager, J.M. (1986). Peroxisomal disorders- a newly recognized group of genetic diseases. *European Journal of Peadiatrics* **144** (5) : 430-440.

Scotto, C., Keller, J-M., Schohn, H., and Dauca, M. (1995). Comparative effects of clofibrate on peroxisomal enzymes of human (Hep EBNA2) and rat (FaO) hepatoma cell lines. *European Journal of Cell Biology* **66** : 375-381.

Shalev, A., Siegrist-Kaiser, C.A., Yen, P.M., Wahli, W., Burger, A.G., Chin, W.W. and Meier, C.A. (1996). The peroxisome proliferator activated receptor α is a phosphoprotein: regulation by insulin. *Endocrinology* **137** (10) : 4499-4502.

Sharma, R.K., Doig, M.V., Lewis, D.F.V. and Gibson, G.G. (1989). Role of hepatic and renal cytochrome P-450 IVA1 in the metabolism of lipid substrates. *Biochemical Pharmacology* **38** (20) : 3621-3629.

Sharma, R.K., Lake, B.G., Foster, J. and Gibson, G.G. (1988). Microsomal cytochrome P452 induction and peroxisome proliferation by hypolipidaemic agents in rat liver: a mechanistic inter-relationship. *Biochemical Pharmacology* **37** : 1193-1201.

Steineger, H.H., Sorensen, H.N., Tugwood, J.D., Skrede, S., Spydevold, O. and Gautvik, K.M. (1994). Dexamethasone and insulin demonstrate marked and opposite regulation of the steady-state messenger RNA level of the peroxisomal proliferator-activated receptor (PPAR) in hepatic cells- Hormonal modulation of fatty-acid-induced transcription. *European Journal of Biochemistry* **225** (3) : 967-974.

Sterchele, P.F., Sun, H., Peterson, R.E. and Vanden Heuval, J.P. (1996). Regulation of peroxisome proliferator-activated receptor- α mRNA in rat liver. *Archives of Biochemistry and Biophysics* **326** (2) : 281-289.

Stromstedt, M., Hayashi, S.I., Zaphiropoulos, P.G. and Gustaffson, J.A. (1990). Cloning and characterization of a novel member of the cytochrome P450 subfamily IVA in rat prostate. *DNA and Cell Biology* **9** (8) : 569-577.

Stromstedt, M., Warner, M. and Gustafsson, JA. (1994). Cytochrome P450S of the 4a subfamily in the brain. *Journal of Neurochemistry* **63** (2) : 671-676.

Styles, J.A., Kelly, M., Pritchard, N.R. and Elcombe, C.R. (1988). A species comparison of acute hyperplasia induced by the peroxisome proliferator methylclofenopate: involvement of the binucleated hepatocyte. *Carcinogenesis* **9** (9) : 1647-1655.

Sundseth, S.S. and Waxman, D.J. (1992). Sex-dependent Expression and Clofibrate Inducibility of Cytochrome P450 4A Fatty Acid ω -Hydroxylases. *Journal of Biological Chemistry* **267** (6) : 3915-3921.

Takagi, A., Sai, K., Umemura, T., Hasegawa, R. and Kurokawa, F. (1991). Short term exposure to peroxisome proliferators, perfluorooctanoic acid and perfluorodecanoic acid causes significant increases of 8-hydroxydeoxyguanosine in liver DNA of rats. *Cancer Letters* **57** : 55-60.

Takagi, A., Sai, K., Umemura, T., Hasegawa, R. and Kurokawa, Y. (1990). Significant increase in 8-hydroxyguanosine in liver DNA of rats following short term exposure to peroxisome proliferators di(2-ethylhexyl)phthalate and di(2-ethylhexyl)adipate. *Japanese Journal of Cancer Research* **81** : 213-215.

Takehara, T., Matsumoto, K. and Nakamura, T. (1992). Cell density dependent regulation of albumin synthesis and DNA-synthesis in rat hepatocytes by hepatocyte growth factor. *Journal of Biochemistry* **112** (3) : 330-334.

Tamburini, P.P., Masson, H.A., Bains, S.K., Makowski, R.J., Morris, B. and Gibson, G.G. (1984). Multiple forms of hepatic cytochrome P450: purification, characterization, and comparison of a novel clofibrate-induced isozyme with other forms of cytochrome P-450. *European Journal of Biochemistry* **139** : 235-246.

Tamura, H., Iida, T., Watanabe, T. and Suga, T. (1990a). Long term effects of peroxisome proliferators on the balance between hydrogen peroxide generating and scavenging capabilities in the liver of Fischer 344 rats. *Toxicology* **63** : 199-213.

Tamura, H., Iida, T., Watanabe, T. and Suga, T. (1990b). Long term effects of hypolipidaemic peroxisome proliferator administration on hepatic hydrogen peroxide metabolism in rats. *Carcinogenesis* **11** : 445-450.

Tamura, H., Iida, T., Watanabe, T., Suga, T. (1991). Lack of induction of hepatic DNA damage on long term administration of peroxisome proliferators in male F344 rats. *Toxicology* **69** : 55-

62.

Tontonoz, P., Graves, R.A., Budavari, A.I., Erdjument-Bromage, H., Lui, M., Hu, E., Tempst, P. and Spiegelman, B.M. (1994b). Adipocyte-specific transcription factor ARF6 is a heterodimeric complex of two nuclear hormone receptors, PPAR β and RXR α . *Nucleic Acids Research* **22** (25) : 5628-5634.

Tontonoz, P., Hu, E., Graves, R.A., Budavari, A.I. and Spiegelman, B.M. (1994a). mPPAR γ 2: Tissue-specific regulator of an adipocyte enhancer. *Genes and Development* **8** : 1224-1234.

Tucker, M.J. and Orton, T.C (eds). (1995). Comparative toxicology of hypolipidaemic fibrates. London, Taylor and Francis.

Tugwood, J.D., Aldridge, T.C., Lambe, K.G., MacDonald, N. and Woodyatt, N.J. (1996). In Peroxisomes: Biology and role in toxicology and disease (Reddy, J.K., Suga, T., Mannaerts, G.P., Lazarow, P.B. and Subramani, S. Eds.). *Annals of the New York Academy of Sciences* **804** : 252-265.

Tugwood, J.D., Holden, P.R., James, N.H., Prince, R.A. and Roberts, R.A. (1998). A peroxisome proliferator-activated receptor alpha (PPAR alpha) cDNA cloned from guinea-pig liver encodes a protein with similar properties to the mouse PPAR alpha: implications for species differences in responses to peroxisome proliferators. *Archives of Toxicology* **72** (3) : 169-177.

Tugwood, J.D., Issemann, I., Anderson, R.G., Bundell, K., McPheat, W.L. and Green, S. (1992). The mouse peroxisome proliferator activated receptor recognizes a response element in the 5' flanking sequence of the rat acyl-CoA oxidase gene. *EMBO Journal* **11** (2) : 433-439.

Usuda, N., Reddy, M.K., Hashimoto, T., Rao, M.S. and Reddy, J.K. (1988). Tissue-specificity

and species differences in the distribution of urate oxidase in peroxisomes. *Laboratory Investigation* **58** (1) : 100-111.

Van den Berg, J., van Ooyen, A., Mantei, N., Schambock, A., Grosveld, G., Flavell, R.A. and Weissmann, C. (1978). Comparison of cloned rabbit and mouse beta-globin genes showing strong evolutionary divergence of two homologous pairs of introns. *Nature*. **276** (5683) : 37-44

Van den Bosch, H., Schutgens, R.B.H., Wanders, R.J.A. and Tager, J.M. (1992). Biochemistry of peroxisomes. *Annual Review of Biochemistry* **61** : 157-197.

Varanasi, U., Chu, R., Huang, Q., Castellon, R., Yeldandi, A.V. and Reddy, J.K. (1996). Identification of a peroxisome proliferator-responsive element upstream of the human peroxisomal fatty acyl-coenzyme A oxidase gene. *Journal of Biological Chemistry*, **271** (4) : 2147-2155.

Veerkamp, J.H. and Vanmoerkerk, H.T.B. (1986). Peroxisomal fatty acid oxidation in rat and human tissues- effect of nutritional state, clofibrate treatment and postnatal-development in the rat. *Biochimica et Biophysica Acta* **875** (2) : 301-310.

Vu-Dac, N., Schoonjans, K., Laine, B., Fruchart, J.C., Auwerx, J. and Staels, B. (1994). Negative regulation of the human apolipoprotein A-I promoter by fibrates can be attenuated by the interaction of the peroxisome proliferator activated receptor with its response element. *Journal of Biological Chemistry* **269** (49) : 31012-31018.

Wagner, R.L., Apriletti, J.W., Mcgrath, M.E., West, B.L., Baxter, J.D. and Fletterick, R.J. (1995). A structural role for hormone in the thyroid-hormone receptor. *Nature* **378** (6558) : 690-697.

Wahlstrom, G.M., Harbers, M. and Vennstrom, B. (1996). The oncoprotein P75gag-v-erbA re-

presses thyroid hormone induced transcription only via response elements containing palindromic half-sites. *Oncogene* **13** (4) : 843-852

Wanders, R.J.A., Romeyn, G.J., Vanroermund, C.W.T., Schutgens, R.B.H., Vandenbosch, H. and Tager, J.M. (1988). Identification of l-pipecolate oxidase in human-liver and its deficiency in the Zellweger syndrome. *Biochemical and Biophysical Research Communications* **154** (1) : 33-38.

Ward, J.M., Diwan, B.A., Ohshima, M., Hu, H., Schuller, H.M. and Rice, J.M. (1986). Tumour-initiating and promoting activities of di(2-ethylhexyl)phthalate *in vivo* and *in vitro*. *Environmental Health Perspectives* **65** : 279-291.

Ward, J.M., Ohshima, M., Lynch, P. and Riggs, C. (1984). Di(2-ethylhexyl)phthalate but not phenobarbital promotes N-nitrosodiethylamine-initiated hepatocellular proliferative lesions after short term exposure in male B6C3F1 mice. *Cancer Letters* **24** : 49-55.

Ward, J.M., Rice, J.M, Creasia, D., Lynch, P. and Riggs, C. (1983). Dissimilar patterns of promotion by di(2-ethylhexyl)phthalate and phenobarbital of hepatocellular neoplasia initiated by diethylnitrosamine in B6C3F1 mice. *Carcinogenesis* **4** (8) : 1021-1029.

Warren, J.R., Simmon, V.F. and Reddy, J.K. (1980). Properties of hypolipidaemic peroxisome proliferators in the lymphocyte [³H]thymidine and *Salmonella* mutagenesis assays. *Cancer Research* **40** : 36-41.

Waxman, D.J., Pampori, N.A., Ram, P.A., Agrawal, A.K. and Shapiro, B.H. (1991). Interpulse interval in circulating growth-hormone patterns regulates sexually dimorphic expression of hepatic cytochrome-P450. *Proceedings of the National Academy of Sciences (USA)* **88** (15) : 6868-6872.

Wilcke, M., Hultenby, K. and Alexson, S.H.E. (1995). Novel peroxisomal populations in sub-cellular fractions from rat liver - implications for peroxisome structure and biogenesis. *Journal of Biological Chemistry* **270** (12) : 6949-6958.

Williams, D.E., Hale, S.E., Okita, R.T. and Masters, B.S.S. (1984). A prostaglandin omega-hydroxylase cytochrome P-450 (P-450_{pg-omega}) purified from lungs of pregnant rabbits. *Journal of Biological Chemistry* **259** (23) : 4600-4608.

Winrow, C.J., Capone, J.P. and Rachubinski, R.A. (1998). Cross-talk between orphan nuclear hormone receptor RZR alpha and peroxisome proliferator-activated receptor alpha in regulation of the peroxisomal hydratase-dehydrogenase gene. *Journal of Biological Chemistry* **273** (47) : 31442-31448.

Woodyatt, N.J., Lambe, K.G., Myers, K.A., Tugwood, J.D. and Roberts, R.A. (1999). The peroxisome proliferator (PP) response element upstream of the human acyl-CoA oxidase gene is inactive among a sample human population: significance for species differences in response to PPs. *Carcinogenesis* **20** (3) : 369-372.

Wu, C.-I. and Li, W.-H. (1985). Evidence for higher rates of nucleotide substitution in rodents than in man. *Proceedings of the National Academy of Sciences (USA)*. **82** : 1741 - 1745.

Wu, C.I. and Li, W.H. (1985). Evidence for higher rates of nucleotide substitution in rodents than in man. *Proceedings of the National Academy of Sciences (USA)* **82** : 1741-1745.

Xing, G., Zhang, L., Heynen, T., Yoshikawa, T., Smith, M., Weiss, S. and Detera-Wadleigh, S. (1995). Rat PPAR δ contains a CGG triplet repeat and is prominently expressed in the thalamic nuclei. *Biochemical and Biophysical Research Communications* **217** (3) : 1015-1025.

Yamada, J, Sugiyama, H, Tamura, H, Suga, T. (1994). Hormonal modulation of peroxisomal enzyme-induction caused by peroxisome proliferators- suppression by growth and thyroid hormones in cultured rat hepatocytes. *Archives of Biochemistry and Biophysics* **315** (2) : 555-557.

Yamada, J., Sugiyama, H., Watanabe, T. and Suga, T. (1995). Suppressive effect of growth hormone on the expression of peroxisome proliferator-activated receptor in cultured hepatocytes. *Research Communications in Molecular Pathology and Pharmacology* **90** (1) : 173-176.

Yamamoto, S., Kusunose, E., Ogita, K., Kaku, M., Ichihara, K. and Kusunose, M. (1984). Isolation of cytochrome P-450 highly active in prostaglandin omega- hydroxylation from lung microsomes of rabbits treated with progesterone. *Journal of Biochemistry* **96** (3) : 593-603.

Yan, Z.H., Karam, W.G., Staudinger, J.L., Medvedev, A., Ghanayem, B.I. and Jetten, A.M. (1998). Regulation of peroxisome proliferator-activated receptor alpha-induced transactivation by the nuclear orphan receptor TAK1/TR4. *Journal of Biological Chemistry* **273** (18) : 10948-10957.

Yokotani, N., Bernhardt, R., Sogawa, K., Kusunose, E., Gotoh, O., Kusunose, M. and Fujii-Kuriyama, Y. (1989). Two Forms of ω -Hydroxylase toward Prostaglandin A and Laurate. *Journal of Biological Chemistry* **264** (36) : 21665-21669.

Zhang, B., Berger, J., Zhou, G.C., Elbrecht, A., Biswas, S., WhiteCarrington, S., Szalkowski, D. and Moller, D.E. (1996). Insulin and mitogen activated protein kinase-mediated phosphorylation and activation of peroxisome proliferator-activated receptor gamma. *Journal of Biological Chemistry* **271** (50) : 31771-31774.

Zhang, B., Marcus, S.L., Sajjadi, F.G., Alvares, K., Reddy, J.K., Subramani, S., Rachubinski, R.A. and Capone, J.P. (1992). Identification of a peroxisome proliferator-responsive element

upstream of the gene encoding rat peroxisomal enoyl-CoA hydratase/3-hydroxyacyl-CoA dehydrogenase. *Proceedings of the National Academy of Sciences (USA)* **89** : 7541-7545.

Zhang, B.H. and Farrell, G.C. (1995). Effects of extracellular Ca^{2+} and HCO_3^- on epidermal growth factor-induced DNA-synthesis in cultured rat hepatocytes. *Gastroenterology* **108** (2) : 477-486.

Zhang, Z.F., Kelly, D.P., Kim, J.J., Zhou, Y.Q., Ogden, M.L., Whelan, A.J. and Strauss, A.W. (1992). Structural organization and regulatory regions of the human medium chain acyl-CoA dehydrogenase gene. *Biochemistry* **31** (1) : 81-89.

Zhou, Y.C. and Waxman, D.J. (1999). Cross-talk between Janus kinase-signal transducer and activator of transcription (JAK-STAT) and peroxisome proliferator-activated receptor-alpha (PPAR alpha) signaling pathways. *Journal of Biological Chemistry* **274** (5) : 2672-2681.

Zou, A.P., Ma, Y.H., Sui, Z.H., Ortizde-Montellano, P.R., Clark, J.E., Masters, B.S. and Roman, R.J. (1994). Effects of 17-octadecynoic acid, a suicide substrate inhibitor of cytochrome P450 fatty acid ω -hydroxylase on renal function in rats. *Journal of Pathology and Experimental Therapeutics* **268** (1) : 474-481.

Zhu, Y., Alvares, K., Huang, Q., Rao, M.S. and Reddy, J.K. (1993). Cloning of a new member of the peroxisome proliferator-activated receptor gene family from mouse liver. *Journal of Biological Chemistry* **258** : 26817-26820.

Zhu, Y., Qi, C., Jain, S., Rao, M.S. and Reddy, J.K. (1997). Isolation and characterization of PBP, a protein that interacts with peroxisome proliferator-activated receptor. *Journal of Biological Chemistry* **272** (41) : 25500-25506.

Zhu, Y.J., Qi, C., Calandra, C., Rao, M.S. and Reddy, J.K. (1996). Cloning and identification of mouse steroid receptor coactivator-1 (mSRC-1), as a coactivator of peroxisome proliferator-activated receptor gamma. *Gene Expression* 6 (3) : 185-195.

Zou, A. P., Imig, J.D., Ortiz de Montellano, P.R., Sui, Z., Falck, J.R. and Roman, R.J. (1994a). Effect of P450 ω -hydroxylase metabolites of arachidonic acid on tubuloglomerular feed back. *American Journal of Physiology* **266** : F934-F941.

Zou, A.P., Imig, J.D., Kaldunski, M., Ortiz de Montellano, P.R., Sui, Z. and Roman, R.J. (1994b). Inhibition of renal vascular 20-HETE production impairs autoregulation of renal blood flow. *American Journal of Physiology* **266** : F275-F282.